Univerzita Karlova

Přírodovědecká fakulta

Studijní program: Geologie

Studijní obor: Geologie

Mgr. Radim Jedlička

Záznam před-exhumačního vývoje silně re-ekvilibrovaných vysoko- až ultra-vysokotlakých hornin v kolizním orogénu

Tracing of the pre-exhumation history of strongly re-equilibrated high-ultrahigh pressure rocks in a collision orogeny

Disertační práce

Školitel: prof. Ing. Shah Wali Faryad, CSc.

Praha, 2017

"Everybody is a genius. But if you judge a fish by its ability to climb a tree, it will live its whole life believing that it is stupid."

- Albert Einstein -

Declaration / Prohlášení

I certify that the work presented in this thesis is my own work or the product of collaboration with other members of the research team. None of the material presented here has been accepted for any other degree or diploma in my name, in any university or other tertiary institution. I used only data acquired from my own research or from sources mentioned in the list of literature for which references has been made in the text.

Prohlašuji, že předkládaná teze je produktem mé vlastní práce nebo spolupráce se členy mého výzkumného týmu. Tato práce ani její podstatná část nebyla předložena k získání jiného nebo stejného akademického titulu na univerzitě či jiné instituci. Použitá data jsou výsledkem mého vlastního výzkumu nebo byly čerpány ze zdrojů, jež jsou řádně ocitovány v textu a uvedeny v seznamu použité literatury.

In Prague, 29/06/2017

V Praze, 29.6.2017

Radim Jedlička

English abstract

The investigation of high- to ultrahigh-pressure rocks in the Bohemian Massif occurring as small bodies enclosed in surrounding rocks with a low degree of metamorphism was always focused on their main metamorphic event in granulite facies conditions at very high temperatures. However, recent studies have shown that these rocks underwent a high-pressure metamorphism that preceded the subsequent high-temperature overprint and exhumation of those rocks. The scientific publications that comprise this dissertation thesis present petrological, mineralogical and geochemical research of these (ultra)high pressure rocks from various parts of the Bohemian Massif that have the potential to preserve information about their pre-exhumation history. The findings of the inclusions of high-pressure phases in metamorphic minerals and, in particular, the study of major and trace elements zoning in garnets together with thermodynamic modelling allowed us to describe new temperature-pressure conditions and to refine the metamorphic paths of these rocks.

The felsic and mafic granulites of the Kutná Hora Complex in the Moldanubian Zone and the Rychleby Mountains in the East Sudetes preserve the evidence of prograde metamorphism. In addition to the inclusions of phengite and omphacite in the garnet cores, the multiple zoning of major and trace elements in garnet declares their prograde evolution. Using thermodynamic modelling, it has been calculated that these rocks have undergone a complex metamorphic evolution from their initial stage at low temperatures and pressures (400-500 °C / 0.8-1.0 GPa) up to UHP conditions in the coesite and diamond stability field. This prograde path took place under a very steep geothermal gradient in the subduction zone. After a partial isobaric ascent of the rocks to the upper mantle levels, significant heating under the granulite facies conditions affected these rocks. This second metamorphic event is linked to the intrusion of a hot mantle magma that penetrated mantle/crust boundary due to the slab break-off and also to later Variscan processes.

The composition of monomineral and polyphase inclusions in garnets from eclogites and clinopyroxenites, which are enclosed as boudins in garnet peridotites in the Moldanubian Zone, shows their origin as derivatives of the lithospheric mantle

above the subduction zone. The temperature-pressure conditions, calculated on the base of preserved prograde zoning in garnets, suggest that the high temperature overprint in granulite facies was relatively short and did not result in total homogenisation of those rocks. This short-term event is also documented in the surrounding felsic granulites. The probable occurrence of the subduction environment and part of the Variscan suture in the Bohemian Massif is also documented by the bodies of eclogites, which occur in the form of a 250 km long bend spreading across the Moldanubian Zone from the southwest to the northeast up to the East Sudetes. Their texture relationships and temperature / pressure conditions (600-650 °C / 2.3 GPa) allow us to determine that these rocks have undergone a steep geothermal gradient during the prograde metamorphism. These hypotheses are also supported by findings of high pressure / low temperature amphiboles of taramitic composition as inclusions in garnets.

Český abstrakt

Výzkum vysoko- až ultra-vysokotlakých hornin vyskytujících se v Českém masívu jako drobná tělesa uzavřená v okolních horninách s nízkým stupněm metamorfózy, byl vždy zaměřen na jejich hlavní metamorfní vývoj v granulitové facii za velmi vysokých teplot. Avšak poslední studie ukázaly, že tyto horniny prodělaly vysokotlakou metamorfózu, jež předcházela pozdějšímu vysokoteplotnímu přetisku a následnému vynoření hornin na zemský povrch. Odborné vědecké publikace, z nichž se skládá tato disertační práce, prezentují petrologický, mineralogický a geochemický výzkum těchto (ultra)vysokotlakých hornin z různých částí Českého masívu, jež mají potenciál zachovat informace o jejich před-exhumační historii. Nálezy inkluzí vysokotlakých fází v metamorfních minerálech a především studie zonality hlavních a stopových prvků v granátech nám společně s termodynamickým modelováním umožnily popsat nové teplotně-tlakové podmínky a zpřesnit metamorfní dráhy těchto hornin.

Felsické a mafické granulity kutnohorské oblasti moldanubika a Rychlebských hor ve východních Sudetech zachovávají znaky prográdní metamorfózy. Vedle inkluzí fengitů a omfacitů v jádrech granátů se pak jedná o prográdní zonalitu hlavních a stopových prvků v granátech. Pomocí termodynamického modelování se podařilo vypočítat, že tyto horniny prodělaly komplexní metamorfní vývoj od svého iniciálního stádia za nízkých teplot a tlaků (400-500 °C / 0.8-1.0 GPa) až po metamorfózu za ultra-vysokých tlaků v poli stability coesitu až diamantu. Tento prográdní vývoj proběhl za velice strmého geotermálního gradientu v prostředí subdukční zóny. Po částečném izobarickém vynoření hornin do úrovní svrchního pláště došlo k jejich výraznému zahřátí v podmínkách granulitové facie. Tato druhá metamorfní událost je spjata s výstupem horkého plášťového magmatu, jež pronikal do rozhraní pláště a kůry díky odlomení části subdukované desky a také s pozdějšími variskými procesy.

Složení monominerálních a polyfázových inkluzí v granátech z eklogitů a klinopyroxenitů, jež tvoří polohy a budiny v granátických peridotitech moldanubické zóny, ukazuje na jejich původ těchto těles, jako na deriváty litosférického pláště nad subdukční zónou. Teplotně-tlakové podmínky, vypočítané díky zachovalé prográdní zonálnosti granátů, naznačují, že vysokoteplotní přetisk těchto hornin

v granulitové facii byl poměrně krátký, tudíž nedošlo k jejich výrazné modifikaci. Tato událost a především její krátkodobost je také zdokumentována v okolních felsických granulitech. Pravděpodobný výskyt subdukčního prostředí a části variské sutury v Českém masívu dokládají i tělesa eklogitů, jež se vyskytují v podobě 250 km dlouhého pásu táhnoucího se napříč moldanubikem od jihozápadu po severovýchod až do oblasti východních Sudet. Jejich texturní vztahy a teplotně-tlakové podmínky (600-650 °C / 2.3 GPa) nám umožňují určit, že tyto horniny prošly strmým termálním gradientem během prográdní metamorfózy. Tyto hypotézy jsou podloženy i nálezy vysokotlakých/nízkoteplotních amfibolů taramitického složení jako inkluzí v granátech.

Acknowledgements

Over the last few years many people have been involved in the creation of this thesis. Whether their contribution was material or spiritual, they all deserve my sincere gratitude. The greatest part in the successful completion of this thesis has my supervisor, Professor Shah Wali Faryad. His great benefit was material assurance and innovative approaches throughout the research. But the most important thing he put into this work was his one hundred percent approach and willingness to be assisted immediately with every problem. These newly acquired experiences will be my model in my future professional and personal life.

I thank my whole family for providing me with a great background in which I studied and worked so that I was able to complete this demanding job. Great thanks also include all colleagues and friends from the Institute of Petrology and Structural Geology at Charles University in Prague, as well as all co-authors and foreign collaborators.

Finally, I thank all the institutions that have financially supported individual parts of this project: Faculty of Science of the Charles University for providing STARS scholarship; Grant Agency of the Czech Republic (13-06958S), research projects No. MSM0021620855 and 210/10/0249, Grant Agency of Charles University (243-250373).

Poděkování

V průběhu posledních několika let se na tvorbě této práce podílelo mnoho lidí. Ať už byl jejich příspěvek hmotný či duchovní, všichni si zaslouží můj upřímný vděk. Největší podíl na zdárném dokončení této teze má můj školitel, professor Shah Wali Faryad. Jeho velkým přínosem bylo materiálové zajištění a inovativní přístupy v průběhu celého výzkumu. To nejdůležitější, co do této práce vložil, byl však jeho stoprocentní přístup a ochota být mi neprodleně nápomocen s každým problémem. Tyto nově nabyté zkušenosti mi budou vzorem v mém budoucím profesním i osobním životě.

Děkuji celé své rodině za to, že mi poskytli vynikající zázemí, ve kterém se mi studovalo a pracovalo tak, že jsem byl schopen tuto náročnou práci dokončit. Velké díky patří take všem kolegům a kamarádům z Ústavu Petrologie a Strukturní Geologie na Univerzitě Karlově v Praze a také všem spoluautorům a zahraničním spolupracovníkům.

Na závěr děkuji všem institucím, které finančně podpořili jednotlivé části tohoto projektu: Přírodovědecké fakultě Univerzity Karlovy za poskytnutí STARS stipendia; Grantové Agentuře České republiky (13-06958S), výzkumným projektům č. MSM0021620855 a 210/10/0249, Grantové Agentuře Univerzity Karlovy (243-250373).

Structure of the thesis

This thesis is presented in seven parts comprising an introduction to the topic, five chapters with the articles published in international impact factor journals, and final part of conclusions derived from this work.

The introduction (part I) is a brief invitation of the readers to the problematics in today´s research approaches in the field of petrology dealing with ultrahigh-pressure metamorphism in collision orogeny. Short presentation of the investigated study areas in the Bohemian Massif takes place here. At last, the main goals, which were dealt in the articles presented in this thesis, have been established.

The study presented in part II is focused on the formation and preservation of major and trace elements zoning in garnet porphyroblasts from felsic granulites in the Kutná Hora Complex of the Bohemian Massif. In addition to prograde zoning of major elements in garnet, the trace elements exhibit a complex core–rim distribution that is preserved as a result of the much slower diffusivities of yttrium and rare Earth elements than of other major cations in garnet. Results presented in this study bring new information about distribution features of those elements in minerals from poly-metamorphosed terranes with high-temperature granulite facies overprint.

Part III treats the prograde mineral inclusions and preservation of compositional zoning in garnets from felsic granulites and embedded layers of eclogite facies rocks in the Rychleby Mountains (East Sudetes). Garnets from both lithologies show typical bell-shaped distributions with no annular peaks near the grain rims. Investigation of major and trace elements zoning were combined with thermodynamic modelling to constrain the early eclogite facies metamorphism. Because of their significant similarities in petrography, mineral inclusions and element distribution in garnets, Rychleby granulites are correlated with other HP-UHP granulites in the Moldanubian Zone.

In the part IV, monomineral and multiphase inclusions in garnet from eclogites and clinopyroxenites, which form layers and boudins in garnet peridotites from two areas in the Moldanubian Zone of the Bohemian Massif, are presented. In addition to complex compositional zoning, garnets from hosting eclogites and clinopyroxenites

preserve inclusions of hydrous phases and alkali silicate minerals. The inclusion patterns and compositional zoning in garnet in combination with textural relations among minerals, suggest that the ultramafic and mafic bodies are derived from lithospheric mantle above the subduction zone and were transformed into garnet pyroxenites and eclogites in the subduction zone.

Part V brings new results of a petrological study of eclogites that occur together with serpentinites within amphibolite facies gneisess in the Moldanubian Zone which form ca 250 km long SW-NE trending zone in the central part of the Bohemian Massif. The presence and distribution of eclogites and comparison of their P-T and age data with HP-UHPM rocks in other units in the Bohemian Massif allow us to constrain the Variscan suture in the south-east of the Teplá-Barrandian Block.

Investigation in part VI deals with leucocratic metagabbro and amphibolite from a mafic-ultramafic body within migmatite and granulite in the Kutná Hora Complex. Phase relations of igneous and metamorphic minerals indicate that magmatic crystallization and subsequent metamorphism occurred as a result of isobaric cooling at a depth of 30–35 km. U–Pb dating on zircon from leucogabbro yielded a Variscan age that is similar or close to the age of granulite facies metamorphism in the Moldanubian Zone.

Finally, in part VII, important and valuable results extracted from the previous chapters are summarized. The conclusions about P-T conditions of the investigated rocks and its geodynamic implication are presented.

List of references cited in the text is attached at the end.

List of published articles presented in the thesis

Jedlicka, R., Faryad, S. W., Hauzenberger, C., 2015. Prograde metamorphic history of UHP granulites from the Moldanubian Zone (Bohemian Massif) revealed by major and Y+REEs zoning in garnets. *Journal of Petrology* 56, 2069-2088. **IF = 3.768**

- Authors contribution: 50 %

Jedlicka, R., Faryad, S. W., 2017. Felsic granulite with layers of eclogite facies rocks in the Bohemain Massif; did they share a common metamorphic history? *Lithos*, accepted. **IF = 3.677**

- Authors contribution: 70 %

Faryad, S. W., **Jedlicka, R.**, Ettinger, K., 2013. Subduction of lithospheric upper mantle recorded by solid phase inclusions and compositional zoning in garnet: example from the Bohemian Massif. *Gondwana Research* 23, 944-955. **IF = 8.122**

- Authors contribution: 30 %

Faryad, S. W., **Jedlicka, R.**, Collett, S., 2013. Eclogite facies rocks of the Monotonous unit, clue to Variscan suture in the Moldanubian Zone (Bohemian Massif). *Lithos* 179, 353-363. **IF = 4.482**

- Authors contribution: 30 %

Faryad, S. W., Kachlík, V., Sláma, J., **Jedlicka, R**., 2016. Coincidence of gabbro and granulite formation and their implication for Variscan HT metamorphism in the Moldanubian Zone (Bohemian Massif), example from the Kutná Hora Complex, *Lithos* 264, 56-69. **IF = 3.723**

- Authors contribution: 20 %

It is to confirm the above given partial involvement (in percentage) of Radim Jedlička in the fieldwork and sampling, responsible for the petrographic descriptions, majority of the collection of chemical data, as well as the thermobarometry and pseudosection modelling. Discussion produced by the student following detailed consultations with the supervisor.

Prof. Shah Wali Faryad (supervisor)

Table of contents

PART I

1.1. Introduction

Recent progress in the research of high- to ultrahigh-pressure (HP-UHP) metamorphic rocks, exposed along the orogenic zones on the Earth, has significantly improved our knowledge about origin, development, transportation and uplift of crustal and mantle rocks during the subduction and subsequent exhumation, and about complexity of processes in this dynamic geological environment. Description, investigation, understanding and unraveling of such high-grade rocks evolution still belong among the most challenging questions in geological research. The main problem is that the rocks usually do not preserve original composition of phases or that the original minerals, which have been stable at high pressure conditions, are no longer in equilibrium with newly adjusted conditions and they undergo breakdown reactions, recrystallization and compositional modification. It is usually due to poly-metamorphic and poly-deformation histories, where former structures are modified and previous minerals are obliterated by medium- to low-pressure assemblages. Metamorphism in low-grade (amphibolite facies) conditions in poly-metamorphic terranes usually results in the total re-equilibration of minerals and their textures formed during the preceding metamorphic processes.

To trace the original metamorphic history of the rocks prior to their exhumation/overprint, a complex and multi-disciplinary approach, involving petrological, geophysical, structural, mineralogical and geochemical methods, is needed. Two main research approaches are used in this thesis to decipher whether the rocks have been subjected to subduction or exhumed from mantle depth along the subduction channel prior to their exhumation to surface. 1) Compositional zoning of phases with a wide stability span are able to preserve growth or multiple zoning of major and even trace elements, which can be used for the reconstruction of previous metamorphic history. 2) Mineral inclusions trapped within resistant phases, which are not in equilibrium with the present chemical composition of the rock, usually bear the information about the prograde pressure-temperature (P-T) path of the rock. In combination with the thermodynamic modelling it is possible to reconstruct changes in pressure-temperature-time-composition (P-T-t-*X*) space and decrypt the probable metamorphic path in these multi-stage geological terranes.

1.2. Geological background and study areas

The Bohemian Massif is located at the eastern border of the Variscan orogenic zone in the Central Europe. It is well known for the presence of eclogite facies and UHP metamorphic rocks of felsic, mafic and ultramafic composition, that are hosted by amphibolite-granulite facies lithology. It is formed by two Blocks (the Brunovistulian and the Teplá–Barrandian) that are separated or surrounded by two Zones (the Moldanubian and the Saxothuringian). The Zones are characterized by the presence of eclogite facies and UHPM rocks that occur as lenses and boudins within amphibolite and granulite facies rocks, while the blocks are free from HP–UHPM rocks. The Moldanubian Zone occurs between the Teplá–Barrandian and Brunovistulian blocks. It is formed by medium-grade (the Monotonous and Varied units) to high-grade (the Gföhl Unit) rocks. They are intruded by Variscan granitoids with two belts of the Central Bohemian Plutonic Complex and the Moldanubian Batholith. The medium- and high-grade rocks contain lenses and blocks of eclogites and peridotites. Most granulite bodies occur along the eastern boundary of the Moldanubian Zone, but some of them are also exposed in its southwestern (the south Bohemian granulite massifs) and northern parts (the Kutná Hora Complex). The estimated P–T conditions for the high-grade rocks are in the range of 1.6–3.1 GPa and 850–1000 °C for granulites, (e.g. Carswell and O'Brien, 1993; Cooke, 2000; Faryad et al., 2010b; Kotková, 2007; Tajčmanová et al., 2006); 2–4 GPa and 800–1 000 °C for the eclogites (Faryad, 2009; Nakamura et al., 2004; Vrána and Frýda, 2003); and 3–5 GPa and 1000–1200 °C for the garnet peridotites (Faryad, 2009; Medaris et al., 2006).

The felsic granulites in the Moldanubian Zone are considered as middle or lower crustal rocks that experienced decompression and cooling from maximum pressures of 1.1–1.6 GPa at 800–1000 °C [Kotková (2007) and references therein]. Some researchers (e.g. Jakeš, 1997; Kotková and Harley, 1999) postulated their formation by crystallization from a melt at high-pressure conditions. Based on mineral inclusions, compositional zoning of garnet and P–T calculations, Faryad et al. (2010b) suggested that prograde eclogite facies metamorphism affected these rocks prior to a granulite facies overprint. This hypothesis was supported by the presence

of HP-UHP mafic and ultramafic rocks that occur within the felsic granulites. These were interpreted as fragments of upper mantle intercalated in the crustal rocks during subduction (Faryad, 2009; Medaris et al., 2006). The UHP conditions of the felsic granulite were later confirmed by the discovery of micro-diamond and coesite inclusions in garnet and zircon in the Kutná Hora Complex (Perraki and Faryad, 2014). This crystalline complex is a composite unit of stacked crustal and mantle rocks metamorphosed in amphibolite to granulite facies conditions (Faryad et al., 2010b; Nahodilová et al., 2011; Pouba et al., 1987; Vrána et al., 2006). It contains granulite and eclogite bodies, which are present also in the central and western parts of the Moldanubian Zone and form ca 200 km long belt from the Kutná Hora Complex in the north to the South Bohemian granulite massifs in the south. These findings concerning ultra-deep subduction of felsic rocks raise questions regarding the P–T trajectory during their exhumation and about the extent of granulite facies re-equilibration of these rocks. According to Perraki and Faryad (2014), the micro-diamond and coesite in the felsic granulite were formed during subduction of crustal rocks to mantle depths and the granulite facies overprint was a subsequent process that occurred after their exhumation to crustal levels (Faryad et al., 2015).

Garnet peridotites, garnet clinopyroxenites and eclogites are exposed in the eastern part of the Moldanubian Zone in Dunkelsteinerwald, where they occur within felsic granulites. The garnet peridotites are highly deformed with a platy fabric affected by late-stage serpentinization. Boudinaged layers or lenses of pyroxenites within the peridotites are relatively unaltered and preserve high-pressure garnet–clinopyroxene assemblages (Carswell, 1991). Most of them show relatively sharp contacts with the host garnet peridotites. Based on the exsolution lamellae of garnet in orthopyroxene, Carswell (1991) assumed cooling and pressure increase from 1350 °C/2.2 GPa to 1000 °C/3.3 GPa. UHP conditions for both garnet peridotites (5.5 GPa / 1100 °C) and for eclogites (5 GPa / 1000 °C) in Nové Dvory were estimated by Medaris et al. (1998) and Nakamura et al. (2004), respectively. Clinopyroxenites from this locality show exsolution lamellae of garnet in clinopyroxene and, similar to that in the Dunkelsteinerwald, a P–T path with cooling and pressure increase from 1300 °C / 2.5 GPa to 900 °C / 4 GPa was estimated (Faryad et al., 2009).

1.3. The main objectives of the thesis

The papers included in this thesis present petrological, mineralogical and geochemical study of (U)HPM rocks from different parts of the Bohemian Massif which, according to previous studies, have the potential to preserve their pre-exhumation history.

Kutná Hora felsic granulites and Rychleby granulites bear the evidence of UHP metamorphism by preservation of prograde zoning garnet. Complex distribution of major and even Y+REEs in those garnets reveal multiple zoning that belongs to garnet growth in different stages of metamorphism. Metagabbro and amphibolite body in the vicinity of those granulites is treated by petrological and geochronological study and the results are used to discuss a possible relationship between the mantle melting process and granulite facies metamorphism in the Moldanubian Zone.

Solid phase inclusions and composition of their host minerals from UHP eclogites, garnet pyroxenites and garnet peridotites are investigated to decipher the origin and metamorphic crystallization of these rocks.

The relationship of eclogite facies and UHPM rocks in the Moldanubian Zone to a possible Variscan suture in the Bohemian Massif is ascertained by investigation of pre-exhumation metamorphic history of the eclogites in the Monotonous unit (Moldanubian Zone).

The results of this work are used to discuss the main geotectonic processes during the Variscan Orogeny leading to the formation of HP-UHP rocks within the Bohemian Massif. All research materials comprising this thesis should bring new knowledge into the problematics of tracing the pre-exhumation history of high-grade metamorphic rocks in a collision orogeny.

PART II

PROGRADE METAMORPHIC HISTORY OF UHP GRANULITES FROM THE MOLDANUBIAN ZONE (BOHEMIAN MASSIF) REVEALED BY MAJOR AND Y+REES ZONING IN GARNETS

Radim Jedlička[1], Shah Wali Faryad[1], Christoph Hauzenberger[2]

[1]Institute of Petrology and Structural Geology, Charles University in Prague, Albertov 6, 12843 Prague, Czech Republic

[2]Institute of Mineralogy and Petrology, Karl-Franzens University, Universitätplatz 2, 8010, Graz, Austria

Abstract

Major and trace element distribution in garnet crystals from felsic granulites of the Kutná Hora Complex provides evidence of two metamorphic events, the first related to continental subduction at ultrahigh pressure (UHP) conditions and the second to a granulite facies overprint that occurred in mid- to lower crustal levels. To reconstruct P-T paths of both metamorphic events, pseudosection modelling was combined with major and trace element zoning in garnet. The granulites contain lenses and boudins of mantle-derived garnet peridotite and eclogite. UHP conditions are confirmed by the presence of inclusions of micro-diamond and coesite in garnet and zircon in the granulites. Compositional zoning in garnet provides evidence for a pre-granulite facies HP-UHP metamorphic history of the rocks. The two distinct metamorphic events are documented by high Y+HREE concentrations in the garnet core with annuli in the mantle part of the garnet grains. The cores of large garnets with relatively high Ca contents and bell-shaped Mn profiles suggest formation during a prograde low- to medium-temperature metamorphic event which was coeval with HP-UHP metamorphism. Decompression and cooling during exhumation of the rocks led to partial resorption of garnet and release of trace elements into the matrix. The new garnet with high Y+HREE in the annuli was formed during the granulite facies event at crustal levels.

Keywords: *granulites; prograde zoning; trace elements distribution; UHP; Y+REE*

2.1. Introduction

Metamorphism under amphibolite- to granulite facies conditions in poly-metamorphic terranes usually results in the total re-equilibration of minerals and their textures formed during the preceding metamorphic history of the rock. However, garnet, as one of the most refractory phases, may preserve growth or multiple zoning that documents previous metamorphic events (Blackburn and Navarro, 1977; Faryad, 2012; Faryad and Chakraborty, 2005; Spear, 1988). This is due to sluggish intracrystalline diffusional equilibration, where the core of garnet porphyroblasts becomes isolated from the reacting volume of rock during garnet growth. Thus it preserves important information about previous metamorphic evolution (e.g. Carlson, 1989; Chakraborty and Ganguly, 1992; Konrad-Schmolke et al., 2008a). Further constraints for multistage or polymetamorphic evolution of basement rocks can be achieved with the use of trace elements, mainly Y+rare earth elements (REE), that are highly compatible within garnet. Their compositional profiles may resist equilibration under granulite facies conditions owing to slow diffusion rates (Otamendi et al., 2002). Good subjects for testing possible preservation of original major and trace element zoning are felsic granulites in the Bohemian Massif. These granulites contain bodies of high-pressure to ultrahigh-pressure (HP–UHP) metamorphic rocks, the origin and emplacement of which within the granulite facies rocks remains uncertain (Faryad, 2011).

The felsic granulites in the Moldanubian Zone are considered as middle or lower crustal rocks that experienced decompression and cooling from maximum pressures of 1.1–1.6 GPa at 800–1000 °C [Kotková (2007) and references therein]. Some researchers (e.g. Jakeš, 1997; Kotková and Harley, 1999) postulated their formation by crystallization from a melt at high-pressure conditions. Based on mineral inclusions, compositional zoning of garnet and P–T calculations, Faryad et al. (2010b) suggested that prograde eclogite facies metamorphism affected these rocks prior to a granulite facies overprint. This hypothesis was supported by the presence of HP-UHP mafic and ultramafic rocks that occur within the felsic granulites. These were interpreted as fragments of upper mantle intercalated in the crustal rocks during subduction (Faryad, 2009; Medaris et al., 2006). The UHP conditions of the felsic

granulite were later confirmed by the discovery of micro-diamond and coesite inclusions in garnet and zircon (Perraki and Faryad, 2014). These findings concerning ultra-deep subduction of felsic rocks raise questions regarding the P–T trajectory during their exhumation and about the extent of granulite facies re-equilibration of these rocks. According to Perraki and Faryad (2014), the micro-diamond and coesite in the felsic granulite were formed during subduction of crustal rocks to mantle depths and the granulite facies overprint was a subsequent process that occurred after their exhumation to crustal levels (Faryad et al., 2015).

This study is focused on the formation and preservation of major and trace element (primarily REE) zoning in garnet porphyroblasts from felsic granulites in the Kutná Hora Complex of the Bohemian Massif. In comparison with other granulite facies rocks in the Moldanubian Zone, these felsic granulites show lower degrees of granulite facies re-equilibration (Faryad et al., 2010b). In addition to prograde zoning of major elements in garnet, the trace elements exhibit a complex core–rim distribution that is preserved as a result of the much slower diffusivities of Y+REE than for major divalent (Mg, Fe, Mn) cations (Chernoff and Carlson, 1999; Hickmott and Schimizu, 1989; Lanzirotti, 1995; Pyle and Spear, 1999). Such complex zoning could be interpreted as a result of major changes in P-T-*X* conditions or a polyphase metamorphic evolution. In the case of UHP rocks with subsequent granulite facies metamorphism, the preservation of such zoning provides important information on the relative timing of geological processes under extreme P-T conditions. The zoning patterns of major and trace elements within garnet in combination with thermodynamic modelling allow us to estimate the different stages of the P-T path during UHP and subsequent granulite facies metamorphism. The results of this work are used to discuss the main geotectonic processes during the Variscan Orogeny leading to the formation of HP-UHP rocks within the Bohemian Massif.

2.2. Geological setting

Metamorphic rocks in the Moldanubian Zone of the Bohemian Massif belong to three tectonic units, the Gföhl Unit and the Variegated and Monotonous Groups (Fig. 1a), which differ in terms of their lithologies and metamorphic conditions (Dallmeyer et al., 1995; Dawson and Carswell, 1990; Medaris et al., 1995). The Gföhl Unit contains granulite and migmatite, which exhibit generally higher metamorphic (granulite facies) conditions compared with the Variegated and Monotonous Groups (amphibolite facies conditions). All three units contain eclogite and peridotite, but garnet peridotite is known only from the Gföhl Unit, where it occurs within or adjacent to granulites and gneisses.

The high-grade metamorphic rocks of the Kutná Hora Complex are exposed in a ~50 km long NW–SE oriented belt near the town of Kutná Hora, where they structurally overlie the medium-grade paragneiss sequence of the Monotonous Group (Fig. 1b). Based on its lithology and metamorphism, the Kutná Hora Complex has been correlated with the Gföhl Unit in the eastern part of the Moldanubian Zone (Synek and Oliveriová, 1993). It consists of two superimposed thrust sheets: at the top are granulites, granulite gneisses and migmatites with amphibolized and serpentinized mafic and ultramafic rocks and calc-silicates, whereas at the bottom are micaschists with lenses of amphibolite. The largest granulite body (the Běstvina granulite) consists mainly of felsic granulites, biotite gneisses and migmatites, additionally containing several small, isolated bodies of peridotite and eclogite (Pouba et al., 1987; Synek and Oliveriová, 1993; Vrána et al., 2005). It is exposed in the eastern part of the Kutná Hora Complex at the boundary with the Monotonous Group (Fig. 1c). The Monotonous Group beneath the Kutná Hora Complex is represented by partly migmatized kyanite/sillimanite + biotite + muscovite ± cordierite paragneiss. At the contact with the micaschist zone, paragneiss from the Monotonous Group encloses several bodies of serpentinized peridotite, eclogite and garnet amphibolite (Synek and Oliveriová, 1993). Controversy exists about the pressure conditions of the Kutná Hora granulites. According to Vrána et al. (2005) and Nahodilová et al. (2014), the felsic granulites reached a maximum pressure of 2.3 GPa at 850–900 °C.

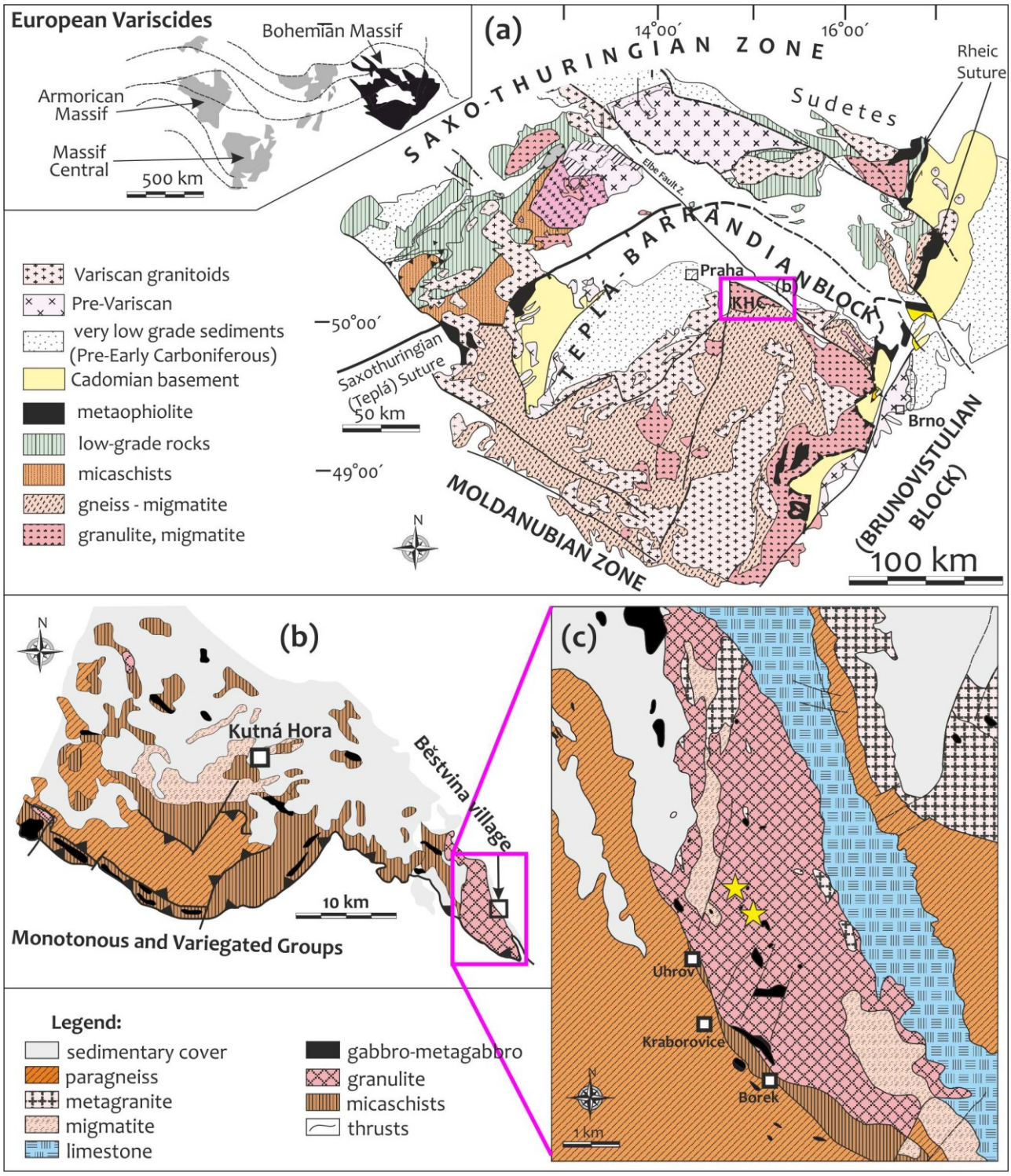

Fig. 1. (a) simplified map of the Bohemian Massif after Franke (2000), Willner et al. (2002), Cháb et al. (2007), Faryad and Kachlík (2013); (b) map of the Kutná Hora Complex, simplified after Synek and Oliveriová (1993); (c) detail of the studied area of the Běstvina granulite, modified after Faryad et al. (2009). Stars indicate sample locations.

However, a UHP prograde P–T path and UHP conditions, similar to the hosted mafic and ultramafic bodies, were postulated by Faryad et al. (2010b).

The samples selected for this study come from the central part of the Běstvina granulite body where lenses of garnet peridotite with eclogite and garnet pyroxenite are exposed. They are from the same outcrop in which micro-diamond and coesite inclusions in garnet and zircon were identified (Perraki and Faryad, 2014). In contrast to other parts of the granulite body, which are characterized by light-colored banding parallel to a weak foliation, here the granulite has a mostly massive, medium-grained appearance.

2.3. Petrography and textural relations

The detailed petrography and textural relations of the Kutná Hora basement rocks, mainly of the Běstvina granulite body, have been discussed by Vrána et al. (2005), Faryad et al. (2010b) and Nahodilová et al. (2011). Two varieties of granulite are present. The most common is a fine- to medium- grained felsic variety with weak foliation highlighted by modal layering of 2–5 cm thick quartzo-feldspathic (leucocratic) layers alternating with garnet-rich (mesocratic) layers [Faryad et al., (2009), Fig. 2a]. Rarely, they may contain lenses (about 3 m in size) of a dark, intermediate variety with porphyroblasts of garnet in a weakly foliated or unfoliated matrix. The two varieties show continuous gradation into one other. The leucocratic layers in the felsic granulite are interpreted as the result of partial dehydration melting during granulite facies metamorphism. The felsic granulite consists of ternary feldspar, quartz, garnet, kyanite, and rutile (Fig. 2b and c). Rarely, inclusions of Ti-phengite are found in garnet (Faryad et al., 2010b). Compared with other felsic granulites in the Moldanubian Zone, kyanite is not replaced by sillimanite or spinel. The presence of biotite depends on the degree of retrogression and/or amphibolite facies overprint.

The samples selected for this study come from the felsic variety of granulite with small amounts of biotite. They include both a mesocratic layer (Fig. 2a and b) with lower silica content (sample RJ34-13) and a leucocratic layer (sample F103-10, Fig. 2c) with higher silica content but lower CaO content. Sample F103-10 has a high

content of quartz that occurs along thin layers with K-feldspar. Garnet and K-feldspar may form ~1 mm sized grains in the fine-grained matrix. Garnet usually contains inclusions of quartz, kyanite, K-feldspar, antiperthitic plagioclase, rutile and rarely phengite (Faryad et al., 2010b). Some garnets have reaction coronas formed by biotite and plagioclase. Small garnet grains are partly chloritized. K-feldspar is usually perthitic (Fig. 3c) but antiperthitic feldspar is also present. Large kyanite grains are rimmed by plagioclase coronas and may contain inclusions of quartz. Apatite is a common accessory phase, which mostly occurs in the matrix at contacts with garnet grains (Fig. 3a) or rarely forms inclusions within garnet (Fig. 3b) or biotite. The apatite may contain exsolution lamellae of monazite. Separate monazite crystals can also be found in contact with apatite crystals (Fig. 3a). Polyphase inclusions (phengite+biotite) pseudomorphic after Ti-phengite were observed (Fig. 3d). Rare tabular-shaped graphite inclusions in garnet were also identified (Fig. 3e).

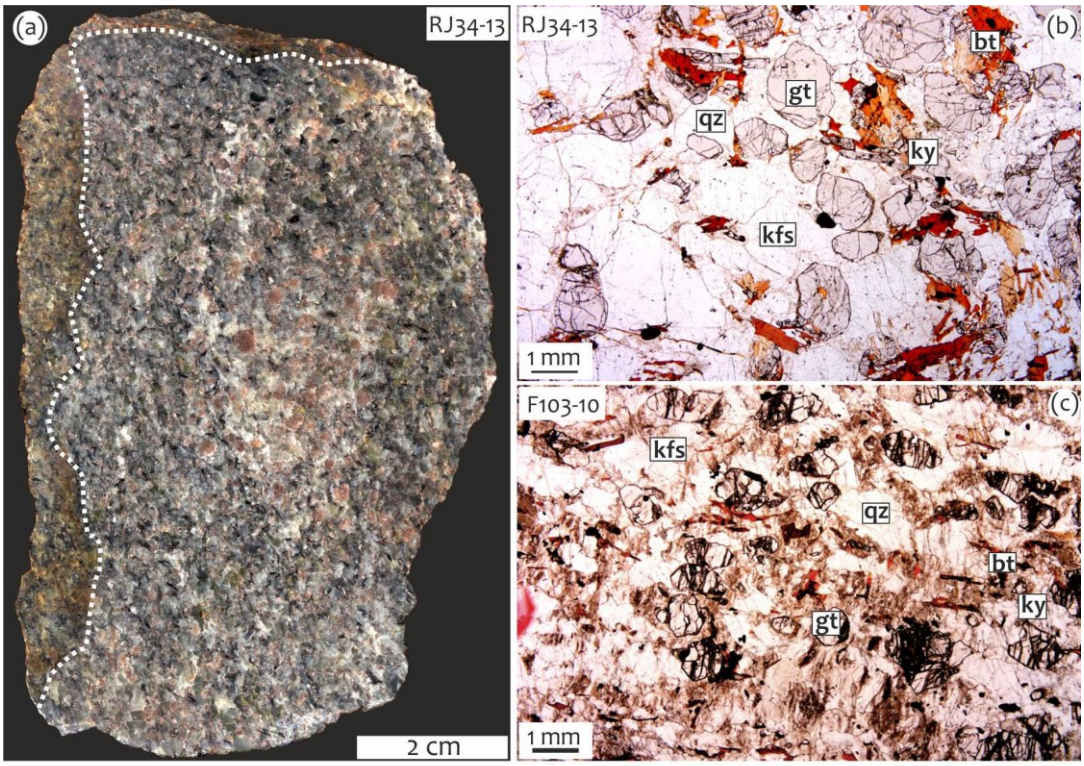

Fig. 2. (a) hand-specimen photograph of a mesocratic layer of granulite with reddish garnet and dark biotite in the quartz+feldspar matrix; Běstvina granulite body (sample RJ34-13). Dotted line separates zone of weathering from fresh part of the sample; (b) photomicrograph of the mesocratic layer RJ34-13; (c) photomicrograph of leucocratic layer F103-10. Abbreviations as in the main text.

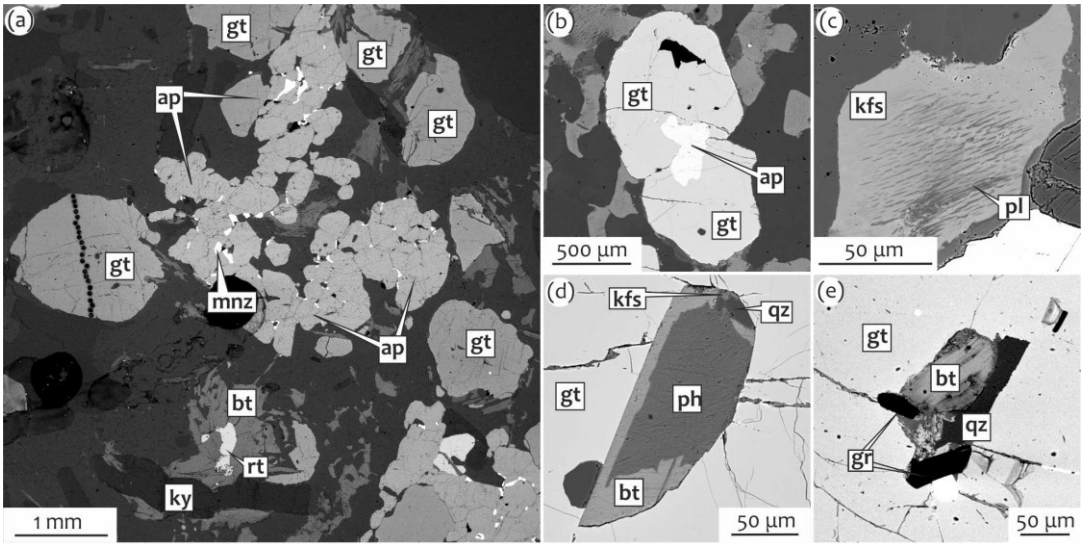

Fig. 3. Back-scattered electron images of felsic granulites. (a) apatite with monazite in matrix (RJ34-13); (b) apatite between two garnet grains (F103-10); (c) perthitic feldspar in matrix (F103-10B); (d) polyphase inclusion after former Ti-rich phengite (F103-10); (e) graphite [gr] inclusions in garnet (F95-10).

2.4. Analytical methods

Bulk-rock major and trace element concentrations were determined by wet chemical analysis and inductively coupled plasma-mass spectrometry (ICP-MS) using a Thermo X-Series II system, respectively, in the Geological Laboratory at Charles University in Prague. Trace elements were determined using a modified total digestion in mineral acids ($HF+HClO_4$) and borate fusion ($Na_2CO_3+Na_2B_4O_7$) technique followed by conventional solution nebulization using a Thermo X-series II ICP-MS system. The ICP-MS analytical procedure and calibration have been described by Strnad et al. (2005). The analytical precision, calculated as one relative standard deviation (RSD), ranged from 0.5 to 5% for most elements. The QA/QC (quality assurance/quality control) was controlled using the AGV-2 and BCR-2 (USGS) reference materials.

Mineral analyses and compositional maps of major elements in garnet were determined by energy-dispersive X-ray analysis using a Vega Tescan scanning electron microscope at Charles University. Analytical conditions include an accelerating potential of 15 kV and a beam current of 800 pA.

For chemical analyses of minerals and variations of elements along garnet profiles a JEOL 6310 scanning electron microscope was used at the Institut für Erdwissenschaften, Karl-Franzens Universität, Graz, Austria, equipped with wavelength- and energy- dispersive spectrometers (WDS and EDS). Standards were garnet (Fe, Mg), adularia (K, Si, Al), rhodonite (Mn), jadeite (Na, WDS), and titanite (Ti, Ca). Sodium content was measured by WDS at conditions of 15 kV and 6 nA on PCD (probe current detector).

Trace element and REE concentrations in garnet were analyzed with a laser ablation (LA)-ICP-MS system (ESI New Wave 193 nm LA system coupled with an Agilent 7500cx ICP-MS system) at the Central Laboratory for Water, Minerals and Rocks, NAWI Graz, Karl-Franzens University Graz and Graz University of Technology, Austria. The material was ablated using a 193 nm laser pulsed at 8 Hz with a 35 lm spot size and energy of 6.5 $J*cm^{-2}$. Helium was used as the carrier gas at a flow rate of 0.7 $liters*min^{-1}$ and data were acquired in time-resolved mode. For each analysis a 30 s gas blank was obtained for background correction. The laser was active for 50 s followed by 45 s washout. The NIST612 standard glass was routinely analyzed

for standardization and to correct for drift, and standard NIST614 and USGS reference material (BCR-2G) were analyzed as unknowns to monitor the accuracy of the measurements. Counting statistics and reproducibility were usually better than 5% relative. However, taking uncertainties in reference material concentrations, elemental mass fractionation and instrumental drift into account, we estimate that the analytical uncertainty may be as much as 10% relative. Results from repeated NIST614 as well as BCR-2G measurements confirmed a reproducibility within ±10% of the reported values. Although the NIST612 reference material and the analyzed garnet contain a silicate-dominated matrix, some analytical uncertainties may arise from matrix effects. To test for matrix effects, the basaltic glass reference material BCR-2G, which contains a significantly different major element matrix, was analyzed. Because the obtained trace element and REE concentrations could be reproduced within the given uncertainties we concluded that matrix effects can be neglected. Data reduction was done using the Glitter software. For NIST612 the concentration values reported by Jochum et al. (2011) were used.

Additional microprobe analyses and X-ray maps of garnets were obtained on the JEOL JXA-8200 at the Eugen F. Stumpfl electron microprobe laboratory of the Universitätszentrum Angewandte Geowissenschaften (UZAG) Steiermark at Montanuniversität, Leoben. The conditions of operation were 15 kV with a 10 nA beam current for analyses and 150 nA for element mapping. Element maps were also acquired on a Cameca SX100 electron microprobe in wavelength-dispersive mode at the Masaryk University in Brno, Czech Republic. Intensities of characteristic X-rays of Ca (Kα), Ti (Kα), P (Kα), Cr (Kα) and Y (Lα) as well as one background for each line were collected at the following conditions: 20 kV, 200 nA, 1 mm beam diameter, 5-8 mm step (depending on the garnet size), and 0.8 s dwell time. The background intensities were subtracted from the characteristic X-ray intensities prior to graphic processing.

Mineral abbreviations in the text, figures and figure captions are those of Whitney and Evans (2010), except garnet, which is abbreviated as gt. Garnet end-members are Alm = Fe^{2+} / (Fe^{2+} + Mg + Ca + Mn), Grs = Ca / (Fe^{2+} + Mg + Ca + Mn), Prp = Mg / (Fe^{2+} + Mg + Ca + Mn) and Sps = Mn / (Fe^{2+} + Mg + Ca + Mn), and X_{Fe} = Fe^{2+} / (Fe^{2+} + Mg).

2.5. Bulk-rock compositions

Bulk-rock SiO_2 contents are 60.3 wt % (RJ34-13) and 71.6 wt % (F103-10). Sample F103-10 has lower Al_2O_3, FeO_t, MgO, CaO and TiO_2, but a higher K_2O content. Both samples have similar Na_2O contents (about 2 wt %) and MnO is below <0.12 wt %. Both of the samples were additionally analyzed for their trace element chemistry, the mesocratic sample recording higher concentrations of REE than the leucocratic sample (Table 1).

Table 1: Whole-rock major and trace elements compositions

Sample	RJ34-13	F103-10	Sample	RJ34-13	F103-10
chemical compositions (wt % oxides)			*in ppm*		
SiO_2	60.31	71.58	Rb	31.17	55.09
TiO_2	1.05	0.34	Sr	95.49	75.12
Al_2O_3	17.41	13.67	Y	53.30	5.20
Fe_2O_3	1.75	0.76	Zr	115.99	14.20
FeO	6.35	3.36	Nb	16.25	2.10
MnO	0.12	0.10	Ba	366.84	266.53
MgO	3.19	1.78	La	79.48	1.94
CaO	3.62	2.26	Ce	204.44	5.25
Na_2O	2.19	2.04	Pr	27.89	0.77
K_2O	1.34	4.06	Nd	117.00	3.95
P_2O_5	1.06	0.07	Sm	26.73	1.32
CO_2	0.60	0.40	Eu	3.67	0.26
			Gd	21.61	1.41
Total	98.99	99.42	Tb	2.57	0.22
			Dy	11.39	1.90
X_{Fe}	0.67	0.65	Ho	1.93	0.19
			Er	5.47	0.54
modal proportions (%)			Tm	0.73	0.08
Qz	28	46	Yb	4.87	0.55
Fsp	42	31	Lu	0.70	0.07
Gt	15	10	Hf	3.78	0.54
Bt	10	7	Pb	29.16	0.19
Ky	3	3	Th	4.79	<0.25
Accesory phases	2	3	U	2.27	0.04

2.6. Compositional zoning in garnet

2.6.1. Major elements

Garnets from both the mesocratic and leucocratic layers of the felsic granulite show strong compositional zoning, differing from each other in terms of grossular and almandine contents [$Grs_{9–20}$ $Alm_{49–57}$ $Prp_{29–36}$ $Sps_{0–21}$ (sample RJ34-13) and $Grs_{18–34}$ $Alm_{39–46}$ $Prp_{16–38}$ $Sps_{1–22}$ (F103-10)]. Although the bulk-rock composition of the mesocratic layer (RJ34-13) shows higher values of all four oxides (FeO, MgO, CaO, MnO; Table 1), the differing garnet compositions reflect the lower value of X_{Ca} = Ca / (Ca + Fe^{2+} + Mg + Mn) = 0.27 and higher X_{Fe} = 0.48 in this sample compared with that in the leucocratic layer (X_{Ca} = 0.30, X_{Fe} = 0.45). Clear prograde garnet zoning is documented by the higher spessartine content in the core of the garnet from the leucocratic sample (Fig. 4d and f). The pyrope, grossular and almandine zoning patterns are complex with at least two segments, which correspond to the core and mantle–rim sections (see below).

In sample RJ34-13 (Fig. 4a and b), grossular content decreases from the core (Grs = 20 mol %) towards the rim, with a weak annular minimum (17 mol %) followed by an increase to 18 mol % and finally a significant decrease at the rim. The pyrope content shows an opposite trend with a less variable compositional profile than grossular. The lowest pyrope value (29 mol %) is recorded in the core with a slight increase (the first maximum at 31 mol %) and then a decrease that is followed by another increase at the rim of the grain. Almandine content has a similar trend to pyrope. The almandine content is lowest in the core (49 mol %) and increases towards the rim. Spessartine content is low and reveals no zonation from core to rim.

Two grains from sample F103-10 (Fig. 4c and e) show similar Ca distribution to that in sample RJ34-13, but with more pronounced zonation. Strong compositional zoning occurs in the larger grain (Fig. 4f) with maximum grossular content of 34 mol % in the core and about 20 mol % in the rim. The rimward decrease in grossular is asymmetrical; it is steep on the left side but relatively flat on the right side, where it shows a slight increase at the rim. Spessartine and almandine also show a rimward

decrease; a slight increase in spessartine at the rim may indicate back-diffusion owing to garnet consumption (Chakraborty and Ganguly, 1992; Kohn and Spear, 2000). Variations in all three constituents are compensated for by pyrope, which has the lowest value of 16 mol % in the core and contents reaching about 39 mol % at the rim. In addition to relatively weaker zoning, the garnet grain in Fig. 4d differs from that in Fig. 4f by comparatively lower grossular and spessartine and higher pyrope contents in the core.

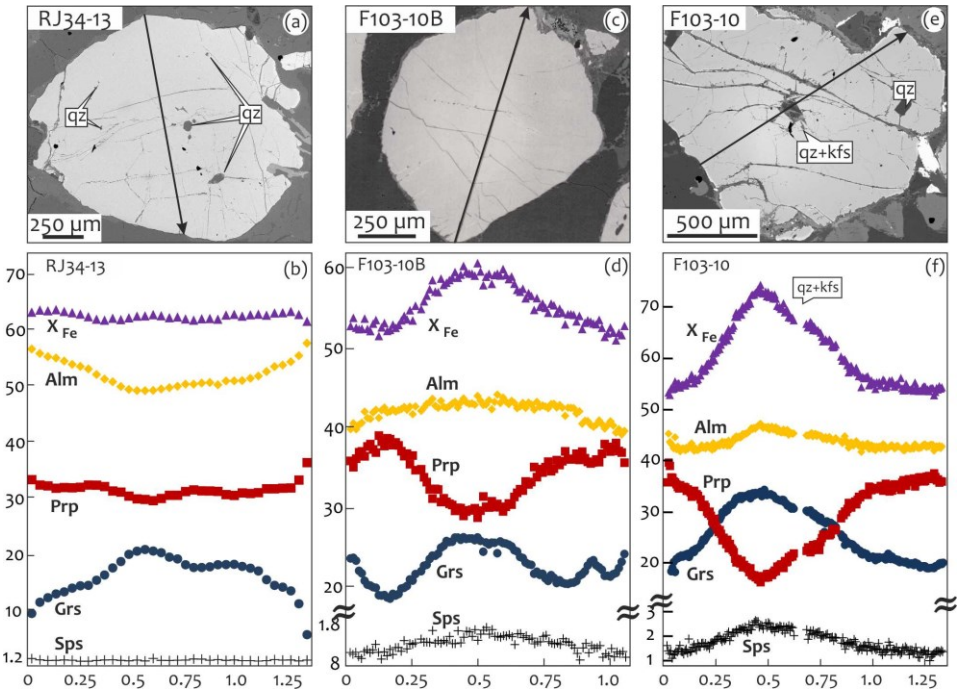

Fig. 4. Back-scattered electron images and major element profiles (rim-core-rim) of the selected garnets from mesocratic granulite RJ34-13 (a, b) and leucocratic granulite F103-10 (c-f). *y*-axes indicate molar percent; *x*-axes of profiles are rim-core-rim distances in millimetres.

2.6.2. Trace elements

To compare the major and trace element zoning in garnet, analyses were obtained along the same garnet profiles from samples RJ34-13 and F103-10 (Figs 4–6; supplementary data are available at www.petrology.oxfordjournals.org). Garnets from both samples display core to rim zonation of Y, Ti, Cr, V and of heavy REE

(HREE; Er, Tm, Yb, Lu), middle REE (MREE; Gd, Tb, Dy, Ho) and light REE (LREE; Nd, Sm, Eu) (Figs 5 and 6). Yttrium and most REE show two maxima, the first in the core section (segment I), which is probably related to nucleation of garnet, and the second in the mantle–rim section (segment II), suggesting a dramatic change in P-T-*X* conditions during garnet crystallization.

Garnet from sample RJ34-13 shows a bell-shaped distribution of Y, HREE, MREE and LREE contents (Fig. 5). Ti shows a high concentration in the core with a decrease towards the border of the core part and second maxima and a subsequent decrease towards the rim (Fig. 5b and f). Vanadium does not show clear zoning at the boundaries of segments I and II, but it generally increases towards the rim (Fig. 5h). The most pronounced zoning is in Y+HREE. After a decrease to a local minimum, all elements start to increase again and reach a second maximum. The second maximum actually shows higher values than in the core of the garnet crystal. The final part of the distribution profile is characterized by a decrease of all elements towards the rim of garnet. Some MREE (Gd, Tb, Dy) show a slight increase at the outermost rim of the garnet (Fig. 5m-o).

Phosphorus content reveals multiple zoning features (Fig. 5d). In addition to high P contents along the rim of the garnet (ring shape), concentric zoning with slightly elevated P content is present in the core. In contrast to the irregular shape of the ring, the core zoning seems to follow the crystallographic planes of the garnet. Three patchy domains with a relatively high P content can also be observed in the mantle part of the garnet grain.

Trace element zoning patterns in sample F103-10 are similar to those in RJ34-10, but the central peak is not clearly visible. However, the second peak of Y+HREE is clear (Fig. 6). Y, Ti, Cr and V increase from the core to the annular maxima. Ti and V reach this point closer to the core (Fig. 6f and g). From the annular maxima, values for all these elements (except vanadium) decrease towards the rim of the garnet. HREE and the heaviest of the MREE (Dy, Ho) increase from the core to the annular maxima. Gd, Tb and LREE have maxima at the garnet core and decrease continuously towards the rim. After reaching the annular maxima, most elements show a significant drop towards the rim. P concentration is low in the garnet core, but high at the outermost rim (Fig. 6d).

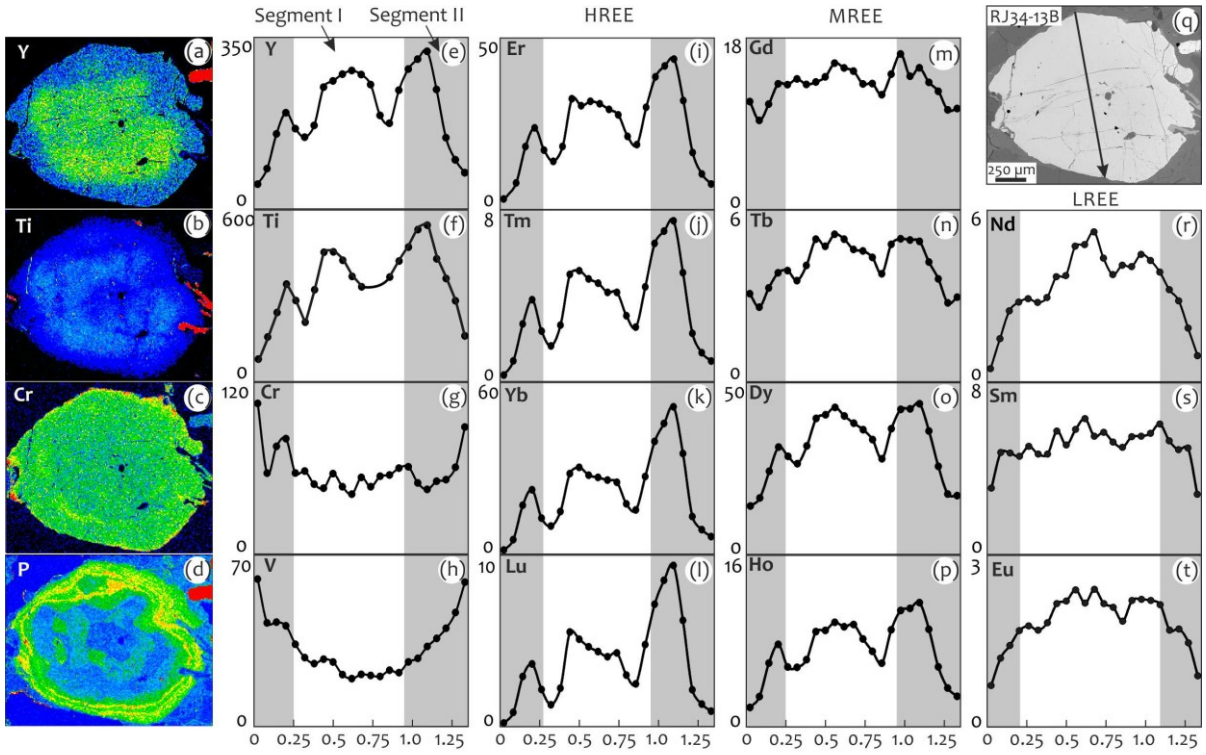

Fig. 5. Garnet from mesocratic layer in granulite RJ34-13; trace element compositional maps of Y, Ti, Cr, P (a-d) and trace element profiles (e-t). Segments I and II are referred to HP-UHP and granulite facies garnet, respectively (for details see text).

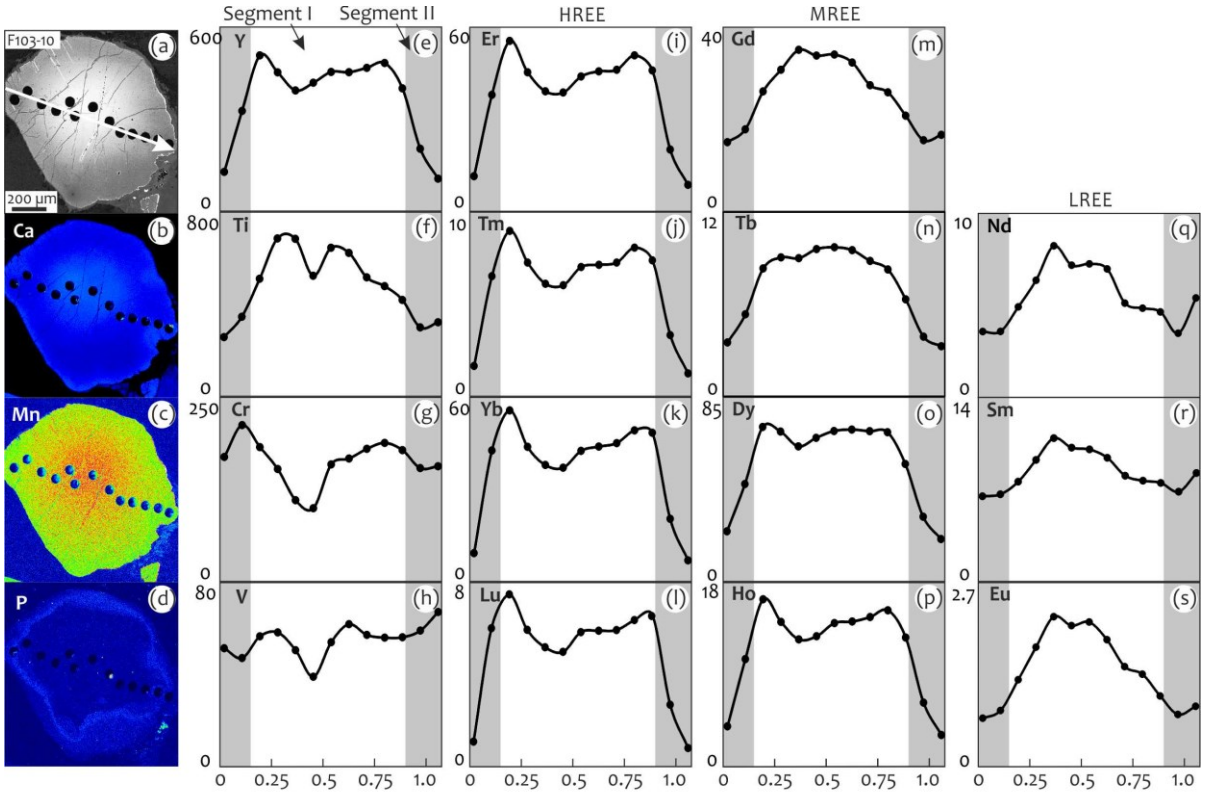

Fig. 6. Garnet from leucocratic layer in granulite F103-10; back-scattered image (a), compositional maps of Ca, Mn and P (b-d) and trace element profiles (e-s) are shown. Segments I and II are as in Fig. 5.

2.7. Pressure-Temperature calculations

To constrain the P–T path for the Kutná Hora felsic granulites, the following points need to be considered: (1) the rocks preserve garnet with prograde zoning; (2) they experienced UHP conditions in the coesite and micro-diamond stability fields (Perraki and Faryad, 2014); (3) they passed through a granulite facies overprint at about 850-900 °C (Nahodilová et al., 2011). Therefore, pseudosection modelling combined with conventional thermobarometry was used to estimate the P-T conditions and trajectory for the HP–UHP event and subsequent granulite facies overprint. It should be noted that a number of uncertainties in the estimated P-T conditions are associated with this approach, owing to the absence of precisely determined thermodynamic data for minerals at such high temperature and pressure conditions and possible modification of garnet composition. However, this approach helps to trace the possible P–T path during the prograde stage of garnet formation and during the granulite facies overprint.

2.7.1. Pseudosection modelling

The pseudosection method was used to decipher the changes in the mineral assemblage and modal volume of garnet in the P-T ranges 400-800 °C and 0.4-4 GPa, and 600-1000 °C and 0.5-2.5 GPa, respectively (Figs 7 and 8). The calculation was performed in the system SiO_2-TiO_2-Al_2O_3-FeO-MgO-CaO-MnO-Na_2O-K_2O-H_2O (KNMnCFMASHT) by Gibbs energy minimization using the computer program Perple_X 6.6.8 (Connolly, 2005) with the internally consistent thermodynamic dataset for mineral end-members and aqueous fluids of Holland and Powell (1998), upgraded in 2004. The following non-ideal solution models were used: garnet (Holland and Powell, 1998), phengite (Coggon and Holland, 2002), biotite (Powell and Holland, 1999), plagioclase (Newton et al., 1980), feldspar (Benisek et al., 2010), omphacite (Holland and Powell, 1996), clinopyroxene (Holland and Powell, 1996), chlorite (Holland et al., 1998) and melt (Holland and Powell, 2001). The effect of ferric iron was explored by adding oxygen as an additional component to the system. Addition of up to 0.08 wt % O_2 leads to the stability of magnetite, but has no significant effects

on omphacite, garnet or biotite equilibria. Considering granite as a potential source material for transformation into felsic granulite (Janoušek et al., 2004), an initial water content of about 0.8 wt % for the low-temperature part of the pseudosection was selected. This water content was calculated based on the approximate mica content in granite [following the method adapted from Proyer (2003)]. To analyze possible P-T conditions for the formation of the garnet core, sample F103-10 with pronounced compositional zoning and high grossular content in garnet was chosen. Because of its slow diffusion coefficients, Ca has a significant effect in preventing the overall compositional modification of garnet through multicomponent diffusion with other divalent cations (Chakraborty and Ganguly, 1992). This is demonstrated by the preserved bell-shaped Mn (Sps) distribution in the garnet core (Fig. 4f). Figure 7a shows the calculated pseudosection, where garnet is stable in all fields in the selected P-T range. Except for sodic clinopyroxene, all phases (including phengite as inclusions in garnet) were observed in the rock. The lack of sodic clinopyroxene in HP felsic granulites was discussed by Faryad et al. (2010b). Based on phase relations in felsic granulite and inclusion patterns in garnet, Faryad et al. (2010b) showed that breakdown of sodic clinopyroxene, which was once in equilibrium with the host Ca-rich garnet, must have occurred relatively early in favor of sodic plagioclase. In contrast, in intermediate rocks the transition to a plagioclase-bearing assemblage occurs at lower pressures, and in very Ca-rich protoliths diopside-rich clinopyroxene coexists with calcic plagioclase and Ca-depleted garnet.

Based on the calculated volume isopleths of garnet in sample F103-10, most garnet (about 5-6 vol. %) was formed below 1 GPa and a subsequent increase to 9 vol. % occurred in the coesite stability field above 3 GPa (Fig. 7a). The high grossular content (34 mol %), measured in the garnet core of sample F103-10 (Fig. 4f), is near the maximum value (36 mol %, Fig. 7b) that was modelled for this sample. This suggests garnet nucleation at a temperature of about 400 °C and pressure of 0.4 GPa [field (1) in Fig. 7b]. Based on the compositional isopleths in garnet, the grossular content in the garnet core was not strongly modified. On the other hand, the corresponding X_{Fe} values for the core were changed by almost 20 % from 91 % (based on the pseudosection, Fig. 7b) to 73 % (measured value in Fig. 4f) in the same

field (1). If we consider that the composition profiles of garnet at the interface between core and mantle–rim parts signify the UHP stage, the grossular isopleth with 22-25 mol % (Fig. 4f) yields temperatures of 650-750 °C in the coesite or even diamond stability field [field (2) in Fig. 7b]. The corresponding X_{Fe} value of about 55-57 % in the measured profile (Fig. 4f) and 70-72 % in the calculated isopleths means about 20 % decrease of X_{Fe} owing to diffusion. However, as the rocks reached the diamond stability field, the measured grossular content should be modified through diffusion by at least 2–3 mol % at the interface between core and mantle-rim parts of the garnet (Fig. 7a).

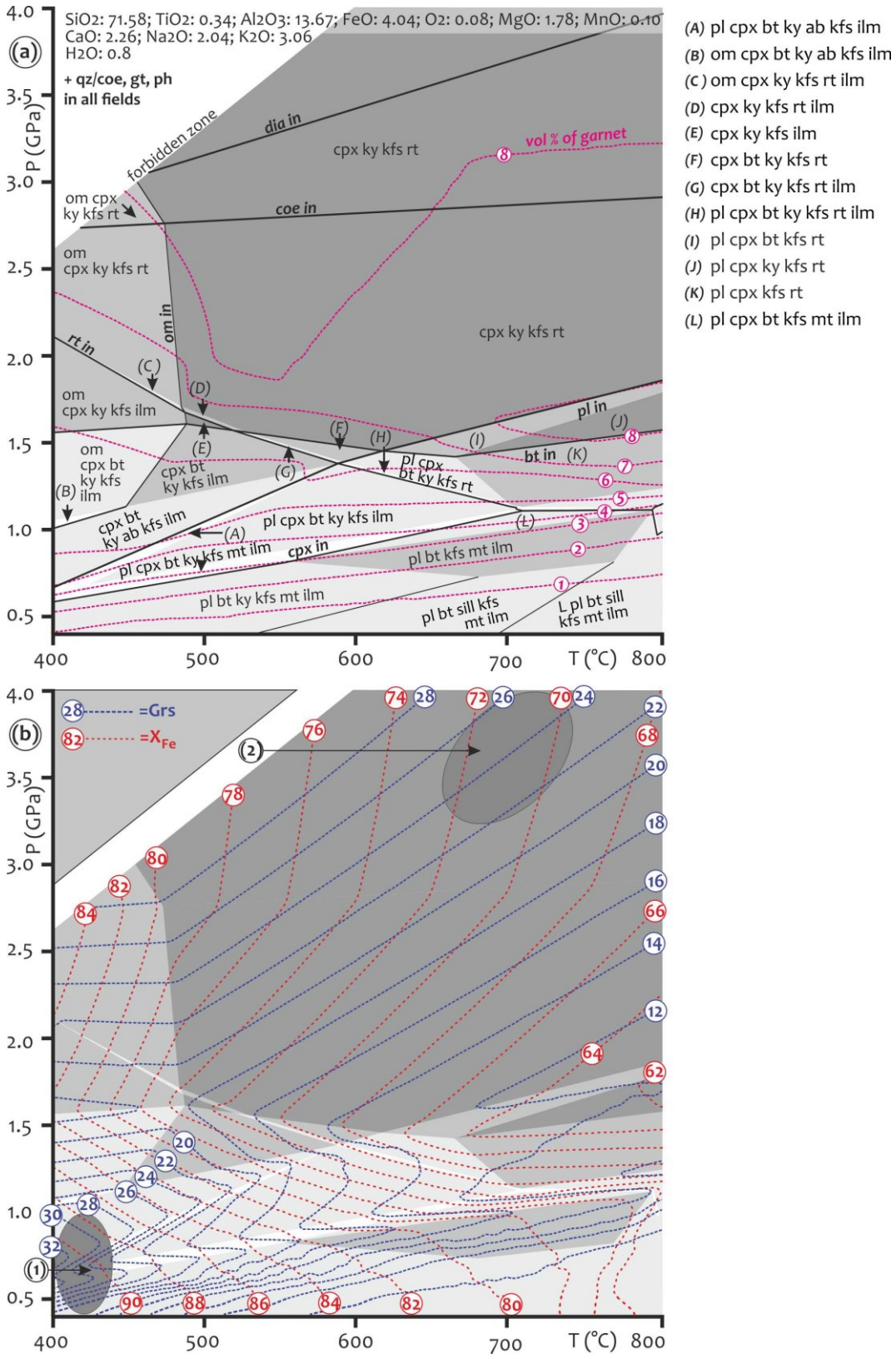

Fig. 7. Low-temperature P-T pseudosection for a felsic layer in the Kutná Hora granulite (F103-10): (a) shows fields of stable mineral assemblage; (b) shows grossular and X_{Fe} isopleths. In (a) bold lines show in-reactions of index minerals and dotted lines indicate modal volume percent of garnet. Labels for small P-T fields are omitted for clarity.

Figure 8a shows the pseudosection calculated for the granulite facies stage (sample F103-10). A water content of 0.33 wt % was determined for the high-temperature stage based on maximum modal content of biotite (up to 5%) in well-preserved (non-retrogressed) samples. The low water content is due to metamorphic dehydration reactions during temperature increase. However, there is some uncertainty in the calculation of P–T conditions for the granulite facies event, as some material is isolated within already crystallized garnet during the HP stage and does not participate in the subsequent metamorphic reactions. Therefore, the core composition of garnet (segment I in Fig. 6) was subtracted from the bulk-rock composition in sample F103-10. The effective bulk composition, used for the pseudosection in Fig. 8a, was calculated by integration of the mineral mode (segment I in Fig. 6) and contents of each element in the microprobe analyses (Konrad-Schmolke et al., 2008a; Stüwe, 1997).

The garnet volume isopleths indicate that most garnet was formed during heating from 800 °C upwards or during a pressure increase above 1 GPa. Assuming that the granulite facies event occurred after exhumation of the rocks to lower-middle crustal levels, about 5 vol. % of garnet should have formed in sample F103-10 during the granulite facies stage at 850–900 °C, as estimated based on thermobarometric calculations for granulites from this locality (Nahodilová et al., 2011, 2014). However, the grossular content of 16–20 mol % in the mantle part of garnet (Fig. 4d and f) indicates a temperature of about 700 °C (Fig. 8b). Further increase of temperature is documented by a decrease of X_{Fe} and Grs (Fig. 4f). The slight increase of Ca and decrease of Mg in the outer rim of garnet (Fig. 4f) could be due to diffusion modification during cooling, as can be postulated from the back-diffusion of Mn.

With increasing temperature, dehydration of phengitic muscovite occurs and melt is produced (Fig. 8a and b). At low pressures, kyanite transforms to sillimanite and rutile changes to ilmenite. Radical change in the chemistry of garnet occurs during temperature increase and pressure decrease owing to the breakdown of pyroxene and creation of plagioclase at the expense of garnet. At high temperatures, only limited amounts of garnet are formed, but significant modification of elemental concentrations occurs at the outermost edge of the garnet crystals in a short time interval (Faryad and Chakraborty, 2005). During cooling and retrogression, newly formed biotite has a significant influence on magnesium and iron diffusion in garnet.

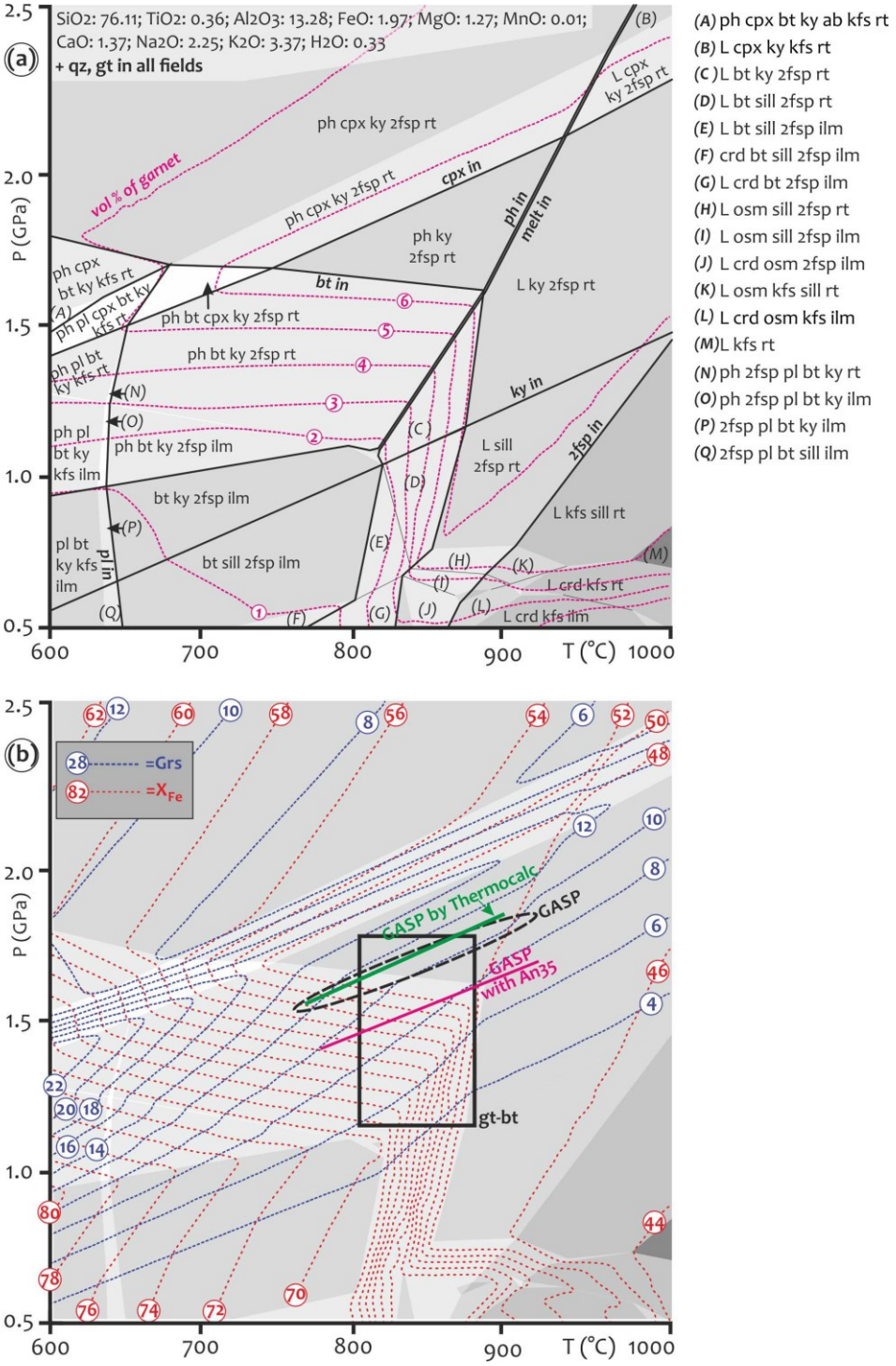

Fig. 8. High temperature P-T pseudosection for a felsic layer in the Kutná Hora granulite (F103-10). (a) shows fields of stable mineral assemblage. Labels for small P-T fields are omitted for clarity. Bold lines show in-reactions of index minerals, dotted lines indicate modal volume percent of garnet (b) shows grossular and X_{Fe} isopleths. Bold rectangle and dashed ellipse indicate temperature range based on garnet-biotite thermometry [calibrations of Bhattacharya et al. (1992); Holdaway (2000)] and GASP barometry [calibrations of Hodges and Spear (1982); Ganguly and Saxena (1984)], respectively (Table 2). Bold lines show pressures obtained by GASP barometry with plagioclase composition An_{35} calculated from pseudosection and GASP barometry using Thermocalc, respectively.

2.7.2. Conventional thermobarometry

Except for kyanite, garnet cores and rutile, all the minerals formed during the HP-UHP event underwent recrystallization during the granulite facies overprint. Therefore, biotite, plagioclase and garnet rims were used to estimate the P–T conditions for the granulite facies event. Based on the pseudosection modelling (Fig. 8a), biotite forms during cooling at about 850 °C. Plagioclase is stable and based on the pseudosection calculations a ternary Na–Ca plagioclase with composition of An_{35} can be stable at 850–900 °C and 1.5– 1.8 GPa. However, most analyzed plagioclase in the matrix of the studied samples is An_{22-23}. The lower anorthite content, consistent with the increase of Grs and decrease of Prp and X_{Fe} at garnet rims (Fig. 4d), suggests that garnet was partly formed during cooling. The garnet-biotite thermometer, used for the high-Mg and low-Ca rim in sample F103-10, yields temperatures in the range 750–900 °C (Table 2). The lowest temperature of 744±29 °C was obtained using the calibration of Perchuk and Lavrent'eva (1983) and the highest temperature of 907±83 °C by using that of Dasgupta et al. (1991). Temperatures calculated using Bhattacharya et al. (1992) and Holdaway (2000) are close to the biotite-in boundary obtained from the pseudosection modelling. GASP barometry used for the analyzed plagioclase (An_{22}) and garnet with the lowest Ca content yielded pressures of 1.6–1.7 GPa at 850 °C. Lower pressures of 1.4–1.5 GPa can be obtained using a plagioclase composition (An_{35}) based on the pseudosection calculation. Similar temperatures of 850 °C and pressures of 1.76±0.02 GPa (Table 2) were obtained by calculation of average P–T using the Thermocalc 3.37 package (Powell et al., 1998; most recent upgrade) and the thermodynamic dataset 5.5 (Holland and Powell, 1998).

Tab. 2: **Representative chemical analyses used for conventional thermobarometry**

Sample: F103-10						
mineral	gt1	gt2	gt3	bt1	bt2	pl
SiO_2 *(wt. %)*	39.05	39.08	39.15	38.66	37.64	62.64
TiO_2	0.07	0.03	0.05	4.93	4.95	0.01
Al_2O_3	22.72	21.85	21.89	17.31	15.18	23.16
FeO	19.70	20.50	21.14	8.68	10.47	-
MnO	0.54	0.60	0.70	0.06	0.05	-
MgO	10.45	9.72	10.27	15.81	15.34	-
CaO	7.05	7.10	6.52	0.08	0.07	4.65
Na_2O	-	0.03	0.06	0.19	0.09	9.05
K_2O	0.03	-	0.02	9.90	9.69	0.08
Total	99.58	98.91	99.80	95.86	94.51	99.47
Si *(per ox.)*	2.95	2.99	2.96	2.90	2.90	2.78
Ti	0.003	0.001	0.003	0.28	0.28	-
Al	2.02	1.96	1.95	1.52	1.38	1.21
Fe	1.17	1.25	1.21	0.54	0.68	-
Mn	0.03	0.04	0.04	0.003	0.003	-
Mg	1.18	1.11	1.16	1.77	1.76	-
Ca	0.57	0.58	0.52	0.006	0.006	0.22
Na	-	-	-	0.03	0.01	078
K	-	-	-	0.95	0.95	-

Temperatures calculated at 1.4 GPa

in °C	gt1-bt1	gt2-bt1	gt3-bt1	gt1-bt2	gt2-bt2	gt3-bt2	average
B92	783	745	761	858	811	832	798 ± 50
Dasg91	865	807	832	1003	949	983	906 ± 88
PL83	728	715	716	785	751	771	744 ± 31
H2000	923	823	881	923	823	881	875 ± 45

Pressures calculated at 850 °C

in GPa	gt1-bt1	gt2-bt1	gt3-bt1	gt1-bt2	gt2-bt2	gt3-bt2	average
HS82	1.60	1.60	1.57	1.60	1.60	1.57	1.59 ± 0.02
GS84	1.79	1.78	1.76	1.79	1.78	1.76	1.78 ± 0.02
HC85	1.72	1.73	1.69	1.73	1.73	1.69	1.72 ± 0.02
K89	1.78	1.79	1.75	1.78	1.79	1.75	1.77 ± 0.02
Tcalc	1.78	1.77	1.73	1.78	1.77	1.73	1.76 ± 0.02

B92=Bhattacharya et al., 1992; Dasg91=Dasgupta et al., 1991; PL83=Perchuk and Lavrent´eva, 1983; H2000=Holdaway, 2000; HS82=Hodges and Spear, 1982; GS84=Ganguly and Saxena, 1984; HC85=Hodges and Crowley, 1985; K89=Koziol, 1989; Tcalc=Thermocalc (Powell et al., 1998)

2.8. Discussion

In addition to major element zoning in garnet from such high-grade rocks, the striking feature of these samples is the presence of two annular trace element and REE maxima in garnet porphyroblasts. To assess or reconstruct the early P-T history of the rocks, we first need to discuss the trace element behavior in garnet during high-grade metamorphism and discuss the possible origins of the annular maxima seen in the garnets.

2.8.1. Origin of the annular maxima of Y+REE in the granulite facies garnet

As indicated by Pyle and Spear (1999), the trace element distribution recorded by any metamorphic rock is a result of the reaction history of the entire rock. Each unique reaction reflects the modal contents of the major phases involved in the reaction. However, also important is the presence of trace element-bearing accessory phases, which buffer trace element activities and can exert very strong trace element partitioning controls. Incorporation of Y+REE into natural garnet is mostly assumed to be by menzerite-like or alkali substitutions with relatively low energetic cost (Carlson et al., 2014). The energetic costs decrease significantly as the host garnet unit-cell dimension expands, decrease very modestly as temperature rises or pressure falls, and decrease substantially with the contraction in ionic radius across the lanthanide series. When studying the origin of compositional zoning in garnet numerous factors controlling the distribution of major and trace elements should be considered (Lanzirotti, 1995; Schwandt et al., 1996). These include the following: (1) element fractionation during mineral growth (e.g. Cygan and Lasaga, 1982; Hickmott et al., 1987; Hollister, 1966); (2) slow re-equilibration of cations by intracrystalline (volume) diffusion (e.g. Anderson and Buckley, 1973; Carlson, 2012; Chakraborty and Ganguly, 1992); (3) limitations of intergranular diffusion of cations at the mineral–matrix interface (e.g. Carlson, 1989); (4) interaction with a metasomatic fluid (e.g. Chamberlain and Conrad, 1993; Erambert and Austrheim, 1993; Hickmott et al., 1987; Jamtveit et al., 1993; Young and Rumble, 1993); (5) the breakdown

or growth of trace element-rich mineral (Chernoff and Carlson, 1999; Hickmott and Spear, 1992). In addition to the classic bell-shaped zoning patterns, which are considered to occur as a result of a fractionation–depletion mechanism during garnet growth (e.g. Hollister, 1966; Tracy, 1982; Tracy et al., 1976), the annular peak of Y and HREE near the rim of garnet crystals can be explained in various ways (Fig. 9). Pyle and Spear (1999) investigated metapelitic rocks in garnet, staurolite, sillimanite and migmatite zones, where they observed high-Y annuli near garnet rims. Those researchers interpreted this high-Y peak as the result of partial garnet consumption in the staurolite zone (Fig. 9a), where Y released into the matrix was incorporated back into garnet during its second stage of growth. Similarly, an annular peak in Y was reported by Yang and Pattison (2006) from pelitic rocks metamorphosed in the garnet to sillimanite zone. The rocks are rich in monazite, and Yang and Pattison (2006) found an yttrium peak in garnet below the staurolite zone (Fig. 9b). Based on monazite geochronology those workers concluded that the annular maximum was the result of decomposition of accessory phases rich in Y and REE. Konrad-Schmolke et al. (2008b) explained an annular peak of REE, observed in garnet from UHP eclogite, by changes in mineral assemblage and fractionation of REE during garnet formation (Fig. 9c). Using pseudosection modelling those workers calculated the modal proportion of minerals along the high-pressure P–T trajectory and interpreted the annular peak, similar to that in calcareous pelites (Hickmott and Spear, 1992), to reflect discontinuous breakdown of zoisite. Therefore, mineral reactions, including resorption of previously crystallized garnet, can liberate REE or change their bulk partition coefficients, and are important for understanding trace element distribution in garnet (e.g. Hickmott et al., 1987; Spear and Kohn, 1996).

A different mechanism for the Y+REE annuli formation in garnets from UHP eclogites was proposed by Skora et al. (2006). According to those researchers, the peak is due to uptake of REE limited by rates of intergranular diffusion during garnet growth (Fig. 9d and e). This occurs when faster diffusion relaxes the concentration gradient in the intergranular medium of the matrix, which allows the garnet to incorporate greater concentrations of the REE when higher temperatures are reached. This model was later adapted by Moore et al. (2013), who studied REE distributions in garnet with annular peaks from quartz pelitic schists and gneisses

(Fig. 9f and g). However, a study by Otamendi et al. (2002) indicated that garnet with strong peaks of Y and HREE in the core without any annuli near the rims can be present in granulite facies rocks (Fig. 9h and i). As shown by Cheng et al. (2007) and Faryad et al. (2010a), annular peak of REE as well as of manganese contents can occur during atoll garnet formation. The early formed small garnet grains or the cores of large crystals can be dissolved owing to their instability at higher P–T conditions. The elements released from the core are transported to the matrix by fluid infiltration through fractures and stabilize new garnet, which continuously overgrows the older crystal. In addition, a patchy and unsystematic distribution of REE, with irregular fluctuations at scales of a few tens of micrometers, can occur in garnet as a result of former accessory phases or pre-existing heterogeneities in the matrix during crystal growth (e.g. Hirsch et al., 2003; Yang and Rivers, 2002).

In all of the above mentioned models, a single metamorphic event is considered for garnet formation. In a polymetamorphic terrane, garnet can be partially replaced during exhumation or cooling and the elements released into the matrix will raise the activity of Y and REE in the environment. This is the case for the Moldanubian Zone granulites, for which two separate metamorphic events are assumed (Faryad et al., 2015; Faryad and Fišera, 2015). The first of these events is the HP–UHP event and the second is the granulite facies overprint following exhumation to lower or middle crustal levels during the Variscan Orogeny. Pseudosection calculations for felsic rocks in the Kutná Hora Complex (Fig. 7) indicate that most of the reactions between minerals occurred below 1.5 GPa and 500 °C, where up to 7 vol. % of garnet was formed. Important information deduced from the pseudosection is that only 2 vol. % of garnet formed at UHP conditions and that no garnet was produced during decompression or cooling. The growth of new garnet during the second event will occur in an environment with higher Y+REE concentrations, resulting in the formation of an annulus. When comparing the distribution of Y+HREE in the felsic granulite from the Kutná Hora Complex (Fig. 9j and k) with those in the literature (Fig. 9), the garnet from the felsic granulite shows higher values of Y+HREE in the annular maximum than in the core. This suggests high concentrations of Y+REE in the matrix that, owing to changing P–T conditions, were incorporated in the new garnet. However, this does not rule out the effect of other factors, as described above, that

could control the overall distribution of Y+REE in garnet. This includes small-scale irregularities or fluctuations in Y+REE concentrations that could relate to the breakdown of former accessory phases or pre-existing heterogeneities in the matrix during crystal growth (Hirsch et al., 2003; Yang and Pattison, 2006; Yang and Rivers, 2002). The best example is patchy and irregular phosphorus zoning in Fig. 5d. The different concentrations of trace elements on the opposite sides of the garnet also signify grain-scale disequilibrium partitioning or uptake of trace elements limited by rates of intergranular diffusion (Skora et al., 2006). It should be noted that apart from apatite, no Y- and REE-bearing accessory phase was observed in garnet.

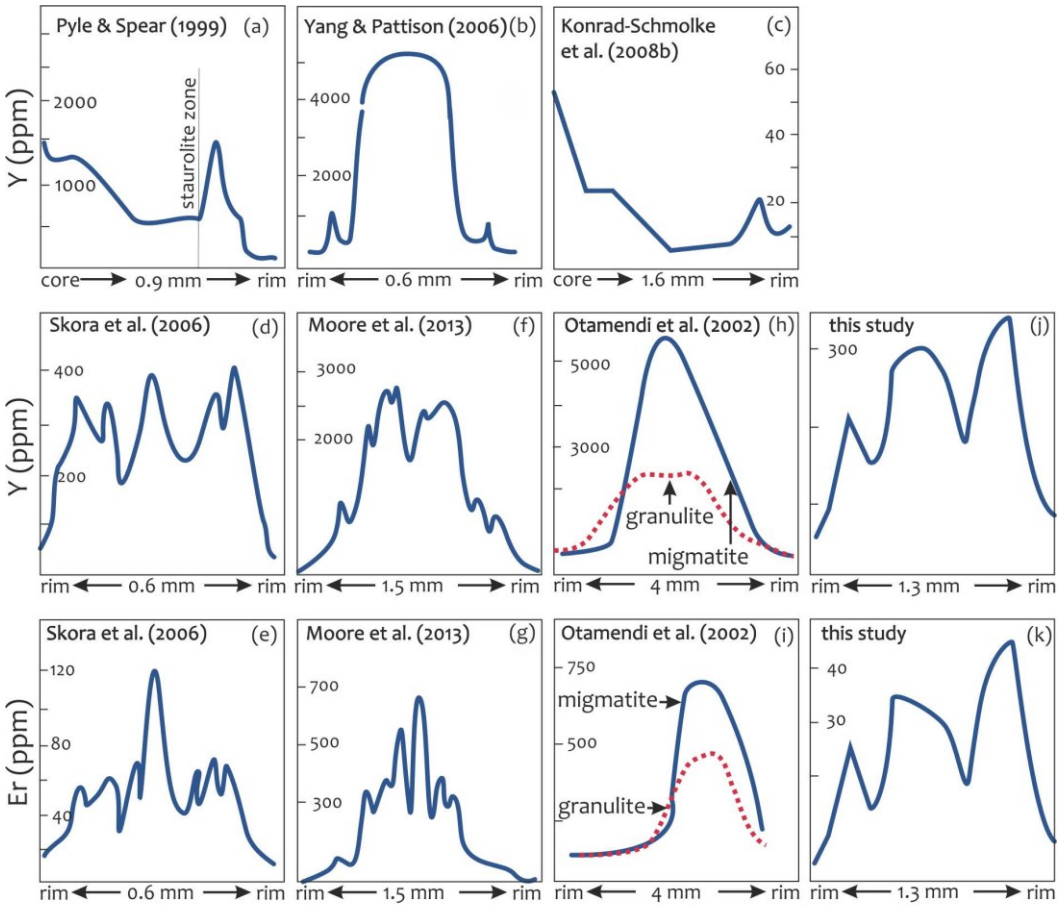

Fig. 9. Summary of distribution of Y+REE and annular peaks in garnet from various metamorphic terranes as discussed in text. (a) staurolite-grade metapelite (British Columbia), (b) staurolite schist (South Dakota), (c) eclogite (Gneiss Complex, Norway), (d, e) eclogite (Zermatt-Saas Zone), (f, g) metapelite (Picuris Mountains), (h, i) migmatite and granulite (Sierra de Pampeanas, Argentina), (j, k) felsic granulite (the Kutná Hora Complex, Bohemian Massif). Data sources are as indicated.

The granulite facies overprint has been assumed to occur by nearly isobaric heating as the result of asthenospheric upwelling and intrusion of ultramafic magma in the Moldanubian crust (Faryad et al., 2015). According to the pseudosection modelling, proportionally 5 vol. % garnet was formed during granulite facies metamorphism, whereas the other 9 vol. % is related to the UHP event. Because of diffusion during the granulite facies event the exact boundary of these two garnets cannot be estimated owing to possible partial resorption of UHP garnet and diffusion modification. Quantitative determinations of rates of diffusion of Y and REE from partially resorbed garnet crystals by Carlson (2012) showed significant change at the outermost rims of garnets. Whereas Nd, Sm, and Eu are strongly depleted in the rims of relict garnet crystals owing to preferential partitioning out of garnet during resorption, Y and some other REE (Er, Tm, Yb, Lu, Tb, Dy, Ho) are strongly concentrated in the relict garnet rims by resorption. Therefore, partial increase of Y and HREE at the rim of UHP garnet could occur by its resorption during exhumation. Figure 10 shows the distribution of REE [normalized to chondrite after Anders and Grevasse (1989)] in bulk-rocks and in garnet from the studied samples. Sample F103-10 has markedly lower REE contents that are probably due to the presence of thin layers of quartz and K-feldspar. The REE content of sample RJ30-13, which has a mineral assemblage similar to that of sample F103-10, is also plotted for comparison. There is generally a decrease, mainly of HREE, from core to rim. All three analysed garnet grains show negative europium anomalies that reflect the overall bulk-rock composition. However, a slight change in Eu anomaly is visible between the core and rim of garnet in sample RJ34-13 (Fig. 10a and b). Considering formation of the garnet rim during the granulite facies stage, this change in the Eu anomaly could be due to simultaneous crystallization of garnet and plagioclase or ternary feldspar. The pseudosection in Fig. 8a indicates the presence of plagioclase with garnet at temperatures below 650 °C, but above this temperature limit two feldspars are stable owing to the inclusion of the melt model in the calculation. The two feldspars are represented here by ternary feldspar.

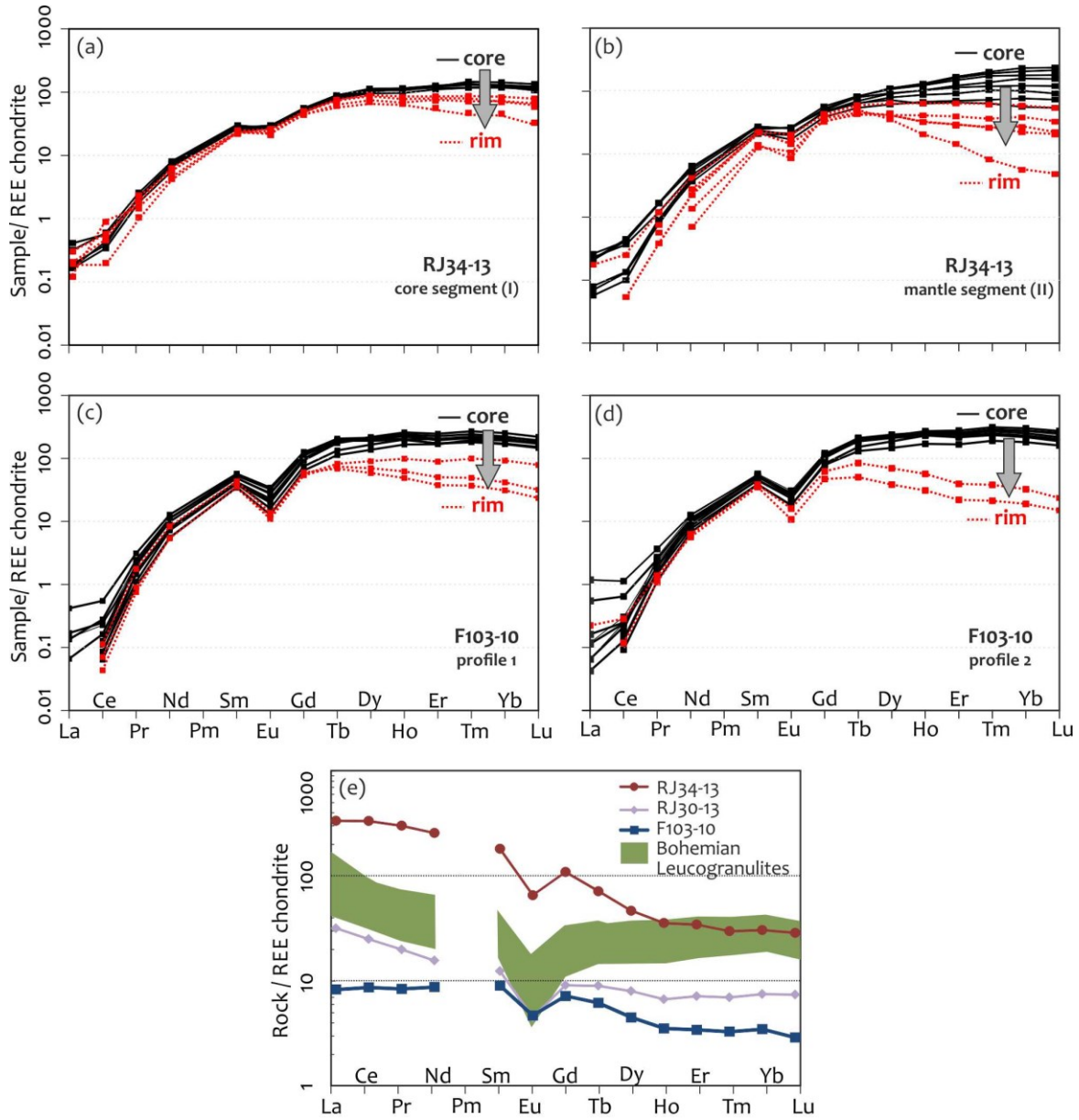

Fig. 10. Chondrite-normalized REE patterns [chondrite values after Anders and Grevasse (1989)] in the studied garnets from mesocratic and leucocratic layers of granulite. (a, b) REE patterns for the core and mantle of garnet in sample RJ34-13 are indicated separately; (c, d) REE patterns for two separate grains in sample F103-10; (e) bulk-rock REE patterns of granulite from the Kutná Hora Complex (RJ34-13, F103-10 and RJ30-13). REE patterns for the South Bohemian granulite (Kotková and Harley, 2010) are also shown for comparison.

2.8.2. Phosphorus zoning in garnet

Apatite is a common phosphate phase in eclogite facies rocks, although moderate amounts of P can enter garnet as pressure and temperature increases (Konzett and Frost, 2009). Because phosphorus diffusion in garnet is slow, phosphorus distribution in garnet can help to decipher its growth history; for example, through preserved growth zones as described by Vielzeuf et al. (2005). By investigating high-grade metapelites containing a sub-solidus assemblage with garnet, Spear and Kohn (1996) showed that phosphorus may increase at the rim of garnet grains, reflecting increased participation of apatite as melting progressed. According to Kawakami and Hokada (2010), the P enrichment in garnet rims from high-grade gneiss in the Lützow–Holm Complex (East Antarctica) was the result of resorption-reprecipitation of garnet during melt formation. One of the most interesting features of the garnet in sample RJ34-13 is the P zoning, particularly at its rims. Detailed compositional maps indicate weak P zoning in the central part and three domains with elevated P concentrations. As mentioned above, apatite is rarely present as an inclusion in garnet, but occurs in the matrix, mainly in direct contact with garnet rims or within intergranular spaces of garnet clusters. Therefore, the three domains could be the result of P diffusion from apatite inclusions below the host garnet surface. According to Brunet et al. (2006), Si–P exchange in garnet under UHP conditions occurs by the $MgPAl_{-1}Si_{-1}$ substitution. The presence of monazite in the matrix (Fig. 3a) as a P-bearing phase can also have influenced P zoning in the garnet rim. In contrast to irregular P zoning at the rim of garnet, the zoning in the central part of the garnet crystal follows its crystallographic planes. This may suggest that the central zoning was a result of continuous garnet crystallization during eclogite facies metamorphism, whereas the rim part was formed after a possible growth gap during granulite facies metamorphism in the presence of a melt. The older eclogite facies garnet that was partly replaced or consumed by matrix phases during exhumation was overgrown by a new P-bearing garnet.

2.8.3. P-T history of felsic granulite from the Kutná Hora Complex and implications for HP-UHP and subsequent granulite facies metamorphism in the Moldanubian Zone

The trace element distribution patterns in garnet, in combination with thermodynamic modelling, in the felsic granulites from the Kutná Hora Complex support the interpretation of two separate Variscan metamorphic events in the Moldanubian Zone (Faryad et al., 2015; Faryad and Fišera, 2015). From the garnet composition, these two events are recorded by the high Y and HREE contents in the core and in the mantle (annulus) part, suggesting nucleation and growth of the first and second garnet, respectively. From the pseudosection modelling, mainly based on grossular isopleths, we interpret that the first garnet was formed during a prograde P–T path from pressure and temperature conditions below 0.6 GPa and 400 °C (Fig. 7b) to 3.2-4.0 GPa at about 700 °C (path 1 in Fig. 11). As the initial profiles of major elements in garnet grains, including calcium contents, were modified to various degrees by diffusion, the intersection of Grs and X_{Fe} isopleth values indicate only an approximate P–T condition for the garnet core, whereas the real values for garnet nucleation were based on pseudosection modelling at even lower pressures and temperatures. However, UHP conditions for these granulites were recently confirmed by the finding of micro-diamond and coesite (Perraki and Faryad, 2014). Modal volume calculations of garnet indicate continuous growth during this UHP event that reached 9 vol. % in the coesite and diamond stability fields (Fig. 7).

There are two alternative scenarios to explain the exhumation of felsic rocks from mantle depths and their subsequent granulite facies metamorphism that could produce the second garnet. The first is decompression and heating to granulite facies conditions of 1.5-2.0 GPa at 800-1000 °C as estimated for the felsic granulite in the Moldanubian Zone (paths a, b and c in Fig. 11). However, such a P–T path will, based on the volume calculations, produce no garnet, even if the rocks are first heated at UHP conditions and then decompressed at high temperatures to granulite facies conditions (Fig. 8). In addition, an isothermal decompression to the granulite facies stage would result in total homogenization of the prograde compositional zoning in garnet (Carlson, 2006; Chakraborty and Ganguly, 1992; Vielzeuf et al., 2005),

unless the exhumation rate from mantle depths to crustal levels was too fast. The second model is an isothermal decompression from UHP conditions at intermediate temperature (path 2 in Fig. 11). After the rocks were exhumed to lower or middle crustal levels, they were subjected to heating at granulite facies conditions (path 3 in Fig. 11). The high peak of Y and HREE concentrations can be the result of partial decomposition of the first garnet during exhumation, during which the trace elements released into the matrix participated in the formation of new garnet. Such a model for granulite facies metamorphism in the Moldanubian Zone has been explained by slab break-off and mantle upwelling as a potential heat source for the granulite facies metamorphism (Faryad et al., 2015). This process was followed by the formation of huge volumes of granitoid magma and their intrusion within the Moldanubian Plutonic Complex (Žák et al., 2014).

In addition to preservation of prograde zoned garnet, the two separate metamorphic events recorded by the felsic granulites can also explain the wide range of age determinations for the felsic granulites and their associated mafic and ultramafic bodies (e.g. Schulmann et al., 2005). Most U–Pb age data on zircon from granulites indicate an age of about 340 Ma that is generally accepted as the culmination of granulite facies metamorphism. However, there are a number of older ages; for example, Sm–Nd ages on garnet of 370–390 Ma from garnet peridotite and pyroxenite (Beard et al., 1992) or of 360 Ma from felsic granulites (Prince et al., 2000), and U–Pb zircon ages of 359–380 Ma from felsic granulites (Nahodilová et al., 2014; Teipel et al., 2012). The older ages are interpreted to date the HP–UHP event, whereas the granulite facies metamorphism occurred at around 340 Ma (Faryad, 2011). The relationship of the granulite facies metamorphism to younger mafic and ultramafic intrusions in the Moldanubian Zone is assumed based on U–Pb age dating on zircon from a metatroctolite with granulite facies coronas around olivine (Faryad et al., 2015).

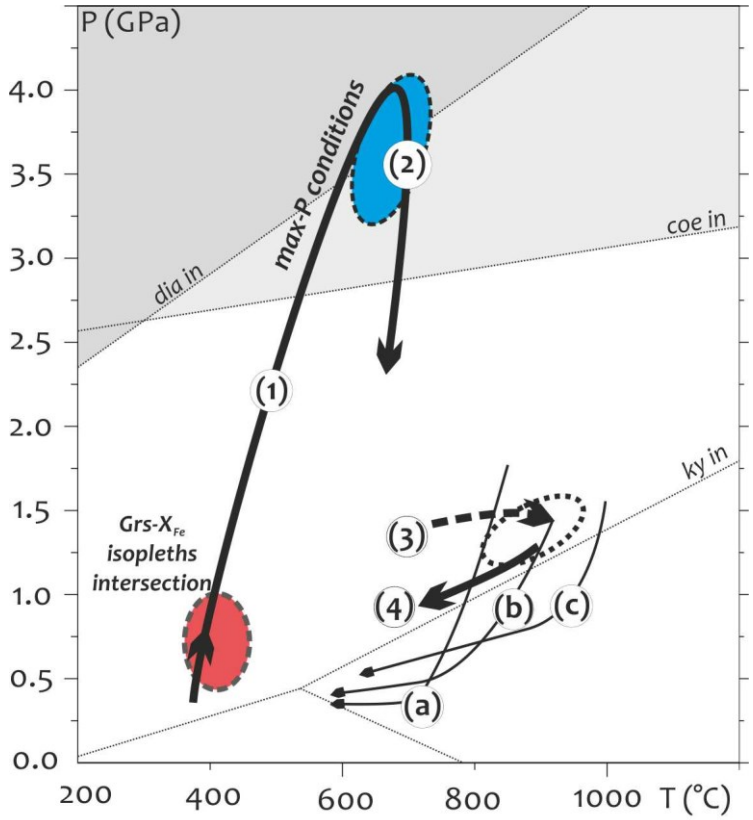

Fig. 11. Inferred P–T paths of the HP granulites in the Moldanubian Zone, based on compositional zoning of garnet and calculated pressure and temperature conditions from the Kutná Hora granulites. (1) Prograde stage reaching UHP conditions. The ellipses indicate P–T fields based on intersection of garnet isopleths for the core and mantle composition of garnet in combination with the data of Perraki and Faryad (2014). It should be noted that garnet nucleates at even lower P–T conditions (see Fig. 7). (2) Exhumation stage to lower crustal levels. (3, 4) Heating and cooling back during the granulite facies overprint for the Kutná Hora felsic granulite, obtained in this study. The cooling and exhumation P–T paths (a–c) of the Moldanubian granulites from different crustal positions are from (a) Strážek Unit (Tajčmanová et al., 2006), (b) South Bohemian granulites (Kotková and Harley, 1999; Vrána, 1992) and (c) granulites of Lower Austria (Carswell and O'Brien, 1993).

2.9. Conclusions

Major and trace element compositional zoning in garnet from felsic granulites in the Kutná Hora Complex (Moldanubian Zone) demonstrates that the rocks experienced two metamorphic events. The first metamorphism occurred in a subduction-zone setting and the second at deep crustal levels, constrained by the following findings.

1. Major element prograde zoning is preserved in the cores of garnets. Thermodynamic modelling indicates that both subduction that reached UHP conditions and subsequent exhumation occurred at relatively low temperatures (below 650-700 °C). These allowed the preservation of prograde zoning, including bell-shaped Mn and Y+HREE profiles in garnet cores.

2. Annular peaks of Y+HREE, developed in the mantle part of garnet crystals, are interpreted as the result of granulite facies metamorphism that mostly occurred in deeper crustal levels. In addition to Y+REE-bearing mineral reactions and partitioning of these elements into garnet during an increase of temperature, the high annular peaks are interpreted to be the result of partial resorption of HP–UHP garnet and the release of trace elements into the matrix during exhumation, followed by their incorporation back into the new garnet during the granulite facies event.

3. The preservation of prograde zoning in garnet, which experienced UHP and subsequent granulite facies metamorphism, suggests that the tectonic and metamorphic processes that occurred during continental collision were too fast to result in total homogenization of the garnet in the felsic rocks.

4. The results of this study support a tectonic model suggesting a short-lived granulite facies overprint that is assumed to have been caused by break-off of the subducting slab and mantle upwelling during the Variscan Orogeny in the Moldanubian Zone.

2.10. Acknowledgements and Funding

The authors thank K. Ettinger and M. Racek for their help with microprobe analyses. We greatly appreciate the constructive reviews by J. F. Otamendi, J. Kotková and an anonymous reviewer. Careful editorial comments of A. Skelton substantially improved the paper.

This work was supported by the Czech Science Foundation (research project number 13-06958S).

PART III

FELSIC GRANULITE WITH LAYERS OF ECLOGITE FACIES ROCKS IN THE BOHEMIAN MASSIF; DID THEY SHARE A COMMON METAMORPHIC HISTORY?

Radim Jedlička, Shah Wali Faryad

[1]Institute of Petrology and Structural Geology, Charles University in Prague, Albertov 6, 12843 Prague, Czech Republic

ABSTRACT

High pressure granulite and granulite gneiss from the Rychleby Mountains in the East Sudetes form an approximately 7 km long and 0.8 km wide body, which is enclosed by amphibolite facies orthogneiss with a steep foliation. Well preserved felsic granulite is located in the central part of the body, where several small bodies of mafic granulite are also present. In comparison to other high pressure granulites in the Bohemian Massif, which show strong mineral and textural re-equilibration under granulite facies conditions, the mafic granulite samples preserve eclogite facies minerals (garnet, omphacite, kyanite, rutile and phengite) and their field and textural relations indicate that both mafic and felsic granulite shared common metamorphic history during prograde eclogite facies and subsequent granulite facies events. Garnet from both granulite varieties shows prograde compositional zoning and contains inclusions of phengite. Yttrium and REEs in garnet show typical bell-shaped distributions with no annular peaks near the grain rims. Investigation of major and trace elements zoning, including REEs distribution in garnet, were combined with thermodynamic modelling to constrain the early eclogite facies metamorphism and to estimate pressure-temperature conditions of the subsequent granulite facies overprint. The first (U)HP metamorphism occurred along a low geothermal gradient in a subduction-related environment from its initial stage at 0.8 GPa / 460 °C and reached pressures up to 2.5 GPa at 550 °C. The subsequent granulite facies overprint (1.6-1.8 GPa / 800-880 °C) affected the rocks only partially; by replacement of omphacite into diopside+plagioclase symplectite and by compositional modification of garnet rims. The mineral textures and the preservation of the eclogite facies prograde compositional zoning in garnet cores confirm

that the granulite facies overprint was either too short or too faint to cause recrystallisation and homogenisation of the eclogite facies mineral assemblage. The results of this study are compared with other granulite massifs in the Moldanubian Zone. In addition, a possible scenario for the Variscan eclogite and subsequent granulite facies metamorphism in the Bohemian Massif is discussed.

Keywords: Bohemian Massif, eclogite facies, granulite, granulite facies overprint, prograde zoning garnet

3.1. Introduction

The prograde metamorphic history of high-pressure to ultrahigh-pressure (HP-UHP) rocks is always difficult to decipher because of strong re-equilibration during subsequent high-temperature overprint and/or exhumation. Minerals stable at high pressure conditions undergo breakdown reactions, recrystallisation and/or compositional modification. This is the case of basement rocks from the Moldanubian Zone in the Bohemian Massif, where numerous lenses and boudins of garnet peridotite and eclogite are present within felsic granulite. Although HP-UHP conditions have previously been estimated for those mafic and ultramafic bodies (Carswell, 1991; Faryad, 2009; Medaris et al., 1995; Nakamura et al., 2004), their common metamorphic history with the host felsic granulite was subject of discussion (Faryad, 2009; Faryad et al., 2010b; Štípská and Powell, 2005). Most of these rocks, cropping-out along the eastern border or in the southern part of the Moldanubian Zone, are collectively called the Gföhl Unit (Fuchs and Matura, 1976; Tollmann, 1995), but similar rocks are also present along the western border of the Moldanubian Zone (for ref. see Faryad and Žák, 2016). Two different scenarios are proposed to explain formation of HP-UHP rocks in the Moldanubian Zone. In addition to the formation of eclogite and garnet peridotite by westward subduction in the Moldanubian Zone (Medaris et al., 2006; Faryad et al., 2013a, b), all these high-grade rocks are assumed either as lower crust material exhumed with fragments of the upper mantle by buckling during compression of the Moldanubian Zone between the Brunovistulian and Teplá-Barrandian Blocks (Schulmann et al., 2005) or formed by subduction of Saxothuringian Zone beneath the Teplá-Barrandian Block (Fig. 1) and their exhumation within the Moldanubian Zone.

In most felsic granulite localities, the main components of these rocks are feldspars and quartz with garnet, which usually shows flat compositional profiles. Minor or accessory phases include kyanite (usually being replaced by sillimanite or symplectitic spinel and plagioclase), rutile, biotite and in some cases also cordierite. Recently, garnet with prograde chemical zoning pattern and containing inclusions of coesite and microdiamond was found in felsic granulite from the Kutná Hora Complex (KHC) in the northern part of the Moldanubian Zone (Jedlicka et al., 2015;

Perraki and Faryad, 2014; Fig. 1a). It was also established that the granulite facies overprint of the HP-UHP crustal lithologies occurred after their exhumation to various crustal levels (Faryad et al., 2015; Jedlicka et al., 2015). Amphibolite-granulite facies overprint at lower pressures (~0.7 GPa) was also confirmed for eclogite occurring within amphibolite facies gneiss and migmatite (Faryad and Fišera, 2015).

The granulite body in the Rychleby Mountains is a part of the Orlica–Śnieżnik dome (Chopin et al., 2012a) in the East Sudetes (Fig. 1b). Small bodies of strongly re-equilibrated granulite and garnet peridotite are also present within gneiss and migmatite in the Góry Sowie Block (Grocholski, 1967; Kryza, 1981; Żelaźniewicz, 1990) in the Central Sudetes (Fig. 1a). The Rychleby granulite is characterised by a low degree of granulite facies recrystallisation and re-equilibration. In contrast to other granulites in the Moldanubian Zone, the eclogite facies assemblages are preserved in thin mafic layers intercalated within felsic granulite. Although phengite and omphacite inclusions in garnet and matrix omphacite were already reported from these mafic granulites (Kryza et al., 2003; Steltenpohl et al., 1993), the possible prograde history of these rocks has not been discussed. This enables to estimate the pre-granulite metamorphic conditions and the degree of recrystallisation and re-equilibration of the rocks during the granulite facies overprint and to correlate them with other granulite massifs within the Moldanubian Zone.

In this paper we investigated mineral compositions and textural relations in mafic and felsic granulite from the Rychleby Mountains in order to constrain the pre-granulite facies metamorphic evolution and to quantify the granulite facies overprint. In addition to mineral inclusions, a study of major and trace elements zoning in garnet combined with thermodynamic modelling is used to trace the prograde metamorphic history during the early eclogite facies metamorphism in the rocks. Mineral textures and P-T conditions of the earlier eclogite and subsequent granulite facies metamorphism are compared with similar granulites from the Gföhl Unit and they are discussed with respect to the Variscan geodynamic evolution of the Bohemian Massif.

3.2. Geological background

The Orlica–Śnieżnik dome (OSD), also called the Orlica-Śnieżnik Massif (Anczkiewicz et al., 2007), is located in the East Sudetes (eastern part of the Bohemian Massif) near the border between Czech Republic and Poland (Fig. 1b). In the east, the OSD is separated from the Neoproterozoic Brunovistulian microcontinent (Schulmann and Gayer, 2000; Štípská et al., 2004) by a thin slice of the Staré Město Formation (Fig. 1b) which is a remnant of a late Cambrian intracontinental rift (Kröner et al., 2001; Lexa et al., 2005; Parry et al., 1997; Štípská et al., 2001). In the south-west and south, the OSD is bounded by low-medium grade rocks of the Nové Město and the Zábřeh Formations (Mazur and Aleksandrowski, 2001; Mazur et al., 2005; Schulmann et al., 2008). The Central, West and East Sudetes are formed by several allochthonous metamorphic complexes of Neoproterozoic to Cambrian-Ordovician protolith age, which are assumed to derive from different continental blocks that were amalgamated during Variscan collision (Mazur et al., 2006). The relationship of the OSD to the Moldanubian (Matte et al., 1990; Mazur et al., 2006) or Saxothuringian Zones (Chopin et al., 2012a; Franke and Żelaźniewicz, 2000) is a subject of discussion. Chopin et al. (2012a) consider the OSD as a part of the Moldanubian Zone that represents a continental orogenic root zone formed during Variscan orogeny. In addition to medium and high-grade metamorphism, Variscan tectonothermal phenomena in the OSD include intense syn-metamorphic burial deformation accompanied by subsequent exhumation of the high-grade rocks (Mazur et al., 2006). In addition to the E-W oriented sub-horizontal shortening, which was related to collision between the West Sudetes and Brunovistulian Block, the recent architecture of the OSD was created by doming and detachment faulting (Jastrzębski, 2009).

The OSD is composed mostly of orthogneiss (migmatitic Gierałtów and Śnieżnik augen orthogneiss) with inliers of (U)HP eclogite facies rocks (Bröcker and Klemd, 1996; Štípská et al., 2004; 2012), but chlorite- to kyanite-grade mica schist, represented by a volcano-sedimentary sequence and metapsammites of the Monotonous Młynowiec and Varied Stronie Formations, composed of paragneiss, metapelite amphibolite and felsic meta-volcanics are also present (e.g. Chopin et al., 2012b;

Don et al., 1990; Jastrzębski, 2009; Jastrzębski et al., 2010). According to detrital zircon ages, Jastrzębski et al. (2010) and Mazur et al. (2012) assume sedimentation of these sequences as middle Cambrian-early Ordovician in age. An age of ca 500 Ma for the magmatic precursor of the orthogneiss was obtained using U-Pb zircon dating (Kröner et al., 2001; Olivier et al., 1993; Turniak et al., 2000).

The felsic granulite, interlayered with mafic granulite (referred to as omphacite-bearing granulite - Pouba et al., 1985), forms an approximately 7 km-long, narrow belt (Fig. 1c). It is part of a gneiss antiform (the Rychleby and Złote Mountains), where the granulites are hosted by the Gierałtów orthogneiss. The surrounding orthogneiss is partially migmatised and contains small bodies of retrogressed eclogite, amphibolite and metagranite (Grześkowiak, 2003). The protolith ages of those granulites are not precisely known, but most likely are older than 470 Ma (Bröcker et al., 1997; Lange et al., 2005; Štípská et al., 2004). There is a wide range of ages (369-337 Ma) obtained mostly using U-Pb dating method on zircons by different authors (Bröcker et al., 2009; Lange et al., 2003; 2005; Szczepański et al., 2004; Štípská et al., 2004), which determines the time of peak pressure-temperature (P-T) conditions for the granulite facies metamorphism. Lu-Hf dating of garnet-whole rock from the Rychleby Mountains granulite yielded 386.6±4.9 Ma, which is interpreted as the age of garnet growth from low-grade to UHP conditions (Anczkiewicz et al., 2007). Similarly, a wide range of P-T conditions were obtained for these granulites. Pouba et al. (1985) estimated temperatures of 850-1000 °C at 1.3-2.0 GPa based on garnet-clinopyroxene Fe-Mg exchange thermometry and assumed stability of plagioclase together with kyanite. Pressure and temperature of 1.8 GPa and 900 °C were obtained by Štípská et al. (2004), but higher pressures (up to 2.7 GPa) were estimated based on the discovery of quartz pseudomorphs after coesite near Stary Gierałtów in the southern part of the granulite body (Bakun-Czubarow, 1992). Recent P-T calculations by Budzyń et al. (2015) for both felsic and mafic granulite in the Rychleby Mountains near Stary Gierałtów are 2.0-2.2 GPa at 900-920 °C and 1.8-2.0 GPa at 950-970 °C, respectively. Pressure and temperature estimate for the Góry Sowie felsic and mafic granulite are about 2.0 GPa and 900-1000 °C (O´Brien et al., 1997). Temperatures of 900 °C and pressures

of 2.2-3.0 GPa were calculated for both the Góry Sowie and the Rychleby Mountains granulites with garnet, orthopyroxene and ternary feldspar by Kryza et al. (1996).

Samples collected for this study come from a 7 km-long belt of felsic and mafic granulite in the Rychleby Mountains (Fig. 1c). The mafic granulite forms centimetre- to decimetre- scale layers within the felsic granulite. Both granulites are enclosed by fine grained (Gierałtów) orthogneiss, which also contains bodies of amphibolite in the vicinity of the granulite belt. The dominant structure within the granulite belt is a NE–SW trending vertical foliation defined by an alternation of mafic and felsic layers varying in thickness from centimetres to several metres (Štípská et al., 2004). The earliest relict structure is marked by mafic layers re-folded by isoclinal folds with steep axial planes.

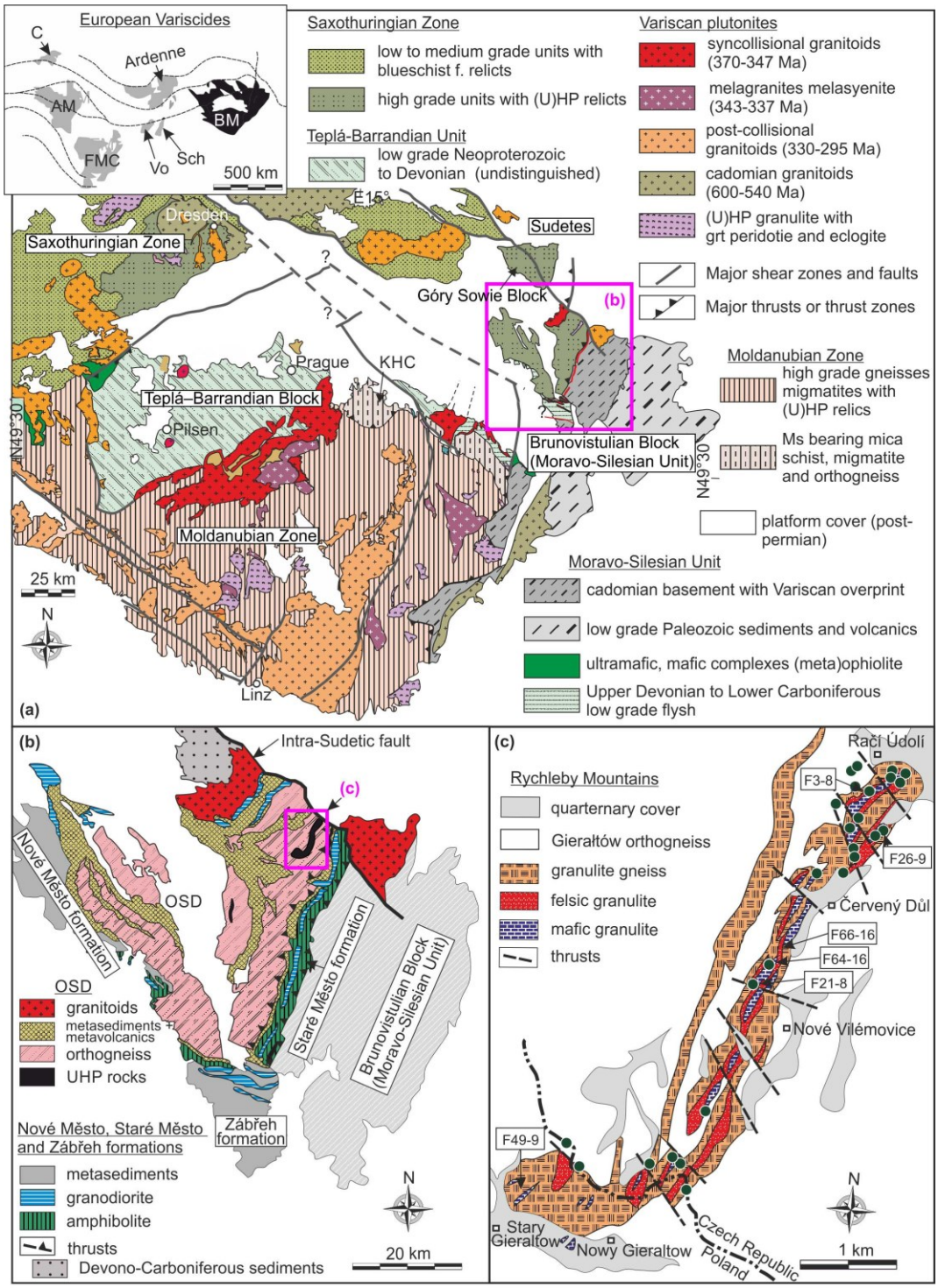

Fig. 1. (a) simplified geological map of the Bohemian Massif after Cháb et al. (2007), Faryad and Kachlík (2013) and Franke (2000) with a sketch of its position within the European Variscan Belt (AM - Armorican Massif, C - Cornwall, FMC - French Massif Central, Vo - Vosges, Sch - Schwarzwald, BM - Bohemian Massif); (b) geological map of the Orlica–Śnieżnik dome (simplified after Aleksandrowski et al., 1997; Don et al., 2003; Żelaźniewicz et al., 2006); (c) detail of the studied area in the Rychleby Mountains (modified after Pouba et al., 1985; Štípská et al., 2004). The solid dots and labels in (c) indicate sample localities.

3.3. Analytical methods

Chemical analyses and X-ray maps were obtained by a JEOL JXA-8530F field-emission gun electron microprobe (FEG-EPMA) equipped with wavelength- and energy-dispersive spectrometers (WDS and EDS) at the Institute of Petrology and Structural Geology, Charles University in Prague. The operating conditions for spot analyses were 15 kV and 30 nA beam current. Standards used were quartz (Si), corundum (Al), periclase (Mg), magnetite (Fe), rhodonite (Mn), calcite (Ca), rutile (Ti), chromium oxide (Cr), vanadinite (V), albite (Na), apatite (P). The same method was applied for detailed compositional profiles of major and trace elements. For high-resolution compositional mapping of major and trace elements, analytical conditions of 20 kV and 120 nA were used.

The bulk rock compositions used for thermodynamic modelling were estimated by quantitative analysis of a representative area of the thin sections using a scanning electron microscope VEGA-TESCAN at the same Institute equipped with an EDS detector in order to mitigate possible sample to thin-section scale heterogeneities (e.g. Peřestý et al., 2016). A total of 20 spectra were acquired in scanning mode at 15 kV and 1.5 nA for 300 s, each spectrum covering an area of ~16 mm^2. The representative areas were defined to incorporate variations in grain size and mineral distributions in order to involve all the phases in their appropriate abundances and to avoid late cracks, alteration zones or veins.

Yttrium and rare earth elements (REEs) in garnet were analysed using an Element 2 high-resolution inductive coupled plasma-mass spectrometer (ICP-MS) coupled with a 213-nm Nd YAG UP-213 laser ablation system at the Institute of Geology of the Czech Academy of Sciences, Prague. The laser was fired at a repetition rate of 10 Hz with beam spot size of 55 μm in diameter and energy density of 11–12 J/cm^2. The data were calibrated against NIST 612 glass using the recommended values from Jochum et al. (2011), and the internal standardisation with Ca was used. Each individual EPMA data were used for laser ablation ICP-MS internal standardisation with Ca to avoid chemical zonality of garnet. The precision of the laser ablation analyses ranges between 2 and 6% (as relative standard deviation - RSD) for most of the detected elements. The accuracy was monitored by analysing basalt

glass BCR2-G and was compared with the values published by Jochum et al. (2005) and ranged between 5 and 10% for most of the elements.

Abbreviations of minerals in the text, figures and figure captions are those from Whitney and Evans (2010), except garnet, which is abbreviated as gt. Garnet end-members are Alm = Fe^{2+} / (Fe^{2+} + Mg + Ca + Mn), Grs = Ca / (Fe^{2+} + Mg + Ca + Mn), Prp = Mg / (Fe^{2+} + Mg + Ca + Mn), Sps = Mn / (Fe^{2+} + Mg + Ca + Mn). Other ratios are X_{Fe} = Fe^{2+} / (Fe^{2+} + Mg); X_{Mg} = Mg / (Fe^{2+} + Mg).

3.4. Petrography of the studied rocks and mineral inclusions in garnets

In total 99 samples of felsic and mafic granulite were collected from three localities (Račí Údolí, Červený Důl and Nové Vilémovice) on the Czech side and one locality (Stary Gierałtów) on the Polish side of the Rychleby Mountains in the OSD (Fig. 1c). Relatively fresh samples of both granulite varieties were selected for detailed study. A total of six samples, three of felsic granulite (F21-8, F26-9, F66-16) and three of mafic granulite (F3-8, F49-9, F64-16) were used for high-sensitive microprobe measurement and thermodynamic modelling.

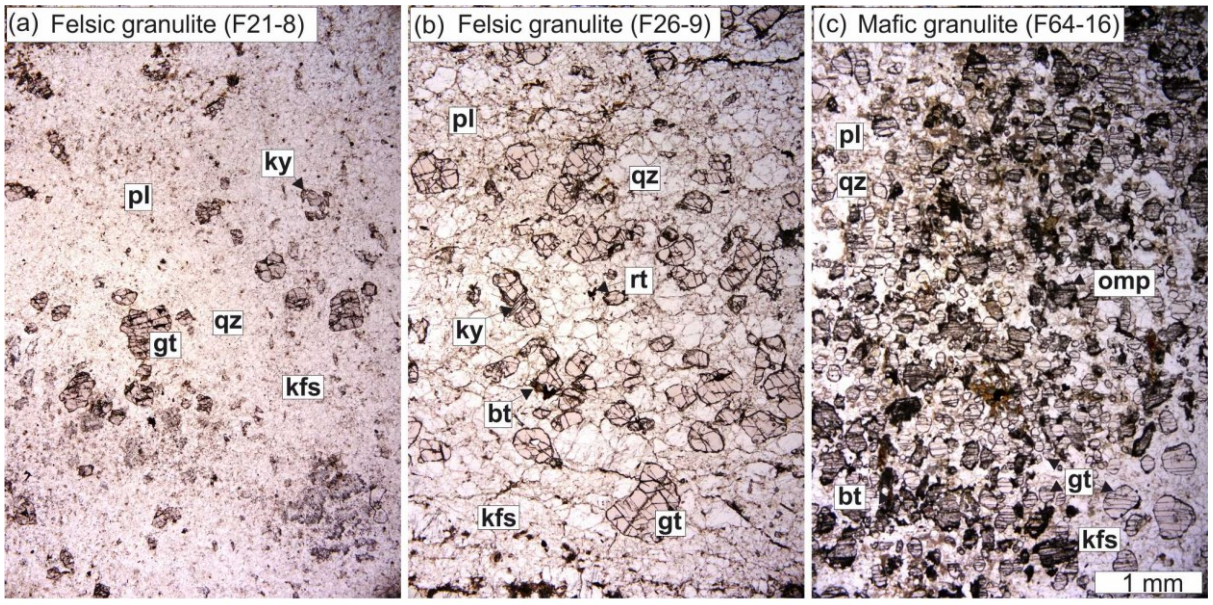

Fig. 2. Microphotographs of the studied rocks in plane polarized light. (a) fine-grained felsic granulite F21-8; (b) felsic granulite (F26-9) near the contact with mafic granulite; (c) mafic granulite (F64-16) with omphacite.

3.4.1. Felsic granulite

The felsic granulite is a fine- to medium-grained massive rock with porphyroblasts of garnet and kyanite in a plagioclase + K-feldspar + quartz matrix (Fig. 2a). Rutile, apatite and zircon can be present as accessory phases. In some samples, biotite or chlorite replace garnet or occur in the matrix. Modal contents of the main phases are: garnet∽10-15%; feldspars∽35%; quartz∽40%; kyanite∽5%. Near to the contact with mafic granulite, garnet size increases and the rock becomes coarse-grained (Fig. 2b). Garnet and some feldspar grains may reach sizes up to 1 mm in diameter (Fig. 3a, b). Perthitic feldspar is present in the matrix (Fig. 3b) and as inclusions in garnet. Kyanite is present both in the matrix (Fig. 2a, b) and as inclusions in garnet porphyroblasts (Fig. 4c). Large kyanite grains in the matrix sometimes have plagioclase coronas (Fig. 3c). Phengite is present only as inclusions in garnet. Representative analyses of garnet are listed in Table 1.

Garnet grains often contain inclusions of quartz, plagioclase, apatite, rutile, phengite, kyanite (Fig. 4a, b, c) and polyphase inclusions of plagioclase+quartz, plagioclase+K-feldspar+quartz. Phengite is always present in the core of garnet and its silica content ranges between 3.22-3.25 a.p.f.u. and titanium content between 0.103-0.209 a.p.f.u. (Table 2). Phengite at contact with garnet is usually replaced by biotite (Fig. 4a). Only one polyphase inclusion of zoisite (Al = 2.65 a.p.f.u.; Fe = 0.37 a.p.f.u.) with an epidote rim (Al = 2.19 a.p.f.u.; Fe = 0.65 a.p.f.u.) together with quartz and chlorite was found in the garnet core (Fig. 4b). It is not clear, whether the rhomboid-shaped zoisite is a pseudomorph after lawsonite or the replacement product of other phase(s) originally enclosed in garnet.

3.4.2. Mafic granulite

Fine- to medium-grained mafic granulite is composed of garnet and omphacitic to diopsidic clinopyroxene, plagioclase, quartz, K-feldspar, kyanite and accessory rutile, apatite and zircon (Fig. 2c, 3d). Modal contents of major phases are: garnet∽25%; clinopyroxene∽25%; feldspars∽20%; quartz∽20%. Garnet

porphyroblasts (around 0.8 mm in size) contain inclusions of phengite, kyanite, omphacite (Fig. 4d, e, f), quartz and rutile. Omphacite is partially transformed to diopside along grain boundaries or to symplectite with plagioclase (Fig. 3e, f). Rare biotite, amphibole and chlorite present in the matrix and in contact with garnet rims are related to late-stage retrogression of the rock. Representative analyses of garnet are listed in Table 1.

Phengite enclosed in garnet may have a tabular shape and is partly replaced by a mixture of plagioclase and biotite (Fig. 4d). Compared to phengite in felsic granulite, it has a slightly lower silica (3.20 a.p.f.u), but similar titanium content (0.138 a.p.f.u. - Table 2). Omphacite is present both in the matrix and as inclusions in garnet. Its jadeite content varies between 27-37.5 mol. %. Omphacite with the highest jadeite content (37.5 mol. %) is present near the core of a garnet (Fig. 4e) and that occurring near the rim (Fig. 4f) has lower jadeite contents (30 to 27 mol. %). Jadeite content in the matrix omphacite is 29 mol. %.

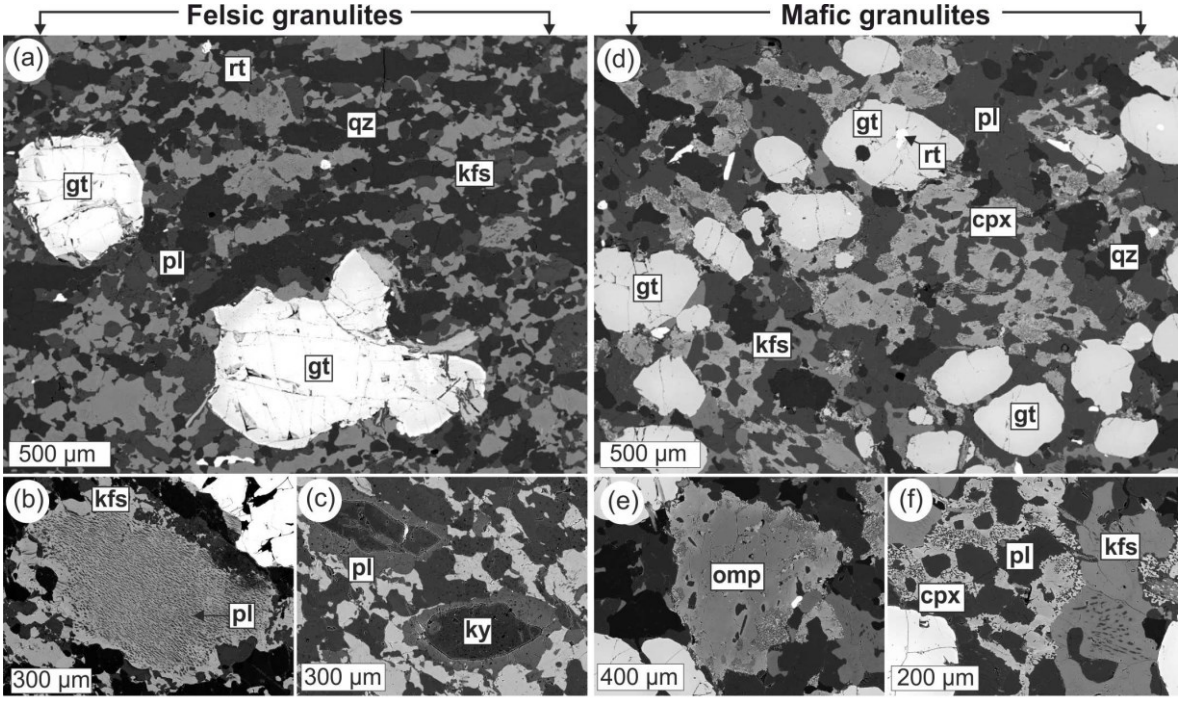

Fig. 3. Back-scattered images of felsic (a, b, c) and mafic granulites (d, e, f), respectively. (a) garnet porphyroblasts in quartzo-feldspathic matrix - sample F66-16; (b) perthitic feldspar in the vicinity of garnet - sample F21-8; (c) kyanite grains with plagioclase rims - sample F21-8; (d) garnet porphyroblasts and omphacite grains in quartzo-feldspathic matrix of mafic granulite - sample F3-8; (e) omphacite core surrounded by diopsidic pyroxene - sample F3-8; (f) symplectite of diopsidic pyroxene and plagioclase - sample F3-8.

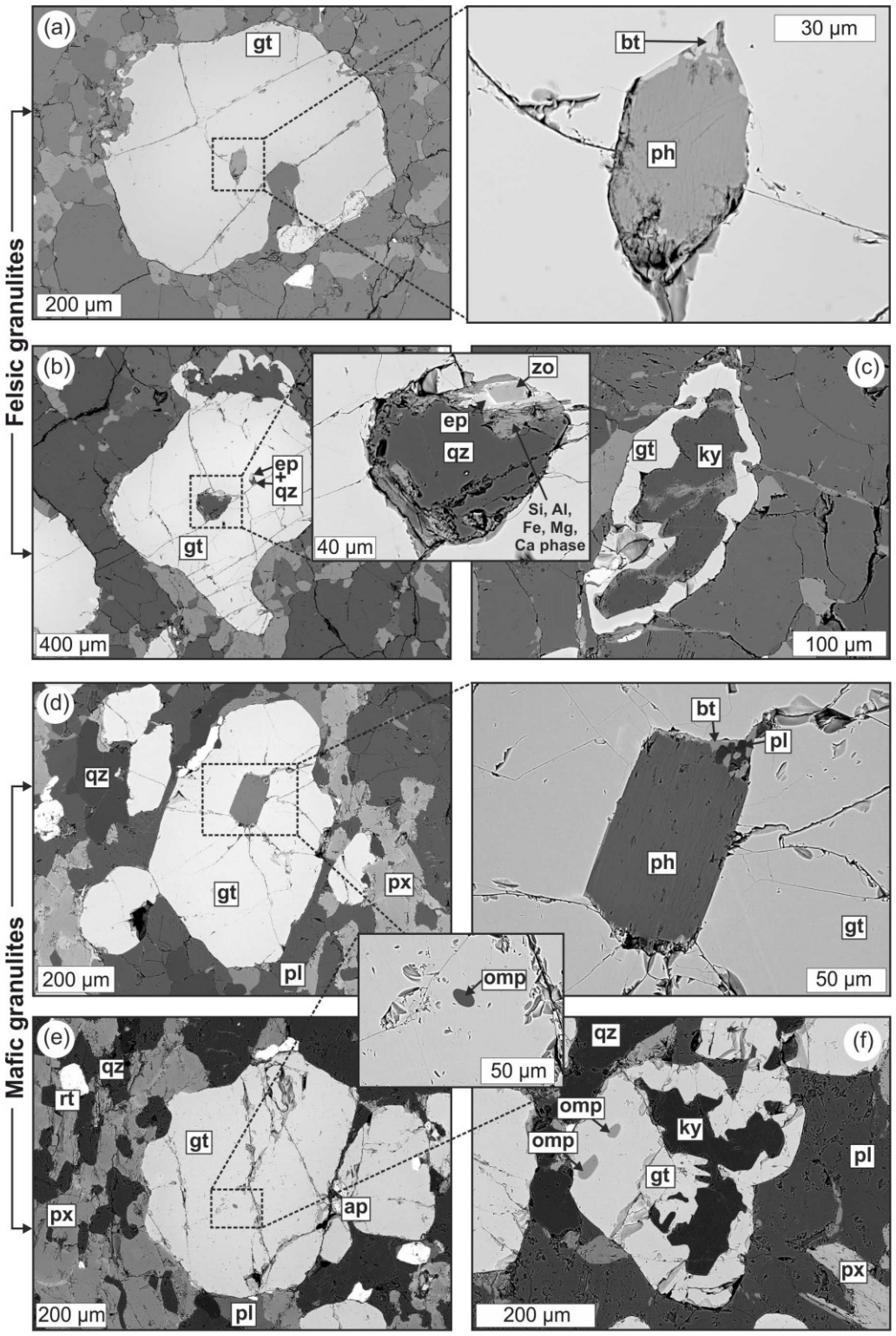

Fig. 4. Back-scattered images of garnets with inclusions of other phases from felsic granulite F26-9 (a, b, c) and mafic granulite F49-9 (d, e, f). (a) phengite inclusion in garnet and its close-up; (b) polyphase inclusion (zoisite+epidote+quartz) in garnet and its detail; note epidote rim (bright) along rhomboid-shaped grain of zoisite (after lawsonite?) (c) kyanite enclosed in garnet; (d) phengite inclusion in garnet and its close-up. Note that phengite in contact with garnet is replaced by a symplectite of biotite and plagioclase; (e) omphacite inclusion in garnet and its detail; (f) kyanite and omphacite inclusions in garnet.

Table 1: Representative chemical analyses of garnets from Rychleby Mountains granulites.

Sample	F26-9	F26-9	F49-9	F49-9	F49-9	F3-8	F3-8
variety	felsic	felsic	mafic	mafic	mafic	mafic	mafic
position	core	rim	core	near inc	rim	core	rim
oxides (wt. %)							
SiO_2	39.116	39.762	38.501	38.459	38.504	39.005	39.386
TiO_2	0.117	0.045	0.116	0.11	0.094	0.086	0.142
Al_2O_3	21.658	22.182	21.554	21.554	21.636	22.004	22.164
FeO	22.255	21.172	21.724	22.277	21.941	20.194	21.986
MnO	0.598	0.388	0.435	0.413	0.416	0.397	0.507
MgO	4.91	8.617	4.419	4.424	5.852	5.124	6.489
CaO	11.809	8.233	12.438	11.912	10.283	13.384	9.751
Na_2O	0.04	0.009	0.023	0.047	0.036	0.014	0.054
Total	100.603	100.436	99.21	99.196	98.762	100.208	100.479
atoms (per 12 ox.)							
Si	3.012	3.010	3.005	3.005	3.002	2.994	3.011
Ti	0.007	0.003	0.007	0.006	0.006	0.005	0.008
Al	1.966	1.979	1.983	1.985	1.989	1.991	1.997
Fe^{2+}	1.433	1.340	1.418	1.456	1.43	1.282	1.405
Mn	0.039	0.025	0.029	0.027	0.027	0.026	0.033
Mg	0.563	0.972	0.514	0.515	0.680	0.586	0.739
Ca	0.974	0.668	1.040	0.997	0.859	1.101	0.799
Na	0.006	0.001	0.003	0.007	0.005	0.002	0.008
Prp	0.184	0.319	0.171	0.172	0.227	0.193	0.242
Alm	0.466	0.439	0.473	0.486	0.477	0.423	0.459
Grs	0.317	0.219	0.347	0.333	0.287	0.363	0.261
Sps	0.013	0.008	0.010	0.009	0.009	0.009	0.011
X_{Fe}	0.718	0.580	0.734	0.739	0.678	0.686	0.655

Table 2: Representative analyses of mineral inclusions from felsic and mafic granulites, as illustrated in Fig. 4

Sample	F26-9	F26-9	F49-9	F26-9	F26-9		F49-9	F49-9	F49-9
variety	felsic	felsic	mafic	felsic	felsic		mafic	mafic	mafic
Mineral	ph	ph	ph	ep	ep		omp	omp	omp
oxides (wt. %)									
SiO_2	48.012	47.605	46.802	38.098	39.352		52.058	52.264	52.243
TiO_2	2.034	4.103	2.676	1.762	0.014		0.659	0.475	0.446
Al_2O_3	29.476	28.46	28.406	23.111	29.222		11.354	8.997	8.084
FeO	2.252	1.674	2.878	9.723	5.696		8.02	7.432	7.682
MnO	0.043	0.009	0.026	0.009	0.007		0.055	0.037	0.019
MgO	2.112	2.192	2.075	0.264	0.092		7.269	9.025	9.522
CaO	-		0.002	22.8	23.701		14.428	16.34	17.137
Na_2O	0.316	0.603	0.318	-	0.009		5.24	4.194	3.748
K_2O	10.64	10.201	10.8	-	-		-	-	-
P_2O_5	-	-	-	0.068	0.022		-	-	-
F	-	-	0.28	-	-		-	-	-
Cl	0.021	0.005	0.014	-	-		-	-	-
Total	94.906	94.852	94.277	95.863	98.115		99.083	98.764	98.881
atoms (per ox.)									
Si	3.246	3.232	3.205	3.059	3.024		1.906	1.925	1.926
Ti	0.103	0.209	0.138	0.106	0.001		0.018	0.013	0.012
Al	2.349	2.278	2.293	2.187	2.646		0.49	0.391	0.351
Fe^{2+}	0.127	0.095	0.158	0.653	0.366		0.209	0.195	0.193
Mn	0.002	0.001	0.002	0.001	-		0.002	0.001	0.001
Mg	0.213	0.222	0.212	0.032	0.011		0.397	0.495	0.523
Ca	-	-	-	1.961	1.951		0.566	0.645	0.677
Na	0.041	0.079	0.042	-	0.001		0.372	0.299	0.268
K	0.918	0.884	0.943	-	-		-	-	-
X_{Mg}	0.626	0.700	0.573			X_{Mg}	0.655	0.717	0.730
						Jd	0.375	0.301	0.273
						En	0.198	0.248	0.262
						Fs	0.104	0.097	0.096
						Wol	0.245	0.291	0.308

3.5. Compositional zoning in garnet

Garnet porphyroblasts from both felsic and mafic granulites reveal a well-preserved core to rim zonation of major and trace elements. Selected compositional maps and profiles of major elements and some trace elements (Y, Na, Ti, P) from both mafic and felsic granulites obtained by detailed X-ray maps are illustrated in Figs. 5-7. As garnet and omphacite in mafic granulite show only replacement textures along their grain boundaries, investigation was directed towards whether the garnet preserves different growth zones indicating distinct metamorphic stages or events. In such high-grade rocks, the overgrowing garnet can be recognized by annular peaks of REEs near the garnet rim (Jedlicka et al., 2015). Distribution of trace elements, including REEs, treated across the garnet grain was obtained by LA-ICP-MS and it is illustrated in Fig. 8.

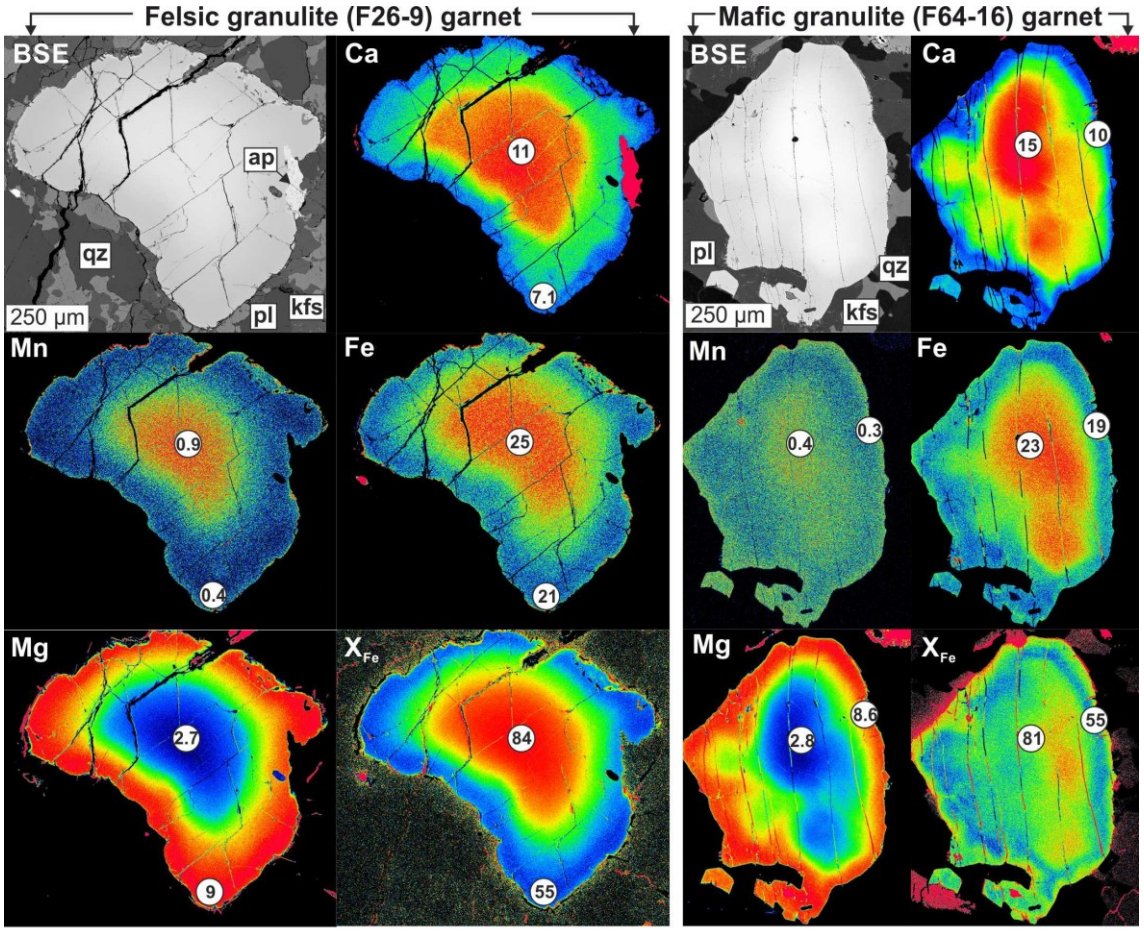

Fig. 5. Selected back-scattered images (BSE) and compositional maps of major elements distribution in garnet porphyroblasts from felsic granulite (F26-9) and mafic granulite (F64-16). Representative spot analyses in wt. % are marked in black circles in the images.

3.5.1. Major element distribution

With the exception of Mg (which shows the lowest values in the core with systematic increase towards the rim), the other three major elements (Fe, Ca, Mn) exhibit the highest concentrations in the core, decreasing towards the rim of grains (Fig. 5).

Garnets from felsic granulite (Fig. 6a, b) indicate clear prograde zoning with high grossular (33 mol. %), spessartine (2 mol. %), almandine (55 mol. %) and X_{Fe} (84) and low pyrope (11 mol. %) contents in the core. Garnet in sample F21-8 (Fig. 6a) has the highest concentration of grossular (35 mol. %) in the core and it decreases towards the mantle part. At the very rim of the grain, the grossular content drops to almost 10 mol. %. Spessartine content is low throughout the grain but a visible decrease towards the rim is recorded. It shows back-diffusion effect due to partial resorption of garnet at the very rim. The larger garnet in sample F26-9 (Fig. 6b) has high spessartine content in the core, however, similar to pyrope, spessartine does not show a central peak. It is not clear, if this is due to the effect of cutting, whereby the plane of the thin section does not cross the core of the grain or if it was modified by diffusion. A small peak in grossular content is compensated by slightly lower almandine content. The almandine, spessartine and X_{Fe} continuously decrease and pyrope increases towards the rim. In contrast, the grossular content changes stepwise in the mantle and rim parts. At the very rim, all elements are modified by diffusion that was related to cooling and resorption of garnet as can be seen from back-diffusion of spessartine.

Similar to felsic granulite, zoned garnets are also present in the mafic granulite (Fig. 6c-f). Two compositional varieties of garnet were observed in sample F64-16. The first variety (Fig. 6c) has complex zoning with weak bell-shaped profile in the core (Grs_{41}, Alm_{48}, Prp_{10} - point 1). The grossular content decreases stepwise from core through mantle (41-35 mol %, points 1-2, Fig. 6c), where it becomes almost flat (35-34 mol %, point 2-3) with steep decrease towards the rim (33-27 mol. %). Pyrope content is low in the core (10 mol. %), increasing to about 14-25 mol. % in the mantle part (point 2-3) and reaching up to 33 mol. % near the rim. It decreases at the very rim, where both spessartine and X_{Fe} increase. The almandine content first slightly increases

towards the mantle and then decreases to the rim, but at the very rim part it increases again. X_{Fe} decreases from its high value (83) in the core, where the decreasing gradient becomes flat in mantle part and finally descends sharply towards the rim. Similar to almandine, X_{Fe} strongly ascends at the very rim. A slight decrease of spessartine towards the rim is visible, but a sharp increase at the very rim of the grain and similar increase of X_{Fe} is a result of garnet consumption and back-diffusion during cooling. If we consider partial resorption and chemical modification of garnet, small inward shift of compositional profile at the most rims can be estimated by qualitative mass-balance of spessartine content (Fig. 6c). The predicted compositional trends of major elements (marked by dashed lines) may indicate about 38 mol. % of pyrope and 21 mol. % of grossular content at the very rim (Fig. 6c). The second variety (Fig. 6d) has the highest grossular/lowest pyrope content (Grs_{44-46}, Alm_{46-48}, Prp_5) in the central part with relatively flat compositional profile in the mantle part that shows rimward decrease of Ca and Fe and increase of Mg. Garnet from sample F49-9 (Fig. 6e) exhibits, despite of small grain size, a bell-shaped distribution of grossular and pyrope with flat spessartine content. Grossular has its maximum concentration in the core with stepwise decrease through mantle towards the rim, while pyrope has the lowest content in the central part with increase towards the rims. This sample contains also second variety garnet with relatively flat compositional profile in central-mantle part. This garnet (Fig. 6f) with inclusion of omphacite (Fig. 4e) has high grossular/low pyrope content in the core (Grs_{34}, Alm_{48}, Prp_{16}). Through the mantle part, grossular and pyrope are almost flat, while almandine content shows a slight decrease. In the rim part, increase of pyrope and decrease of grossular can be observed. On the left side of the profile is documented partial modification of all elements (slight decrease of pyrope and grossular and increase of almandine and X_{Fe}) at the very rim, nevertheless it is typical for all studied grains. Spessartine shows no zoning pattern with low (<1 mol %) values.

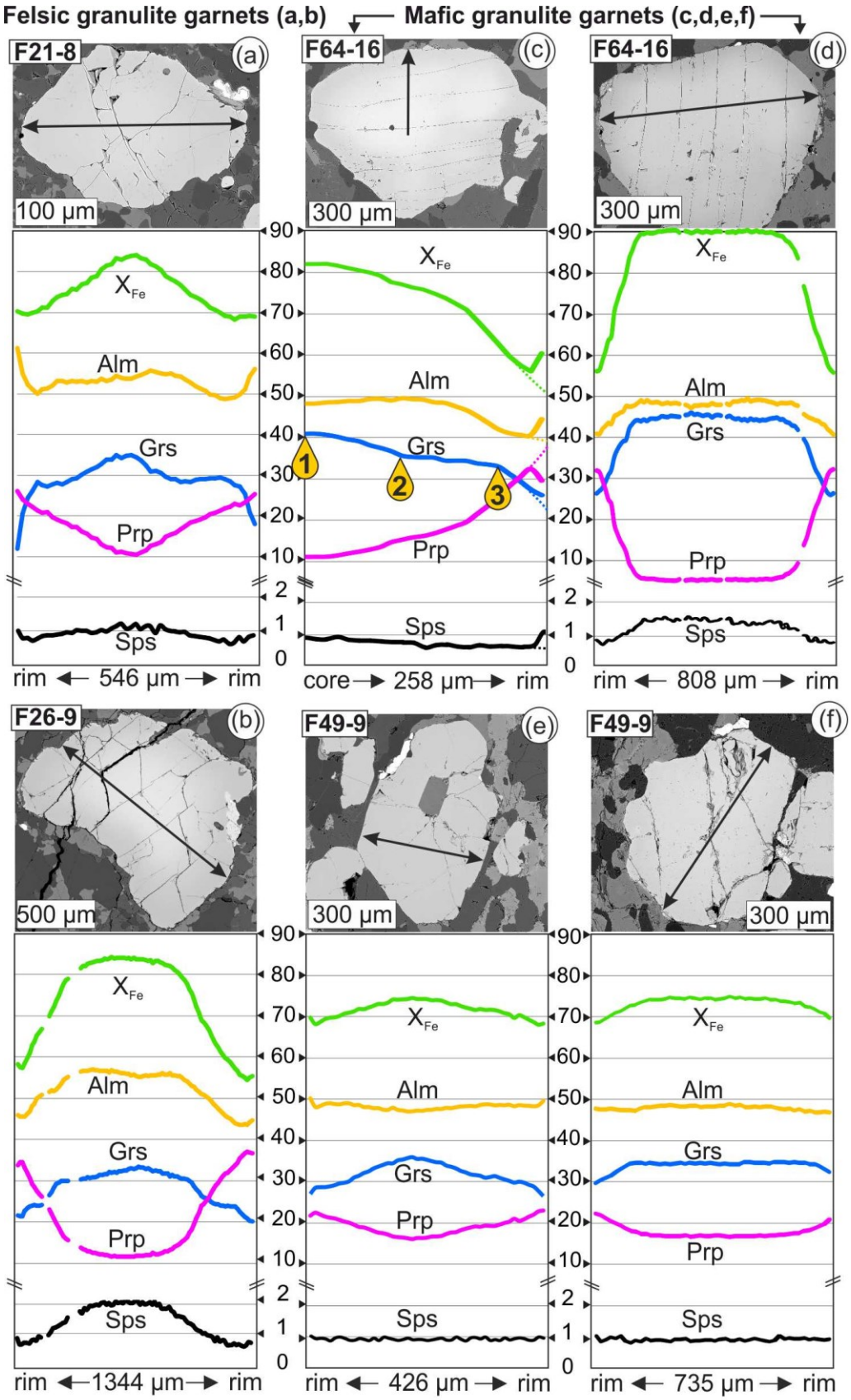

Fig. 6. Back-scattered images and major element profiles of selected garnets from felsic granulites (a, b) and mafic granulites (c-f). Y-axes indicate molar % *100.

3.5.2. Trace element zoning

Garnet from two samples of felsic and mafic granulite were analysed for Y, Na, Ti and P concentrations (Figs. 7, 8). Compositional maps (Fig. 7) indicate a high concentration of yttrium and sodium in the core and their decrease towards the rims in garnets from both felsic and mafic granulites (Fig. 7a, b, e, f). However, titanium concentration trends are not the same for felsic and mafic granulite, respectively. In garnet from the felsic granulite, titanium has a low concentration in the core, while that from mafic granulite has lower values at the rim (Fig. 7c, g). Phosphorus indicates first increase followed by decrease in garnet from felsic granulite, but its content in garnet from mafic granulite is very low and lacks any zoning (Fig. 7d, h).

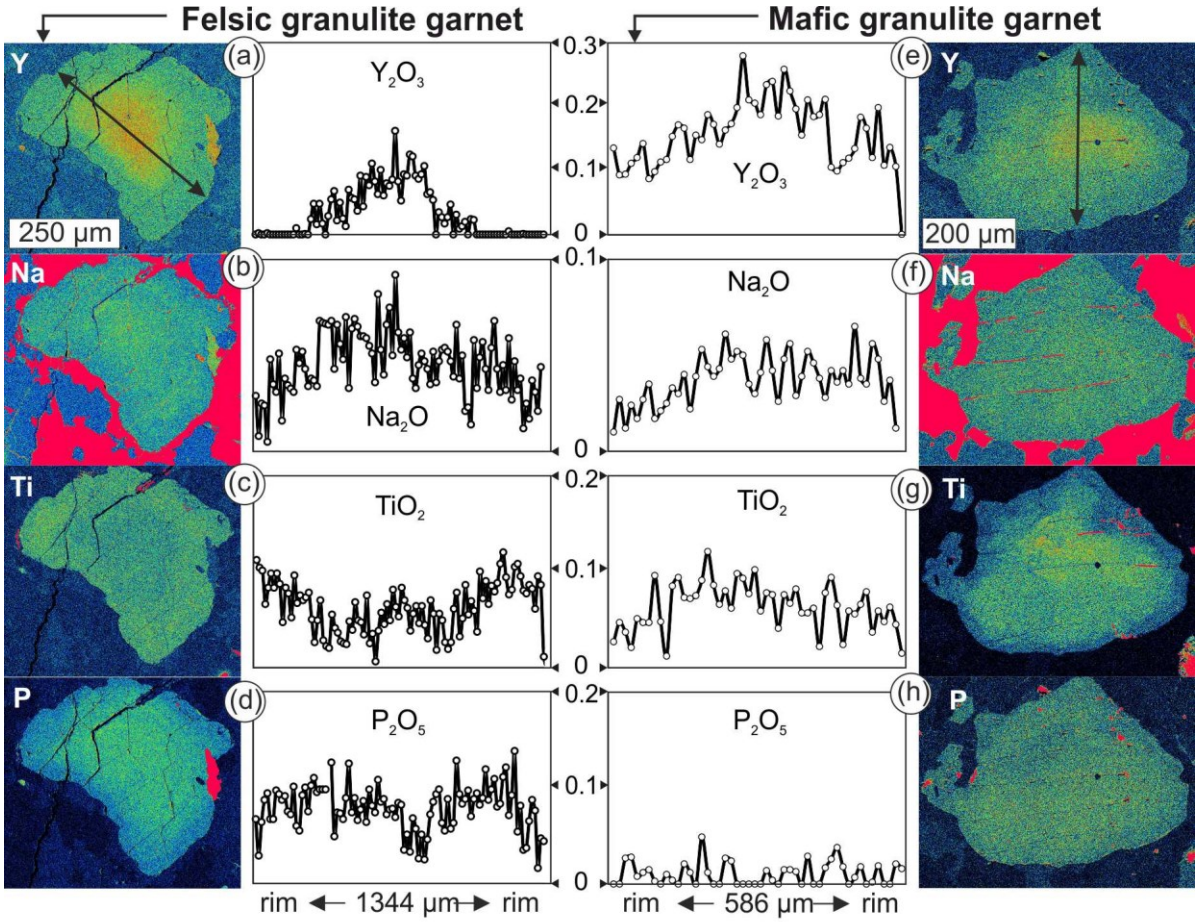

Fig. 7. Compositional maps and profiles of trace elements in garnet porphyroblast from felsic granulite – sample F26-9 (a-d) and mafic granulite - sample F64-16 (e-h). Y-axes indicate wt. %.

The largest garnet with strong major elements and yttrium zoning from felsic granulite (F26-9) was selected for analysing REEs distribution by LA-ICP-MS (Fig. 8). In addition to Y, the heavy REEs (HREEs - Er, Tm, Yb, Lu) values indicate a classical bell-shaped zonation with strong peak in the core that is also characteristic for the spessartine and grossular contents (Fig. 6b). While the middle REEs (MREEs - Ho, Dy, Gd, Tb) indicate rounded crest in the core with abrupt decrease to the rim, the light REEs (LREEs - Nd, Sm, Eu, Ce and Pr) exhibit plateau profiles in the central part followed by a small crest in the mantle part prior to their decrease at the garnet rims. The weak elevation of the LREEs corresponds well with the rapid decrease of grossular content in the mantle part of garnet (Fig. 6b).

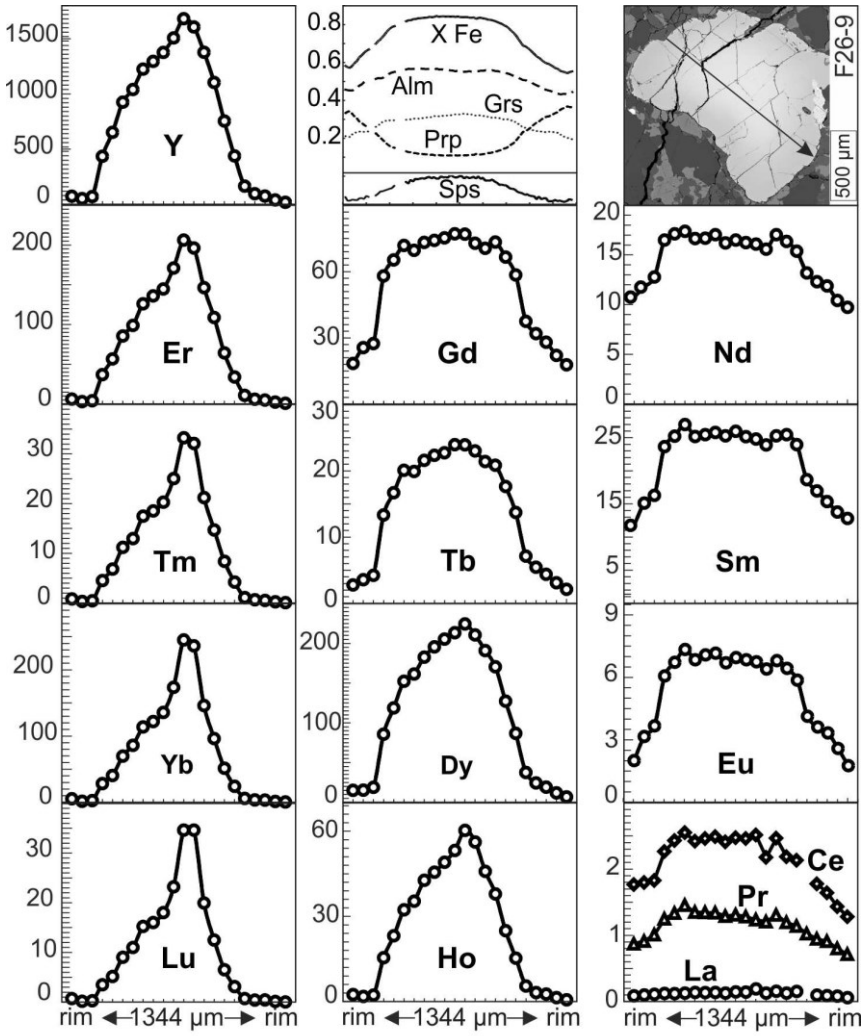

Fig. 8. Compositional profiles of Y+REEs in garnet from felsic granulite (F26-9), measured by LA-ICP-MS; Y-axes indicate concentrations in ppm. The major elements distribution is also shown.

3.6. Compositional zoning in omphacite

Although omphacite is partially replaced by symplectite of plagioclase and diopside that penetrates the grain along thin stripes, it still shows complex compositional zoning (Fig. 9). The concentration of Na, Mg, Al, Ca and Fe usually change at the contact with symplectite or around inclusions. However, long-distance profile set from the jadeite-rich core towards the rim indicates relatively flat profile in the central domain with continuous decrease of Na, Al and increase of Ca, Mg and Fe towards the rim. Relatively strong increase of Ca and Mg at the rim is compensated by decrease of Al and partly by Na. The X_{Mg} ratio of zoned omphacite grains in the matrix decreases from the core (75) to mantle part (74-71) and it is significantly modified at the rim (75) (Fig. 9).

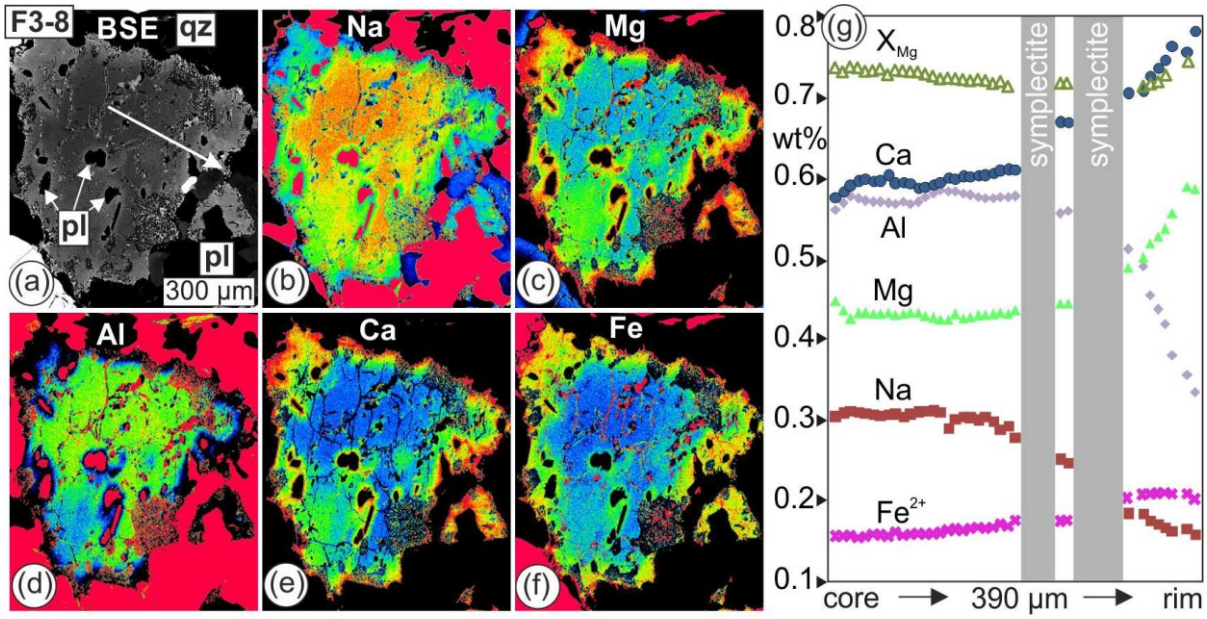

Fig. 9. (a) Back-scattered image, (b-g) compositional maps and major element profile of zoned omphacite grain from mafic granulite (F3-8). Note that the omphacite grain is partially replaced by a symplectite of diopside and plagioclase, which forms thin veins or occurs along the grain boundaries. Major compositional change occurs also at contact with plagioclase inside the omphacite grain. Y-axes in (g) indicate element concentrations in wt. %.

3.7. Tracing the metamorphic P-T path of the Rychleby Mountains granulite

Calculation of P-T conditions in high-grade metamorphic rocks with a HP history suffers from a number of uncertainties, that includes disequilibrium conditions of minerals, lack of precisely determined thermodynamic data for minerals at HP conditions, etc. If the rocks preserve prograde zoned garnet, mineral equilibria modelling, combined with isopleths of mineral compositions, help us to trace the reaction progress and to quantify modification of the measured compositional profiles in minerals from that calculated based on the bulk rock composition. However, it should be noted that Mn, Fe and Mg zoning can be easily modified due to their faster diffusion rates comparing to Ca which has the slowest diffusion coefficient among other major elements in garnet (Carlson, 2006; Chakraborty and Ganguly, 1992). As the rocks reached granulite facies conditions, the P-T estimates can be further complemented by combination with conventional thermobarometry, which uses reactions intersection points of minerals in equilibrium. This may include matrix minerals that have been formed or re-equilibrated during the HT stage in granulite facies conditions. To trace the probable P-T path of the studied rocks during their prograde stage, thermodynamic modelling was undertaken using the Perple_X programs (Connolly, 2005). Mafic granulite with relatively well preserved prograde zoned garnet was chosen for the pseudosection modelling. Textural relationships in these samples also show very low degrees of garnet resorption and omphacite replacement.

3.7.1. Eclogite facies metamorphism

To constrain the P-T path from initial stage to possible peak pressure conditions during eclogite facies metamorphism, the pseudosection method was applied to the samples which contain grossular-rich garnet and inclusions of phengite and/or omphacite, respectively. In addition to changes in mineral assemblage, we wanted to know to what extent the observed compositional profiles in zoned garnet

are modified compared with those predicted by the pseudosection method. Based on data from the literature regarding UHP conditions of the Rychleby Mountains granulite (Bakun-Czubarow, 1992; Kryza et al., 1996) and the presence of omphacite and phengite inclusions, a P-T space in the range of 0.5-3.5 GPa at 400-800 °C was selected (Fig. 10, 11). The calculation was performed for mafic granulite samples F64-16 and F49-9 in the system SiO_2–TiO_2–Al_2O_3–FeO–MgO–CaO–MnO–Na_2O–K_2O–H_2O (KNMnCFMASHT) by Gibbs energy minimisation using the computer program Perple_X, version 6.6.8 (Connolly, 2005) with the internally consistent thermodynamic dataset for mineral end-members and aqueous fluids of Holland and Powell (1998), upgraded in 2004. The following non-ideal solution models were used: garnet (Holland and Powell, 1998), phengite (Coggon and Holland, 2002), biotite (Powell and Holland, 1999), plagioclase (Newton et al., 1980), omphacite (Holland and Powell, 1996), clinopyroxene (Holland and Powell, 1996), ortho- and clino-amphibole (Dale et al., 2005) and chlorite (Holland et al., 1998). Because we have no information about the water content in the protolith of the rocks (if they derived from sediments or from igneous rocks similar to the granitic precursor of the felsic granulite in the Moldanubian Zone), pseudosection calculations were performed with water contents of 1, 2, 5 wt. % as well as with water in excess. Testing of different amounts of water indicated a shift in the modal amount of garnet to lower pressures and temperatures with decreasing water content. In the system with water in excess, garnet starts to nucleate at approximately 400 °C / 0.8 GPa in the presence of hydrous phases (zoisite, amphibole). With increasing pressure, the amount of water is reduced and the modal amount of garnet increases up to the coesite stability field.

Figs. 10 and 11 show the pseudosections and compositional isopleths for samples F64-16 and F49-9 calculated for H_2O = 1 wt. %. This low water content is in accordance with the presence of anhydrous phases (except of phengite) in the eclogite facies stage. The low P-T limit of 400 °C for the pseudosections was selected based on testing of various water contents, where garnet starts to nucleate at ca 0.8 GPa / 400-450 °C in water-saturated system. Both pseudosections are generally similar and the assemblage observed in garnet cores with omphacite, garnet, phengite, kyanite, quartz and rutile is stable above 2.4-1.5 GPa / 400-600 °C (Figs. 10a, 11a). Feldspars are usually present in garnet, but it is not always clear, if they are the original

inclusions or they formed by recrystallization or replacement of former phengite. Omphacite modal content in sample F64-16 decreases with temperature increase and more diopsidic clinopyroxene is stabilized around 550-600 °C (Fig. 10b). The total amount of clinopyroxene does not change markedly in the P-T space above 1.5 GPa and 400-800 °C. The same apply for sample F49-9.

Sample F64-16 containing garnet with the highest grossular content and still preserved the bell-shaped spessartine distribution in the core (Fig. 6d) was used to estimate pressure and temperature conditions for the initial stage of eclogite facies event (Fig. 10). In addition to the slowest diffusion rate of Ca among major elements in garnet (Carlson, 2006; Chakraborty and Ganguly, 1992), the high grossular content with the flat compositional profile (without concentration gradient) allows us to estimate P-T conditions relevant to the initial stage of eclogite facies metamorphism. The garnet content in this sample increases with pressure from about 2 modal % at 0.8 GPa / 400-450 °C to 16 modal % at 3 GPa / 580 °C (Fig. 10c) in a system with limited water content (1 wt. %). This modal amount of garnet (16 modal %) is almost the same as that estimated from image analyses in the investigated sample, which means that almost all garnet was formed during the first prograde stage from low P-T to (U)HP conditions. The grossular content decreases with pressure and temperature increase up to ca 1.2-1.5 GPa / 400-500 °C (Fig. 10d), where around 8 modal % of garnet is formed (Fig. 10c). Considering that the grain size reflects the volume content of garnet, based on the compositional profiles (Fig. 6c, d), most part of garnet was formed during the initial stage of metamorphism. Because of the flat compositional profile (lack of concentration gradient, Fig. 6d), almandine and pyrope contents are also less modified and their isopleths intersect with grossular isopleths (Fig. 10d-f) at around 0.8-0.9 GPa and 460 °C (Point X in Fig. 10a). This point represents P-T conditions for the initial stage of prograde eclogite facies metamorphism. On the other hand, the garnet with the complex zoning profile (Fig. 6c) has lower grossular content in the core that could be either due to the cutting effect or the garnet started to nucleate later at relatively higher pressure and temperature than garnet in Fig. 6d. The stepwise decrease of grossular content in the mantle part of this garnet grain (Fig. 6c) probably signifies the amphibole breakdown reaction boundary at 0.8-1.4 GPa (Fig. 10a). Further

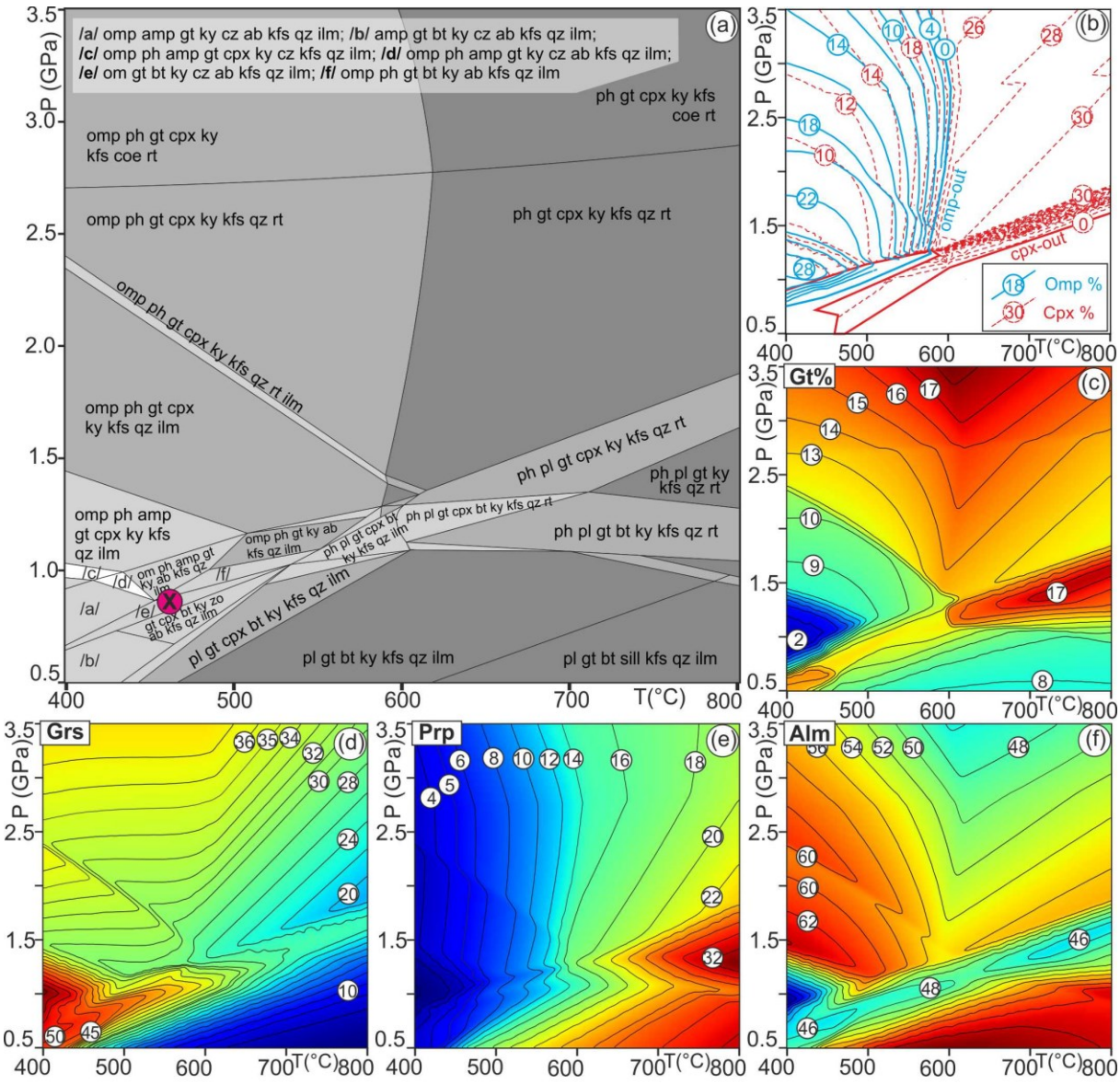

Fig. 10. (a) P-T pseudosection constrained for mafic granulite (F64-16) in the Rychleby Mountains based on the bulk rock composition (in wt. %) of SiO_2=66.48; Al_2O_3=14.11; TiO_2=0.68; FeO=4.65; MnO=0.09; MgO=3.14; CaO=5.35; Na_2O=3.34; K_2O=2.18; H_2O=1.0. Labels for small P-T fields are omitted for clarity. Diagrams with the isopleths of modal % of omphacite and clinopyroxene (b) and garnet (c) are shown as well as isopleths of molar % of grossular (d), pyrope (e) and almandine (f).

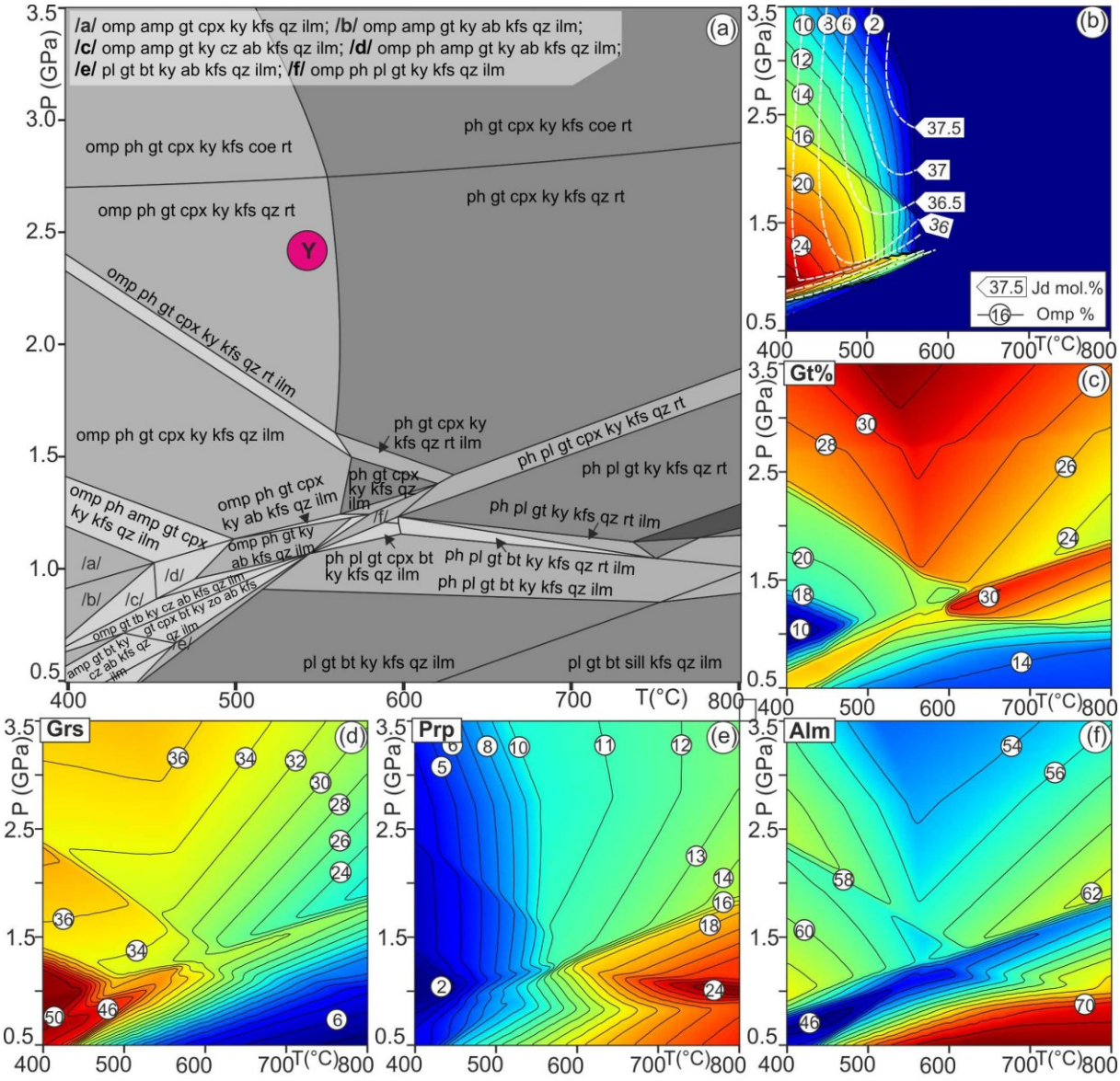

Fig. 11. (a) P-T pseudosection constrained for mafic granulite (F49-9) in the Rychleby Mountains based on the bulk rock composition (in wt. %) of SiO_2=58.64; Al_2O_3=15.59; TiO_2=1.65; FeO=8.52; MnO=0.15; MgO=2.97; CaO=7.16; Na_2O=4.38; K_2O=0.74; H_2O=1.0. Labels for small P-T fields are omitted for clarity. Diagrams with the isopleths of modal % of omphacite (b) and garnet (c) are shown as well as isopleths of molar % of grossular (d), pyrope (e) and almandine (f). In addition, jadeite content in omphacite is shown in (b).

flattening of the compositional profile towards point 3 (Fig. 6c) was probably governed by garnet growth along the grossular isopleths of nearly fixed composition (33-35 mol. %; Fig. 10d) up to the quartz/coesite boundary. The rim part above point 3 with > 25 mol. % of pyrope, < 33 mol. % of grossular and < 42 mol. % of almandine could be formed by increase of temperature (above 700 °C) but at lower pressure to almost 1.5 GPa, while no garnet is formed during temperature increase and pressure decrease based on isopleths modelling from UHP conditions (Fig. 10c). On the other hand, if we compare compositional profiles in Fig. 6c with the calculated isopleths in Fig. 10, we can observe that both pyrope and almandine contents were strongly modified.

As composition of the garnet rim with omphacite in the matrix could be easily modified during HT granulite facies event, garnet with omphacite inclusions in sample F49-9 were used to estimate possible high-pressure and low-temperature conditions reached during eclogite facies stage (Fig. 11). In this sample, the garnet content increases from 10 modal % at 1.0 GPa / 400-450 °C to 30 modal % at 3.0 GPa / 500 °C. The calculated modal content of omphacite in this sample (Fig. 11b) is almost similar to that in sample F64-16 (Fig. 10b) and its decrease to higher pressures and temperatures is compensated by the increase of diopsidic clinopyroxene. The best results were obtained for omphacite inclusion and host garnet in Fig. 4e, which has almost flat central part with high grossular (Fig. 6f). The grossular content in the core of garnet (34 mol. %, Fig. 6f), comparing to that calculated based on the pseudosection (Fig. 11d) suggest that either garnet nucleated later during eclogite facies metamorphism or crystal cut is beyond the core of garnet grain. The grossular isopleths (34-35 mol. %) of garnet intersect the jadeite isopleth (37.5 mol. %) of hosted omphacite inclusion at 2.4-2.5 GPa / 540-560 °C (Point Y in Fig. 11). This point represents the peak pressure of eclogite facies metamorphism, which we are able to calculate by direct textural observations from the natural sample.

3.7.2. Granulite facies metamorphism

To obtain P-T conditions for the granulite facies stage, both pseudosection modelling and conventional geothermobarometry were combined. The granulite facies conditions were treated with zirconium in rutile thermometry (Tomkins et al., 2007) and GASP barometry (Ganguly and Saxena, 1984; Hodges and Crowley, 1985; Hodges and Spear, 1982; Koziol, 1989; Koziol and Newton, 1988) for plagioclase in the matrix and garnet rims in felsic granulite with kyanite. While it is clear that biotite was formed later in the rock, the garnet-biotite thermometry (Perchuk and Lavrent´eva, 1983) was used for biotite in the matrix and garnet rim in felsic granulite. We also used garnet-clinopyroxene thermometry (Ravna, 2000) for diopsidic clinopyroxene in the matrix with garnet rim from mafic granulite. The results listed in Table 3 and 4 and shown in Fig. 12 indicate a temperature range of 800-870 °C for the pressure range of 1.6-1.8 GPa.

Based on the results of GASP barometry, garnet-clinopyroxene and zirconium in rutile thermometry, a pseudosection was calculated in the range of 0.7-2.0 GPa at 750-950 °C with a modified effective bulk rock composition (Fig. 12). Because some material is isolated within already crystallized garnet and/or clinopyroxene during the HP stage and does not participate in the subsequent metamorphic reactions, it is essential to subtract adequate amount of material from bulk rock analyses. This was obtained based on the calculated mineral mode and contents of each element in the microprobe analyses (Konrad-Schmolke et al., 2008a; Stüwe, 1997). Two alternatives of the effective bulk composition (EBC) were used to constrain the pseudosections, the first obtained by subtraction of garnet only and the second by subtraction of both garnet and clinopyroxene.

Fig. 10 shows that about 16 mol. % of garnet was created up to UHP conditions and very small amount of garnet could form at HT conditions (over 700 °C at 1.5 GPa), where pyrope content increases up to 32 mol. % and grossular decreases below 20 mol. %. From this information, we subtracted 90 % of garnet according to profile in Fig. 6c from the bulk rock composition in sample F64-16. A similar approach was used for the additional subtraction of 95 % of clinopyroxene (according to Fig. 9) that changes from 24 to 30 mol. % in the selected P-T range above 1.5 GPa (Fig. 10).

Water content of 0.3 wt. % was calculated based on the modal amount of biotite (up to 5%), that could crystallize during cooling from granulite facies conditions in the presence of melt. The pseudosection calculated using the EBC obtained only by subtraction of garnet shows that only a very small amount of garnet can be formed at temperatures above 800 °C at 1.5-1.7 GPa, but it will be extremely rich in pyrope with low grossular content (Fig. 12). This is consistent with the predicted trend of compositional profile of garnet (Fig. 6c), if assume that the most rim part of the profile was affected by cooling and resorption. Based on these predictions, the calculated isopleths (Grs_{21}, Prp_{38}; Fig. 6c) intersect at ca 1.6-1.8 GPa / 800-870 °C, which is the same as obtained by conventional thermobarometry (Fig. 12). Using an EBC with additional subtraction of clinopyroxene will result in the formation of Mg-richer garnet, but its molar amount remains largely unchanged. The high compositional gradient of Mg in the system can be easily modified at the rim of garnet and will accelerate diffusion across the garnet profile, depending on the rate of diffusion coefficients from the fastest to slowest elements: Mn, Mg, Fe, Ca (Chakraborty and Ganguly, 1992). Calculation of a pseudosection using of EBC obtained by subtraction of both garnet and clinopyroxene, yields very low grossular content (about 6 mol. %) at 800 °C / 1.5 GPa.

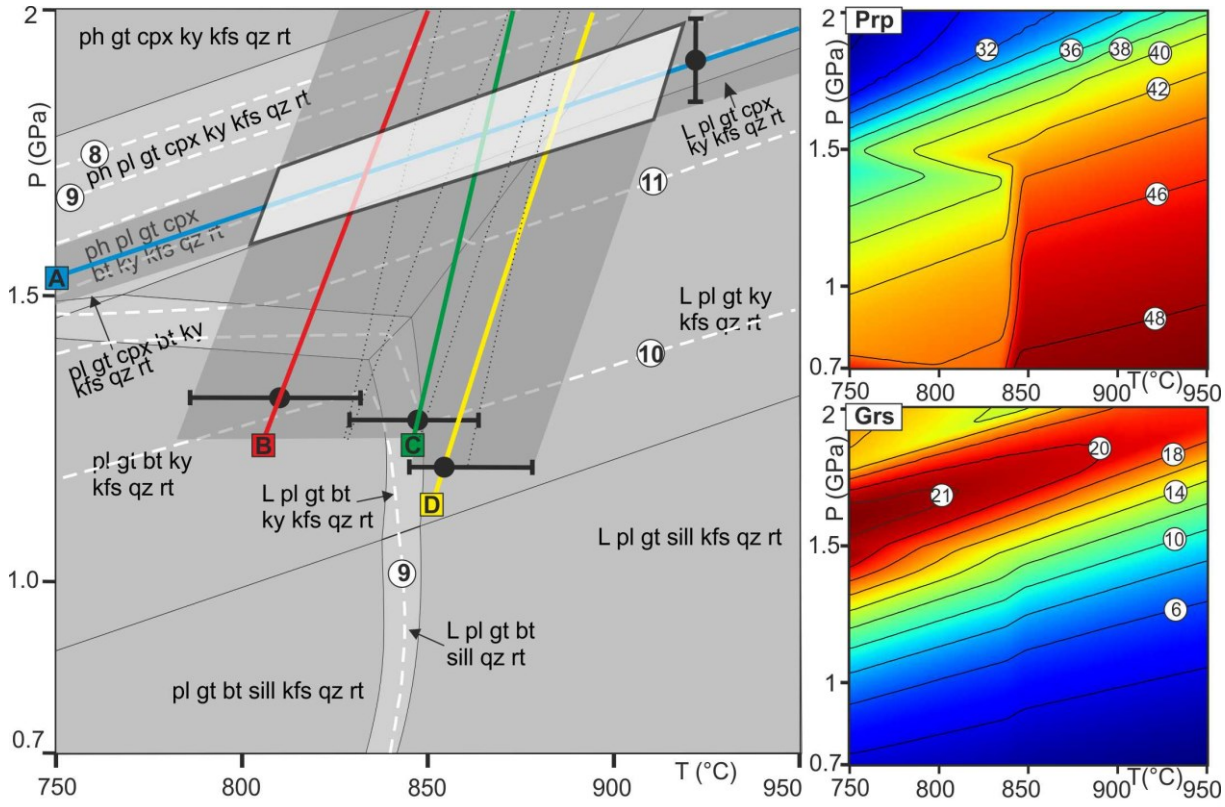

Fig. 12. High-temperature P-T pseudosection for mafic granulite (F64-16) in the Rychleby Mountains constrained for an effective bulk composition (in wt. %): SiO_2=71.53; Al_2O_3=12.67; TiO_2=0.80; FeO=1.69; MnO=0.05; MgO=2.59; CaO=4.16; Na_2O=3.95; K_2O=2.18; H_2O=0.3. Dashed lines show modal % of garnet, thick solid lines (A-D) point out temperature and pressure conditions with range bars based on the results of thermobarometry in Table 3 and 4. Labels for small P-T fields are omitted for clarity. Diagrams show isopleths of pyrope and grossular contents.

Table 3: Selected chemical analyses used for conventional thermobarometry and its results.

Sample	F26-9	F49-9	F49-9	F49-9	F49-9	F26-9	F26-9
used for	GASP, gt-bt	gt-px	gt-px	gt-px	gt-px	gt-bt	GASP
mineral	gt1	gt2	gt3	px1	px2	bt	pl
SiO_2 *(wt. %)*	39.21	38.50	38.84	53.18	50.70	37.16	62.60
TiO_2	0.11	0.09	0.08	0.43	0.44	4.16	-
Al_2O_3	22.15	21.6	21.79	8.56	6.80	15.13	21.81
FeO	21.36	21.9	22.2	8.12	9.16	14.77	0.07
MnO	0.41	0.41	0.47	-	-	0.05	-
MgO	8.71	5.85	6.12	9.05	10.30	12.55	-
CaO	7.64	10.28	9.92	17.09	21.32	0.01	4.73
Na_2O	-	0.03	0.04	4.18	1.71	0.08	8.17
K_2O	-	-	-			9.97	0.4
Total	99.62	98.73	99.46	100.65	100.47	94.23	97.76
Si *(per ox.)*	2.996	3.005	3.007	1.928	1.874	2.912	2.852
Ti	0.006	0.006	0.005	0.012	0.012	0.245	-
Al	1.993	1.990	1.989	0.366	0.297	1.397	1.171
Fe	1.358	1.432	1.439	0.198	0.229	0.968	0.003
Mn	0.026	0.027	0.031	0.489	0.568	0.003	-
Mg	0.990	0.681	0.706	0.664	0.844	1.465	-
Ca	0.625	0.86	0.823	0.294	0.122	-	0.231
Na	-	-	-			0.012	0.722
K	-	-	-	-	-	0.997	0.022

GASP barometry - reaction (A) in Fig. 11

Temperature	HS82	GS84	HC85	K89	KN88
850 °C	1.59 GPa	1.77 GPa	1.72 GPa	1.77 GPa	1.88 GPa

garnet-pyroxene thermometry (R2000) - reaction (B) in Fig. 11

Pressure	gt2-px1	gt2-px2	gt3-px1	gt3-px2
1.75 GPa	825 °C	824 °C	827 °C	825 °C

garnet-biotite thermometry (PL83) - reaction (C) in Fig. 11

Pressure	PL83
1.75 GPa	864 °C

GS84=Ganguly and Saxena, 1984; HC85=Hodges and Crowley, 1985; HS82=Hodges and Spear, 1982; K89=Koziol, 1989; KN88=Koziol and Newton, 1989; PL83=Perchuk and Lavrent´eva, 1983; R2000=Ravna, 2000

Table 4: Chemical analyses of rutile grains used for Zr-in-rutile thermometry and its results.

	rt1	rt2	rt3	rt4	rt5	rt6	rt7	rt8	rt9	rt10	rt11	detect. limit (ppm)
TiO_2 (wt. %)	98.72	98.44	98.96	99.04	97.48	98.91	98.77	98.91	99.28	99.17	98.66	73
Zr (ppm)	2100	2160	2100	2130	2040	2320	2050	2680	2130	2240	2090	37
Fe (ppm)	2380	3150	2000	1700	6790	2080	2700	2300	1880	2180	2690	38
Si (ppm)	390	260	220	200	360	160	220	210	170	240	220	72

P (GPa)	T (°C) at different pressures calculated for each grain (line D in Fig. 12)											average T
1.0	838	841	838	840	835	850	835	867	840	846	838	843
1.5	864	867	864	866	861	876	861	894	866	872	863	869
2.0	890	893	890	892	886	902	887	920	892	898	889	895

3.8. Discussion

3.8.1. Pre-granulite facies history and preservation of prograde zoning in garnet in the Rychleby Mountains granulite

Similar to other granulite bodies in the Moldanubian Zone, only cooling and decompression P-T paths from UHP-UHT conditions were proposed for granulite in the Rychleby Mountains (Bakun-Czubarow, 1992; Budzyń et al., 2015; Kryza et al., 1996; Pouba et al., 1985; Štípská et al., 2004). In addition to mineral inclusions, the prograde metamorphic history in both felsic and mafic varieties of granulite is confirmed by the distribution of major and trace elements in garnet. The classic bell-shaped pattern of major and some trace elements is considered to occur due to strong affinity of these elements into garnet and also as the result of fractionation-depletion mechanism during garnet growth (e.g. Hollister, 1966; Otamendi et al., 2002; Tracy, 1982; Tracy et al., 1976). In contrast to garnet from granulite in the Kutná Hora Complex (Jedlicka et al., 2015), we did not observe annular peaks of Y+HREEs near the rim of garnet crystals in the study samples (Fig. 13). The annular peak in garnet from the Kutná Hora granulite is interpreted as the result of two stages of garnet growth that occurred during HP-UHP metamorphism and subsequent granulite facies overprint. The first garnet, formed during the HP-UHP event, was partially consumed during exhumation of the rocks, where Y+HREEs released from the resorbed garnet into the matrix were incorporated back into garnet during the second stage in granulite facies conditions in lower to middle crustal positions. The lack of annular peaks in garnet from the Rychleby granulite suggests its formation by a single HP-UHP event, where almost all garnet (ca 16 modal %, Fig. 10 and also observed in thin-section) was created. If a small amount of garnet was formed during the granulite facies stage, it could continuously overgrow the HP garnet without resorption of the core garnet or enrichment of the system by REEs from an external source by fluid or melt. In comparison with the Rychleby Mountains, the granulite in the Kutná Hora shows higher

temperature during granulite facies overprint with formation of leucocratic layers as result of partial melting (Nahodilová et al., 2011) and overgrowth of granulite facies garnet with annular peaks of Y+REEs (Jedlicka et al., 2015). Higher temperature and degree of granulite facies overprint was responsible for local garnet resorption-regrowth in the Kutná Hora Complex.

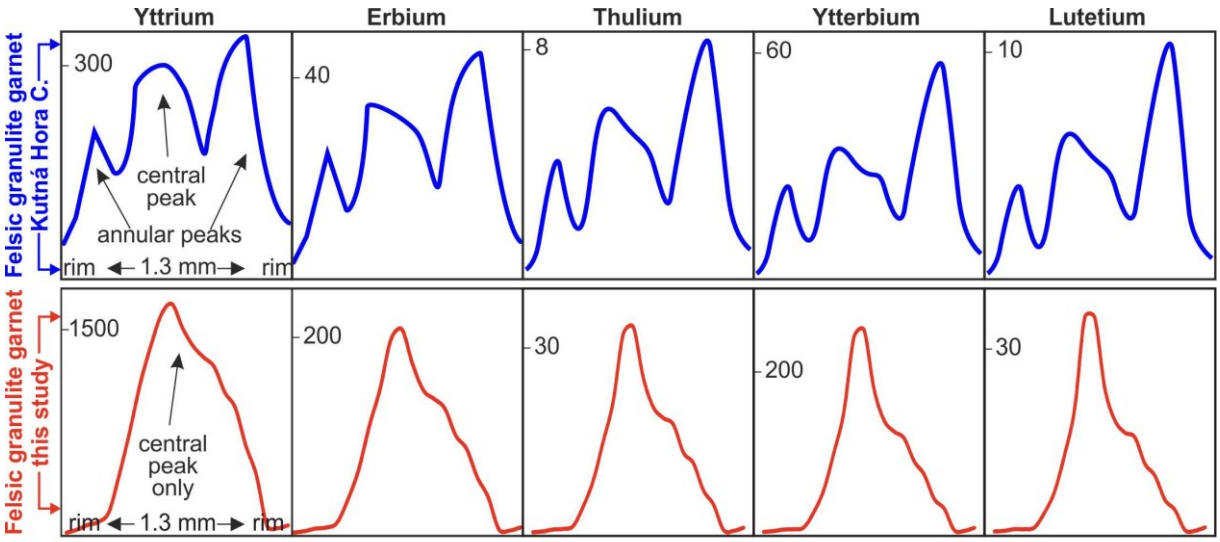

Fig. 13. Comparison of Y+HREEs distribution in garnet from the Rychleby Mountains felsic granulite (this study) and in garnet with two annular peaks from Kutná Hora Complex felsic granulite in the Moldanubian Zone (Jedlicka et al., 2015).

The preservation of prograde zoning in garnet is an important attribute for constraining P-T history and geodynamic reconstruction of the subduction and/or collision zone. In contrast to the slow diffusion rates of Y and REEs in garnet (Carlson, 2012; Carlson et al., 2014), the major elements (mainly Mn) can be easily homogenized, if the rocks experienced high temperature overprint (Carlson, 2006; Chakraborty and Ganguly, 1992; Vielzeuf et al., 2007). Considering that the Rychleby granulite reached pressure conditions in the stability field of coesite (Bakun-Czubarow, 1992; Kryza et al., 1996), two alternative scenarios exist to explain the exhumation of felsic rocks from the mantle depth and their subsequent granulite facies metamorphism. 1) peak temperatures were already reached during peak pressure conditions and then the rocks were exhumed by isothermal decompression (path 1 in Fig. 14) to depths comparable to ca 1.5-1.8 GPa (Bakun-Czubarow, 1992; Budzyń et al., 2015; Kryza et al., 1996; Štípská et al., 2004). Such a P-T path would however

result in total homogenisation of prograde compositional zoning in garnet (Carlson, 2006; Chakraborty and Ganguly, 1992; Vielzeuf et al., 2007); 2) heating to granulite facies conditions after partial decompression (path 2 in Fig. 14). A similar P-T path was constrained for felsic granulite in the Kutná Hora Complex (Jedlicka et al., 2015). The short-term heating during decompression was the reason for the preservation of the bell-shaped zonation even for Mn which has the fastest diffusion coefficient among other elements in garnet. There is a general agreement that further exhumation from the granulite facies stage occurred by cooling of the rocks back to amphibolite facies conditions of 600-650 °C / 0.4-1.1 GPa (Klemd et al., 1995) which were similar to that in the surrounding orthogneiss.

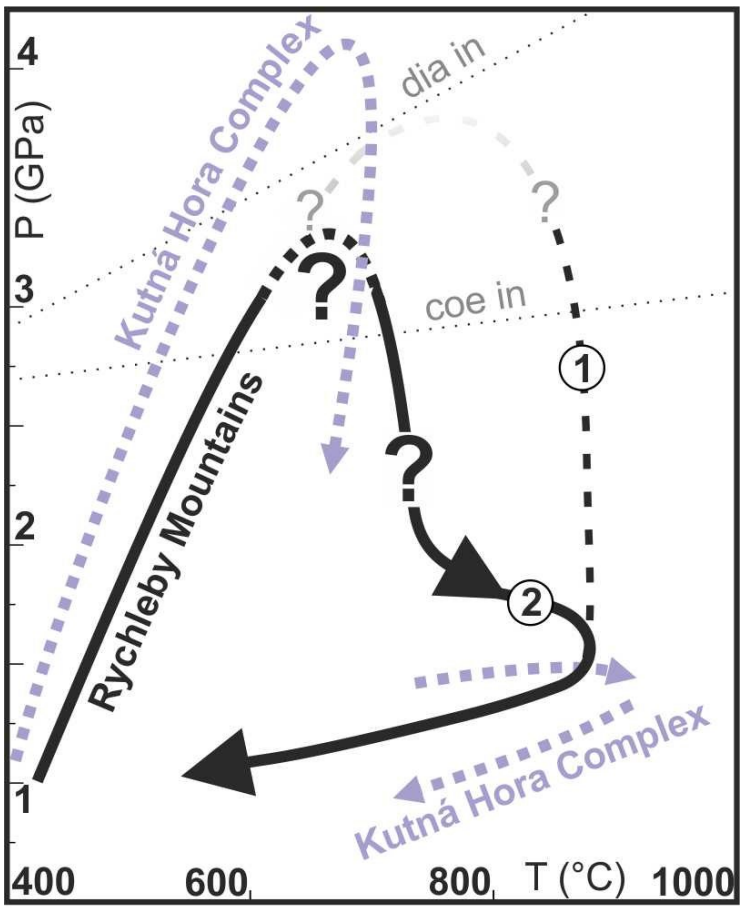

Fig. 14. Inferred P-T path (2) for mafic and felsic granulites from the Rychleby Mountains. The dashed curve (1) to high-temperature conditions is an alternative P-T path based on the data from literature (see text for discussion). P-T path of granulites from the Kutná Hora Complex (Jedlicka et al., 2015) is indicated for comparison.

3.8.2. Geodynamic implication

Recent studies of felsic granulite in the Gföhl Unit of the Moldanubian Zone (Faryad et al., 2010b; 2015; Jedlicka et al., 2015; Perraki and Faryad, 2014) and from some eclogites in the Monotonous and Variegated units (Faryad and Fišera, 2015; Scott et al., 2013) showed that they both experienced an earlier HP-UHP event and were subsequently overprinted by granulite-amphibolite facies metamorphism in lower and middle crustal positions at 0.7-1.5 GPa. Except for granulite of the Kutná Hora Complex, where prograde zoned garnet with phengite inclusions was observed, most granulites are strongly re-equilibrated and their earlier HP history is difficult to establish (for ref. see Faryad and Žák, 2016). In most cases, the eclogite bodies within granulite were interpreted as result of tectonic imbrication of rocks, which differs in their metamorphic history (Nakamura et al., 2004; Medaris et al., 2006). The close spatial and textural relations between mafic and felsic granulites in the Rychleby Mountains indicate that they both underwent prograde eclogite facies metamorphism and were subsequently overprinted by the granulite facies metamorphism. The presence of omphacite in the matrix and strong compositional zoning in garnet, even in small grains in granulite, suggest that the granulite facies recrystallisation and mineral modification was relatively weak. On the other hand, the presence of ternary feldspars in some parts of the granulite body, e.g. near Stary Gierałtów (Kryza et al., 1996, Fig. 1b) suggests that the whole body was not heated or recrystallised uniformly. Variation in the intensity of recrystallisation and re-equilibration was also recognized in the Kutná Hora granulite body (3x9 km in size). The prograde zoned garnet with phengite inclusions was observed in the central domains of the body, where partially serpentinised boudins of garnet peridotite with garnet pyroxenite are also present.

The two stage metamorphic history of the Rychleby granulite, the first at HP-UHP and the second in MP granulite facies conditions suggests their common geodynamic evolution with granulites in the Moldanubian Zone for which a similar P-T path was constrained (Jedlicka et al., 2015; Faryad and Žák, 2016). In the Moldanubian Zone, granulite facies metamorphism is assumed to have occurred after exhumation of the HP-UHP rocks by a syn-convergent mechanism (Chemenda et al., 1995) into

lower-middle crustal positions (Faryad et al., 2015). The heat source for this short-lived granulite facies metamorphism is explained by slab break-off and mantle upwelling triggering melting and emplacement of magma in a lower stress field beneath the accretionary complex. Based on geochronological data, the emplacement of mafic-ultramafic magma (norite, troctolite, gabbro) occurred in various crustal levels between 360–340 Ma (Faryad et al., 2015; 2016). Extreme heating, produced by mafic-ultramafic intrusions, resulted in granulite facies overprint of the already exhumed HP-UHP bodies and migmatisation of their host lithologies. After this short-lived thermal process (Faryad and Fišera, 2015; Jedlicka et al., 2015), the high-grade rocks were transported to the upper crustal levels due to the subduction of the Rheic oceanic plate (Finger et al., 2007) and subsequent tectonic underplating of the Brunovistulian Block beneath the Moldanubian Zone (Schulmann et al., 2005).

Relation of the Rychleby Mountains and the Góry Sowie Block to other geological units in the Bohemian Massif is interpreted in different ways. Aleksandrowski and Mazur (2002) in their tectono-stratigraphical model interpreted the OSD as a part of the Moldanubian terrane. The Góry Sowie Block is considered as a separate block, which collided with the OSD at around 370 Ma and later merged with the West Sudetes (the Saxothuringian Zone) to the west and Brunovistulian Block to the east (Mazur et al., 2006). According to Kröner and Hegner (1998) the Góry Sowie Block is a klippe of the Moldanubian Zone. A model of buckling of thickened crustal layers due to lateral shortening, similar to that assumed for granulites in the Moldanubian Zone (Schulmann et al., 2005) is considered also for the Rychleby granulite by Štípská et al. (2004). As regional correlation of geological units needs a multidisciplinary approach with various information about stratigraphy, magmatism, geophysics, etc., this is outside the scope of this contribution. However, the P-T history of the granulite from the Rychleby Mountains with their subduction-related metamorphism and subsequent granulite facies overprint is similar to that in the Moldanubian Zone. They could be formed and exhumed along the Moldanubian suture, which is assumed to continue across all basement massifs along the European Variscan Belt from the Bohemian Massif to the Iberian Massif in the southwest (Faryad et al., 2015; Franke, 2000). The East Sudetes with HP granulite in the Rychleby Mountains and Góry Sowie might indicate a triple point of three suture zones, the Moldanubian,

Saxothuringian and the Rheic sutures. Although the timing of subduction of crustal rocks could vary along the Variscan Belt, the UHP rocks with granulite facies overprint indicate close similarity with those in the Moldanubian Zone. The difference in age data mainly of zircon from felsic granulite in the eastern part of the Moldanubian Zone (about 340 Ma), in the Kutná Hora Complex (up to 365 Ma) and up to 369 Ma in the Rychleby Mountains could be due to different degree of recrystallisation of HP rocks during granulite facies overprint.

3.9. Conclusions

Mineral and textural relations in felsic and mafic granulites from the Rychleby Mountains in the East Sudetes indicate that they both shared a common metamorphic history from their HP conditions and preserve evidence of the earlier HP metamorphism despite subsequent granulite facies overprint. This is documented by:

1. Preservation of omphacite in the matrix of mafic granulite, which forms thin, centimetre- to decimetre- scale, layers within felsic granulite. Garnet from both felsic and mafic varieties contains inclusions of phengite and show prograde zoning related to the eclogite facies event.

2. Thermodynamic modelling of the compositional zoning in garnet suggests a steep geothermal gradient in a subduction environment from its initial stage (0.8-0.9 GPa / 460 °C) up to HP-UHP conditions (2.4-2.5 GPa / 550 °C). Trace elements zoning in garnet, including REEs, does not show annular peaks, which might signify garnet overgrowth during granulite facies overprint. This is confirmed by observed and calculated modal contents of garnet which indicates that almost all garnet was formed during the eclogite facies stage.

3. The granulite facies overprint occurred within crustal levels at ca 1.6-1.8 GPa 800-870 °C, but it was too short to recrystallize the rocks and to homogenize garnet both in felsic and mafic varieties.

4. The results of this study indicate a close similarity between the metamorphic history of granulite in the Rychleby Mountains with those in the Moldanubian Zone.

3.10. Acknowledgement

This work was supported by the Czech Science Foundation (research project number 13-06958S), the Charles University (project GA UK no. 243-250373) and by institutional project Progres Q45. The authors thank M. Svojtka (Czech Academy of Sciences) for his help with LA-ICP-MS analyses of garnet and S. Collett for English correction of the manuscript. We gratefully acknowledge constructive reviews by E. Skrzypek and an anonymous reviewer. M. Scambelluri is thanked for careful editorial handling.

PART VI

SUBDUCTION OF LITHOSPHERIC UPPER MANTLE RECORDED BY SOLID PHASE INCLUSIONS AND COMPOSITIONAL ZONING IN GARNET: EXAMPLE FROM THE BOHEMIAN MASSIF

Shah Wali Faryad[1], Radim Jedlička[1], Karl Ettinger[2]

[1]Institute of Petrology and Structural Geology, Charles University in Prague, Albertov 6, 12843 Prague, Czech Republic

[2]Institute of Earth Science, University of Graz, Universitätplatz 2, 8010 Graz, Austria

Abstract

This paper presents monomineral and multiphase inclusions in garnet from eclogites and clinopyroxenites, which form layers and boudins in garnet peridotites from two areas in the Moldanubian Zone of the Bohemian Massif. The garnet peridotites occur in felsic granulites and reached UHP conditions prior to their granulite facies overprint. In addition to complex compositional zoning, garnets from hosting eclogites and clinopyroxenites preserve inclusions of hydrous phases and alkali silicate minerals including: amphiboles, chlorites, micas and feldspars. Amphibole, biotite and apatite inclusions in garnet have a high concentration of halogens; CO_2 and sulfur are involved in carbonates and sulfide inclusions, respectively. The inclusion patterns and compositional zoning in garnet in combination with textural relations among minerals, suggest that the ultramafic and mafic bodies are derived from lithospheric mantle above the subduction zone and were transformed into garnet pyroxenites and eclogites in the subduction zone. Based on compositional, mineral and textural relations, all of these rocks along with the surrounding crustal material were overprinted by granulite facies metamorphism during their exhumation.

Keywords: *Bohemian Massif, eclogite, garnet pyroxenite, multiphase inclusions, petrology, tectonics,*

4.1. Introduction

Recent progress in high- to ultrahigh-pressure (HP/UHP) metamorphic rocks, exposed along orogenic zones on the Earth, has significantly improved our knowledge about the depths reached by crustal and mantle rocks during subduction (for references see Dobrzhinetskaya, 2012; Dobrzhinetskaya and Faryad, 2011; Ernst and Liou, 2000; Liou et al., 2009). As the crustal basement rocks are dragged down the subduction channel along with sediments, origin of mafic, but mainly ultramafic rocks is not always clear, whether they are part of oceanic crust and depleted mantle or they are derived from mantle wedge above the subduction zone. Understanding of the geotectonic position of the source area of HP rocks and their P–T paths are essential for geodynamics of convergent plate tectonics (e.g. Brueckner, 1998; Brueckner and Medaris, 2000; Medaris et al., 2005; Oncken et al., 2007; Sempere et al., 2008; van Roermund, 2009; Sajeev et al., 2012; Schellart and Rawlinson, 2010). To define source material from which the rocks were derived, conventional geochemical and isotope analyses are usually used (Carlson and Irving, 1994; Demidjuk et al., 2007; Smith, 2003). These methods provided valuable information about the geotectonic position of the rocks. However, it was also shown that the overlying mantle wedge above the subduction zone is usually affected by fluid flux and melt, derived from the subducting slab (Bebout, 2003; Bebout et al., 1999; Hilton et al., 2002; Sadofsky and Zheng et al., 2003; Zhang et al., 2009). Therefore, the major and trace elements as well as the isotopic system may or may not accurately reflect the chemical signatures of the mantle wedge. Additional changes in geochemistry of these rocks can occur during their exhumation, because these rocks are usually surrounded by various lithologies, mostly sedimentary material that was subjected to metamorphism and dehydration. On the other hand, several studies of UHPM rocks indicated that relict minerals and their inclusions provide significant information to trace the metamorphic path of the rocks from their original stage through subduction and exhumation (e.g. Liu et al., 2001; Sobolev and Chopin, 1995; Zhang et al., 2006).

The Moldanubian Zone of the Bohemian Massif provides the best opportunity to study the mantle peridotites and eclogites, which occur as lenses and boudins

in felsic granulites. Geotectonic position of the source material of the eclogites, garnet peridotites and garnet pyroxenites is interpreted by different ways. Based on geochemistry and P–T conditions, Medaris et al. (2005) classified the eclogites and peridotites in two main groups. The first group is represented by peridotites and associated eclogites that are derived from subcontinental lithospheric mantle having medium to high P–T regime. The second group is formed from depleted oceanic mantle and MORB type basalts and they show low to medium P–T regime. Based on geochemistry, Obata et al. (2006) argued that some kyanite-bearing eclogites from the first group (from Nové Dvory in this study), for which UHP conditions were estimated (Nakamura et al., 2004), were derived from cumulate gabbros. Carswell (1991) interpreted garnet peridotites and garnet pyroxenites with garnet exsolution lamellae in pyroxene from Dunkelsteinerwald (Lower Austria) as a result of cooling and pressure increase from shallow levels of the mantle. This paper focuses on the occurrence and composition of solid phase inclusions and their host minerals from UHP eclogites, garnet pyroxenites and garnet peridotites to decipher the origin and metamorphic crystallization of these rocks. Two areas with garnet peridotites and eclogites in Dunkelsteinerwald (Lower Austria) and in Nové Dvory (south Moravia) were selected for this research. The results are used to localize the geotectonic positions of the source materials and their subsequent metamorphic history.

4.2. Geological setting and sampling

The Moldanubian and the Saxothuringian Zones of the Bohemian Massif are represented by the presence of amphibolite to granulite facies basement rocks that are intruded by Variscan granitoids (Fig. 1). Both Zones surround and underplate the Teplá–Barrandian Block from the northwest and southeast, respectively. In contrast to the Teplá–Barrandian Block with low- to medium- grade metamorphic sedimentary sequences, the Moldanubian and the Saxothuringian Zones are characterized by the presence of lenses of eclogites and garnet/spinel peridotites within gneisses and felsic granulites. In the Moldanubian Zone, lenses of spinel

peridotites and medium temperature eclogites occur in the medium-grade rocks (the Monotonous and Varied groups), while the high-grade rocks (the Gföhl Unit) contain lenses and boudins of garnet peridotites and high temperature eclogites. Most of the granulites with garnet peridotites and eclogites are exposed along the eastern border of the Moldanubian Zone, but some occur also in the western border of this Zone (Fig. 1).

The felsic granulites reached HP/UHP conditions (Faryad et al., 2010b; Klemd and Bröcker, 1999; O'Brien, 2008). They consist of ternary feldspar, quartz, garnet, kyanite and rutile and show various degrees of re-equilibrium through medium- to low- pressure conditions. Some mafic varieties may contain clino- and ortho-pyroxene. Well preserved mafic granulites may contain omphacite as a relic phase from eclogite stage. UHP conditions of 4–5 GPa and 1000–1200 °C for garnet peridotites and eclogites were estimated based on mineral compositions (Faryad, 2009; Medaris et al., 1990, 2006; Nakamura et al., 2004; Vrána and Frýda, 2003). They contain relicts of olivine, orthopyroxene, clinopyroxene and garnet, which form porphyroblasts (reaching 5 mm in size) with kelyphitic coronas of orthopyroxene, spinel and amphibole. In addition to boudins of eclogites, the garnet peridotites contain layers or veins of garnet clinopyroxenites. In some cases, they preserve a coarse-grained variety with porphyroclasts of clinopyroxene, which have exsolution lamellae of garnet+orthopyroxene with ilmenite rods. Unmixing and exsolution of garnet+pyroxene occurred due to cooling and pressure increase from 1400-1300 °C / 2.2-2.5 GPa to 1100–900 °C / 4.5-5.0 GPa (Faryad et al., 2009).

The studied garnet peridotites, garnet clinopyroxenites and eclogites come from Dunkelsteinerwald (Austria) and from Nové Dvory (Czech Republic) (Fig. 1b, c). In the Dunkelsteinerwald, the rocks occur within felsic granulites, which are exposed south of the Danube River near Krems an der Donau. The garnet peridotites are highly deformed with a platy fabric affected by late-stage serpentinization. Boudinaged layers or lenses of pyroxenites within the peridotites are relatively unaltered and preserve high-pressure garnet–clinopyroxene assemblages (Carswell, 1991). Garnet peridotites have composition of lherzolite, harzburgite, and rarely of dunite (Becker, 1997a, 1997b).

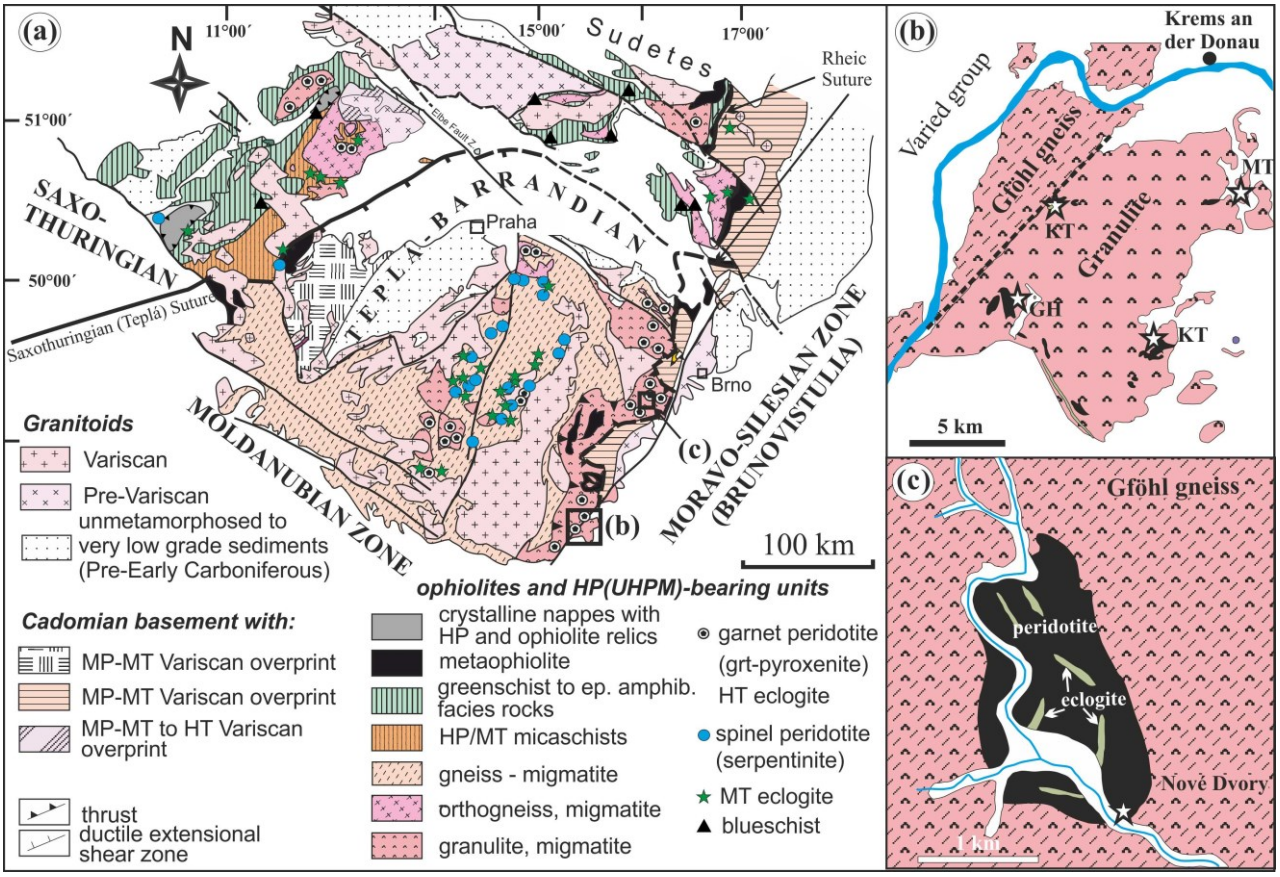

Fig. 1. Schematic geological map of the Bohemian Massif (a) [modified from Franke (2000), Willner et al. (2002), Cháb et al. (2007), Faryad and Kachlík,(2012)] with location (squares) of the studied area from Dunkelsteinerwald (b) and Nové Dvory (c). Sample locations: GH - Gurhof, KT - Karlstetten, MT - Meidling im Tal, PG - Plaimberg.

Garnet clinopyroxenites occur as millimeter to decimeter thick layers within garnet peridotites. Most of them show relatively sharp contacts with the host garnet peridotites. Garnetites with more than 90 vol. % of garnet are also present within peridotites (Becker, 1997a, 1997b). Based on the exsolution lamellae of garnet in orthopyroxene, Carswell (1991) assumed cooling and pressure increase from 1350 °C / 2.2 GPa to 1000 °C / 3.3 GPa. Samples selected for this study come from four localities (Fig. 1b): Meidling im Tal (peridotite–clinopyroxenites, samples M-6/IEC and DS27D), Karlstetten (peridotites, samples K1-IEC, K9-IEC, and K14-IEC), Plaimberg (clinopyroxene-rich eclogite or garnet-rich clinopyroxenite, sample DS-27E) and from Gurhof (eclogite, sample F15-10 and garnet clinopyroxenite, sample F12-10). The peridotite block at Nové Dvory is serpentinized garnet lherzolite (Medaris et al.,

1998) within migmatitic and granulite gneisses. It contains several large (up to 500 m long) lenses of eclogite (Fig. 1c) and thin layers of clinopyroxenite. UHP conditions for both garnet peridotites (5.5 GPa / 1100 °C) and for eclogites (5 GPa / 1000 °C) were estimated by Medaris et al. (1998) and Nakamura et al. (2004), respectively. Clinopyroxenites from this locality show exsolution lamellae of garnet in clinopyroxene and, similar to that in the Dunkelsteinerwald, a P–T path with cooling and pressure increase from 1300 °C / 2.5 GPa to 900 °C / 4 GPa was estimated (Faryad et al., 2009). Samples selected for this study are from garnet peridotites (F46-6) and from eclogites (D6-11, D8-11, D9-11 and D12-11), exposed in the southern part of the peridotite body (Fig. 1c).

4.3. Petrology of investigated samples

4.3.1. Peridotite

The rocks are strongly serpentinized, but relatively well preserved parts show inequigranular texture with porphyroblasts of garnet (up to 1 cm in size), that occurs in a medium- to fine- grained matrix with relicts of olivine, clino- and orthopyroxenes. Some samples may contain red-brown spinel, which occurs as inclusion in garnet (Fig. 2a, b). Garnet is surrounded by an inner, fine-grained pyroxene–spinel kelyphite and an outer, fibrous amphibole–spinel kelyphite. In some cases, the garnet porphyroblasts are totally replaced by kelyphite. If the garnet peridotite contains layers of pyroxenite, it may have a foliation, which is parallel to the pyroxenite layers. Garnet may contain inclusions of olivine and pyroxene.

4.3.2. Clinopyroxenite

Clinopyroxenite occurs in both areas, where it forms layers or veins in garnet peridotites. The layers and veins have a thickness from millimeters to several centimeters. In the Nové Dvory, they may have a porphyroclastic texture with relicts

of large igneous clinopyroxene porphyroclasts, which have exsolution lamellae of garnet and clinopyroxene (Fig. 2c), occurring in a fine-grained recrystallized matrix. In Meidling im Tal, the clinopyroxenite forms thin veins and preserves garnet, which is in contrast to the host peridotites, where garnet is totally replaced by kelyphite–symplectite.

4.3.3. Eclogite

Two samples (DS27E and F12-10) of eclogite were selected from the Dunkelsteinerwald. The first sample has a high amount of clinopyroxene (about 70 vol. %) and transitions to clinopyroxenite. In the pyroxene-rich sample, garnet porphyroblasts occur in a finegrained matrix consisting of clinopyroxene, plagioclase and amphibole. The garnet porphyroblasts contain many solid phase inclusions (Fig. 2d–f). Although the matrix is strongly recrystallized, the shapes of primary omphacite crystals (transformed to plagioclase, clinopyroxene and amphibole) can be recognized. Some relatively large grains of clinopyroxene have open fractures in the central parts with fracture-free rims (Fig. 2g). The fractures have parallel orientation in two directions. The main and relatively long fractures follow the *c*-axis of pyroxene crystal. Most samples of the eclogite were selected from Nové Dvory. They are foliated to various degrees and the foliation is defined by omphacite and its replacement products and also by prolonged garnet grains. The eclogites are medium- to coarse- grained with garnet porphyroblasts having sizes between 1 and 3 mm, locally up to 8 mm. Garnet content varies between 50 and 60 vol. % of the rock. Garnets may have mono- or multiphase inclusions (Fig. 3a–e). Some samples are rich in rutile and apatite, which occur in garnets and also in the matrix. Rutile is usually replaced by ilmenite. Apatite contains thin rods of monazite. Garnet has usually a corona of fine-grained symplectite. Green amphibole is present in the symplectite after omphacite, but red-brown amphibole occurs at contact with ilmenite. The omphacite may contain very small inclusions (needles, samples D8-11 and D12-11), which have direction parallel to the crystallographic shape of the host grains (Fig. 3f).

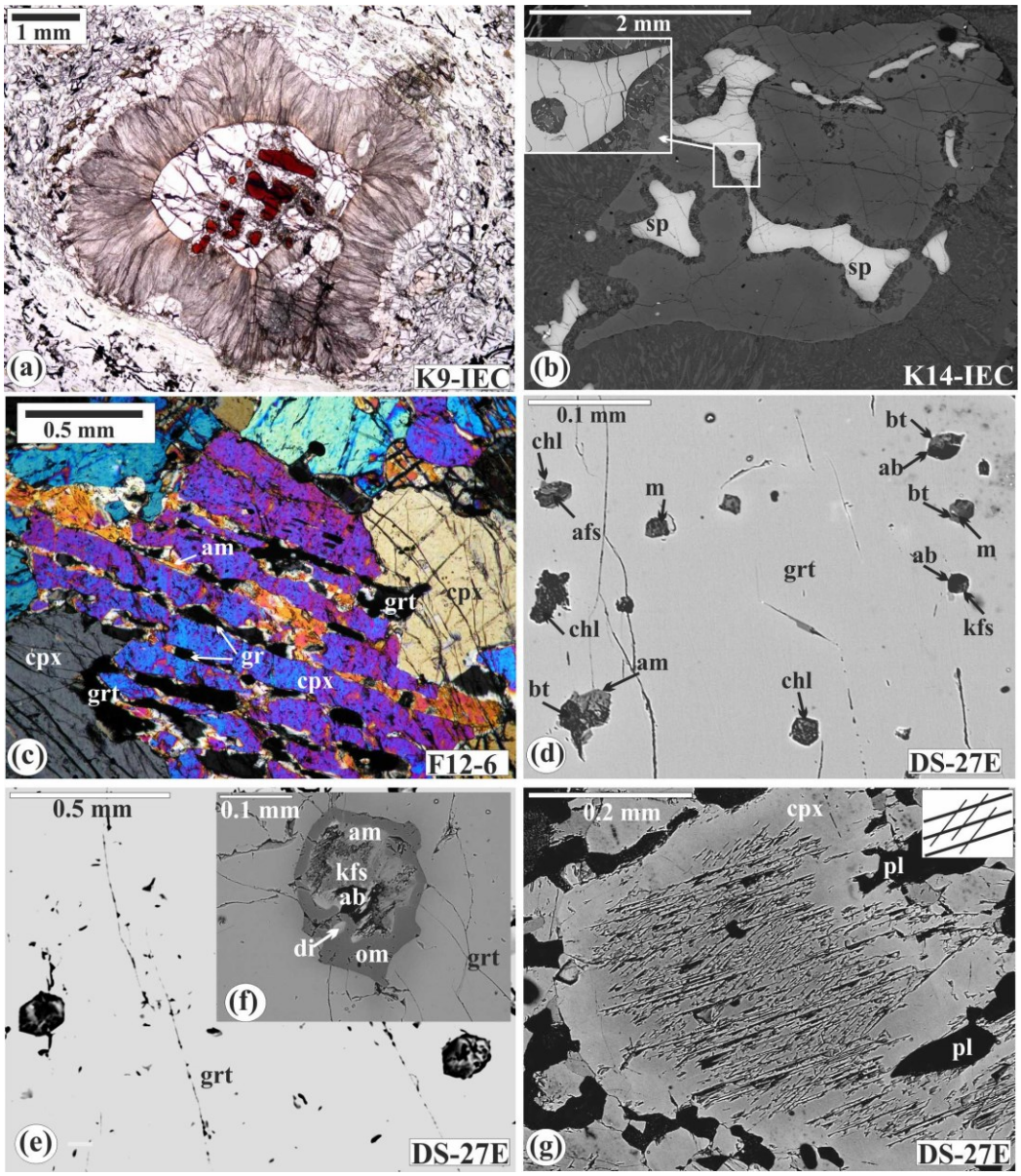

Fig. 2. Photomicrograph (a) and BSE image (b) of garnet with Cr-spinel inclusions from peridotites in the Dunkelsteinerwald. (a) shows garnet with thick kelyphitic corona. It has numerous Cr-spinel inclusions (K9-IEC). Interface between spinel and garnet is formed by thin zone of ortho- and clinopyroxene symplectite (see detail in the upper left corner of b). (c) photomicrograph of clinopyroxenite with clinopyroxene porphyroclast from Nové Dvory. The clinopyroxene has lamellae of garnet and orthopyroxene, which are partly replaced by amphibole. (d–f) inclusion patterns in garnet from clinopyroxene-rich eclogite in Dunkelsteinerwald. (d) monomineral and multiphase inclusions in garnet (detail from Fig. 5a). (e) undefined melt inclusions in garnet. Note the negative hexagonal shape of the inclusions. (f) large inclusion of omphacite (om) with K-feldspar (kfs), albite (ab) and amphibole (am) in the core. Note diopside inclusion in omphacite. Other abbreviations are: afs - alkali feldspar, bt - biotite, chl - chlorite, m - melt. (g) relatively coarse grains of clinopyroxene in the matrix have cores with open fractures. The scheme in the upper right corner shows two directions of the fractures. The main fractures are along the *c*-axis of pyroxene crystal.

Table 1: Microprobe analyses of selected garnet and clinopyroxene from clinopyroxenite and eclogite

Rocks	Clinopyroxenite-eclogite			Eclogite			Cpx-Ecl		Eclogite		
Sample	DS27E			D8-11			DS27E		D8-11	D9-11	D6-11
Mineral	Garnet						Clinopyroxene				
Position	c	rc	r	c	rc	r		In grt		In grt	In grt
SiO_2	41.44	41.30	40.83	39.96	39.76	40.03	50.73	53.45	56.86	54.23	55.44
TiO_2	0.11	0.04	0.01	0.23	0.17	0.15	0.44	0.30	0.24	0.40	0.00
Al_2O_3	22.95	23.05	22.66	22.32	22.31	22.72	11.90	9.19	12.39	10.13	13.61
Cr_2O_3	0.04	0.08	0.07	0.00	0.00	0.05	0.00	0.07	0.00	0.08	0.00
FeO	12.58	13.26	16.46	16.41	15.14	16.50	3.37	3.05	3.66	4.48	4.69
MnO	0.20	0.22	0.41	0.45	0.34	0.30	0.02	0.11	0.01	0.06	0.03
MgO	17.68	15.97	14.71	9.94	9.21	8.58	12.10	12.82	7.29	9.76	7.08
CaO	5.22	6.58	5.14	10.76	12.73	12.16	18.55	17.05	13.86	17.11	12.69
Na_2O	0.00	0.00	0.00	0.00	0.00	0.00	2.86	3.82	6.46	4.19	6.57
Total	100.22	100.49	100.29	100.07	99.65	100.49	99.97	99.86	100.78	100.44	100.11
Per			12 (O)						6 (O)		
Si	2.980	2.985	2.993	2.991	2.987	2.997	1.822	1.909	2.013	1.948	1.974
Al	1.945	1.963	1.957	1.969	1.976	2.006	0.504	0.387	0.517	0.429	0.571
Ti	0.006	0.002	0.001	0.013	0.009	0.009	0.012	0.008	0.006	0.011	0.000
Cr	0.002	0.005	0.004	0.000	0.000	0.003	0.000	0.002	0.000	0.002	0.000
Fe^{3+}	0.080	0.058	0.052	0.024	0.031	0.000	0.018	0.041	0.000	0.000	0.000
Fe^{2+}	0.676	0.743	0.956	1.003	0.920	1.033	0.083	0.050	0.108	0.135	0.140
Mn	0.012	0.013	0.026	0.029	0.022	0.019	0.001	0.003	0.000	0.002	0.001
Mg	1.895	1.721	1.607	1.109	1.031	0.958	0.648	0.683	0.385	0.523	0.376
Ca	0.402	0.510	0.404	0.863	1.024	0.975	0.714	0.653	0.526	0.659	0.484
Na	0.000	0.000	0.000	0.000	0.000	0.000	0.199	0.264	0.443	0.292	0.454
Alm (Aug)	22.4	24.7	31.8	33.3	30.6	34.6	68.5	69.5	48.9	65.6	54.6
Prp (Jd)	62.9	57.2	53.4	36.8	34.3	32.1	17.9	28.2	44.2	29.8	47.6
Grs (Aeg)	12.9	16.6	13.1	28.6	34.0	32.5	1.8	0.8	0.7	0.0	0.0
Sps (ts)	0.4	0.4	0.8	1.0	0.7	0.6	11.7	1.5	4.0	1.7	5.3
X_{Mg}	0.74	0.70	0.63	0.52	0.53	0.48	0.90	0.80	0.76	0.80	0.73

c. rc. and r for garnet in sample DS27Eand D8-11 represent core. core-rim and rim compositions as indicated in Fig. 5b and d.

4.4. Mineral compositions

Most minerals were analyzed at the Institute of Earth Sciences in Graz, using a JEOL JSM-6310 scanning electron microscope (SEM) equipped with wavelength- and energy-dispersive spectrometers. Standards were pyrope (Mg, Al), adularia (K), rutile (Ti), tephroite (Mn), jadeite (Na, Si), and andradite (Fe, Ca). Na and F were measured with a Microspec wavelength-dispersive spectrometer, and operating conditions were 15 kV and 10 or 15 nA, with 20 s counting time on peak and 10 s on each background. Representative analyses of some selected minerals are given in Tables 1 and 2.

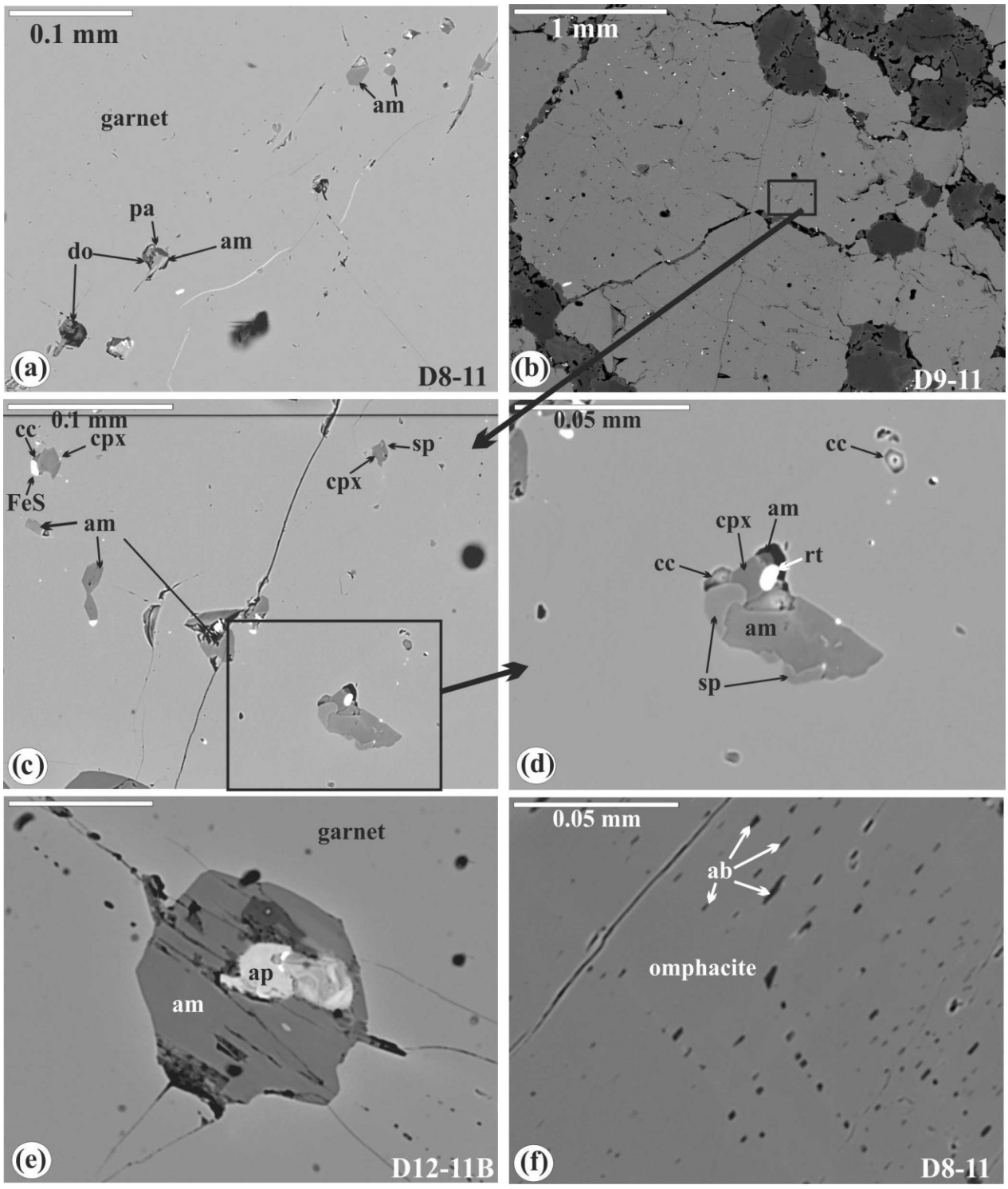

Fig. 3. BSE images of garnet (a–e) and pyroxene (f) from eclogite in the Nové Dvory. (a) monomineral and multiphase inclusions (pa - paragonite, do - dolomite) in garnet. (b) garnet with detail in (c) and (d) shows various inclusions with calcite (cc), diopsidic clinopyroxene (cpx), and Fe-sulfide. Note that spinel (sp) occurs at contact between amphibole and garnet. (e) amphibole with apatite and albite occurs in inclusion, which primarily had an idiomorphic shape and now the garnet is partly replaced by amphibole. (f) albite rods in omphacite.

4.4.1. Garnet

Figure 4a shows compositional variation of garnet from garnet peridotite, garnet clinopyroxenite and eclogite, where pyrope content decreases and almandine and grossular increase from peridotites through clinopyroxenites to eclogites. Cr_2O_3 content in garnet from peridotite ranges from 0.4 wt % in sample K1-IEC through 1.9 wt % in F46-6 to 2.9 wt % (DS27D). It shows slight increase toward the rims, which is similar to Fe, but opposite to the change of Mg content.

Garnet from thin clinopyroxenite veins (sample M6-IEC) has relatively high Fe content, comparing to that in the peridotites (Fig. 3a). More Fe-rich garnet is in sample DS27E, which has transitioned from clinopyroxenite to eclogite. Cr_2O_3 content in garnet from clinopyroxenites is relatively low (below 0.6 wt %), but similar to that in the peridotites, it systematically increases toward the rim (Fig. 4b). In the clinopyroxene rich sample (DS27E), garnet shows compositional zoning with increase of grossular and decrease of pyrope in the core, followed by decrease of grossular toward the rim (Fig. 5a, b, Table 1). However, pyrope shows first an increase and then decrease at the rim. Almandine has a flat profile in the core, but similar to X_{Fe} it shows systematic increase toward the rim.

Small garnet grains in eclogite are usually homogeneous in composition with only slight decrease of Mg and increase of Fe toward the rim. However, some larger garnet porphyroblasts may preserve compositional zoning, which could be more complex. Fig. 5c–d shows zoning profiles of garnet from eclogite in the Nové Dvory, where grossular content first increases and then decreases at the rim (see Table 1). Pyrope shows first a decrease, then slight increase, followed by its decrease at the rim. The almandine values indicate a decrease in the core and an increase near the rim. X_{Fe} contents are flat in the core and increase toward the rim. Ti contents, observed in most garnets, show a slight decrease toward the rim. Cr content is very low and shows no zoning in garnet from eclogite.

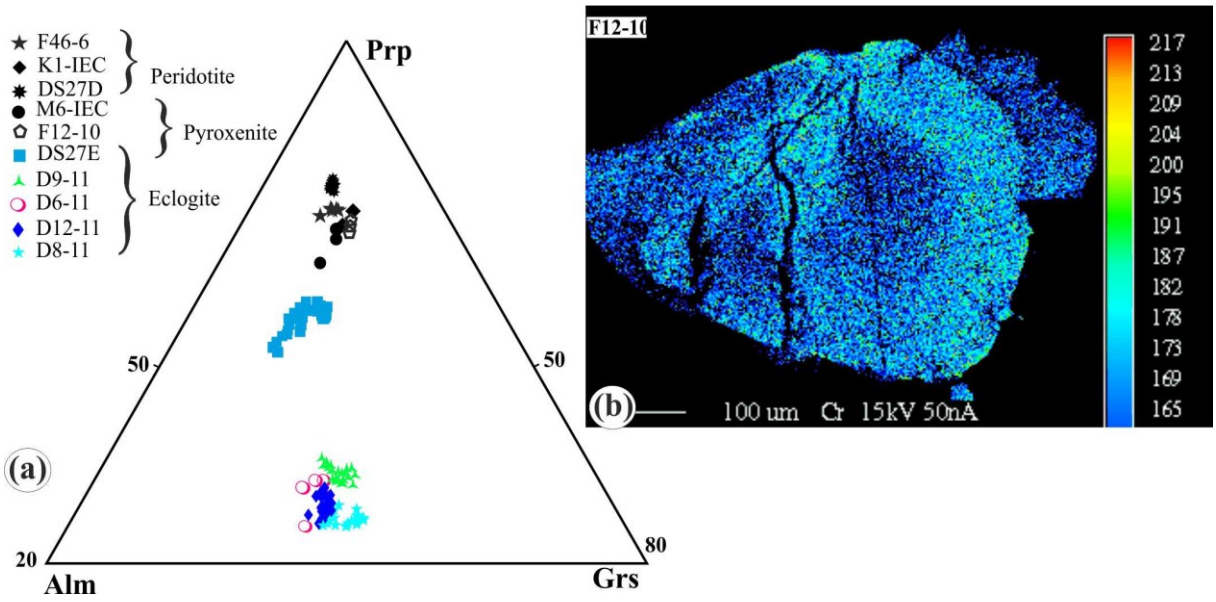

Fig. 4. Composition of garnet (a) from peridotite, clinopyroxenite and eclogite from Dunkelsteinerwald and Nové Dvory. (b) shows compositional map with rimward increase of Cr content in garnet from clinopyroxenite.

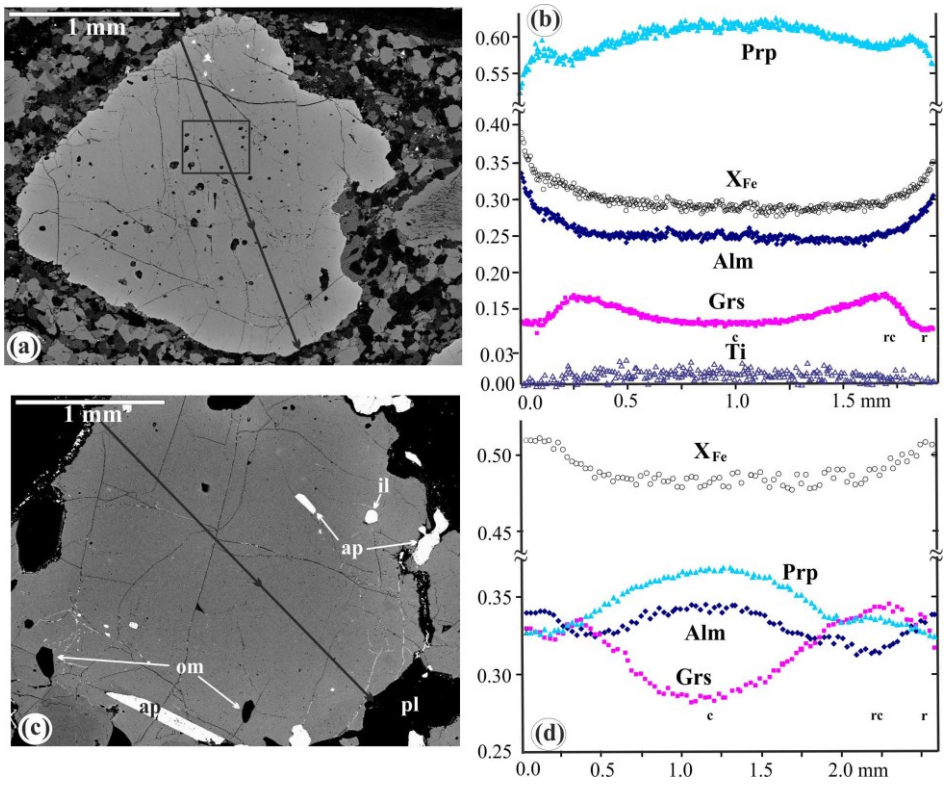

Fig. 5. BSE images (a, c) and compositional profiles (b, d) of garnet from eclogite from Dunkelsteinerwald (DS27E) and Nové Dvory (D8-11). Box in (a) shows position of Fig. 2d. Note that garnet (c) contains inclusions of omphacite (om) and apatite (ap). In addition to molar proportion of Alm, Grs and Prp, Fig. 5b shows Ti content (a.p.f.u.). c, rc and r are position analyses listed in Table 1.

4.4.2. Clinopyroxene

Clinopyroxene from garnet peridotite is rich in diopside and has jadeite content between 3 and 7 mol % in samples from Dunkelsteinerwald and between 11 and 13 mol % fromthe Nové Dvory. Reintegrated composition of exsolution phases (garnet+orthopyroxene) and of host pyroxene indicated that the primary pyroxene in the clinopyroxenite from the Nové Dvory was rich in Al and contained 8 mol % of Tschermak components (Faryad et al., 2009). There is no significant difference in clinopyroxene between garnet peridotite and clinopyroxenite layers from the Dunkelsteinerwald (M6-1EC and F12-10).

Clinopyroxene in the inclusions in garnet from clinopyroxene-rich eclogite (sample DS27E) is omphacite ($Jd_{25–28}$), but the matrix clinopyroxene with plagioclase has $Jd_{15–17}$ (Table 1). As mentioned before, no phase was observed in the fractures inside the relatively coarse grains of clinopyroxene crystals (Fig. 2g). It is not clear if the fractures are results of volume change during cooling or they are tracks after fluid flow that migrated during later granulite facies overprint. Jadeite-rich omphacite (up to Jd_{44} and Jd_{47}) occurs in eclogites (samples D8-11 and D6-11, see Table 1). The albite exsolutions in omphacite (Fig. 3f) can be explained as result of quartz precipitation from relatively Si-rich clinopyroxene (Ca-Eskola component) and then by the decompression reaction of quartz + jadeite = albite (Tagiri et al., 1995).

4.4.3. Orthopyroxene

Orthopyroxenes in garnet peridotites from both areas are enstatite (X_{Mg} = 0.90-0.94), but they differ from each other in Al_2O_3 content, which is ≤0.9 wt % in the Nové Dvory and higher (1.2–3.6 wt %) in the Dunkelsteinerwald. Cr_2O_3 content in both localities is ≤0.6 wt %.

4.4.4. Olivine

Olivine in garnet peridotites from both areas is rich in forsterite content (Fo = 89–91 mol %). Some pyroxene-rich samples from Nové Dvory have olivine with lower Fo = 83 mol %.

4.4.5. Spinel

Al-rich spinel occurs in kelyphitic rims and in symplectites around garnet. Cr-rich spinel occurs as inclusions in garnet. It has X_{Al}=Al / (Al+Cr+Fe^{3+}) ratios ranging from 0.68 to 0.78.

4.5. Inclusions in garnet

Garnets from peridotites contain inclusions of Cr-spinel, olivine and in some cases also of ortho- and clinopyroxene. The olivine and orthopyroxene inclusions are usually replaced by serpentine. The clinopyroxene in the inclusions in garnet from peridotite may contain exsolution lamellae of orthopyroxene. Cr-spinel in the inclusions is preserved, but it may have a thin zones formed by symplectite of ortho- and clinopyroxene (Fig. 2b).

A wide variety of inclusions was observed in garnet from eclogites (sample D6-11, D8-11, D9-11, D12-11, and F15-10), including clinopyroxene-rich eclogite (sample DS27E) (Tables 2 and 3). In addition to one phase inclusion, most inclusions are multiphase or have undefined composition. Table 3 shows monomineral and multiphase inclusions observed in garnet from eclogite. The monomineral inclusions are represented by omphacite, apatite, rutile, amphibole, biotite, chlorite and calcite. Omphacite in the inclusions has usually higher jadeite content compared to that in the matrix.

Table 2: Selected microprobe analyses of minerals observed as inclusions in garnet.

Sample	D8-11			D8-11		DS27E	D12B-11		D9-11	D8-11	F15-10
Mineral	Amphibole			Biotite		Pl	Epidote	Prh?	Spinel	Dol	Hbs
SiO_2	39.30	39.54	38.17	40.94	34.20	62.26	38.06	44.36	0.13	0.00	39.41
TiO_2	1.14	0.73	0.38	0.86	4.75	0.00	0.30	0.00	0.04	0.00	0.01
Al_2O_3	19.61	18.93	18.40	15.59	18.05	22.57	28.19	26.33	61.83	0.00	22.11
Cr_2O_3	0.05	0.00	0.06	0.03	0.00	0.00	0.00	0.00	0.11	0.00	0.01
FeO	7.58	9.01	11.22	3.59	17.47	0.27	5.91	0.40	21.68	7.21	1.54
MnO	0.04	0.04	0.00	0.01	0.07	0.00	0.00	0.00	0.04	0.41	0.40
MgO	11.91	11.55	11.53	25.00	11.28	0.00	0.63	0.00	14.26	16.39	0.92
CaO	11.31	12.32	12.12	0.06	0.44	4.18	22.94	26.63	0.25	29.68	35.10
Na_2O	3.18	1.97	2.57	1.81	0.57	7.64	0.00	0.06	0.00	0.00	0.04
K_2O	1.09	1.03	0.37	9.07	6.96	1.72	0.02	0.02	0.00	0.00	0.03
ZnO	0.00	0.00	0.00	0.00	0.00	0.00	0.00	0.00	1.75	0.00	0.00
BaO	0.00	0.00	0.00	0.00	0.00	1.22	0.00	0.00	0.00	0.00	0.00
F	1.70	1.27	0.31	0.00	0.00	0.00	0.00	2.28	0.00	0.00	0.27
Cl	0.65	1.02	1.76	0.52	0.81	0.00	0.00	0.03	0.00	0.00	0.02
Total	97.55	97.42	96.88	97.47	94.61	99.86	96.06	100.11	100.08	53.69	99.87
Per		23 (O)		11 (O)		8 (O)	12.5 (O)	11 (O)	4 (O)		12 (O)
Si	5.844	5.895	5.720	2.838	2.709	2.815	2.986	2.975	0.003	0.000	2.968
Al	3.437	3.326	3.249	1.273	1.685	1.203	2.606	2.080	1.938	0.000	1.963
Ti	0.128	0.082	0.043	0.045	0.283	0.000	0.018	0.000	0.001	0.000	0.000
Cr	0.000	0.000	0.000	0.002	0.000	0.000	0.000	0.000	0.002	0.000	0.001
Fe^{3+}	0.000	0.016	0.508	0.004	0.000	0.000	0.388	0.000	0.000	0.000	0.097
Fe^{2+}	0.942	1.107	0.898	0.204	1.157	0.010	0.000	0.022	0.482	0.096	0.000
Mn	0.004	0.005	0.000	0.001	0.005	0.000	0.000	0.000	0.001	0.006	0.025
Mg	2.639	2.568	2.576	2.583	1.332	0.000	0.074	0.000	0.565	0.390	0.104
Ca	1.801	1.969	1.946	0.004	0.037	0.203	1.926	1.913	0.007	0.508	2.833
Na	0.917	0.570	0.748	0.243	0.088	0.670	0.000	0.008	0.000	0.000	0.005
K	0.207	0.197	0.070	0.802	0.703	0.099	2.986	0.002	0.000	0.000	0.003
Zn	0.000	0.000	0.000	0.000	0.000	0.000	0.000	0.000	0.034	0.000	0.000
Ba	0.000	0.000	0.000	0.000	0.000	0.022	0.000	0.000	0.000	0.000	0.000
F	0.802	0.600	0.147	0.000	0.020	0.000	0.000	0.483	0.000	0.000	0.063
Cl	0.163	0.258	0.446	0.062	0.000	0.000	0.000	0.003	0.000	0.000	0.003
X_{Mg}	0.737	0.699	0.742	0.927	0.535				0.540		

Except sample DS27E of clinopyroxenite–eclogite from Dunkelsteinerwald. the rest of the samples are eclogites from Nové Dvory.
Abbreviations: hbs — hibschite. pl — plagioclase. prh — prehnite.

4.5.1. Amphibole

In addition to individual grains, amphibole occurs with one or more phases in the inclusions. It is pargasite with Si = 5.6–6.3 a.p.f.u. and high Al^{VI} (above 1.0 a.p.f.u.), which based on the amphibole nomenclature (Leake et al., 2003) can be classified as aluminopargasite. The X_{Mg} ratios in amphibole range from 0.7 in eclogites to 0.9 in pyroxene-rich sample (DS27E). It shows no systematic variation between monomineral and multiphase inclusions. No compositional relationship to the coexisting phase was observed. In one case a potassic amphibole with

K = 0.63 a.p.f.u. was analyzed. The total Cl+F content is usually between 0.40 and 0.96 a.p.f.u. (Table 2). Maximum F = 0.82 a.p.f.u. was analyzed in Al-rich amphibole with Al^{VI} = 1.28 a.p.f.u. The F/Cl ratio changes from one inclusion to another and similar to the main cation contents, no systematic relationship to monomineral and multiphase inclusions was observed.

4.5.2. Clinopyroxene

In addition to monomineral inclusions of omphacite, diopside usually occurs together with one or more minerals (Table 3). It has low jadeite content (≤10 mol %) and slightly higher X_{Mg} = 0.83 compared to omphacite (X_{Mg} ≤ 0.8). Spinel associated with diopside is poor in Cr and has X_{Mg} = 0.54 (Table 2) and 3.4 mol % of gahnite end-member ($ZnAl_2O_4$).

4.5.3. Micas

Phlogopite was analyzed in garnet from pyroxene-rich sample (DS27E). It occurs in multiphase inclusion and has X_{Mg} = 0.92 (Table 2). Biotite with X_{Mg} = 0.5–0.6 is present in garnet from eclogite. In addition to paragonite with amphibole and dolomite, a Na-rich phase having a composition similar to paragonite was also analyzed in one inclusion. The X site of the mineral formula of mica $XY_2Z_3O_{10}(OH)_2$ is occupied by 0.70 Na, 0.14 Ca and 0.02 K a.p.f.u.

4.5.4. Feldspars

Albite and K-feldspar are the most common inclusions. In addition to alkali feldspar, plagioclase with $An_{30–50}$ was also found in many multiphase inclusions. BaO content analyzed in K-feldspar is 1 wt % and 1.22 wt % in plagioclase (Table 2).

4.5.5. Carbonates

In addition to almost pure calcite, dolomite with dolomite–ankerite solid solution was found. It has a composition of $Cal_{51–53}$ $Dol_{39–40}$ Ank_{10} $Rds_{4–6}$ (Table 2) and occurs in a multiphase inclusion with amphibole and paragonite.

4.5.6. Apatite

Apatite is common in eclogite from Nové Dvory. It occurs in the matrix and also as inclusions in garnet and omphacite. Total amount of halogens ranges between 2.7 and 3.7 wt % in apatite. It is rich in fluorine (2–3 wt %) and has a maximum chlorine content of 1.1 wt %. Apatite has a dusty appearance, which is the result of very fine exsolution lamellae of monazite that has an orientation parallel to the *c*-axis of apatite crystal.

4.5.7. Other minerals

Epidote was observed in three inclusions from sample DS27E. It has a composition of X_{Al} = (Al-2) / (Al-2+Fe) = 0.48–0.63, but in some cases it is zoned with lower X_{Al} in the core. In one case, a phase having a composition similar to prehnite (Table 2) was analyzed. However, it has F = 2.28 wt %. Prehnite, pumpellyite and hydrogrossular (hibschite) with plagioclase were analyzed in several grains of garnet from eclogite sample F15-10. The hibschite with a composition of $Grs_{85–92}$ $And_{4–8}$ $Prp_{2–5}$ Alm_{0} has 0.2–0.3 wt % of F in the analyses (Table 2). However, the inclusions with hydrous minerals are connected with matrix by fractures. Chlorite is common as separate inclusion as well as in multiphase inclusions. As it seems to be a replacement product, its composition varies in relation to the phases occurring in the inclusions. Iron sulfide was observed in two polyphase inclusions with amphibole+calcite and plagioclase+amphibole+diopside, respectively. In both cases it has an almost pure FeS composition without having detectable amounts of Ni, Cu or As.

4.5.8. Melt?

There are a number of not-well identified inclusions in garnet. Mostly, they were found in garnet from clinopyroxene-rich rock (DS27E). These inclusions have the negative shape of crystals (Fig. 2c, d). Based on oxide content, they can be subdivided into two groups. The first group has low FM (FeO+MgO) = 6–8 wt %, but high SiO_2 = 53–66 wt %. The second group has higher FM = 24–30 wt % and lower SiO_2 = 36–47 wt %. There is no systematic variation in Al_2O_3, CaO, MgO, FeO, Na_2O and K_2O contents. The total oxide content ranges between 92.86 and 98.65 wt %. Fig. 6 shows variation of major oxide contents of the melt (?) inclusions along with the polyphase inclusions, calculated using microprobe analyses and modal contents of the phases (Tables 2 and 3).

Table 3: Monomineral and multiphase inclusions in garnet from eclogite and clinopyroxenite with estimated mode of each phase in the inclusions

Sample	Phase														
	Rt	Ap	Om	Di	Am	Sp	Bt	Pa	Cc	Do	FeS	Pl	Kfs	Prh?	Ep
DS27E	x	x	x		x		x		x			x	x	x	x
D8-11		x	x		x		x	x		x		x			
D9-11		x	x	x	x	x			x		x				
D6-11		x	x		x										
D12-11		x					x					x	x		x

Numbers (column 1) and estimated modal abundance of phase in selected inclusions

1	1														
1		1													
1			1												
1					1										
1							1								
1									1						
2		0.2					0.8								
2		0.2	0.8												
2				0.8		0.2									
2	0.1				0.9										
2					0.8	0.2									
2												0.4	0.6		
3		0.18			0.7									0.13	
3				0.4	0.25							0.35			
3		0.4					0.4								0.2
3					0.7				0.1		0.2				
3					0.6			0.2		0.2					
4	0.05			0.2	0.5	0.25									
4				0.3	0.4						0.15	0.15			
5			0.4	0.02	0.3							0.1	0.18		

Ep - epidote. Prh - prehnite. other abbreviations are as in Figs. 2 and 3.

4.6. Discussion and interpretation

The occurrence of millimeter to decimeter thick layers of pyroxenites and the compositional variation of mafic–ultramafic rocks from peridotites through clinopyroxenites and eclogites to garnetites (with more than 90 vol.% of garnet) in the studied areas suggest that all these mafic and ultramafic lithologies represent fragments of mantle, which were involved in the subduction zone. This is consistent with the interpretation of Medaris et al. (2005) and Ackermann et al. (2009), who assumed that mafic–ultramafic layers had formed from melt that migrated through the lithospheric mantle wedge above the subduction zone. However, this process was not coeval with the formation of solid phase inclusions in garnet as discussed below.

4.6.1. Origin of solid phase inclusions in garnet from garnet peridotites, pyroxenites and eclogites

4.6.1.1. Garnet peridotites

Inclusions of olivine and pyroxene are common in garnet from peridotites, however the succession of mineral formation in relation to pressure or temperature changes can hardly be evaluated. On the other hand, spinel inclusions in garnet indicate that the peridotites crossed the spinel–garnet stability field either by an increase of P or a decrease of T (e.g. Brey et al., 1999; Grütter et al., 2006; Klemme and O'Neill, 2000; Nickel, 1986; O'Neill, 1981; Webb and Wood, 1986). In addition to high concentration of Cr around spinel inclusions, the increase of Cr content from core to rim of garnet can be interpreted as result of spinel breakdown in the matrix during garnet formation (Faryad, 2009).

4.6.1.2. Pyroxenites

Spinel inclusions are also present in garnet from clinopyroxenite which, similar to that in peridotite, suggest pressure increase and temperature decrease (Faryad et al.,

2009). Garnet exsolution lamellae in Al-rich clino- and orthopyroxene porphyroclasts was formed by the reactions 2Di + Ca – Ts = En + Grs and 2En + Ca – Ts = Di + Prp, which occurred due to cooling and pressure increase during metamorphism (Carswell, 1990; Faryad et al., 2009). Such P–T trend is supported by compositional zoning in garnet from clinopyroxene-rich sample DS27E (Fig. 5b), which has transitioned from clinopyroxenite to eclogite. Garnet from this sample is rich in solid phase inclusions, similar to that in eclogite (see below).

4.6.1.3. Eclogite

Apart from mineral inclusions, garnet from eclogites contains numerous inclusions, which are difficult to define as their compositions do not match with any mineral. As shown in Figs. 2 and 3, most of the inclusions are not connected with the matrix by fractures. These, together with negative shapes of some inclusions (Fig. 2e), mainly those following crystallographic planes, suggest that they were precipitated or crystallized from a fluid-bearing phase or from melt, which was present during garnet formation. Polyphase inclusions in garnet that precipitated from melt have recently been reported from several UHP terrains (e.g. Gao et al., 2011; Lang and Gilotti, 2007; Zheng et al., 2011). However, Perchuk et al. (2008), based on experimental works on eclogite facies garnet, showed that the melt could form by decomposition of former hydrous minerals, e.g. epidote, amphibole, titanite etc., which were included in garnet during prograde stage of garnet growing. Direct features of minerals enclosed during prograde stage in HP/UHP garnet are difficult to find, because of possible melting and subsequent recrystallization during decompression.

In addition to high concentrations of Na and K that are incorporated in alkali feldspars, most inclusions studied here consist of mineral phases that contain one or more of the volatiles H_2O, F, Cl, CO_2 and SO_4. High concentrations of halogens occur in apatite (up to 3.69 wt %) and in amphibole (up to 2.35 wt %), but also in biotite with up to 0.8 wt % (Table 2). Apart from calcite and dolomite, other CO_2-bearing phases were not observed. Fluid and solid phase inclusions with similar components in minerals have been investigated from many HP/UHPM terrains (e.g. Andersen et al., 1990; Ferrando et al., 2005; Fu et al., 2001; Gao et al., 2011;

Malaspina et al., 2006; Philippot, 1993; Svensen et al., 2001; Zheng et al., 2011). Origin of the fluid and other lithophile elements are interpreted as a result of dehydration and melting of subducted crustal rocks. Fluids generated by dehydration accelerate the reaction progress, control material transport in the subduction zone and finally result in melting and syn-subduction magmatism (e.g. Manning, 2004; Schmidt and Poli, 1998). Crustal material undergoes dehydration and prograde metamorphism by both P and T increases, but the hot mantle rocks can be recrystallized by cooling as well as fluid and melt infiltration.

Mineral analyses and modal amounts of phases in the studied inclusions within garnet indicate that their composition varies from one inclusion to another, even in the same grain of host mineral. In addition to the monomineralic phases, e.g. biotite, calcite, amphibole, etc., the reintegrated composition of polyphase inclusions shows a large range of major oxide contents (SiO_2, Al_2O_3, MgO, FeO_t, K_2O and Na_2O, Fig. 6). This is in contrast to the in situ melt inclusions trapped during crystallization in the magmatic system, where equilibrium magma is enclosed by the host mineral (for reference see Kent, 2008). Although potential modification of trapped melt compositions can occur during entrapment or post trapping equilibration, the melt inclusions reflect the same compositional range present within the host magmatic system (e.g. Shimizu, 1998; Slater et al., 2001; Sobolev, 1996).

4.6.2. Significance of the solid phase inclusions for the origin of UHPM mafic and ultramafic rocks in the Moldanubian Zone

Melt and fluid infiltration into the lithospheric mantle is a continual process, which supplies magmatic activity in the arc. However, a portion of the melt interacting with mantle rocks can crystallize as layers and veins of pyroxenites and gabbros in different levels of the mantle above the subduction zone. As shown by Medaris et al. (2005), this is the case of clinopyroxenites and some eclogite bodies within peridotites in the Moldanubian Zone. The data presented in this paper indicates that the eclogites and garnet pyroxenites are not products of direct HP crystallization from melt, but they were in solid state prior to their transformation into eclogites and garnet peridotites or garnet pyroxenites. Their recrystallization occurred both

with and without the presence of fluids. Spinel inclusions in garnet from peridotites and formation of garnet lamellae in pyroxenes in pyroxenites are examples of recrystallization in a relatively dry environment, while the eclogites with inclusions of hydrous phases in garnet suggest the presence of fluids. Both rocks show evidence of cooling and pressure increase.

Metamorphic P–T conditions estimated for garnet peridotites and eclogites from Nové Dvory (Medaris et al., 2005; Nakamura et al., 2004) and from Dunkelsteinerwald (Becker, 1997a, 1997b; Carswell, 1991) indicate that they passed UHP conditions at temperatures above 1000 or 1100 °C. All these rocks occur within felsic granulites, which together with mafic and ultramafic bodies shared granulite facies metamorphism at about 900–1000 °C (Faryad et al., 2010b; Kotková, 2007; O'Brien and Carswell, 1993; Tajčmanová et al., 2006). Despite such high-temperature metamorphic events, compositional zoning in garnet from eclogites is preserved. This suggests that the UHP and subsequent granulite facies metamorphism were not long enough to entirely homogenize the major element composition in garnet. The increase of Ca and decrease of Mg in the core of garnet grains, both in garnet clinopyroxenite and eclogite (Fig. 5b and c) can be interpreted as the result of pressure increase and temperature decrease. This fits with the transformation of spinel to garnet and formation of garnet lamellae both in Al-rich clino- and orthopyroxene. The granulite facies process can be also reproduced from the zoning profile near the rim of garnet grains, where Mg shows increase and Ca decrease. A short-term granulite facies overprint is documented by preservation of prograde zoning garnet in felsic granulite (Faryad et al., 2010b). This zoning is preserved despite of relatively low Ca, the element which has slow diffusion coefficient (Chakraborty and Ganguly, 1992) and prevents homogenization of compositional profile of garnet at high temperature.

4.7. Acknowledgment

This work is part of research projects MSM0021620855 and P 210/10/0249. S. Ulrich is thanked for providing sample DS27E. We would like to thank two anonymous reviewers for their careful and thorough reviews of the manuscript.

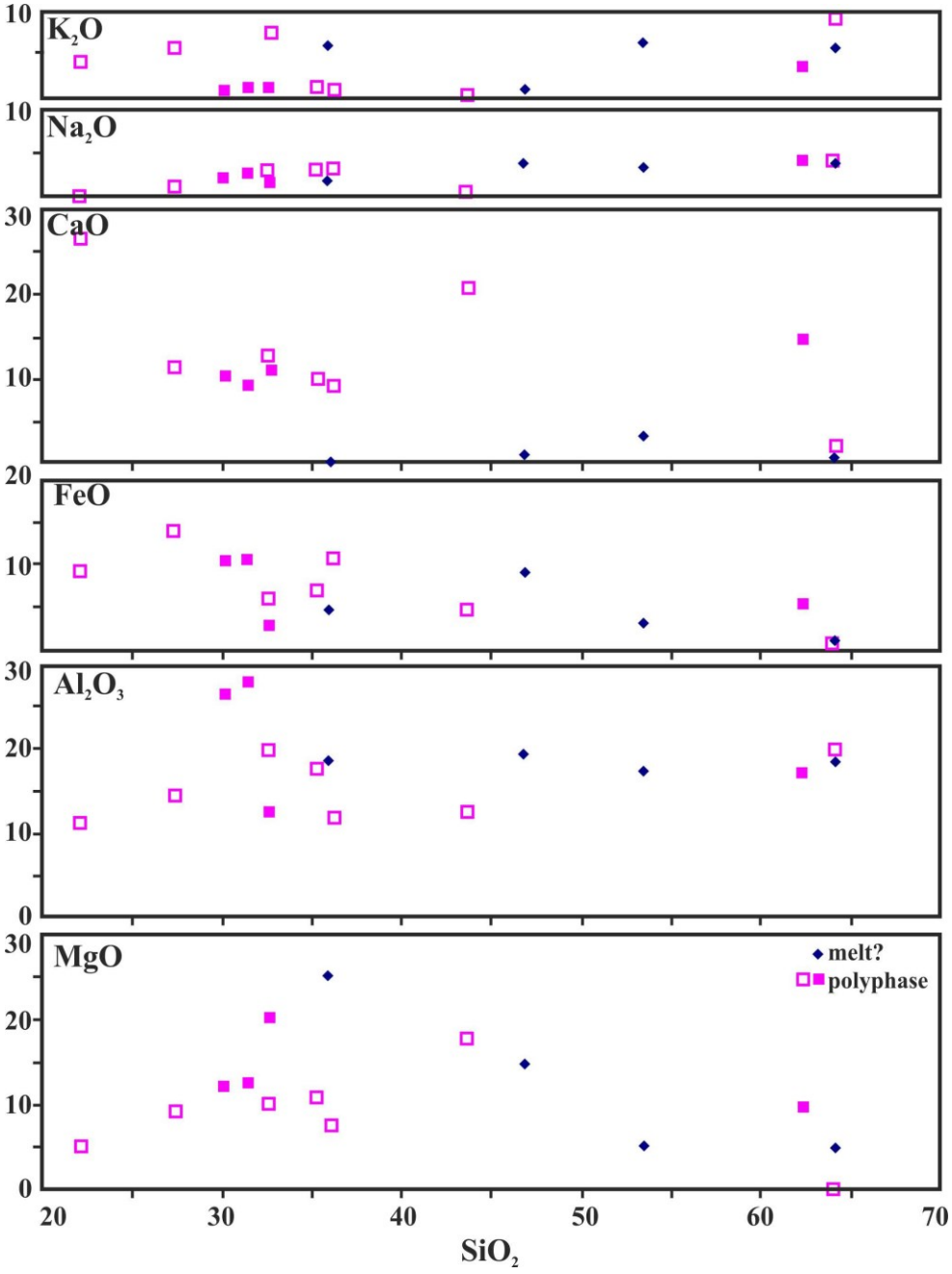

Fig. 6. Plots of selected oxides (wt.%) against silica of potentially melt and reintegrated polyphase inclusions in garnet (Tables 2 and 3). Filled symbols are from garnet-rich clinopyroxenite (sample DS27E) and open symbols are from eclogite (samples D8-11 and D9-11).

PART V

ECLOGITE FACIES ROCKS OF THE MONOTONOUS UNIT, CLUE TO VARISCAN SUTURE IN THE MOLDANUBIAN ZONE (BOHEMIAN MASSIF)

Shah Wali Faryad, Radim Jedlička, Stephen Collett

Institute of Petrology and Structural Geology, Charles University in Prague, Albertov 6, 12843 Prague, Czech Republic

Abstract

The formation and exhumation of Variscan high- to ultrahigh-pressure metamorphic rocks from the Moldanubian Zone in the Bohemian Massif is the subject of controversy regarding their unclear relationship to possible subduction zones. In this paper we present the results of a petrological study of eclogites that occur together with serpentinites within amphibolite facies gneisses in the Moldanubian Zone, east of the Teplá–Barrandian Block. More than 100 bodies of retrogressed eclogite and serpentinite follow an approximately 250 km long SW–NE trending zone in the central part of the Bohemian Massif. Together with surrounding gneisses, the eclogites share a medium to low-pressure amphibolite facies metamorphism. P–T conditions estimated for the eclogite facies stage indicate a relatively low-temperature geothermal gradient similar to those observed in the Saxothuringian Zone, which occurs north and northwest of the Teplá–Barrandian Block. The presence and distribution of eclogites and comparison of their P–T and age data with HP–UHPM rocks in other units in the Bohemian Massif allow us to constrain the Variscan suture, which straddles the SE of the Teplá–Barrandian Block. The existence of this suture in relation to available geotectonic models and its possible continuation through other allochthonous units along the European Variscan Belt are discussed.

Keywords: *Bohemian Massif, eclogite, Variscan suture*

5.1. Introduction

Definition and localization of suture zones responsible for the formation and/or exhumation of HP–UHPM rocks along old orogenic belts are among the most challenging questions in geological research. This is usually due to poly-metamorphic and poly-deformation histories, where former structures are modified and HP minerals are obliterated by medium- to low- pressure assemblages (Banno et al., 2000; Chopin, 2003; Ernst, 1988; Faryad and Kachlík, 2013; Janák et al., 2009; O'Brien, 1997). To trace the original suture zones, a complex and multi-disciplinary approach, involving geophysical, structural, mineralogical and geochemical methods, is needed. Mineral inclusions and mineral zoning are the best tracers to decipher, whether the rocks have been subjected to subduction or exhumed from mantle depth along the subduction channel (e.g. Liu et al., 2001; Sobolev and Chopin, 1995; Zhang et al., 2006).

The Bohemian Massif is well known for the presence of Variscan eclogite facies and UHPM rocks that are hosted by amphibolite and granulite facies lithologies, respectively. The HP–UHPM rocks are restricted to the Saxothuringian and the Moldanubian Zones which surround the Teplá–Barrandian Block in the core of the Bohemian Massif. Many newly discovered occurrences of HP–UHPM rocks or refinement of P-T conditions of known localities (Faryad, 2009; Kotková et al., 2011; Medaris et al., 2006; Naemura et al., 2011; Nakamura et al., 2004) help to localize subduction zones or sutures which need to be considered when creating or modifying a geotectonic model for the European Variscan Belt (Franke, 2000; Kröner and Romer, 2010; Linnemann et al., 2010; Matte, 1986; Schulmann et al., 2005, 2009). The Saxothuringian Zone is characterized by the presence of blueschist facies rocks that form a discontinuous belt related to the Teplá Suture at contact with the Teplá–Barrandian Block (Faryad and Kachlík, 2013; Franke, 2000; Mazur and Alexandrowski, 2001). By contrast, the relationship of eclogite facies and UHPM rocks in the Moldanubian Zone to a possible Variscan suture is the subject of discussion and controversy. Some authors (Babuška and Plomerová, 2013; Franke, 2000; Medaris et al., 2006) consider formation of HP–UHPM rocks as the result of closure of the Moldanubian basin that was situated east from the Teplá–Barrandian Blocks. On the other hand, Schulmann et al. (2005, 2009), Lexa et al. (2011) and Guy et al.

(2011) assume that the HP–UHPM rocks in the Moldanubian Zone came from the Saxothuringian Zone by underplating the Teplá–Barrandian Block.

In this paper, we present mineral textural relations and maximum P–T conditions reached by eclogites that form lenses and boudins within amphibolite facies gneisses in the Moldanubian Zone. The eclogites record evidence of rapid subduction and exhumation and their occurrence along a SSW–NNE traverse (200 × 50 km) signifies a possible remnant of the Variscan suture zone. The results of this study are combined with the available information about HP–UHPM rocks in the Moldanubian Zone to analyze the interplay between petrological data and existing geotectonic models for Variscan Orogeny in the Bohemian Massif.

5.2. Geological position

The Bohemian Massif represents the easternmost segment of the European Variscan Belt and is formed by two blocks (the Brunovistulian and the Teplá–Barrandian) that are separated or surrounded by two zones (the Moldanubian and the Saxothuringian, Fig. 1). The zones are characterized by the presence of eclogite facies and UHPM rocks that occur as lenses and boudins within amphibolite and granulite facies rocks, while the blocks are free from HP–UHPM rocks. The Saxothuringian Zone occupies the northern part of the Bohemian Massif, including the Erzgebirge in the west and the Sudetes in the east (Fig. 1). In addition to eclogite facies and UHPM rocks, it contains blueschist facies rocks that are strongly overprinted by greenschist facies metamorphism. The estimated P–T conditions are: 1–2 GPa at 300–550 °C for blueschists (Faryad and Kachlík, 2013; Kryza et al., 2011; Žáčková et al., 2010) and 1.5–2.7 GPa at 600–650 °C for eclogite (Bakun-Czubarow, 1998; Klápová et al., 1998; Massonne and O'Brien, 2003). UHP conditions are estimated for some eclogites, garnet peridotites (Schmädicke et al. 1992; 2010), garnet pyroxenite (Massonne and Bautsch, 2004) and for diamond-bearing gneiss and granulite (Kotková et al., 2011; Nasdala and Massonne, 2000). The Saxothuringian Zone with the Sudetes and Erzgebirge is also characterized by the presence of blueschist facies rocks. The contact between the south-eastward-dipping Saxothuringian plate beneath

the Teplá–Barrandian Block is called the Saxothuringian (Teplá) Suture (Franke, 2000; Matte, 2001; Seston et al., 2000), which is assumed to continue along the Saxothuringian and Teplá–Barrandian boundary to the NE, where it is partly covered by Upper Palaeozoic and Mesozoic sedimentary rocks (Faryad and Kachlík, 2013). Ophiolite complexes are exposed at the contact with the Teplá–Barrandian Block (the Mariánské Lázně Complex) in the west and at the contact with the Brunovistulian Block in the east, where they follow the Rheic/ Rhenohercynian Suture. In the eastern part of the Sudetes, both the Saxothuringian and the Rheic Sutures are cut and reoriented to the south and north due to westward compression and underplating of the Brunovistulian plate beneath the Moldanubian Zone and the West Sudetes (Kryza and Pin, 2010; Mazur et al., 2006).

The Moldanubian Zone occurs between the Teplá–Barrandian and Brunovistulian blocks. It is formed by medium-grade (the Monotonous and Varied units) to high-grade (the Gföhl Unit) rocks. They are intruded by Variscan granitoids with two belts (Fig. 1) of the Central Bohemian Plutonic Complex (CBPC) and the Moldanubian Batholith (MB). Similar to that in the Saxothuringian Zone, the medium- and high-grade rocks contain lenses and blocks of eclogites and peridotites. Most granulite bodies occur along the eastern boundary of the Moldanubian Zone, but some of them are also exposed in its southwestern (the south Bohemian granulite massifs) and northern parts (the Kutná Hora Complex, Fig. 1). The estimated P–T conditions for the high-grade rocks are in the range of 1.6–3.1 GPa and 850–1 000 °C for granulites, (e.g. Carswell and O'Brien, 1993; Cooke, 2000; Faryad et al., 2010b; Kotková, 2007; Tajčmanová et al., 2006); 2–4 GPa and 800–1 000 °C for the eclogites (Faryad, 2009; Nakamura et al., 2004; Vrána and Frýda, 2003); and 3–5 GPa and 1 000–1 200 °C for the garnet peridotites (Faryad, 2009; Medaris et al., 2006). Based on geochronological data, the HP–UHP and subsequent granulite to amphibolite facies metamorphism occurred in a time scale of 370–340 Ma (Brueckner et al., 1991; Carswell and Jamtweit, 1990; Friedl et al., 2011; Kröner and Willner, 1998; Kröner et al., 2000; Schulmann et al., 2005; Wendt et al., 1994).

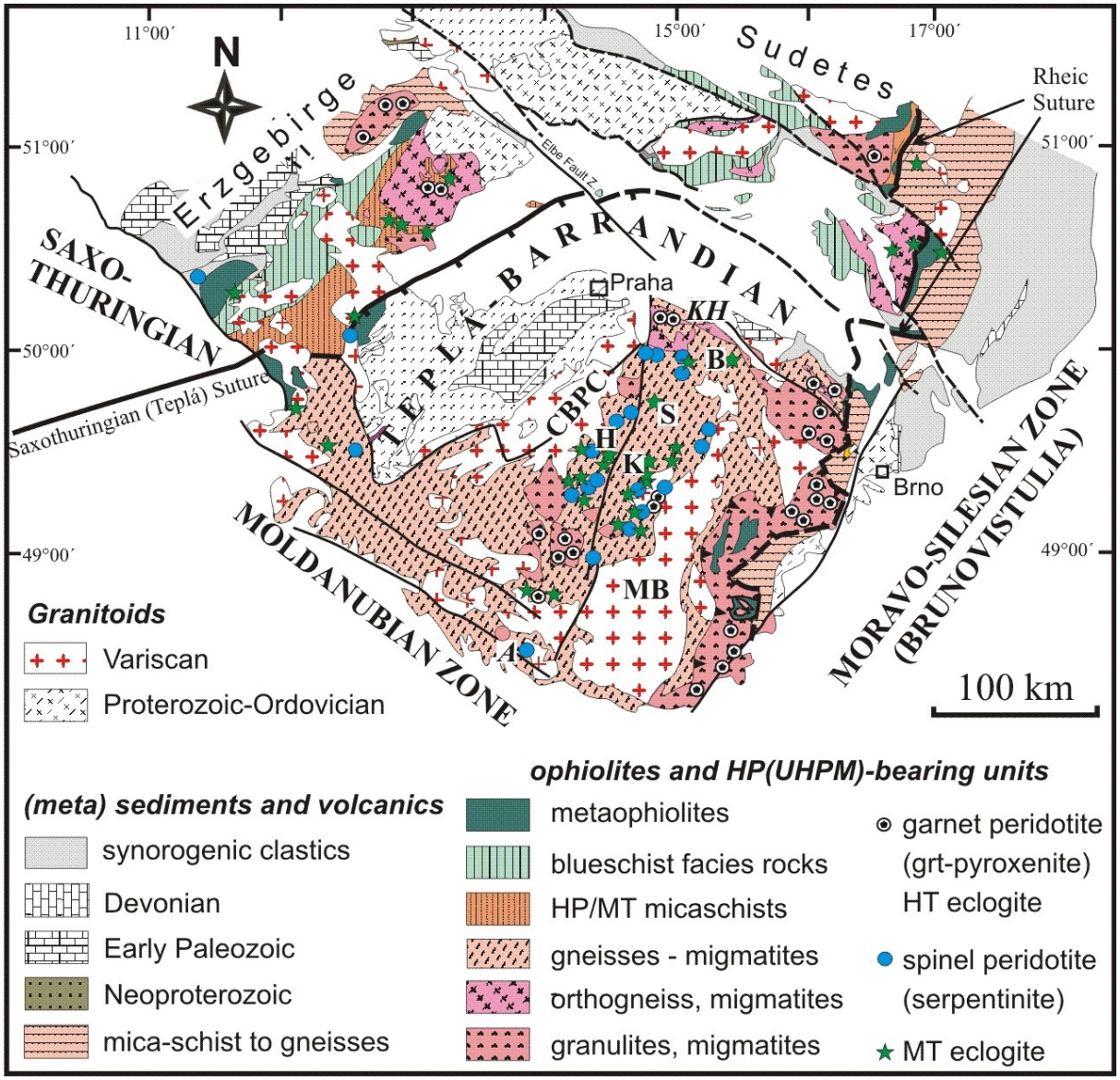

Fig. 1. Simplified geological map of the Bohemian Massif and location of HP–UHPM rocks (compiled from data after Cháb et al., 2007; Faryad and Kachlík, 2013; Franke, 2000; Machart, 1984; Willner et al., 2002). A-Aubach CBPC-Central Bohemian Plutonic Complex, KH-Kutná Hora and MB-Moldanubian Batholith. The studied eclogite localities are: B-Borek, S- Šelmberk, K-Katov and H-Hutě.

The medium-grade rocks of the Moldanubian Zone contain numerous bodies of retrogressed eclogite and serpentinized peridotites. They were mapped by Machart (1984), who described about 100 occurrences of eclogite with or without serpentinites that form an approximately 200 km long belt parallel to the CBPC (Fig. 1). The size of bodies ranges from several meters to almost 4 km in length. P–T conditions of twelve eclogite occurrences were summarized by Medaris et al. (1995). Temperatures, calculated using garnet–pyroxene thermometry, are in the range of 615–705 °C with an average 657 ± 26 °C and minimum pressure values of 1.3–1.5 GPa are based on the maximum jadeite content in omphacite. Higher temperatures of about 800 °C and pressures of 1.6 to 2.0 GPa, that are comparable with eclogite in the Gföhl unit, were calculated for eclogites associating with pyroxenites in the southern part of the Bohemian Massif (Faryad et al., 2006; O'Brien and Vrána, 1995). The presence of disordered graphite as possible precursor of microdiamond was also reported in these eclogites (Faryad et al., 2006). The surrounding rocks are mostly gneiss, some may contain relicts of kyanite, and they are usually re-equilibrated at lower pressure, where andalusite or cordierite may form as result of granite intrusion. The studied eclogite samples come from four localities (Fig. 1): 1) In Borek (B), about 60–70 m thick lens of eclogite that is part of serpentinite body with ca. 400 × 250 m in size (Synek and Oliveriová, 1993). The serpentinized peridotite consists of harzburgite with minor lherzolite and dunite (Fiala and Jelínek, 1992). In addition to olivine (Fo_{90}), it contains orthopyroxene (En_{90}), minor diopsidic clinopyroxene and accessory spinel. 2) Eclogite from Hutě (H) forms about 400 × 100 m large body within biotite gneiss–migmatite (Machart, 1984). K–Ar data from amphibole yields age of 366 ± 26 Ma (Udovkiny et al., 1977). 3) Eclogite body (200 × 100 m in size) near Katov (K) is exposed within two mica gneiss. 4) Serpentinite body (1100 × 500 m) near Šelmberk (S) ruin contains several boudins of eclogite (the largest being 200 × 20 m in size). It is dunite in composition and contains relicts of clinopyroxene and orthopyroxene (Schovánek, 1977) and occurs at contact between orthogneiss and two mica gneiss.

5.3. Petrography

Two samples, one with and the other without kyanite, were selected from the Borek locality for detailed study. The kyanite free eclogite (sample 8B-4) is coarse-grained with weak foliation and consists of garnet, relict omphacite and quartz, amphibole, rutile and ilmenite. Garnet forms porphyroblasts (up to 5 mm) that may contain inclusions of rutile, ilmenite, amphibole and locally omphacite (Fig. 2a). Sample RJB1-11 has up to 5 vol % of kyanite or its pseudomorphs (Fig. 2b) formed by plagioclase + spinel. Garnet has only inclusions of rutile and it is usually rimed by plagioclase and amphibole coronas. Omphacite is fully replaced by symplectite of amphibole + plagioclase. The sample from Hutě (F120-12) is fine- to medium-grained and consists of garnet, omphacite, ilmenite, quartz, amphibole and accessory amounts of epidote, titanite and rutile. Garnet may contain inclusions of amphibole. Omphacite is transformed into plagioclase + amphibole ± diopside symplectite. In comparison to eclogites from other localities, this rock has high ilmenite content of up to 10 vol %. Together with omphacite it defines foliation of the rock. The sample from Katov (F146-12) is coarse-grained with garnet porphyroblasts surrounded by symplectite of amphibole + plagioclase + diopside with relicts of omphacite. All eclogites in the studied localities are strongly retrogressed. Amphibole and plagioclase first form symplectite after omphacite or thin coronas around garnet and finally large amphibole crystals overgrow the symplectite and stabilize amphibolite facies assemblage.

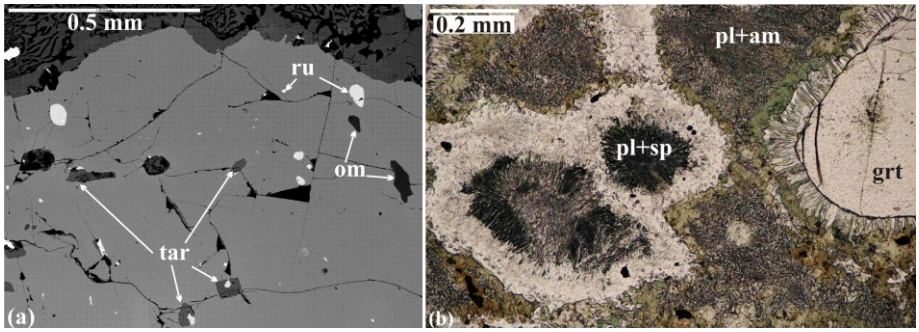

Fig. 2. BSE image (a) of garnet with inclusions of taramite (tar) in the core and omphacite near to the rim (sample 8B-4). Garnet has numerous inclusions of rutile (ru). (b) shows retrogressed eclogite (sample RJB1-11) with symplectite of amphibole (am) + plagioclase (pl) after omphacite and of spinel (sp) + plagioclase after kyanite. Garnet has corona of amphibole and plagioclase.

5.4. Mineral compositions

5.4.1. Garnet

Fig. 3 and Table 1 show composition of garnet from all four localities and it ranges from almandine-rich variety ($Alm_{54}Prp_{22}Grs_{23}$) in samples F146-12, F120-12 and 8B-4 to relatively pyrope-rich type ($Alm_{23}Prp_{54}Grs_{20}$) in sample F3-6. The spessartine content is low with a maximum of 4 mol % in samples from Borek. Garnet from both kyanite-free and kyanite-bearing samples in Borek shows strong and complex zoning, but generally with increase of pyrope and decrease of grossular and spessartine towards the rim (Fig. 4). In garnet from the kyanite-bearing sample almandine indicates a rimward decrease, but shows a flat profile in kyanite-free sample (Fig. 4c, d).

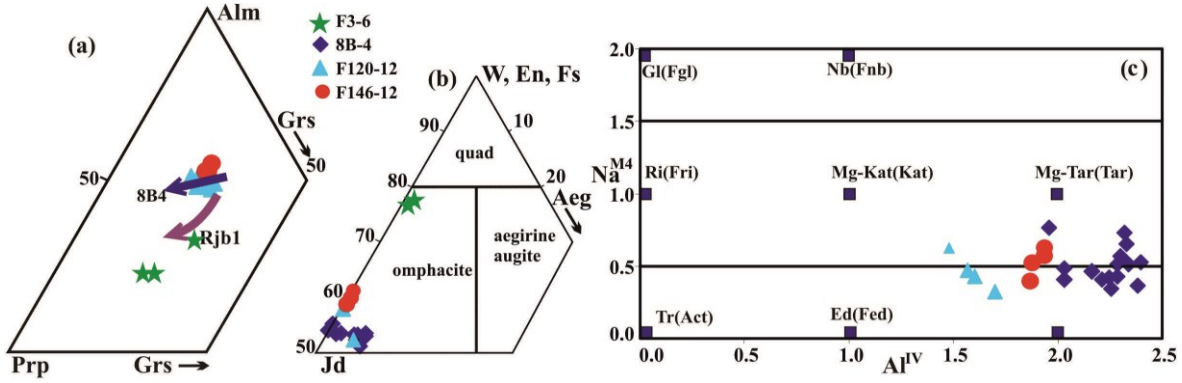

Fig. 3. Composition of garnet (a), pyroxene (b) and amphibole (c) from the studied eclogites in the Monotonous Unit. Abbreviations in the Na^{M4} and Al^{IV} diagram (c) are: Gl–glaucophane, Nb-nyböite, Ri-richterite, Kat-katophorite, Tar-taramite, Tr-tremolite, and Ed-edenite. F and Mg refer to ferro- and magnesian prefixes.

5.4.2. Clinopyroxene

Jadeite contents analyzed in clinopyroxene range between 23 and 43 mol % while aegirine is up to 3 mol % (Fig. 3b). Maximum jadeite-rich omphacite comes from kyanite-free samples (8B-4 and F120-12) and the lowest jadeitic clinopyroxene occurs in the sample from Šelmberk (F3-6). Clinopyroxene in the symplectite with plagioclase and amphibole is diopside with low jadeite content (below 20 mol %).

5.4.3. Amphibole

Amphibole in the matrix is pargasite and hornblende. At contact with ilmenite, it may have high Ti content and corresponds to titanium hornblende. Composition of amphiboles enclosed in garnet from the studied samples is shown in Fig. 3c. Taramite is present in the sample from Borek. Its B site is occupied by 0.51 to 0.76 Na atoms per formula unit (a.p.f.u.) and the A site contains 0.6–0.8 Na + K a.p.f.u. (the ferric/ferrous ratio in amphibole was calculated by normalization to 13 cations and 46 charges). The X_{Mg} = Mg / (Mg + Fe^{2+}) ratio is about 0.5. Inclusions of taramite to barroisite occur also in garnet from samples in Hutě and Katov.

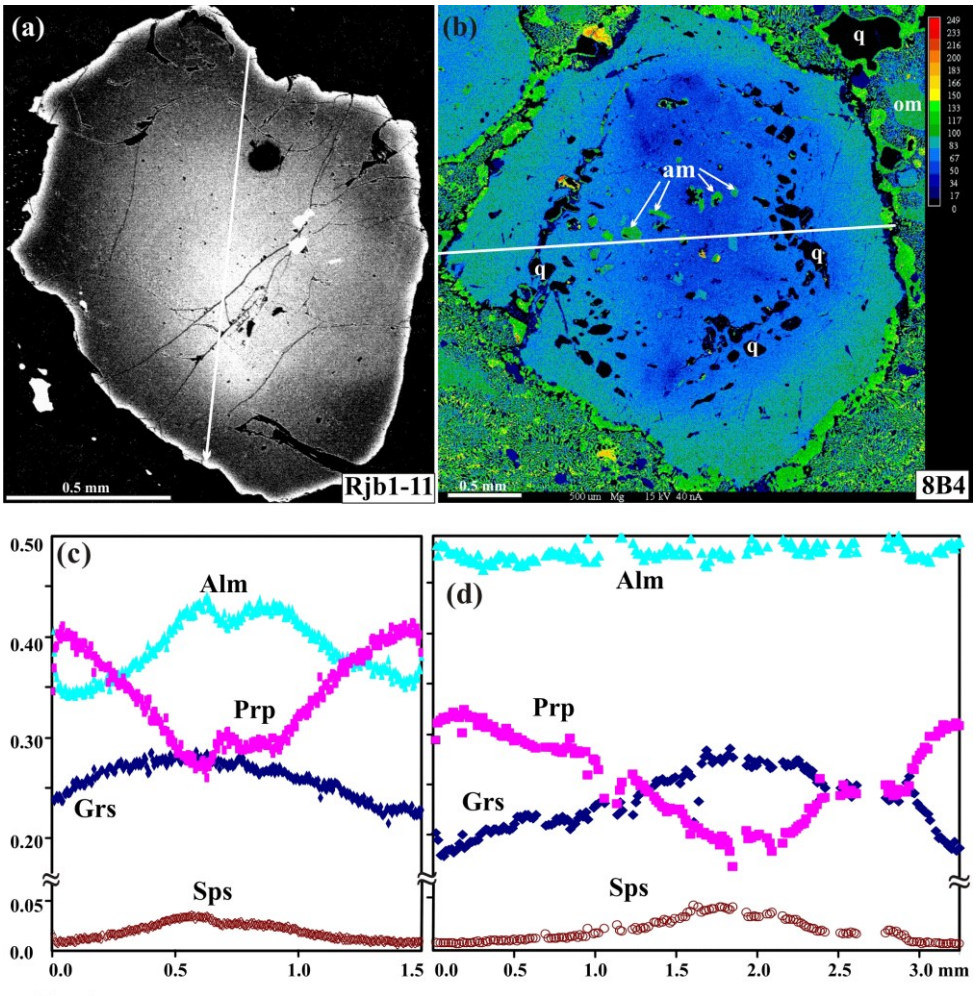

Fig. 4. BSE images (a) and compositional map of Mg (b) of garnet with inclusions of quartz (q) and Na–Ca amphibole (am). The matrix omphacite is replaced by symplectite of amphibole + plagioclase. (c and d) show compositional profiles with mol fractions of almandine, pyrope, grossular and spessartine contents.

Table 1: Microprobe analyses of selected garnet and clinopyroxene from clinopyroxenite and eclogite

Mineral	Garnet								
Sample	8B-4			RJB1-11		F120-12		F146-12	F3-6
Position	r	rc	c	c	r		c		om
SiO_2	39.33	38.71	38.39	39.06	40.49	38.50	38.63	39.42	40.09
TiO_2	0.05	0.06	0.14	0.03	0.02	0.03	0.05	0.09	0.07
Al_2O_3	22.43	22.10	22.05	21.99	22.45	21.69	21.66	21.73	22.76
FeO	22.78	23.31	22.60	20.36	16.58	24.08	23.01	25.13	14.50
MnO	0.35	0.97	1.93	1.55	0.38	0.72	0.71	0.37	0.28
MgO	8.62	6.97	5.18	6.25	11.12	6.73	7.49	5.66	11.83
CaO	7.18	8.23	10.41	10.22	8.91	7.83	7.75	8.36	10.90
Total	100.74	100.34	100.71	99.47	99.95	99.58	99.30	100.77	100.43
Si	2.971	2.959	2.944	3.016	2.999	2.982	2.985	3.019	2.947
Ti	0.003	0.003	0.008	0.002	0.001	0.002	0.003	0.005	0.004
Al	1.997	1.991	1.993	2.001	1.981	1.980	1.972	1.981	1.972
Fe^{3+}	0.056	0.085	0.111	0.000	0.018	0.054	0.054	0.000	0.121
Fe^{2+}	1.391	1.423	1.358	1.314	1.019	1.505	1.432	1.625	0.770
Mn	0.022	0.063	0.126	0.102	0.024	0.047	0.047	0.024	0.017
Mg	0.971	0.794	0.593	0.720	1.242	0.777	0.863	0.652	1.297
Ca	0.581	0.674	0.856	0.846	0.715	0.650	0.641	0.693	0.859
alm	46.6	47.7	45.7	44.1	34.0	50.2	47.7	54.3	25.8
prp	32.5	26.6	20.0	24.1	41.4	25.9	28.7	21.8	43.5
grs	19.2	22.1	28.1	28.4	23.8	21.5	21.2	23.1	27.6
sps	0.7	2.1	4.2	3.4	0.8	1.6	1.6	0.8	0.6
X_{Fe}	0.59	0.64	0.70	0.65	0.46	0.66	0.62	0.71	0.37

Table 1 *(continued)*

Mineral	Clinopyroxene					Amphibole				
Sample	8B-4		F120-12	F146-12	F3-6		F146-12	F120-12	8B-4	8B-4
SiO_2	55.46	55.65	56.21	56.45	55.11	SiO_2	43.13	46.96	41.75	39.2
TiO_2	0.14	0.10	0.06	0.16	0.07	TiO_2	0.52	0.21	1.98	3.92
Al_2O_3	10.83	10.10	9.51	9.05	6.64	Al_2O_3	19.15	13.38	17.80	20.5
FeO	4.92	4.68	4.04	5.12	1.87	FeO	11.83	9.91	13.39	12.1
MnO	0.04	0.00	0.03	0.07	0.00	MnO	0.05	0.00	0.12	0.12
MgO	8.89	8.20	9.52	10.64	13.30	MgO	11.04	15.07	9.57	8.93
CaO	13.66	14.12	14.55	14.73	19.14	CaO	9.43	9.27	7.97	8.73
Na_2O	6.52	6.72	5.69	5.01	3.46	Na_2O	3.49	3.25	5.53	5.13
						K_2O	0.17	0.12	0.07	0.04
Total	100.46	99.57	99.61	101.23	99.60	Total	98.80	98.17	100.66	100.92
Si	1.963	1.988	2.013	1.999	1.972	Si	6.063	6.519	6.044	5.671
Ti	0.004	0.003	0.002	0.004	0.002	AlIV	1.937	1.481	0.956	2.330
Al	0.452	0.425	0.401	0.378	0.280	AlVI	1.235	0.708	1.080	1.166
Fe^{3+}	0.042	0.038	0.000	0.000	0.004	Ti	0.055	0.022	0.216	0.426
Fe^{2+}	0.103	0.102	0.121	0.152	0.051	Fe^{3+}	0.770	1.075	0.404	0.153
Mn	0.001	0.000	0.001	0.002	0.000	Fe^{2+}	0.621	0.075	1.217	1.311
Mg	0.469	0.437	0.508	0.562	0.710	Mn	0.005	0.000	0.015	0.014
Ca	0.518	0.540	0.558	0.559	0.734	Mg	2.313	3.120	2.066	1.926
Na	0.448	0.465	0.395	0.344	0.240	Ca	1.420	1.379	1.236	1.353
aug	45.9	53.3	56.2	55.8	75.0	NaM4	0.580	0.621	0.767	0.652
jd	36.4	42.3	40.0	34.9	23.6	Na(A)	0.371	0.255	0.784	0.788
aeg	3.8	3.8	0.0	0.0	0.5	K	0.030	0.021	0.013	0.007
						A	0.401	0.275	0.798	0.795

5.5. P–T conditions

The compositional zoning and the presence of Na–Ca amphibole inclusions in garnet from eclogite suggest a prograde metamorphism from high-temperature blueschist facies to eclogite facies conditions (Faryad and Bernhardt, 1996). To estimate maximum P–T conditions in the eclogite, garnet–pyroxene thermometry (Ai, 1994; Ravna, 2000) was used for all four localities. End-member reactions for garnet with inclusions of taramite and omphacite in sample 8B-4 were calculated based on Thermocalc software V3.21 (Holland and Powell, 2003) and the Holland et al. (1998) dataset. The Gibbs-free energy minimization technique [Perplex 09 by Connolly (2005)] was used for kyanite bearing eclogite (sample RJB1-11). We used the solution models for garnet, chlorite and omphacite after Holland et al. (1998), updated by Holland and Powell (2003), plagioclase after Newton et al. (1980) and amphibole after White et al. (2003). The results of garnet–clinopyroxene thermometry for different samples and different localities (Table 2) are in the range of 640–670 °C. A temperature of 650 °C at 2.3 GPa was obtained by calculation of endmember reactions among amphibole, clinopyroxene and garnet in sample 8B-4:

(1) prp + hed = di + alm

(2) parg + q = prp + grs + di + jd + H_2O

(3) parg + alm + q = prp + grs + jd + hed + H_2O

(4) parg + hed + q = grs + di + jd + alm + H_2O.

Table 2: Results of thermobarometric calculations.

Calibration	Ravna (2000)	Ai (1994)	Thermocalc	
Samples	T (°C)[a]	T (°C)[a]	T (°C)a	P (GPa)
8B-4	667 ± 11	642 ± 16	650	2.3
RJB1-11	651 ± 19	641 ± 20		
F146-12	660 ± 36	649 ± 34		
F120-12	665 ± 22	645 ± 22		
F3-6	659 ± 29	649 ± 27		

[a] Temperature calculation at 2.0 GPa

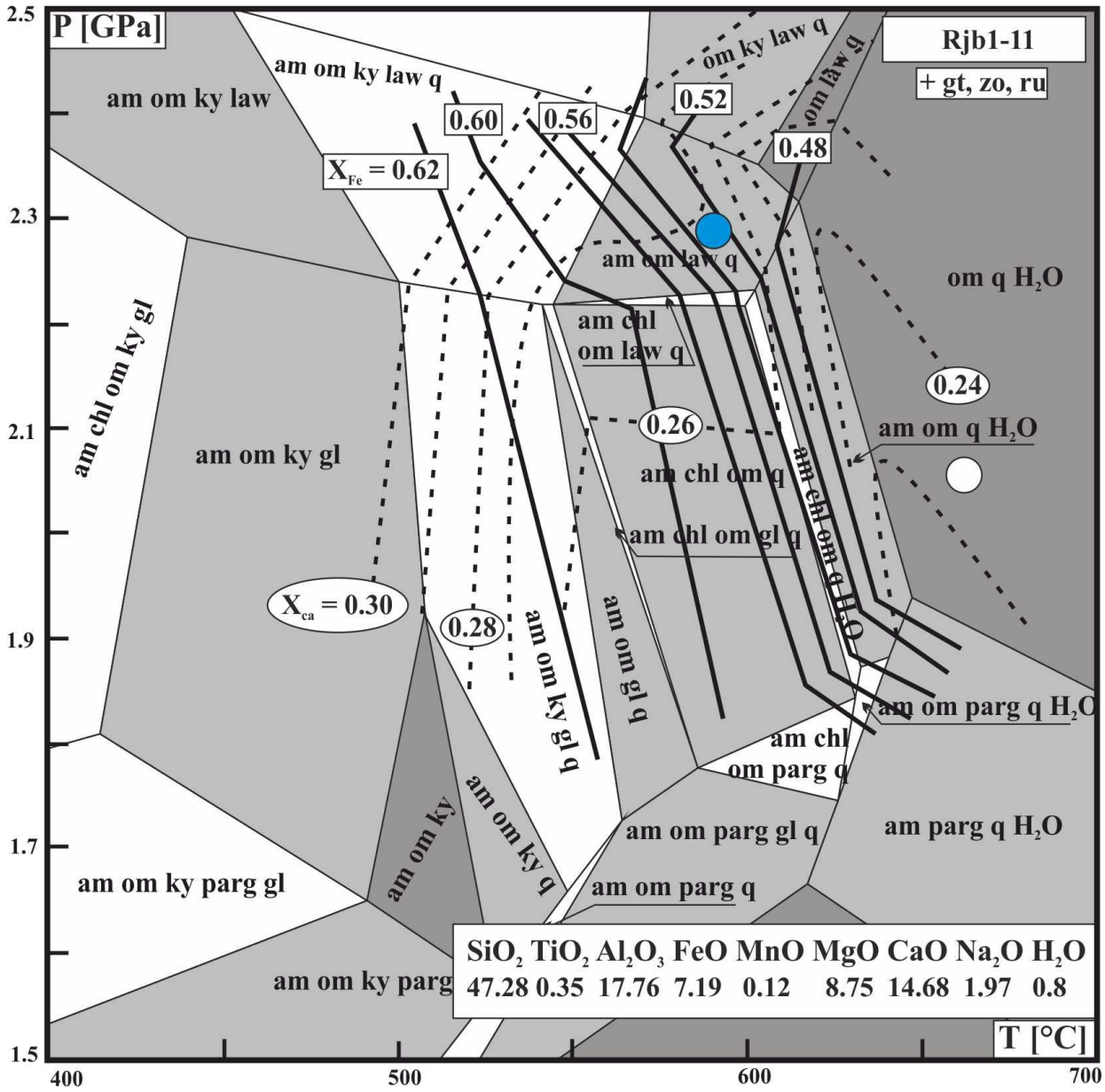

Fig. 5 shows pseudosection constrained for kyanite-bearing sample (RJB1-11) from Borek. All fields in the selected P–T range (400– 700 °C and 1.5–2.5 GPa) contain garnet, zoisite and rutile. Kyanite is present at relatively low temperature (below 550 °C). Mantle composition near the rim of garnet (X_{Ca} = 0.27, X_{Fe} = 0.53) yields pressure above 2.3 GPa at cca 600 °C which is similar to that obtained by the end-member equilibrium reactions. The rim composition of garnet shows lower pressure of 2.0 GPa, but higher temperature of about 660 °C. It should be noted that most garnets in this sample indicate various degree of replacement with amphibole + plagioclase coronae.

5.6. Discussion

5.6.1. Significance of pressure–temperature variations

Textural relations and estimated P–T conditions of eclogite bodies within amphibolite facies basement rocks in the Moldanubian Zone enable us to constrain the earlier subduction history of HP–UHPM rocks and compare them with similar rocks in the Saxothuringian Zone. The calculated temperature conditions for eclogites in the amphibolite facies Monotonous and Varied units (600–650 °C, Fig. 6) are consistent with those already reported by Medaris et al. (1995). Pressures of 1.3–1.5 GPa, reported by these authors, were obtained using jadeite content in clinopyroxene and indicate only minimum values for the eclogite facies event. Maximum pressure, calculated based on the pseudosection method and equilibrium reactions among minerals, is almost one order higher (about 2.3 GPa, Fig. 6). Compared to the high-grade Gföhl Unit, the pressures and temperatures of eclogite facies metamorphism are low, however intermediate P–T conditions between these two units have been reported from the nearby South Bohemian Granulite massif (Faryad et al., 2006; Kobayashi et al., 2011; Kotková et al., 1997).

When comparing P–T conditions of eclogites in amphibolite facies units from the Moldanubian Zone with those occurring in the Erzgebirge and Sudetes [the Saxothuringian Zone, Massonne and Koppe (2005), Klemd and Bröcker (1999)], both show a P–T gradient of 7–9 °C/km (Fig. 6) with prograde P–T paths crossing the epidote and lawsonite eclogite facies boundary. These features, as well as preservation of strong compositional zoning of garnet with taramite inclusions, similar to that in eclogites from Mariánské Lázně Complex (Faryad, 2012), suggest a rapid and/or relatively cool subduction environment. In contrast to eclogites in amphibolite facies units in the Erzgebirge and from Sudetes, where decompression and cooling history (path 2 in Fig. 6) are defined by formation of barroisitic amphibole, overgrowing or replacing the eclogite facies assemblage, the eclogites in the Moldanubian Zone show almost isothermal decompression (path 1). Amphibole in the matrix is pargasite or hornblende. It is not clear, if the isothermal decompression path, deduced from compositional zoning in garnet, was due to

re-equilibration during exhumation, or it was a result from later amphibolite facies overprint. This process was documented by geochronological dating of amphibole occurring at around 370–380 Ma (Ar–Ar method) in the Mariánské Lázně Complex (Dallmeyer and Urban, 1998; Zulauf, 1997) and 365 Ma (K–Ar method) in the Hutě eclogite (Udovkiny et al., 1977).

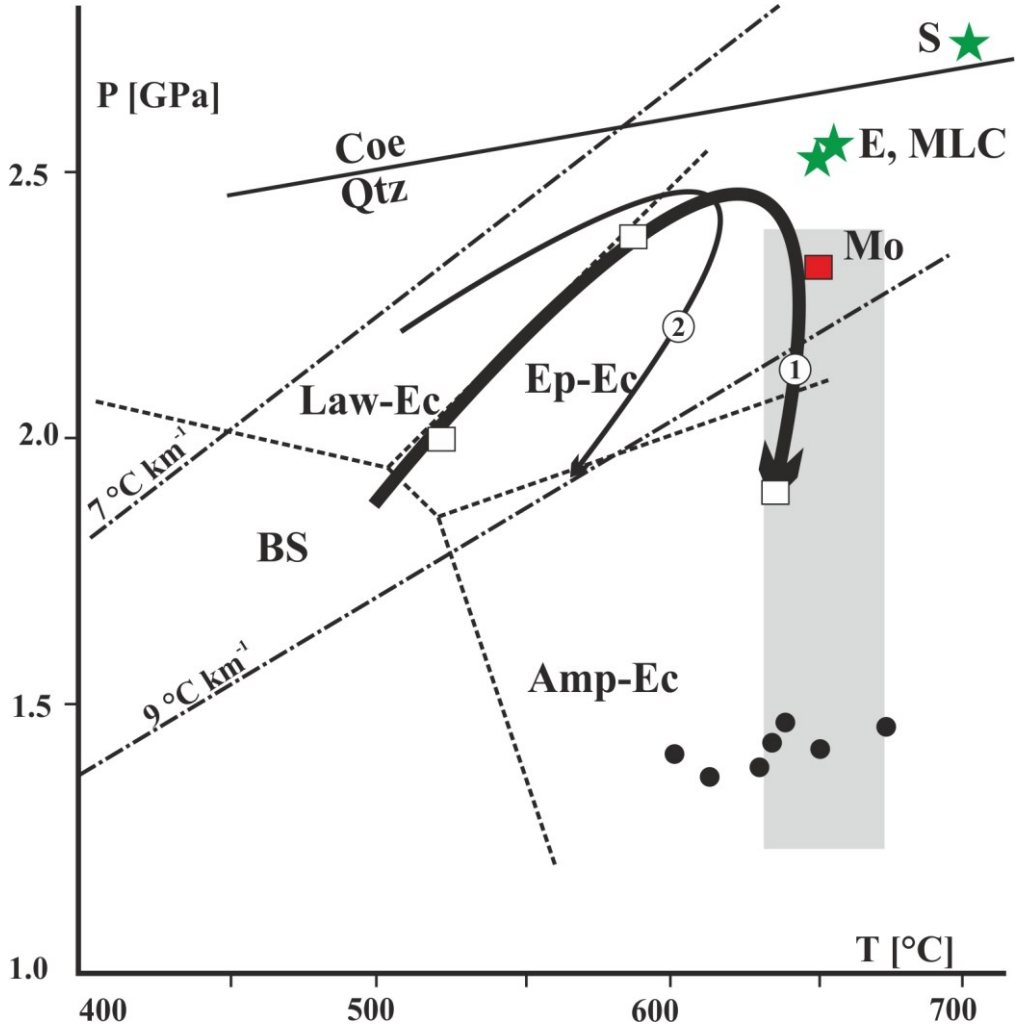

Fig. 6. Summary of P–T data from eclogites in theMoldanubian Zone, east from the Teplá–Barrandian Block. Gray shaded field shows average temperatures, obtained by garnet–pyroxene thermometry for the studied samples (Table 2). Solid square corresponds to P and T values obtained by the end-member reactions (1–4). Filled circles are P–T data by Medaris et al. (1995) from eclogite in this area. The thick solid line arrow (1) is P–T path, obtained by mantle and rim compositions (open squares) of garnet in Fig. 5. P–T data from medium-temperature eclogite in the Saxothuringian Zone are also shown for comparison: E-Erzgebirge (Klápová et al., 1998; Massonne and Koppe, 2005), MLC-Mariánské Lázně Complex (Faryad, 2012), and S-Sniežnik in the Sudetes (Bröcker and Klemd, 1996). P–T path (2) is from eclogite in the Erzgebirge (Faryad et al., 2010a).

5.6.2. Geodynamic implication of the medium-temperature eclogites for Variscan Orogeny in the Moldanubian Zone

Figure 7 shows tectonic zonation along the European Variscan Belt with location of major allochthonous Units (Massifs) (Franke, 2000; Matte, 1986). All massifs are characterized by the presence of ophiolites and HP rocks and they are crossed by one or more suture zones. The most prominent Variscan suture is formed by north- or northwest-verging subduction in all massifs. In the Bohemian Massif, two sutures are considered to be formed by closure of the Saxothuringian and Moldanubian Oceans (Franke, 2000). In the present geographic situation, the two oceans were closed by opposite subductions beneath the Teplá–Barrandian Block from northwest and southeast, respectively. A younger subduction beneath the Moldanubian Zone is assumed by closure of the Rhenohercynian (Rheic) Ocean with the suture following the eastern border of the Moldanubian Zone, including Sudetes (Fig. 1) (Finger et al., 2007). Because of similarity of felsic granulites with HP–UHPM rocks both in Saxothuringian and Moldanubian Zones, Schulmann et al. (2009) consider only one subduction from the Saxothuringian side beneath the Teplá–Barrandian Block. In this model, a part of subducted material, now occurring in the Saxothuringian Zone, was exhumed back along the subduction channel, but a part penetrated the lower crust–mantle boundary beneath the Teplá–Barrandian Block and Moldanubian Zone and then exhumed due to buckling of crustal layers in the Moldanubian Zone. The calculated P–T conditions in eclogites from the Monotonous and Varied units and the preservation of the prograde P–T paths even in HT eclogites and host granulites (Faryad et al., 2010b) in the Moldanubian Zone, however do not support long distance transport beneath continental blocks (zones) but testify a rather cooler environment both for their subduction and exhumation. Therefore, the westward subduction by closure of the Moldanubian Ocean (Franke, 2000), where burial and exhumation of HP–UHPM rocks occurred along the same subduction channel, seems to be the relevant model for the Moldanubian rocks. The Moldanubian suture was adapted by Medaris et al. (2006) to explain formation and exhumation of eclogites and garnet peridotites in the eastern part of the Bohemian Massif and its existence is supported by geophysical data (Babuška and Plomerová, 2013).

The 250 km long suture in the Moldanubian Zone, from Aubach (A) in the SW to the Kutná Hora (KH) in the NE (Fig. 1), is followed not only by the presence of eclogites and serpentinites, but also by granulites with HT eclogites and garnet peridotites. Its continuation to the northeast is not clear due to the Cretaceous sedimentary cover, however Vrána et al. (2009) correlate the high-grade rocks from the Kutná Hora Complex (the Moldanubian Zone) with those in the Sudetes. Formation of HP–UHPM rocks, occurring along the Saxothuringian Zone from Sudetes to the Erzgebirge (Fig. 1) by one subduction zone and from a similar source material is generally accepted (for ref. see Faryad, 2011). Based on similarity in lithologies, P–T regime and age of metamorphism (see below) of HP–UHPM rocks between the Saxothuringian and Moldanubian zones, we assume that they were formed by a single subduction that related to the closure of the Moldanubian Ocean. The Moldanubian Zone with melange-like structure is characterized by volumetrically larger amounts of HP–UHPM rocks with greater regional extent than that occurring in the Saxothuringian Zone (Fig. 1). The present position of HP–UHPM rocks surrounding the Teplá–Barrandian Block from north and west could be partly explained by orocline bend of the Moldanubian suture in the north, and mostly by tectonic transport after their exhumation to various crustal levels. A hairpin bend suture model north of the Teplá–Barrandian Block with oroclinal bending in the Sudetes was proposed to explain distribution of ophiolites and HP rocks (Finger and Steyrer, 1995). This model, primarily assumed connection of the Saxothuringian suture with much younger Rhenohercynian suture, can fit for possible continuation of the Moldanubian suture to the north of the Teplá-Barrandian Block. Statistical evaluation of paleomagnetic data documents various degrees of clockwise and anticlockwise block rotations in the Bohemian Massif since Devonian (Edel et al., 2003; Krs et al., 1995; Tait et al., 1994). In addition to more than 90° rotation in the East Sudetes and Silesian Block, up to 60° block rotation against each other can be documented when comparing paleomagnetic data from Carboniferous sediments in the Teplá–Barrandian Block (cca 30° anticlockwise rotation, Krs et al., 1995) and Variscan plutonites in the Moldanubian Zone (ca. 25° clockwise rotation, Edel et al., 2003). This implies significant displacement and tectonic transport of material around rigid block as that of the Teplá–Barrandian. The block rotations occurred

during convergence and closure of the Rhenohercynian Ocean during Carboniferous (Edel et al., 2003) which was followed by crustal thickening in the Moldanubian Zone as a result of deep-level westward wedging (indentation) of Brunovistulian Block (Schulmann et al., 2005). The presence of amphibolite facies Moldanubian rocks surrounding the Teplá–Barrandian Block from south to south-west and the occurrence of eclogite bodies further west near Winklarn in Germany and of the Mariánské Lázně Complex at contact with the Saxothuringian Zone (Fig. 1) are the best examples of possible tectonic transport from their main Variscan suture.

It is commonly accepted that closure of the oceans in the central part of the Variscides occurred in the Devonian (see Franke, 2000; Timmermann et al., 2004; Zulauf, 1997), as indicated for example by the 400 Ma age for high-pressure metamorphism. Some younger ages of 340 Ma from HP granulite and diamondiferous gneiss in the Erzgebirge are explained by crustal thickening, where the HP rocks were maintained in the crustal root for about 50 Ma and then exhumed due to delamination of lithospheric mantle (Willner et al., 2000). Although, ages of about 340 Ma are known from HP granulite in the Moldanubian Zone and in Sudetes, there are an increasing number of new geochronological data indicating 390–370 Ma age of HP–UHP metamorphism (Bröcker et al., 2009; Lange et al., 2005; Nahodilová et al., 2014; Prince et al., 2000; Teipel et al., 2012). A similar age is also reported from garnet pyroxenite (Brueckner et al., 1991). Based on the preservation of prograde zoning in garnet from granulites and associated eclogites and pyroxenite (Faryad et al., 2010b, 2013), we assume that the younger ages could be the results of granulite facies overprint. This process related to subduction of the Rhenohercynian Ocean and subsequent collision between the Moldanubian Zone and Brunovistulian Block (Babuška and Plomerová, 2013; Finger et al., 2007; Schulmann et al., 2005).

Fig. 7. Position of the pre-Carboniferous Moldanubian type allochthonous units along the European Variscan Belt (Franke, 2000; Matte, 1986). The allochthonous units are followed by a suture that continues from the Iberian Massif, through French Massif Central, Vosges (V), Schwarzwald (S) to the Moldanubian Zone.

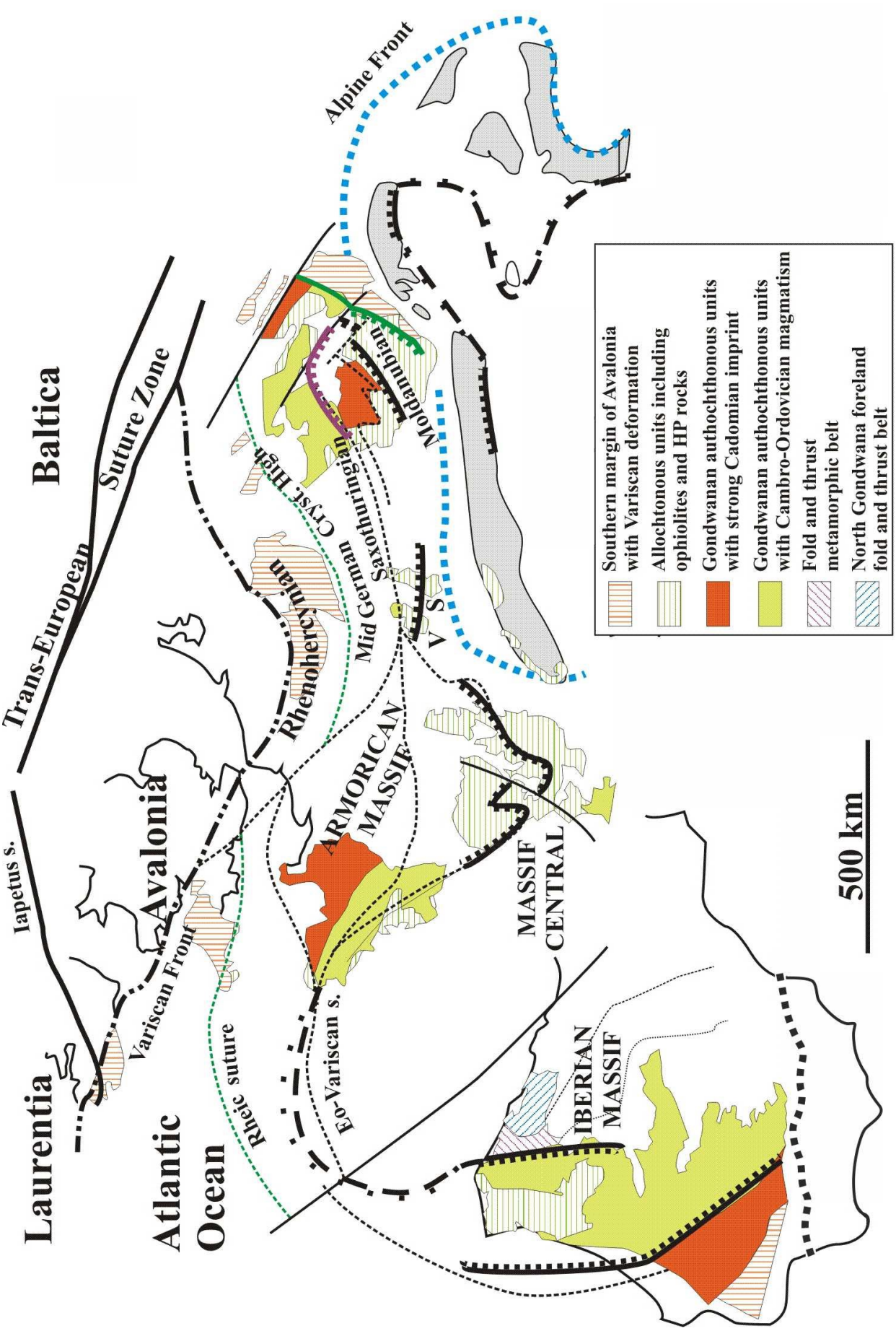
Laurentia
Baltica
Atlantic Ocean
Iapetus s.
Trans-European Suture Zone
Avalonia
Variscan Front
Rheic suture
Eo-Variscan s.
Rhenohercynian
Mid German Crystl. High
Saxothuringian
Moldanubian
S A
ARMORICAN MASSIF
MASSIF CENTRAL
IBERIAN MASSIF
Alpine Front
500 km
Southern margin of Avalonia with Variscan deformation
Allochtonous units including ophiolites and HP rocks
Gondwanan authochthonous units with strong Cadomian imprint
Gondwanan authochthonous units with Cambro-Ordovician magmatism
Fold and thrust metamorphic belt
North Gondwana foreland fold and thrust belt

5.7. Conclusions

The occurrence of eclogite bodies with serpentinite along cca 250 km zone southeast of the Teplá–Barrandian Block is interpreted as Variscan suture formed by closure of the Moldanubian Ocean (Franke, 2000). The eclogites and serpentinites are part of the amphibolite facies Monotonous and Varied units and the suture zone is followed by the presence of granulite massifs that contain bodies of garnet peridotite, showing UHP conditions. The Moldanubian suture is part of the main Variscan suture that can be traced within other allochthonous massifs along the European Variscan Belt. In the Bohemian Massif, it continues from the Moldanubian Zone to Sudetes in the northwest. The calculated P–T conditions from eclogite bodies in the Moldanubian Zone indicate low geothermal gradient, similar to that in eclogites from the Saxothuringian Zone and suggest their formation by rapid subduction and exhumation process. Based on their analogy in lithology, P-T regime and ages of metamorphism of HP–UHP rocks, we assume that the Moldanubian suture was responsible for the formation and exhumation of these rocks both in the Moldanubian and Saxothuringian zones. Present position of HP–UHPM rocks in the Saxothuringian Zone could be the result of tectonic transport after their exhumation to crustal levels.

5.8. Acknowledgements

This work is part of the research projects MSM0021620855 and P 13-06958S (Czech Sciences Foundation). We thank V. Babuška, V. Kachlík and P. Pruner for helpful discussion during the manuscript preparation. We are grateful for constructive comments and suggestions of M. Janák and an anonymous reviewer. M. Scambelluri is thanked for careful editorial comments.

PART VI

COINCIDENCE OF GABBRO AND GRANULITE FORMATION AND THEIR IMPLICATION FOR VARISCAN HT METAMORPHISM IN THE MOLDANUBIAN ZONE (BOHEMIAN MASSIF), EXAMPLE FROM THE KUTNÁ HORA COMPLEX

Shah Wali Faryad[1], Václav Kachlík[2], Jiří Sláma[3], Radim Jedlička[1]

Institute of Petrology and Structural Geology, Charles University in Prague, Albertov 6, 12843 Prague, Czech Republic

Institute of Geology and Paleontology, Charles University in Prague, Albertov 6, 12843 Prague, Czech Reublic

Institute of Geology AS CR, Rozvojová 269, 16500 Prague, Czech Republic

Abstract

Leucocratic metagabbro and amphibolite from a mafic–ultramafic body within migmatite and granulite in the Kutná Hora Complex were investigated. The mafic–ultramafic rocks show amphibolite facies metamorphism, but in the central part of the body some metagabbro preserves cumulus and intercumulus plagioclase, clinopyroxene and spinel. Spinel forms inclusions in both clinopyroxene and plagioclase and shows various degree of embayment structure, that was probably a result of reaction with melt during magmatic crystallization. In the metagabbro, garnet forms coronae around clinopyroxene at the contacts with plagioclase. Amphibolite contains garnet with prograde zoning and plagioclase. Phase relations of igneous and metamorphic minerals indicate that magmatic crystallization and subsequent metamorphism occurred as a result of isobaric cooling at a depth of 30–35 km. U–Pb dating on zircon from leucogabbro yielded a Variscan age (337.7 ± 2 Ma) that is similar or close to the age of granulite facies metamorphism (cca 340 Ma) in the Moldanubian Zone. Based on the calculated P-T conditions and age data, both the mafic–ultramafic body and surrounding granulite shared the same exhumation path from their middle–lower crustal position at the end of Variscan orogeny. The coincidence of mafic–ultramafic intrusives and granulite–amphibolite facies metamorphism is explained by lithospheric upwelling beneath the Moldanubian Zone that occurred due to slab break-off during the final stages of subduction of the Moldanubian plate beneath the Teplá Barrandian Block. The model also addresses questions about the preservation of minerals and/or their compositions from the early metamorphic history of the rocks subjected to ultradeep subduction and subsequent granulite facies metamorphism.

Keywords: *Granulite, Heat source, Spinel-bearing gabbro, Variscan age*

6.1. Introduction

The Kutná Hora Complex is a composite unit of stacked crustal and mantle rocks metamorphosed in amphibolite to granulite facies conditions (Faryad et al., 2010b; Nahodilová et al., 2011; Pouba et al., 1987; Vrána et al., 2006). It contains granulite and eclogite bodies, which are present also in the central and western parts of the Moldanubian Zone and form a cca 200 km long belt from the Kutná Hora Complex in the north to the South Bohemian granulite massifs in the south (Fig. 1). The felsic granulites and granulite gneisses contain lenses and boudins of garnet peridotite, garnet pyroxenite and eclogite for which high-pressure to ultrahigh-pressure (HP–UHP) conditions were estimated (Faryad, 2009). The high-grade rocks of the Kutná Hora Complex have been traditionally correlated with the Gföhl Unit (Synek and Oliveriová, 1993), which is characterized by the presence of bodies of felsic granulite, which are mostly exposed along the eastern border of the Moldanubian Zone [Fuchs and Matura (1976), Fig. 1]. Mineral inclusion studies by Perraki and Faryad (2014) indicated that some felsic granulite from the Kutná Hora Complex experienced an earlier UHP metamorphism. Based on major and trace element zoning in garnet, Jedlicka et al. (2015) concluded that the UHP conditions in felsic rocks were reached at relatively low temperature and that the granulite facies metamorphism occurred after the UHP rocks were exhumed and emplaced in a mid-crustal position. While the first metamorphism is related to subduction of the Moldanubian plate beneath the Teplá-Barrandian Block (Faryad et al., 2013; Franke, 2000; Medaris et al., 2005), the mechanism and source for granulite facies heating remains unclear. According to Lexa et al. (2011), the granulite facies metamorphism in the Bohemian Massif occurred due to the radioactive heat production within the lithospheric felsic lower crust. Willner et al. (2000, 2002) consider delamination and detachment of mantle lithosphere under the crustal root for the generation and exhumation of high-pressure and high-temperature rocks. Jedlicka et al. (2015) and Faryad and Fišera (2015) showed that the granulite facies metamorphism was a short-lived process, otherwise the prograde compositional zonation in garnet from the HP–UHP event would totally homogenize. By investigating the coronitic troctolite, occurring adjacent to granulite in the eastern part of the Moldanubian Zone, Faryad et al. (2015)

proposed that the heat source for granulite facies metamorphism of HP–UHP rocks in the Moldanubian accretionary complex was upwelling of asthenospheric magma, a process governed by slab break-off.

In this paper we present results of a petrological and geochronological study within a several km long mafic–ultramafic body that occurs within migmatite and granulite gneiss in the southeastern part of the Kutná Hora Complex. In composition the mafic-ultramafic rocks range from norite, pyroxenite, troctolite to anorthositic gabbro. In contrast to the surrounding granulites, which experienced an earlier UHP metamorphism, the mafic–ultramafic body shows only a single amphibolite facies metamorphism, where igneous phases are preserved mostly in the central part of the body. The zircon U–Pb data from plagioclase rich gabbro yielded Variscan magmatic crystallization age which is similar to the age of granulite facies metamorphism in the nearby rocks. Phase and textural relations of igneous and metamorphic minerals are used to define the crystallization depth of magma and subsequent metamorphism of the mafic–ultramafic rocks. The results of petrological and geochronological study are discussed to decipher a possible relationship between the mantle melting process and granulite facies metamorphism in the Moldanubian Zone. The relationship of high–ultrahigh pressure metamorphism to post-collisional magmatism in the Moldanubian is also discussed.

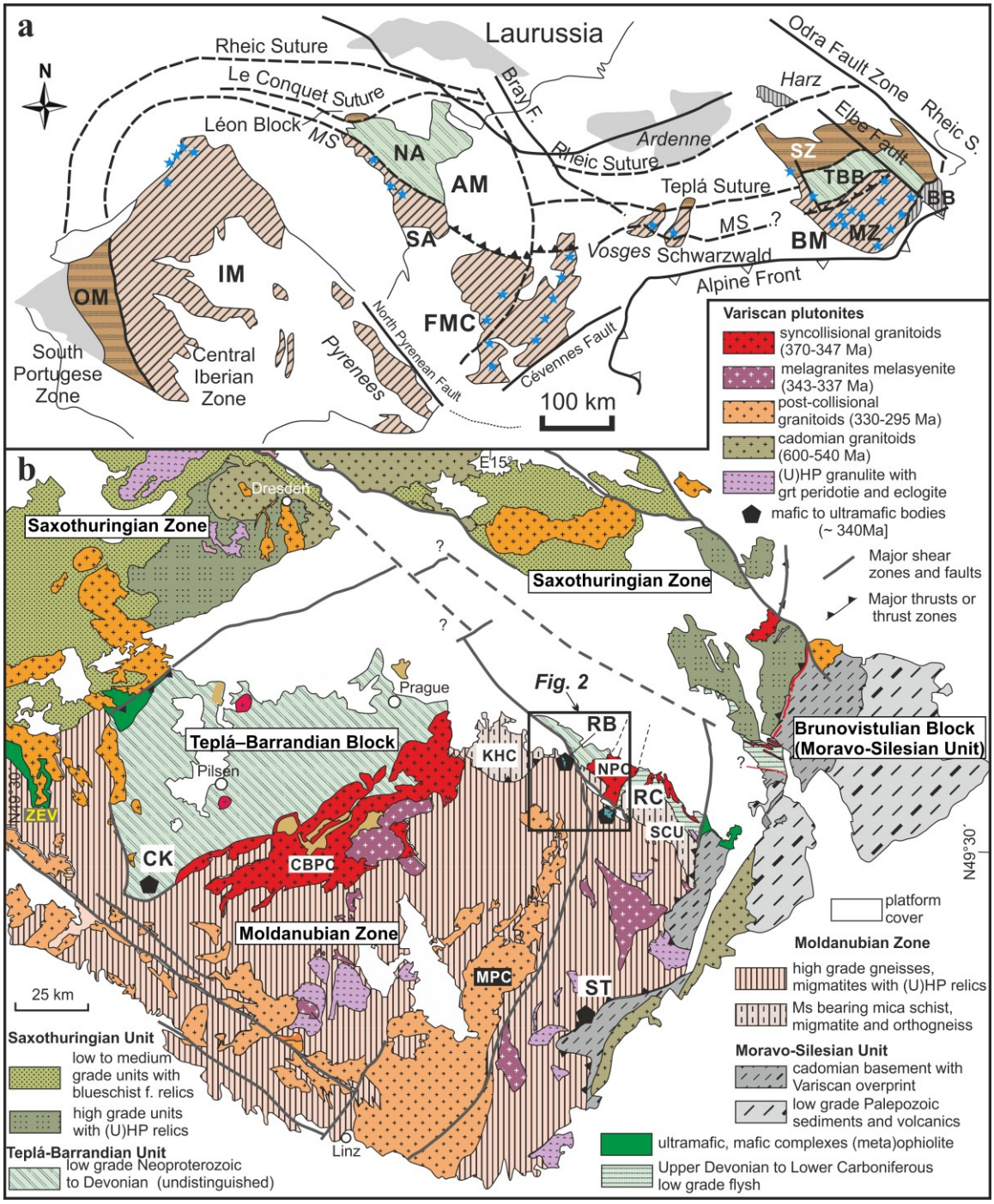

Fig. 1: (a) Position of the pre-Carboniferous Moldanubian type allochthonous units along the European Variscan Belt with presumed Moldanubian suture = MS [modified from Franke (2000), Faure et al. (2014)]. The stars indicate the occurrences of HP-UHP rocks (Faryad and Kachlík, 2013) within basement massifs: AM = Armorican Massif (NA = North Armorica, SA = South Armorica), BM = Bohemian Massif, FMC = French Massif Central, IM = Iberian Massif with Ossa-Morena Zone (OM). Basement units in the Bohemian Massif are: BB = Brunovistulian Block, MZ = Moldanubian Zone, SZ= Saxothuringian Zone, TBB = Teplá-Barrandian Block; (b) Simplified geological map of the Bohemian Massif, modified from Franke (2000), Cháb et al. (2007) and Faryad and Kachlík (2013). KHC = Kutná Hora Complex, SCU = Svratka Crystalline Unit, CBPC = Central Bohemian Plutonic Complex, MPC = Moldanubian Plutonic Complex. Variscan (~340Ma) mafic and ultramafic intrusions are: CK = Čertův Kámen, RB = Ronov body, RC = Ransko Complex, ST = Stálky, NPC = Nasavrky Plutonic Complex.

6.2. Geological setting

The Bohemian Massif is the easternmost segment of the European Variscan Belt (Fig. 1a) and it consists of four major tectonic domains: (i) the Saxothuringian Zone, (ii) the Moldanubian Zone, (iii) the Teplá-Barrandian Block and (iv) the Moravo-Silesian (Brunovistulian) Block. The Saxothuringian Zone occupies the northern part of the Bohemian Massif, while the Moldanubian Zone is located in the southern part between the Teplá-Barrandian Block in the West and the Brunovistulian Block in the east. The zones are characterized by the presence of lenses and boudins of HP and UHP metamorphic rocks within amphibolite to granulite facies rocks, while the Brunovistulian and the Teplá-Barrandian blocks have no HP–UHP metamorphic rocks. In addition to eclogite facies and UHP metamorphic rocks (see Kotková et al., 2011; Massonne and O'Brien, 2003), the Saxothuringian Zone contains blueschist facies rocks that are strongly overprinted by greenschist facies metamorphism (Faryad and Kachlík, 2013).

The Teplá-Barrandian Block with its crustal units tectonically overlies Moldanubian Zone along a dextral oblique shear zone in the Železné hory area (Fig. 2). It is formed by Neoproterozoic and Early Paleozoic sedimentary and volcanic rocks. The Neoproterozoic rocks are black shales, greywackes with intercalations of conglomerate. They are intruded by Neoproterozoic (cca 580 Ma) tonalite and Ordovician (cca 480 Ma) granite with numerous bodies of co-magmatic gabbro (Fig. 2). The Early Paleozoic sequence consists of Cambrian to Devonian sediments with Cambrian intermediate to acid calc-alkaline volcanics. The Neoproterozoic and Early Paleozoic rocks, imbricated along the Železné hory Fault zone show various degrees of metamorphism, ranging from lower greenschist to amphibolite facies conditions. The degree of metamorphism increases generally towards the underlying Moldanubian Zone. Some rocks in the southwestern edge of the Teplá-Barrandian Block (Fig. 1b) show up to granulite facies conditions (Bues and Zulauf, 2000).

The Moldanubian Zone is formed by medium-grade (the Monotonous and Varied units) to high-grade (the Gföhl Unit) rocks with Paleoproterozoic to Devonian protolith ages (Košler et al., 2014; Schulmann et al., 2005 and references therein). The Monotonous and Varied groups, collectively known as the Drosendorf Unit (Fuchs

and Matura, 1976), consist of various types of paragneisses and migmatites. The Varied Unit additionally contains lenses and layers of marbles, amphibolite, quartzite and graphite-bearing paragneiss. Both the Monotonous and Varied units contain bodies of retrogressed eclogite and spinel peridotite. The Gföhl Unit is represented by felsic granulite, orthogneisses and various types of migmatite including kyanite-bearing migmatite. The felsic granulite forms up to 10 × 20 km large bodies that are imbricated within the Drosendorf Unit rocks. They contain lenses of garnet peridotite and eclogite. Recent thermobarometric and mineral inclusion studies (Faryad et al., 2010b; Jedlicka et al., 2015; Perraki and Faryad, 2014) showed that the felsic granulite experienced HP–UHP metamorphism prior to their granulite facies overprint. Fig. 1a shows that rocks of Moldanubian affinity are present along the internal and most eroded part of the European Variscan Belt. The most striking feature of the Moldanubian Zone in the Bohemian Massif is the presence of more than one hundred bodies of retrogressed eclogite and serpentinized spinel peridotites (Machart, 1984; Medaris et al., 2015), which together with bodies of granulite (former HP–UHP rocks) are interpreted as integrated members of the Moldanubian accretionary complex or orogenic wedge (Faryad et al., 2013). The distribution of HP–UHP rocks along the whole Moldanubian Zone from the Bohemian Massif in the east to the Iberian Massif in the southwest (Fig. 1a), is consistent with the subduction and exhumation hypothesis of Franke (2000) and related to the Moldanubian suture (Faryad et al., 2013).

Variscan igneous rocks of the Moldanubian Zone, some also intruding the overlying Teplá-Barrandian Block, can be classified into four groups. The first group (cca 350–346 Ma) is represented by arc-related intrusions [the Central Bohemian Plutonic Complex = CBPC; Žák et al. (2014)] and synkinematic gabbro-tonalite bodies within the Upper Devonian to Lower Carboniferous flysh complexes, (Fig. 1a), which occur along the boundaries between the Moldanubian Zone and Teplá-Barrandian Block (Fig. 1b). The second group (cc0. 360–340 Ma) consists of separate intrusive bodies of mafic–ultramafic rocks (Figs. 1b, 2) that include the Čertův Kámen (Bues et al., 2002), Stálky (Faryad et al., 2015) and the Ransko Complex (Ackerman et al., 2013). They show different degrees of post-magmatic and metamorphic recrystallization. Several gabbroic bodies are present in the Nasavrky Plutonic

Complex dominated by a tonalite to granite suite (Schulmann et al., 2005; Fig. 2a). The largest Ransko gabbro-peridotite Complex (up to several km in size) is not affected by metamorphism, but others, e.g. the metatroctolite at Stálky in the Drosendorf stack at the Moldanubian-Moravian Boundary (Fig. 1b), show granulite facies recrystallization. The third group is represented by unmetamorphosed plutons (melagranite, melasyenite, Fig. 1b) and dyke swarms of ultrapotassic rocks (343–337 Ma) that penetrated the Moldanubian Zone rocks (Holub, 1997; Kotková et al., 2010; Kusiak et al., 2010). The youngest (cca 329–305 Ma) anatectic granitoids of the Moldanubian Plutonic Complex (MPC) are related to formation of the dome like structure generated along the Přibyslav Mylonite Zone (PMZ in Fig. 2) as a response to underthrusting of Brunovistulian Block under the Moldanubian Zone (Žák et al., 2011, 2014).

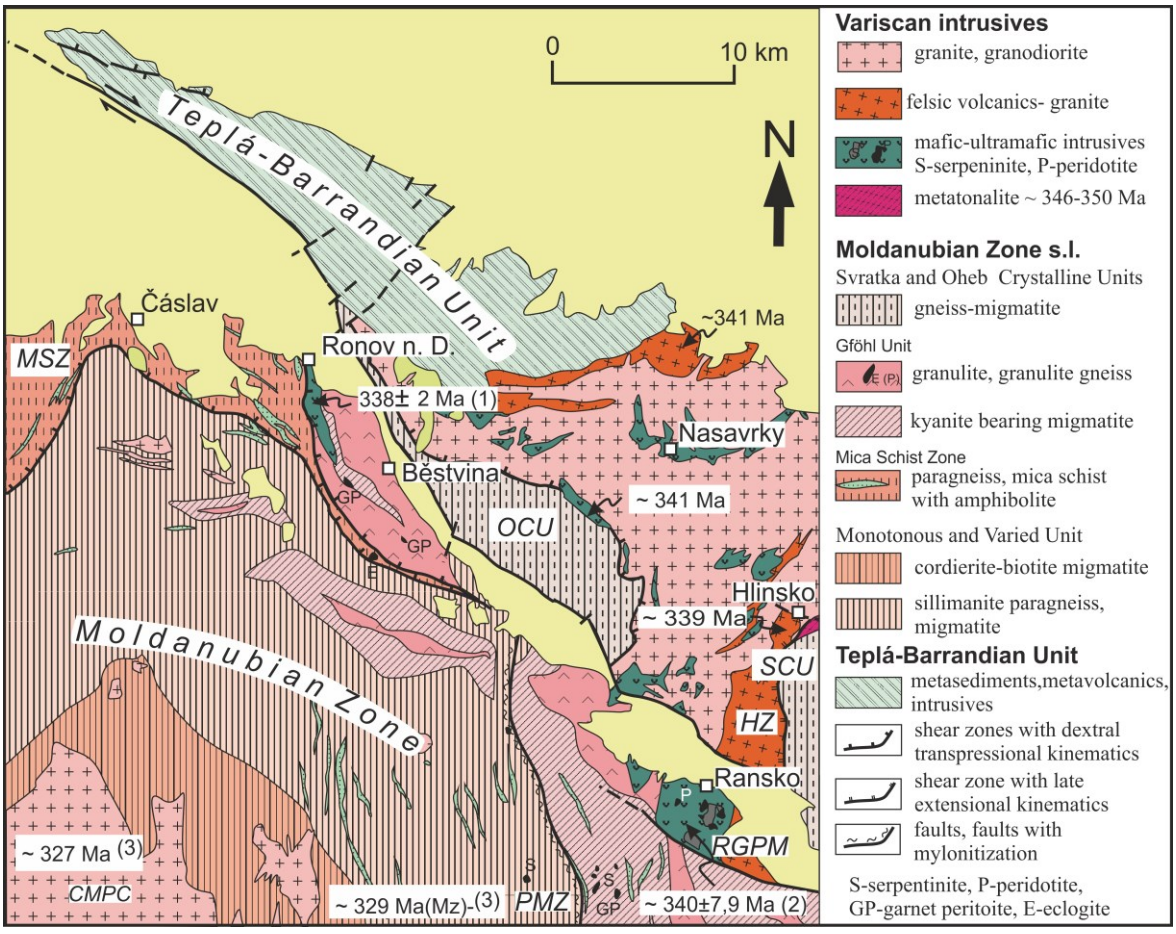

Fig. 2. Geological map and relations between the Moldanubian Zone and Teplá-Barrandian Block near Čáslav showing widespread occurrences of Variscan mafic-ultramafic intrusions. The age data are: Ronov (this work), Ransko (2; Ackerman et al., 2013), CMPC (3; Žák et al., 2011).

The Kutná Hora Complex (KHC) including the Ronov mafic-ultramafic body is located in the uppermost part of the Moldanubian Zone (Fig. 1b). It tectonically overlies the Drosendorf Unit. The KHC consists mostly of orthogneisses at the base, structurally overlain by migmatites and micaschists that contain tectonic bodies of granulites and granulite gneisses (Štědrá and Nahodilová, 2009) that are usually correlated with the Gföhl Unit (Pouba et al., 1987; Synek and Oliveriová, 1993). UHP conditions for felsic granulites, hosting boudins of garnet peridotite and garnet pyroxenites, were confirmed by the presence of microdiamond and coesite inclusions in garnet and zircon (Perraki and Faryad, 2014). The age of ~365 Ma, obtained using U–Pb method on zircon from less re-equilibrated granulite in the Kutná Hora Complex (Nahodilová et al., 2014), is interpreted to date the HP–UHP event (Jedlicka et al., 2015).

The Ronov mafic–ultramafic body (4.5 × 0.5–1.0 km) is exposed within granulite and migmatite at the contact with micaschist (Fig. 1b) and it is partly covered by quaternary sediments. In composition it ranges from norite through pyroxenite, troctolite to anorthositic gabbro (Munshi, 1981; Holub and Munshi, 1984). The mafic varieties are transformed mostly into banded amphibolite and norite is completely serpentinized. Relict igneous and coronitic textures are preserved in small (decimeter-meter in size) boudins in the northern and central parts of the body. The long axes of the boudins are elongated in the NNW–SSE direction parallel to the orientation of the whole body. The asymmetry of the boudins and asymmetric pressure shadows show mostly oblique dextral sense of shear. Coronitic metagabbro was investigated by Holub and Munshi (1984) and they deduced their formation by subsolidus reactions that occurred at 0.7–0.8 GPa and 900–950 °C.

3. Methods

In addition to analyses of the bulk rock and minerals, the rock was dated using LA-ICP-MS U–Pb analysis of zircon. The whole rock geochemistry was undertaken at the Laboratories of the Geological Institutes, Charles University in Prague. Major oxides, analysed by classical wet chemical methods together with normative mineral contents are listed in Table 1. Chemical analyses and X-ray maps were obtained by the

JEOL JXA-8530F microprobe equipped with wavelength- and energy-dispersive spectrometers (WDS and EDS) at the Department of Petrology and Structural Geology, Charles University in Prague. Quantitative analyses and maps were obtained by WDS only. The operating conditions were 15 kV and 30 nA beam current for spot analyses and 20 kV and 120 nA for element mapping. Standards were quartz (Si), corundum (Al), periclase (Mg), magnetite (Fe), rhodonite (Mn), calcite (Ca), rutile (Ti), chromium oxide (Cr), vanadinite (V), albite (Na), apatite (P). Representative analyses of selected minerals are given in Table 2. Mineral abbreviations are: ab = albite, am = amphibole, an = anorthite, and = andalusite, cpx = clinopyroxene, fo = forsterite, sil = sillimanite, gt = garnet, parg = pargasite, pl = plagioclase, opx = orthopyroxene, sp = spinel, tr = tremolite, ts = tschermakite, garnet: alm = Fe / (Ca + Fe + Mg + Mn), prp = Mg / (Ca + Fe + Mg + Mn), grs = Ca / (Ca + Fe + Mg + Mn), sps = Mn / (Ca + Fe + Mg + Mn), X_{Mg} = Mg / (Fe + Mg).

Table 1: Major element and normative mineral contents in olivine metagabbro from the Ronov mafic-ultramafic body.

Wt %	V878	V890	Mineral	V878	V890
SiO_2	44.68	42.64	Plagioclase	57.06	55.89
TiO_2	0.15	0.12	Diopside	18.18	16.41
Al_2O_3	22.82	23.97	Olivine	17.18	23.62
Fe_2O_3	1.18	2.07	Orthopyroxene	7.08	3.08
FeO	3.27	4.5	Magnetite	0.51	1.00
MnO	0.1	0.12			
MgO	9.17	9.43			
CaO	15.56	14.73			
Na_2O	0.91	0.3			
K_2O	0.04	0.02			
P_2O_5	0.07	0.07			
Total	97.95	97.97			

Table 2: Selected microprobe analyses of minerals from metagabbro and amphibolite from the Ronov mafic-ultramafic body.

Mineral	Clinopyroxene					Amphibole						
Sample	V890	V890	V890	V878		V890	V890	V890	V878	V878	R124	R124
Position	cpx oi	cpx oi				in cpx	in grt		with grt	with cpx		
SiO_2	53,09	53,14	52,39	53,02	SiO_2	43,13	46,50	46,41	44,63	46,28	42,88	46,68
TiO_2	0,18	0,29	0,30	0,00	TiO_2	0,20	0,02	0,28	0,19	0,07	1,30	0,72
Al_2O_3	3,67	4,18	5,63	2,86	Al_2O_3	17,26	13,12	13,41	15,25	11,80	11,58	8,41
Cr_2O_3	0,00	0,10	0,04	0,15	Cr_2O_3	0,00	0,01	0,30	0,19	0,07	0,10	0,04
FeO	4,49	4,09	4,63	3,86	FeO	8,90	7,80	7,18	8,86	7,69	14,43	13,37
MnO	0,05	0,00	0,06	0,00	MnO	0,10	0,05	0,08	0,06	0,13	0,13	0,15
MgO	16,90	16,20	14,43	16,22	MgO	13,12	14,79	14,23	14,62	16,76	10,70	12,72
CaO	21,82	21,90	22,30	23,82	CaO	12,37	13,26	12,75	12,32	12,35	11,70	11,88
Na_2O	0,00	0,00	0,02	0,01	Na_2O	0,10	0,47	0,64	0,99	0,58	1,65	1,24
K_2O	0,05	0,05	0,02	0,04	K_2O	0,24	0,04	0,07	0,00	0,08	0,62	0,31
Total	100,26	99,94	99,83	99,99	Total	95,42	96,05	95,36	97,11	95,81	95,08	95,51
Si	1,934	1,940	1,900	1,937	Si	6,217	6,672	6,707	6,356	6,608	6,503	6,940
Ti	0,005	0,008	0,008	0,000	Al^{IV}	1,783	1,328	1,293	1,644	1,392	1,497	1,060
Al	0,158	0,180	0,241	0,123	Al^{VI}	1,149	0,891	0,990	0,915	0,593	0,574	0,413
Cr	0,000	0,003	0,001	0,004	Ti	0,022	0,002	0,031	0,020	0,007	0,148	0,081
Fe^{3+}	0,000	0,000	0,000	0,001	Cr	0,000	0,001	0,035	0,021	0,008	0,012	0,005
Fe^{2+}	0,137	0,125	0,140	0,117	Fe^{3+}	0,546	0,401	0,066	0,395	0,601	0,209	0,281
Mn	0,002	0,000	0,002	0,000	Fe^{2+}	0,527	0,536	0,802	0,660	0,317	1,621	1,381
Mg	0,918	0,882	0,780	0,883	Mn	0,012	0,006	0,010	0,007	0,016	0,017	0,019
Ca	0,844	0,861	0,925	0,932	Mg	2,819	3,164	3,066	3,103	3,568	2,419	2,820
Na	0,000	0,000	0,001	0,001	Ca	1,915	1,947	1,974	1,879	1,889	1,901	1,892
K	0,002	0,002	0,001	0,002	Na^{M4}	0,020	0,053	0,026	0,121	0,111	0,099	0,108
					Na^{A}	0,000	0,078	0,153	0,152	0,051	0,385	0,249
X_{Mg}	0,87	0,88	0,85	0,88	K	0,043	0,007	0,013	0,000	0,013	0,119	0,059
augite	85,64	84,60	90,30	93,83	A	0,063	0,085	0,166	0,152	0,064	0,504	0,308
Ca-tsch	0,00	0,00	3,08	0,00								
FeMgts	7,18	8,01	5,14	4,03								
Opx	6,16	6,00	0,00	1,51								

Table 2: *(continued)*

Mineral	Spinel					
Sample	V878	V890	V877	V890	V890	V890
Position	in grt	cpx-oi	in pl	in cpx	in pl	in pl
Al_2O_3	59.22	60.26	63.00	60.89	60.39	63.36
Cr_2O_3	0.00	2.16	0.00	0.00	2.11	0.02
FeO	34.39	24.16	23.03	27.54	27.08	23.85
MnO	0.55	0.27	0.16	0.51	0.35	0.28
MgO	5.46	12.91	13.65	9.95	9.21	11.91
CaO	0.35	0.04	0.10	0.11	0.01	0.03
ZnO	0.00	0.12	0.08	0.00	0.16	0.07
Total	99.97	99.92	100.02	99.01	99.31	99.52
Al	1.947	1.895	1.952	1.954	1.950	1.986
Cr	0.000	0.046	0.000	0.000	0.046	0.000
Fe^{3+}	0.053	0.060	0.048	0.046	0.005	0.017
Fe^{2+}	0.750	0.479	0.459	0.581	0.616	0.514
Mn	0.013	0.006	0.004	0.012	0.008	0.006
Mg	0.227	0.513	0.535	0.404	0.376	0.472
Ca	0.010	0.001	0.003	0.003	0.000	0.001
Zn	0.000	0.003	0.002	0.000	0.003	0.002
Spinel	22.64	57.79	53.49	40.31	43.18	47.15
Galaxite	2.60	0.81	0.48	1.55	1.26	0.84
Hercynite	72.15	35.94	43.64	56.47	44.88	51.53
Gahnite	0.00	0.28	0.19	0.00	0.47	0.18
Chromite	0.00	2.28	0.00	0.00	2.62	0.02
Magnetite	2.56	2.73	2.21	1.59	7.60	0.26

Garnet

	V890	V890	V890	V878	V878	R124	R124	R124
Domine	light	dark	light	with pl	dark	core	rim	rim
SiO_2	39.10	40.74	38.37	39.16	40.18	37.92	37.91	38.30
TiO_2	0.00	0.00	0.00	0.00	0.07	0.15	0.00	0.00
Al_2O_3	22.51	22.93	22.01	22.30	22.61	21.30	21.39	21.39
Cr_2O_3	0.00	0.02	0.00	0.02	0.00	0.01	0.01	0.04
FeO	18.62	15.73	21.78	19.27	16.28	26.36	26.36	24.51
MnO	1.09	0.18	2.62	0.83	0.20	2.85	0.23	0.55
MgO	6.78	14.15	3.50	5.86	11.65	2.07	2.96	3.66
CaO	11.29	6.64	11.78	11.86	9.11	9.53	10.53	10.99
Total	99.40	100.39	100.06	99.32	100.10	100.19	99.39	99.44
Si	2.998	2.996	2.992	3.000	2.980	3.007	3.001	2.998
Ti	0.000	0.000	0.000	0.000	0.000	0.009	0.000	0.000
Al	2.034	1.987	2.023	2.010	1.980	1.990	1.996	2.010
Cr	0.000	0.001	0.000	0.000	0.000	0.000	0.001	0.002
Fe^{3+}	0.000	0.020	0.000	0.000	0.040	0.000	0.002	0.000
Fe^{2+}	1.194	0.947	1.420	1.230	0.970	1.748	1.743	1.604
Mn	0.071	0.011	0.173	0.050	0.010	0.191	0.015	0.037
Mg	0.775	1.551	0.407	0.670	1.290	0.245	0.350	0.427
Ca	0.928	0.486	0.984	1.020	0.720	0.810	0.893	0.922
Alm	40.23	31.53	47.59	41.41	32.22	58.37	58.06	53.64
Prp	26.12	1.65	13.64	22.46	42.96	8.18	11.64	14.29
Grs	31.26	16.01	32.97	34.25	23.80	27.02	29.70	30.71
Sps	2.39	0.37	5.79	1.82	0.42	6.39	0.51	1.22

Table 3: LA ICP-MS zircon U-Pb data from the sample KHC46c

		Measured isotopic ratios									Ages (Ma)						
Nr.	Zircon type[a]	Th	U	^{206}Pb	^{207}Pb	2σ	^{206}Pb	2σ	^{207}Pb	2σ	^{207}Pb	2σ	^{206}Pb	2σ	^{207}Pb	2σ	Disc. [§]
		(ppm)	(ppm)	^{204}Pb	^{235}U	(abs)	^{238}U	(abs)	^{206}Pb	(abs)	^{238}U	(abs)	^{238}U	(abs)	^{206}Pb	(abs)	(%)
0	(a)	151	1310	370	0.3971	0.016	0.0535	0.0018	0.0543	0.0010	339	11	335.9	11	365	42	8.0
1	(a)	538.2	3309	1030	0.3957	0.016	0.0538	0.0018	0.0538	0.0010	338.4	11	337.7	11	349	42	3.2
2	(a)	492	2398	580	0.3959	0.016	0.0538	0.0018	0.0537	0.0010	338.5	11	337.8	11	351	43	3.8
3	(a)	213.5	1716	480	0.3911	0.016	0.0537	0.0018	0.0531	0.0010	334.9	11	337.3	11	320	43	-5.4
4	(a)	293	2091	570	0.3955	0.016	0.0543	0.0018	0.0531	0.0010	337.9	11	340.7	11	317	41	-7.5
5	(b)	245.6	1006	210	0.3711	0.015	0.0504	0.0017	0.0536	0.0011	319.9	11	317.1	11	338	44	6.2
6	(b)	150.8	1142	150	0.3872	0.016	0.0531	0.0018	0.0532	0.0011	332	12	333.2	11	318	46	-4.8
7	(b)	140.2	1274	360	0.3895	0.015	0.053	0.0018	0.0535	0.0010	333.6	11	332.9	11	332	43	-0.3
8	(b)	95.5	1291	320	0.3746	0.015	0.0512	0.0017	0.0532	0.0010	322.7	11	321.8	11	323	42	0.4
9	(a)	168.3	1083	230	0.3944	0.016	0.0541	0.0019	0.053	0.0011	337	12	339.7	11	311	45	-9.2
10	(a)	437.9	2666	610	0.3988	0.016	0.0546	0.0018	0.0533	0.0010	340.8	12	342.5	11	330	43	-3.8
11	(a)	195.9	1625	340	0.391	0.016	0.0535	0.0018	0.0532	0.0010	334.6	11	336.1	11	324	43	-3.7
12	(a)	192.6	1746	20	0.3953	0.016	0.054	0.0018	0.0533	0.0010	337.8	11	338.7	11	327	42	-3.6
13	(a)	269.4	1938	70	0.3941	0.016	0.0537	0.0018	0.0534	0.0010	337	11	337.1	11	333	41	-1.2
14	(a)	54	1057	92	0.4002	0.016	0.0544	0.0019	0.0536	0.0011	341.3	12	341.4	11	335	45	-1.9
15	(a)	40.11	840	109	0.3961	0.017	0.0537	0.0019	0.0538	0.0012	338	12	336.8	12	342	52	1.5
16	(a)	242.9	1668	0	0.3901	0.015	0.0533	0.0018	0.0531	0.0010	334.1	11	334.7	11	321	41	-4.3
17	(b)	125.6	2766	310	0.3835	0.015	0.0519	0.0018	0.0539	0.0010	329.3	11	326.1	11	357	44	8.7
18	(a)	95.7	986	-39	0.3901	0.016	0.0532	0.0018	0.0532	0.0010	334	11	334	11	320	43	-4.4
19	(a)	2.342	498	-16	0.3955	0.018	0.0531	0.0020	0.0544	0.0014	337.6	13	333.2	12	361	58	7.7
20	(c)	0.294	112.9	-3.4	0.4269	0.019	0.0566	0.0020	0.0557	0.0016	358.7	13	354.5	12	364	60	2.6
21	(c)	0.334	161.6	14	0.3821	0.017	0.0509	0.0018	0.0554	0.0016	327.4	13	319.8	11	364	63	12.1
22	(c)	1.331	249.2	-7	0.3814	0.016	0.0517	0.0018	0.0541	0.0013	326.7	12	325	11	330	50	1.5
23	(a)	1.038	199.8	-6	0.395	0.017	0.0533	0.0019	0.0542	0.0015	336.2	13	334.8	11	331	58	-1.1
24	(a)	0.58	137.3	-9	0.4016	0.017	0.0543	0.0019	0.0547	0.0014	340.8	13	340.4	11	335	55	-1.6
25	(a)	1.187	182	-28	0.3968	0.017	0.0536	0.0018	0.0535	0.0013	337.5	12	336.5	11	307	52	-9.6
26	(c)	0.279	149.7	-13	0.3887	0.017	0.0529	0.0018	0.0533	0.0014	331.4	12	332.5	11	284	56	-17.1
27	(c)	1.392	422.3	-30	0.3904	0.017	0.0531	0.0019	0.0533	0.0013	334	12	333.5	11	315	54	-5.9
28	(b)	2.27	441.2	-33	0.3778	0.015	0.0511	0.0017	0.0534	0.0011	324.4	11	321.5	11	318	47	-1.1
29	(c)	3.018	325.1	-9	0.4002	0.016	0.052	0.0018	0.0557	0.0012	340.7	12	326.8	11	404	48	19.1
30	(c)	119.3	1050	-120	0.3476	0.014	0.0473	0.0016	0.0531	0.0011	302.4	11	298.1	10	316	46	5.7
31	(b)	212.6	1610	-190	0.3837	0.015	0.0519	0.0018	0.0536	0.0010	329.3	11	325.8	11	339	42	3.9
32	(c)	172.6	1473	-120	0.3917	0.016	0.0500	0.0017	0.0563	0.0011	335.2	11	314.5	10	450	42	30.1
33	(a)	455.8	3567	-650	0.3964	0.016	0.0541	0.0018	0.0528	0.0010	338.9	11	339.7	11	307	42	-10.7
34	(b)	18.32	596.6	-199	0.3851	0.016	0.0515	0.0018	0.0536	0.0011	330.3	12	323.5	11	333	47	2.9
35	(b)	188.3	1620	-280	0.3779	0.015	0.0509	0.0017	0.0533	0.0010	325.3	11	320.1	11	330	43	3.0
36	(c)	1.709	193.2	-45	0.3812	0.018	0.0504	0.0018	0.0549	0.0019	327.3	13	316.9	11	346	71	8.4
37	(c)	0.41	162.8	-33	0.3828	0.016	0.0512	0.0018	0.0543	0.0015	327.7	12	321.6	11	319	56	-0.8
38	(c)	1.175	452.8	-93	0.3644	0.015	0.0491	0.0017	0.0534	0.0012	314.6	11	308.8	10	314	47	1.7
39	(a)	0.747	180.2	-41	0.3948	0.017	0.0534	0.0018	0.0533	0.0013	336.4	12	335.1	11	295	51	-13.6
40	(c)	1.348	234.3	-61	0.3872	0.016	0.0526	0.0018	0.0532	0.0013	330.5	12	330.4	11	283	52	-16.7
41	(c)	1.868	316.7	-73	0.3853	0.016	0.0517	0.0018	0.0536	0.0012	329.9	12	324.5	11	321	49	-1.1
42	(a)	82.9	963	-213	0.3911	0.016	0.0533	0.0018	0.0528	0.0010	334.9	11	334.6	11	303	42	-10.4
43	(a)	133.1	1386	-380	0.3929	0.016	0.0535	0.0018	0.0527	0.0010	336.2	11	335.6	11	305	42	-10.0
44	(a)	213.2	1914	-390	0.3962	0.016	0.0537	0.0018	0.0532	0.0010	338.8	11	337.2	11	322	44	-4.7

[a] Zircon type corresponds to the description in the text; [§]Disc. = (1 - (($^{206}Pb/^{238}U$) / ($^{207}Pb/^{206}Pb$))) * 100.

A Nu AttoM High resolution ICP-MS coupled to a 193 nm ArF excimer laser (Resonetics RESOlution M-50 LR) at the University of Bergen, Norway, was used to measure the Pb/U and Pb isotopic ratios in zircons (Table 3). The laser was fired at a repetition rate of 5 Hz and energy of 80 mJ with 19 μm spot size. Typical acquisitions consisted of 15 s measurement of blank followed by measurement of U, Th and Pb signals from the ablated zircon for another 30 s. The data were acquired in time resolved – peak jumping – pulse counting mode with 1 point measured per peak for masses ^{204}Pb + Hg, ^{206}Pb, ^{207}Pb, ^{208}Pb, ^{232}Th, ^{235}U, and ^{238}U. Due to a non-

linear transition between the counting and attenuated (=analog) acquisition modes of the ICP instrument, the raw data were pre-processed using a purpose-made Excel macro. As a result, the intensities of ^{238}U are left unchanged if measured in a counting mode and recalculated from ^{235}U intensities if the ^{238}U was acquired in an attenuated mode. Data reduction was then carried out off-line using the Iolite data reduction package version 3.0 with the VizualAge utility (Petrus and Kamber, 2012). Full details of the data reduction methodology can be found in Paton et al. (2010). The data reduction included correction for gas blank, laser-induced elemental fractionation of Pb and U and instrument mass bias. For the data presented here, blank intensities and instrumental bias were interpolated using an automatic spline function while down-hole inter-element fractionation was corrected using an exponential function. No common Pb correction was applied to the data but the low concentrations of common Pb were controlled by observing $^{206}Pb/^{204}Pb$ ratio during measurements. Residual elemental fractionation and instrumental mass bias were corrected by normalization to the natural zircon reference material Plešovice (Sláma et al., 2008). Zircon reference materials GJ-1 {nr. 63} (Jackson et al., 2004) and 91500 (Wiedenbeck et al., 1995) were periodically analysed during the measurement for quality control and the obtained mean values of 596 ± 3Ma (2σ) and 1071 ± 5Ma (2σ) are 1 % accurate within the published reference values [600.5 ± 0.4 Ma, Schaltegger et al. (2015); 1065 Ma,Wiedenbeck et al. (1995), respectively]. The zircon U–Pb ages are presented as concordia (pooled) age plot generated with the ISOPLOT program v. 3.70 (Ludwig, 2008).

6.4. Petrological characteristics

Detailed petrographical characteristics of the Ronov mafic–ultramafic body was reported by Munshi (1981), who distinguished several varieties of mafic and ultramafic rocks that include norite, pyroxenite, troctolite, anorthositic gabbro and gabbro-diorite. The ultramafic rocks are strongly serpentinized, but may contain relicts of clinopyroxene. The gabbro and anorthositic rocks are extensively deformed and recrystallized into amphibolite with various degrees of foliation. They consist mostly of amphibole and plagioclase with quartz and rarely titanite. Amphibole

and quartz define a foliation in the rocks. In some cases, amphibolite shows thin leucocratic banding formed by plagioclase with quartz. Locally, garnet-bearing amphibolite is present. Two varieties of garnet were observed. The first forms porphyroblasts of up to 2 mm in size and it is a main phase in the amphibolite. The second occurs in isolated boudins of metagabbro in the central part of the body (Culek, 1951), where it forms coronae around amphibolized clinopyroxene at the contacts with plagioclase. In some case, spinel can be also present in the coronae. Two varieties of mafic rocks with different degree of metamorphic recrystallization were selected for this study. The first is a metagabbro with igneous plagioclase, clinopyroxene and spinel (samples V877, V878, V890) and the second is a garnet amphibolite (sample R124) with no observed igneous phases. Sample (KHC-46c), utilized for U–Pb age dating of zircon, is a garnet-free amphibolite.

6.4.1. Spinel-bearing metagabbro

Based on normative (CIPW) mineral composition (Table 1), the metagabbro corresponds to plagioclase-rich olivine gabbro near to leucogabbro with 17–23 mol % olivine and 3–7 mol % orthopyroxene. It consists of amphibole, plagioclase, with relics of clinopyroxene and small amounts of spinel and garnet. Plagioclase may form up to 5 mm large crystals, but mostly it is fine- to medium- grained. No pseudomorphs after olivine or orthopyroxene were observed. Except small amounts of garnet most of the replacement product is amphibole. Mineral textures show two stages of crystallization and/or their transformation. The first is related to a magmatic stage, where two varieties of clinopyroxene can be distinguished. The first ones are oikocrysts with abundant spinel inclusions (Fig. 3a, b). Most clinopyroxene grains contain various amounts of spinel inclusions (Fig. 3d, e), but some are also free of spinel inclusions.

Several textural varieties of spinel can be distinguished. The first comprises inclusions in clinopyroxene. Some inclusions show various degrees of embayment structure development (Fig. 3e) that seems to be the result of reaction with intercumulus melt during crystallization. This is supported also by a channelized structure of spinel inclusions (Fig. 3f). Spinel is present also as inclusions in plagioclase

as well as in amphibole (Fig. 4a), the latter formed by replacement of original clinopyroxene. Spinel may form clusters of several relatively large grains within amphibole or at the contacts with plagioclase. In some cases, spinel forms seams along boundaries between plagioclase and clinopyroxene pseudomorphs, where garnet coronae forms. It is not always clear, if the spinel seams relate to a magmatic stage or formed by reactions between clinopyroxene and plagioclase. Garnet is a later phase and usually contains inclusions of spinel.

Clinopyroxene shows varying degrees of replacement to amphibole. It starts with formation of thin amphibole crystals following cleavage planes of clinopyroxene (Fig. 4b). In most cases the clinopyroxene is completely replaced by amphibole and its shape can be deduced by the garnet coronae (Fig. 4c, d). Garnet is present also in the matrix, but usually it forms coronae around clinopyroxene. Detailed BSE images show thin bright smears (Fig. 4e) following probably boundaries of grains formed by multiple nucleation and coalescence processes. In some garnets with inclusions of spinel, relatively dark domains (Fig. 4f), representing diffusive contact after spinel inclusions, are present.

6.4.2. Garnet-bearing amphibolite

Most amphibolite samples are bi-mineralic formed by hornblende and plagioclase with minor quartz and accessory ilmenite, titanite and apatite. In some cases, relics of clinopyroxene can be also observed. The selected sample for this study contains hornblende (50 vol %), plagioclase (40 vol %), garnet (5–10 vol %) and small amounts of quartz. The rocks show foliation, defined by amphibole and porphyroblastic garnet (up to 3 mm in size). The garnet grains are rimmed by a plagioclase + amphibole corona.

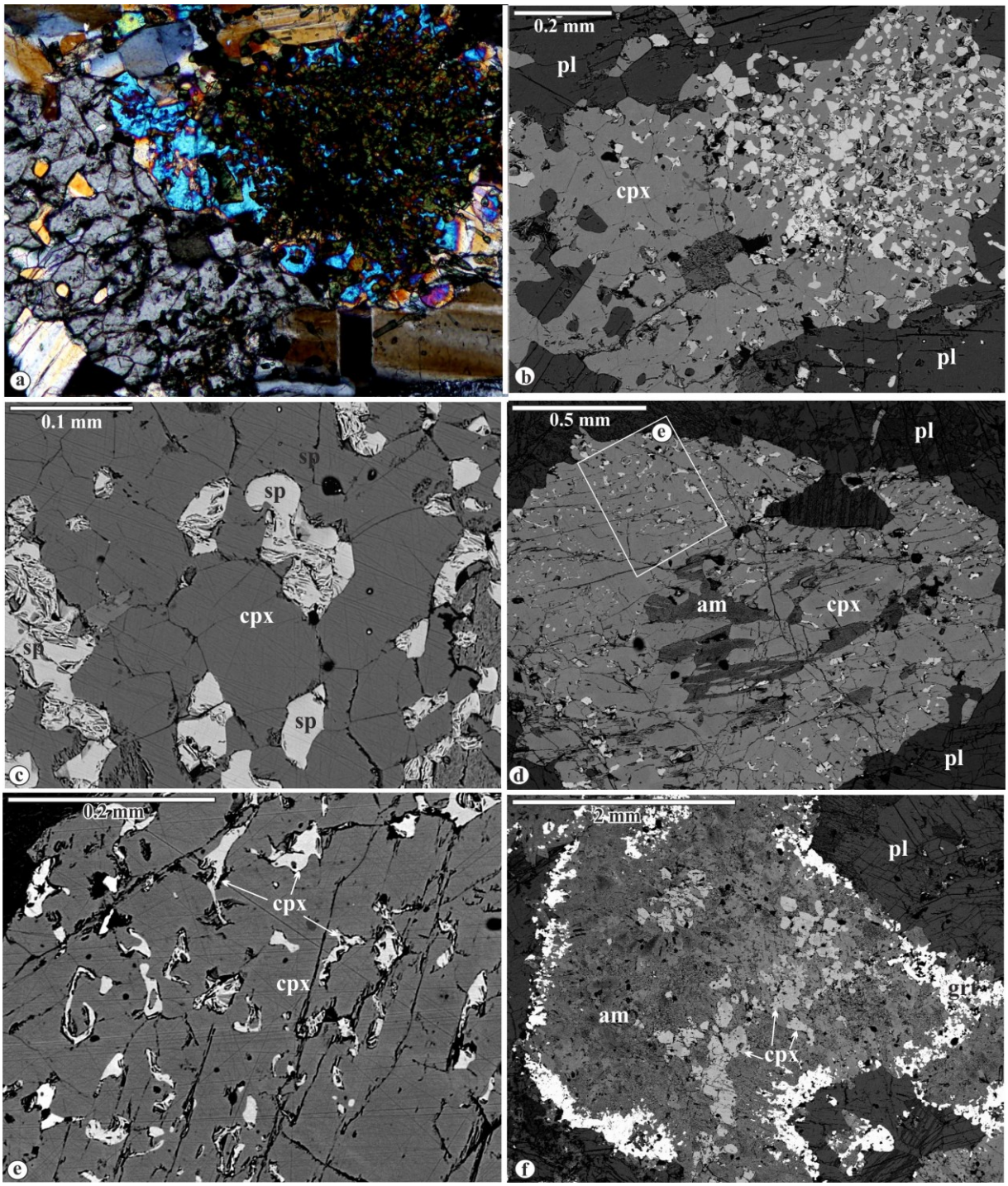

Fig. 3. Subsolidus mineral textures in metagabbro. (a and b) clinopyroxene oikocryst with spinel inclusions (sample V890). Note the optically continuous clinopyroxene oikocryst (a), in which densely scattered spinel crystals are embedded, occurs at contact with intercumulus clinopyroxene grain. (c) spinel inclusions in clinopyroxene (sample V877) show embayment structure due to reaction with fluid or melt, (d) the clinopyroxene grain is partly replaced by amphibole (sample V890). (e) is detail from (d), (f) primary clinopyroxene, now replaced by amphibole, has corona of garnet with clinopyroxene and spinel (sample V878).

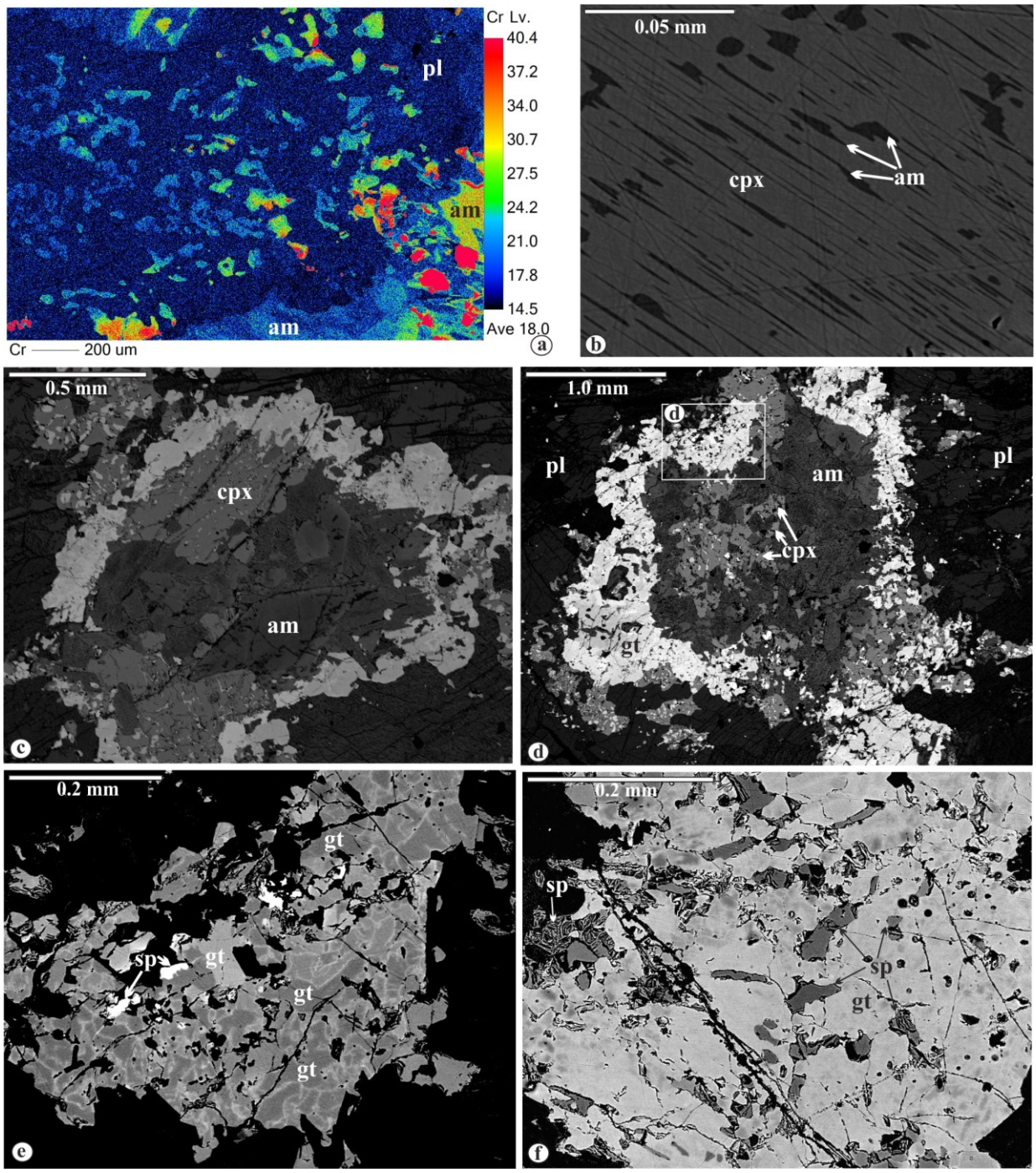

Fig. 4. Post-magmatic and metamorphic textures in metagabbro. (a) chromium concentration map of plagioclase with spinel inclusions (sample V890). Note compositional variation of Cr in spinel as well as in amphibole. (b) replacement of clinopyroxene along cleavage planes (sample V890), (c and d) garnet corona around clinopyroxene that is partly replaced by amphibole (sample V890). (e) is detail of garnet from (d) and shows thin bright channels along boundaries of micrograins. Note relict grains of Fe-rich spinel partly enclosed by garnet. (f) Garnet with Mg-rich spinel inclusions (sample V878). Some darker domains indicate probably diffusive contact with spinel under polished surface.

6.5. Mineral compositions

6.5.1. Plagioclase

Most analysed plagioclase in both samples of coronitic metagabbro (V787, V890) is pure anorthite ($An_{99.9}$). The Na_2O and K_2O contents are below 0.06 and 0.04 wt % in the analyses. No variation was observed among different sizes of grains or between the core and rim of plagioclase crystals. Only locally plagioclase has small domains or thin veins with composition of An_{80}. Normative contents, calculated for the analysed samples, indicate plagioclase with An_{92} and An_{95}.

Plagioclase in amphibolite has anorthite content ranging from 0.37–0.43. The higher anorthite content was measured at the coronae around plagioclase.

6.5.2. Clinopyroxene

Clinopyroxene is augite with 73–88 mol % diopside and 10–13 mol % hedenbergite end-member components analysed in different samples. It is relatively rich in Al with 4–9 mol % Fe-Mg-tschermak end-members. No systematic core to rim zoning was observed. The oikocrystic clinopyroxene grains with spinel inclusions show slightly elevated MgO and Al_2O_3 contents compared to those free of spinel (Table 2). No diffusion zoning was observed in clinopyroxene at the contacts with spinel inclusions.

6.5.3. Spinel

There is a wider range in spinel composition. Spinel densely scattered in oikocryst has elevated Cr with 2.0–2.3 mol % chromite content. This spinel is also relatively rich in spinel end-member (Sp_{58} Hc_{35}). Spinel clusters in plagioclase show strong variation in Cr content ranging from 0.1 to 2.1 wt %. The grains are variably zoned (Fig. 4a). Most of spinel in plagioclase or in pyroxene and amphibole lacks or has very

insignificant amounts of chromite end-member content and its spinel and hercynite contents range between 42–54 mol %. A hercynite-rich spinel ($Sp_{23–27}$ $Hc_{71–72}$) was found in garnet. All spinel has variable amounts of magnetite end-member ranging between 2–4 mol %. Zinc and titanium is very low in spinel and they are mostly under detection limit.

6.5.4. Garnet

Major component contents in garnet from different samples of coronitic metagabbro are in range of $alm_{30–48}$ $prp_{14–34}$ $grs_{26–38}$ $sps_{1–4}$ (Table 2, Fig. 5). Compositional change in garnet is irregular and depends on its occurrence at contacts with other phases, which supplied major elements to garnet. Up to 5 wt % increase of FeO and decrease of CaO was observed in garnet at contact with clinopyroxene in a distance of 20 μm. This zone also shows an increase of MnO to about 2 wt % compared to the rest of garnet with MnO <1 wt %. However, this variation is not gradual and it probably relates to the element availability during garnet growth. BSE images with high contrast (Fig. 4e) show the presence of thin irregular channels with light shades in garnet. These light thin zones have higher Fe and lower Mg and Ca content. Vice versa, darker domains in garnet occur around spinel inclusions (Fig. 4f).

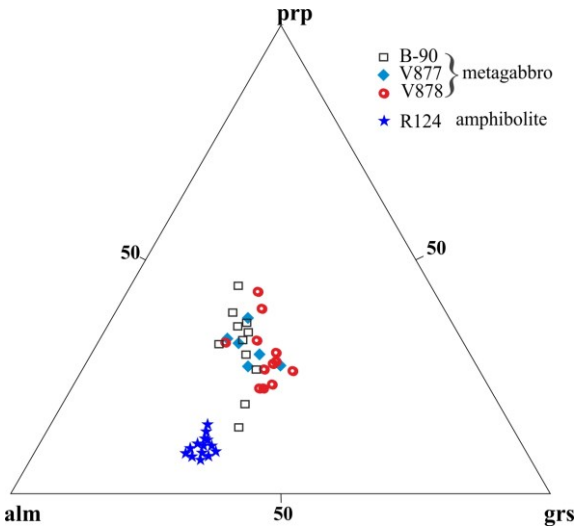

Fig. 5. Compositional range of garnet in coronitic metagabbro and amphibolite from the Ronov mafic–ultramafic body.

Garnet from amphibolite has higher almandine and lower pyrope and grossular content comparing to that in metagabbro (Fig. 5) and large porphyroblasts show core to rim zoning. The core is rich in Mn and Ti and the Mg values show an increase towards the rims (Fig. 6). Slight increase toward the rims can be seen also in Fe and Ca content, but most of the central part of garnet contains several domains with different Ca contents. The most rim part shows first increase of Ca with decreasing of Mg and Fe and then decrease of Ca and increase of Mg and Fe.

6.5.5. Amphibole

Amphibole in coronitic metagabbro is tschermakite with transition to magnesiohorblende (Hawthorne et al., 2012) with Si = 6.3–6.6 atoms per formula unit (a.p.f.u.). The X_{Mg} content ranges between 0.78–0.92, depending on its position within other phases and in different samples. The highest X_{Mg} occurs in amphibole at the contact with clinopyroxene. Amphibole has a relatively low Na <0.27 a.p.f.u. (<1 wt % Na_2O) content. Al-rich amphibole with Al^{VI} = 1.14 a.p.f.u. occurs at contact with spinel. Compositional mapping in Fig. 4a shows that amphibole near spinel clusters has relatively higher (0.3 wt %) Cr content (Table 2). Some amphibole grains show weak zoning characterized by the decreasing Mg and increasing Al and Fe from core to rim of grains.

Amphibole from garnet amphibolite is magnesiohornblende with X_{Mg} about 0.7 with Si = 6.52–6.92 a.p.f.u. Na content is about 0.4 a.p.f.u. with 0.1 a.p.f.u. in Na^{M4} site.

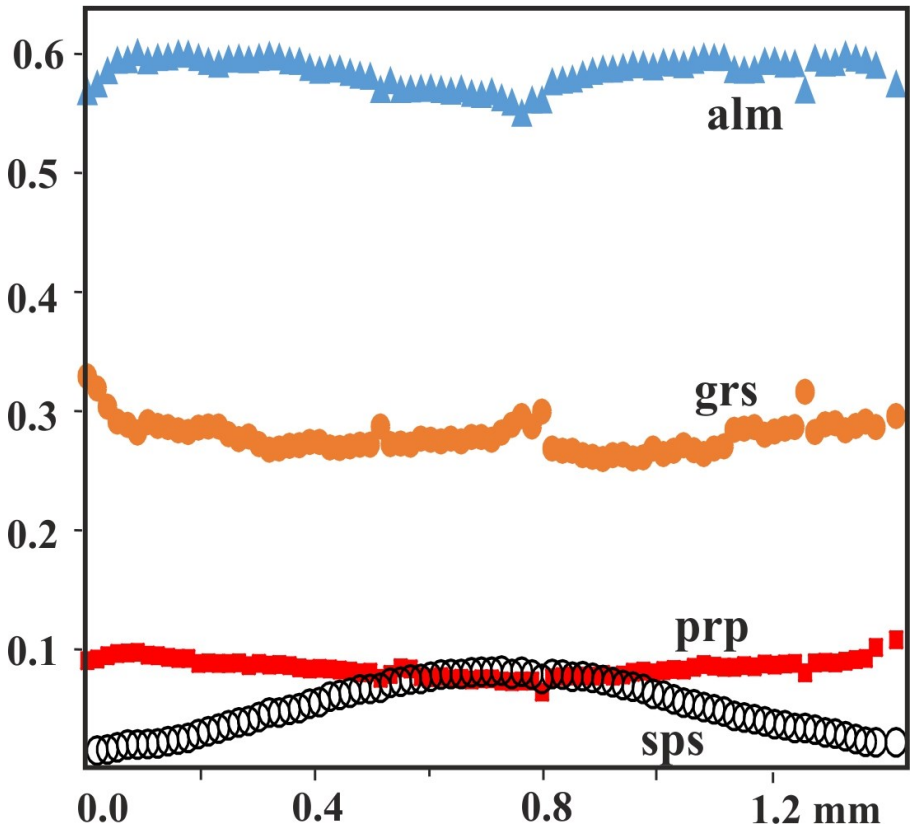

Fig. 6. Compositional profile of garnet from amphibolite (sample R124). Note the irregular variation in Ca and Mg contents, mainly near rim of garnet.

5.6. Metamorphic P-T conditions

To quantify the metamorphic overprint in both coronitic metagabbro and garnet-bearing amphibolite, amphibole–garnet–plagioclase thermobarometry (Dale et al., 2000) was used. Ferric and ferrous iron contents in amphibole were calculated based on the charge balance. The temperature-depending reaction (1) in this calculation is based on Fe–Mg exchange between garnet and amphibole end-members (actinolite, tremolite, pyrope and almandine):

(1) fact + prp = tr + alm

This multivariant reaction calculated for coronitic metagabbro yields temperatures of 680–780 °C for the pressure range of 0.7 to 1.4 GPa (Fig. 7). Very high temperatures exceeding 900 °C could be obtained, if the most Mg-rich garnet with spinel inclusions is used. The pressure-depended reactions (2–4) involve pargasite and grossular end-members with anorthite, albite and quartz:

(2) ts + grs + prp + q = tr + an

(3) parg + grs + prp + q = tr + an + ab

(4) gl + gr + prp + q = tr + an + ab

Free quartz was not observed, however its solution in fluid during the garnet forming reaction is assumed. The reactions are calculated for $a_{SiO_2} = 1$. Using lower a_{SiO_2} contents (e.g. 0.9, 0.8), the changes in P-T values are not significant and they are in the range of error calculated for different mineral analyses. We used both plagioclases with 21 and 0.6 mol % albite component. There is no change in the position of the reaction curve (2) and it gives pressure of about 0.7–1.0 GPa at 700–750 °C, but the curves of reactions (3) and (4) give higher pressure for plagioclase with 0.6 mol % albite and lower for plagioclase with 21 mol % albite component.

In garnet-bearing amphibolite, the near-rim composition of garnet with high Mg content yielded temperatures of 720–770 °C at pressures of 1.0–1.2 GPa. Lower temperatures up to 700 °C at 0.8 GPa were obtained by using garnet composition from the mantle and central part of zoned garnet.

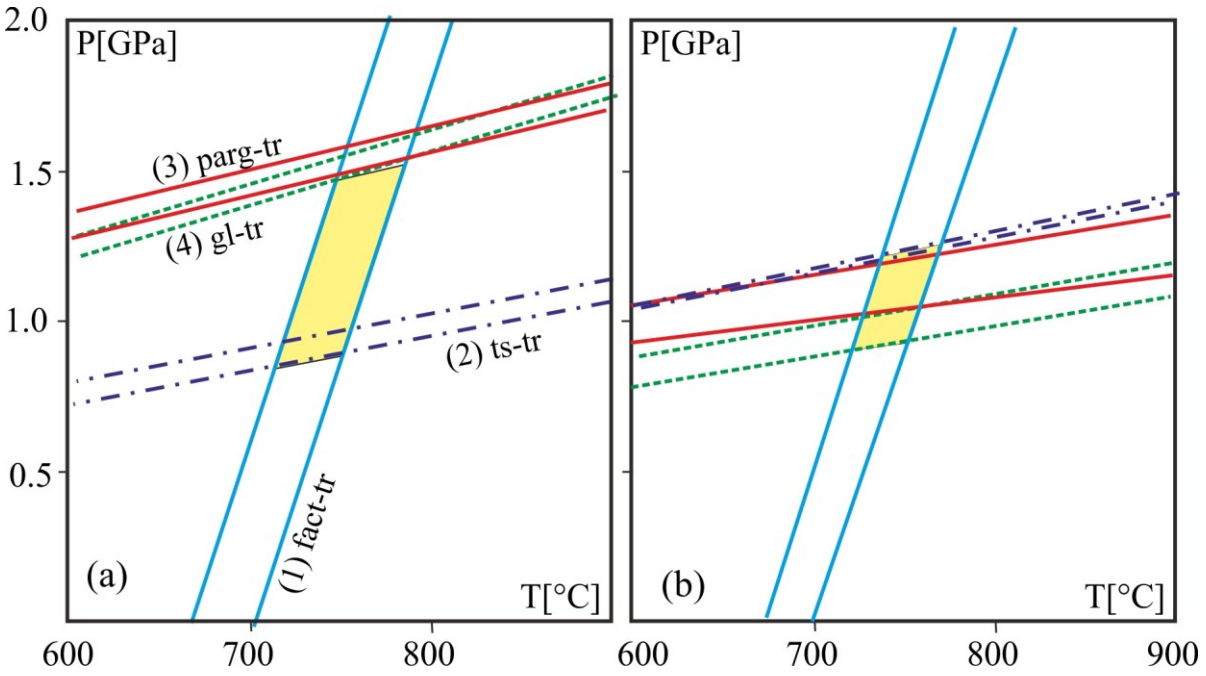

Fig. 7. Pressure–temperature diagram and position of reaction curves, calculated using garnet-amphibole–plagioclase thermobarometry (Dale et al., 2000) in coronae from metagabbro (a) and garnet-bearing amphibolite (b).

6.7. Geochronology

Only a limited amount of zircon was extracted from the sample and thus available for U–Pb dating. The cathodoluminescence (CL) imaging revealed 3 types of zircon in the polished section (Fig. 8): (a) long prismatic grains, dark in CL with oscillatory zonation and partially resorbed rims overgrown by thin CL bright zircon; (b) CL dark prismatic grains with irregular zonation, sometimes with remnants of oscillatory zonation; (c) CL bright zircons with sector zonation forming either isometric grains, sometimes with remnants of CL dark zircon in the centre, or thin rims around the dark cores.

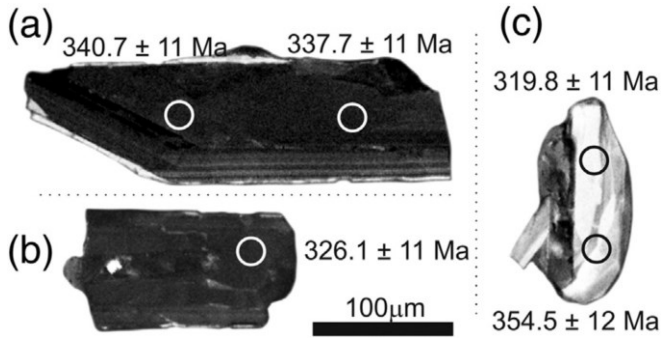

Fig. 8. Representative CL images of zircon together with respective $^{206}Pb/^{238}U$ ages in the sample KHC-46c. The individual zircon types are described in the text; see Fig. 9 for the corresponding U–Pb data. Note the two distinctly different ages detected in (c), the zircon type characterized by isotopic disequilibrium.

The U–Pb data from the type (a) zircon grains form a homogenous cluster in the concordia diagram with a pooled (Concordia) age of 337.7 ± 2.0 Ma (2σ) in Fig. 9. They have relatively high U, Th and Pb concentrations (average values of 1455 ppm, 186 ppm and 93 ppm respectively) and Th/U ratio of 0.13. The type (b) zircon has similar composition (average concentrations of U: 1305 ppm, Th: 131 ppm, Pb: 67 ppm; Th/U: 0.10) to the type (a) but its U–Pb data are more or less discordant and scattered between cca 335–320 Ma (Fig. 9). The type (b) zircon most probably represents isotopically disturbed grains of the type (a) zircon. The type (c) zircon did not provide meaningful U–Pb data (Fig. 9). The spread of slightly to more discordant

ages between cca 305–355 Ma together with lower trace element concentrations (U: 319 ppm, Th: 11 ppm, Pb: 6 ppm) point to an isotopic disequilibrium during type (c) zircon growth. Its lower Th/U ratio of cca 0.03 indicate that this zircon grew probably under metamorphic conditions while the types (a) and (b) most probably represent magmatic stage. The temporal separation of the two events are not distinguishable using the obtained data but the presence of oscillatory zonation and U, Th and Pb concentration typical of magmatic rocks in zircon (a) and (b) indicate, that the Concordia age of 337.7 Ma dates the magmatic emplacement and the metamorphic overprint followed shortly after.

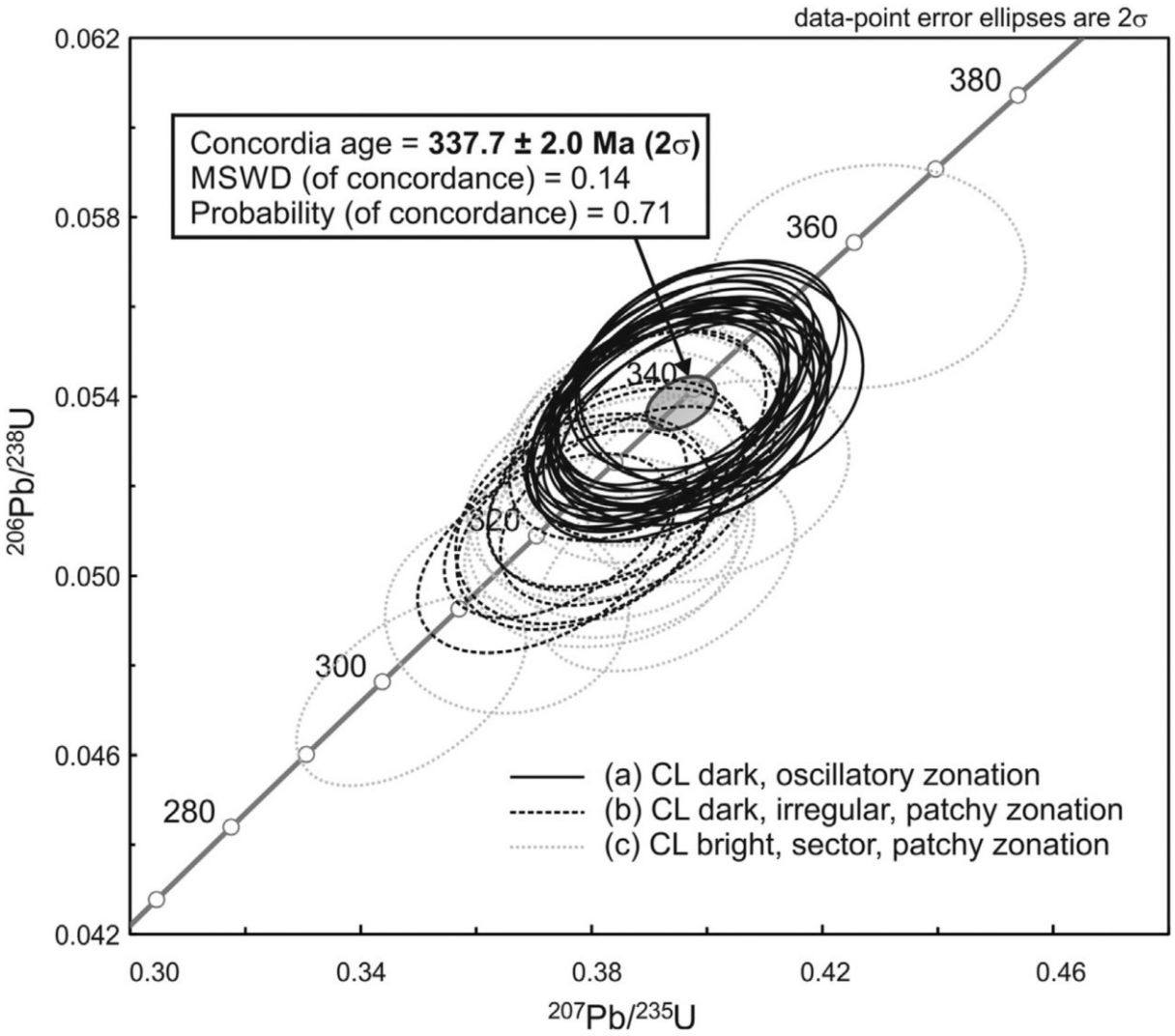

Fig. 9. Concordia plot of the U–Pb data of the sample KHC-46c. For the calculation of Concordia age only the type (a) zircon data (solid black ellipses) were used based on the textures observed in CL.

6.8. Discussion

6.8.1. Textural and phase relations

The bulk rock chemistry and normative mineral contents of coronitic metagabbro combined with the liquidus phase relations (Fig. 10) suggest that most spinel are formed during the magmatic stage. The projection of the spinel field in relation to the An-Di-Fo triangle diagram in the Al_2O_3–CaO–MgO–SiO_2 (Morse, 1980; Osborn and Tait, 1952) shows that crystallization continued along the spinel+clinopyroxene cotectic line from about 1430 °C to the eutectic point at 1410 °C. This is consistent with the textural relations, where spinel occurs as inclusions in clinopyroxene and plagioclase. Depending on the crystallization depth or pressure conditions (Cameron and French, 1977; Presnall et al., 1978), the plagioclase field will shrink and the diopside and spinel fields will expand with pressure increase (Fig. 10b, c). Considering the experimental data of Kinzler and Grove (1992) on basaltic melt with bulk rock Mg# = Mg / (Mg + Fe_t) = 0.7–0.8 similar to the studied metagabbro, the pressure conditions for its crystallization range between 1.0–1.4 GPa at temperatures above 1330–1430 °C. However, the high CaO in the gabbro (up to 14 wt %, Table 1) suggests that pressures could be below 1.0 GPa (Villiger et al., 2007). Longhi et al. (1999) indicated that mantle basaltic magma may produce anorthositic rocks up to 1.1 GPa. The presence of different compositional varieties of spinel inclusions in clinopyroxene and plagioclase suggest either mixing of replenishing magma with existing (cooler) resident magma, with subsequent crystal settling (Dunham and Wilkinson, 1985; Henderson, 1975; O'Driscoll et al., 2009) or partial modification by a residual melt (Hoshide and Obata, 2014). Regarding the first alternative, the relatively Mg-rich clinopyroxene with spinel having higher Cr contents, may represent different crystal populations grown at slightly different sites in the magma chamber.

In a mafic-ultramafic system, the plagioclase rich members (e.g. anorthosite) rise to the top of magma chamber and they may ascent as crystal mush plutons because of density–buoyancy relations with the overlying crust (Ashwal, 1993). Depending on the crystallization rate and composition, the An content in plagioclase decreases

with crystallization and fractionation (Maaloe, 1978; Wager and Brown, 1968). The presence of almost pure anorthite plagioclase with no rimward zoning, but with only local domains and veins with elevated Na content in the studied metagabbro, could be due to rapid cooling and concentration of Na in the residual melt that resulted in plagioclase alteration during the subsolidus stage.

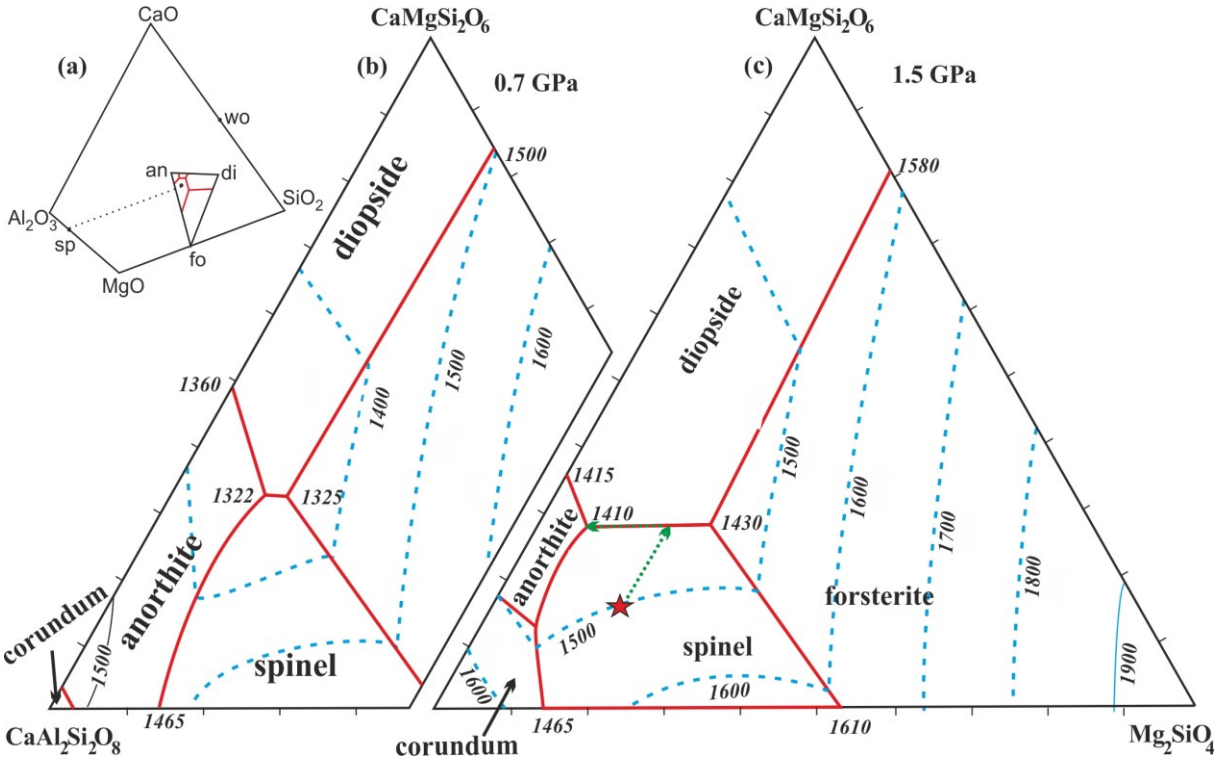

Fig. 10. Liquidus phase relations on the join $CaMgSi_2O_6$ (Di) – Mg_2SiO_4 (Fo) – $CaAl_2Si_2O_8$ (An) at 0.7 and 1.5 GPa after Presnall et al. (1978). (a) shows position of spinel and Di-Fo-An triangle in $CaO–Al_2O_3–MgO–SiO_2$ tetrahedron. Heavy (red) lines are liquidus boundaries. Star indicates bulk rock composition of metagabbro. Note that with pressure increase the anorthite field shrinks while spinel field increases (b, c).

Stabilization of garnet instead of spinel in gabbro occurred after cooling down below subsolidus conditions. The formation of only small grains of garnet in the corona at the contacts between plagioclase and clinopyroxene or around spinel suggests that garnet forming reaction was a short term process. This can be confirmed also by the preservation of Fe-rich capillaceous zones that escaped compositional modification due to rapid cooling. This process was accompanied by the presence of fluid which stabilized amphibole formation. Transformation of clinopyroxene oikocrysts with spinel into amphibole resulted in relatively high concentration of Cr

in the new amphibole (Fig. 4a). It is not clear, whether the deformation of plagioclase occurred partly during diapiric ascent of gabbro or it was only related to the post-consolidation amphibolite facies overprint. In contrast to metagabbro in the central part, the other mafic rocks of this massif show higher degrees of deformation and metamorphism that is defined by amphibole and may contain garnet porphyroblasts.

6.8.2. Geotectonic implication

Figure 11 summarizes the results of this work on the Ronov mafic–ultramafic body in relation to the metamorphic history of the surrounding rocks in the Kutná Hora Complex. Considering different varieties of rocks within the Ronov body, the metagabbro represents a more evolved member with composition near to the boundary of gabbro-anorthosite. The presence of almost pure anorthite in metagabbro suggests its formation by fractionation of a mantle ultramafic magma without or with only limited contamination with crustal material. Based on the phase relations in Fig. 10, the metagabbro crystallized at middle to lower crustal levels. This is supported also by the experimentally determined pressure stability field of the assemblage with spinel, plagioclase and clinopyroxene (Gasparik, 2003) that ranges between 0.8–1.4 GPa (Fig. 11). Pressures of 0.9–1.0 GPa are favoured by a combination of both igneous and metamorphic mineral equilibria. This also suggests a near isobaric cooling to amphibolite facies overprint at about 750–700 °C and 1.0 GPa (position III in Fig. 11). The presence of kyanite in granulite and migmatite suggest that further exhumation of the rocks to their present position occurred in the kyanite stability field. No sillimanite was observed in the surrounding gneiss and granulite as well as in the whole Kutná Hora Complex.

The position of the Ronov mafic–ultramafic body, surrounded by granulite gneiss and granulite, in combination with the new age data from coronitic metagabbro has important implication for geodynamic interpretation of the Variscan orogeny in the Moldanubian Zone. The metamorphic history of granulite facies rocks with lenses of eclogites and garnet peridotites adjacent to the Ronov mafic–ultramafic body has

been the subject of extensive study (Faryad, 2009; Faryad et al., 2010b; Jedlicka et al., 2015; Perraki and Faryad, 2014). These authors indicated that the felsic granulite and hosting rocks were first subducted to UHP conditions (path I in Fig. 11) and after their exhumation into the middle crustal levels within an accretionary wedge they were shortly heated and overprinted by granulite facies metamorphism (path II in Fig. 11). Most of the age data, obtained for zircon in granulite range from 365–342 Ma (Nahodilová et al., 2014), which date both the UHP event about 370 Ma (Brueckner et al., 1991) and the granulite facies metamorphism of cca 340 Ma in the Moldanubian Zone (for ref. see Schulmann et al., 2005; Friedl et al., 2011). The Variscan (337.7 ± 2 Ma) age obtained for the leucocratic member of the Ronov mafic–ultramafic body suggests that crystallization of its parent magma was probably coeval or slightly younger than the granulite facies peak temperature conditions. Jedlicka et al. (2015) calculated peak pressure for the granulite facies event at about 1.5 GPa. This means that the Ronov mafic–ultramafic body crystallized at relatively higher crustal levels (30–35 km), comparing to the surrounding granulites. In contrast to granulite facies assemblages (garnet+sapphirine+clinopyroxene+orthopyroxene) in the coronitic troctolite at Stálky (Faryad et al., 2015), recrystallization and corona formation in the Ronov body occurred in amphibolite facies conditions. During exhumation, the mafic body was sampled by granulites, which reached higher temperatures close to the asthenosphere. Both the host granulite and the Ronov mafic–ultramafic body then shared a common P-T path from their crystallization depth corresponding to 1.0 GPa.

Fig. 2 shows that the Variscan mafic–ultramafic intrusives are not only restricted to a single occurrence, but they are widespread in the Moldanubian Zone and even penetrated the hanging wall of Teplá-Barrandian Block. Some of them are unmetamorphosed and their relations to post-collisional Variscan magmatism is clear, others show recrystallization under amphibolite facies conditions and they were intruded into the middle crustal levels and subsequently metamorphosed and transported into their present positions. The coincidence of magmatic crystallization of mafic–ultramafic bodies and granulite facies metamorphism of HP-UHP rocks is a good argument for the interplay of mantle-derived magmas and granulite–amphibolite facies metamorphism. Mantle dynamics and related magma

generation during Variscan post-collisional events is supported by ultrapotassic magmatism in the Bohemian Massif (Holub, 1997; Janoušek and Holub, 2007). The extensive mantle-related melting process not only caused formation of various mafic and ultramafic rocks but also operated as heat source for the granulite facies metamorphism in the Moldanubian Zone. The role of asthenospheric magma as a heat source for the granulite facies metamorphism, mainly at UHT conditions, is widely considered (see Brown and Korhonen, 2009; Mints, 2015; Miyashiro, 1994). In our case, a rapid heating and short-lived process for the granulite facies metamorphism is supported by the preservation of prograde zoning garnet in felsic granulite which formed during the high-pressure metamorphism.

The common occurrence of both mafic–ultramafic intrusive and granulite facies rocks within or adjacent to amphibolite facies gneisses and migmatites are indicative for crustal scale tectonic zones along which these rocks were exhumed. In the case of the Ronov amphibolite facies mafic–ultramafic body and surrounding felsic granulite this will mean their common exhumation from the middle–lower crustal levels. Faryad et al. (2013) proposed that the 200 km long zone with retrogressed eclogite and serpentinite that occurs east of CBPC (Fig. 1) might represent the relic of a suture created by subduction of the Moldanubian plate beneath the Teplá-Barrandian Block (Franke, 2000). This zone is also characterized by bodies of felsic granulite with former UHP history that include the south Bohemian granulite massifs, Podolsko Complex (see also Faryad and Žák, 2016) and the Kutná Hora Complex. Possible continuation of this suture along the European Variscan belt through Schwarzwald, Vosges, the French Massif Central, the Armorican Massif to the Iberian Massif (Fig. 1a) is assumed by the affinity of the Moldanubian Zone rocks in other crystalline massifs (Franke, 2000). However, surface tectonic features of this suture zone were probably destroyed due to syn- to post-collisional metamorphism and associated granite magmatism mainly within Moldanubian lower plate.

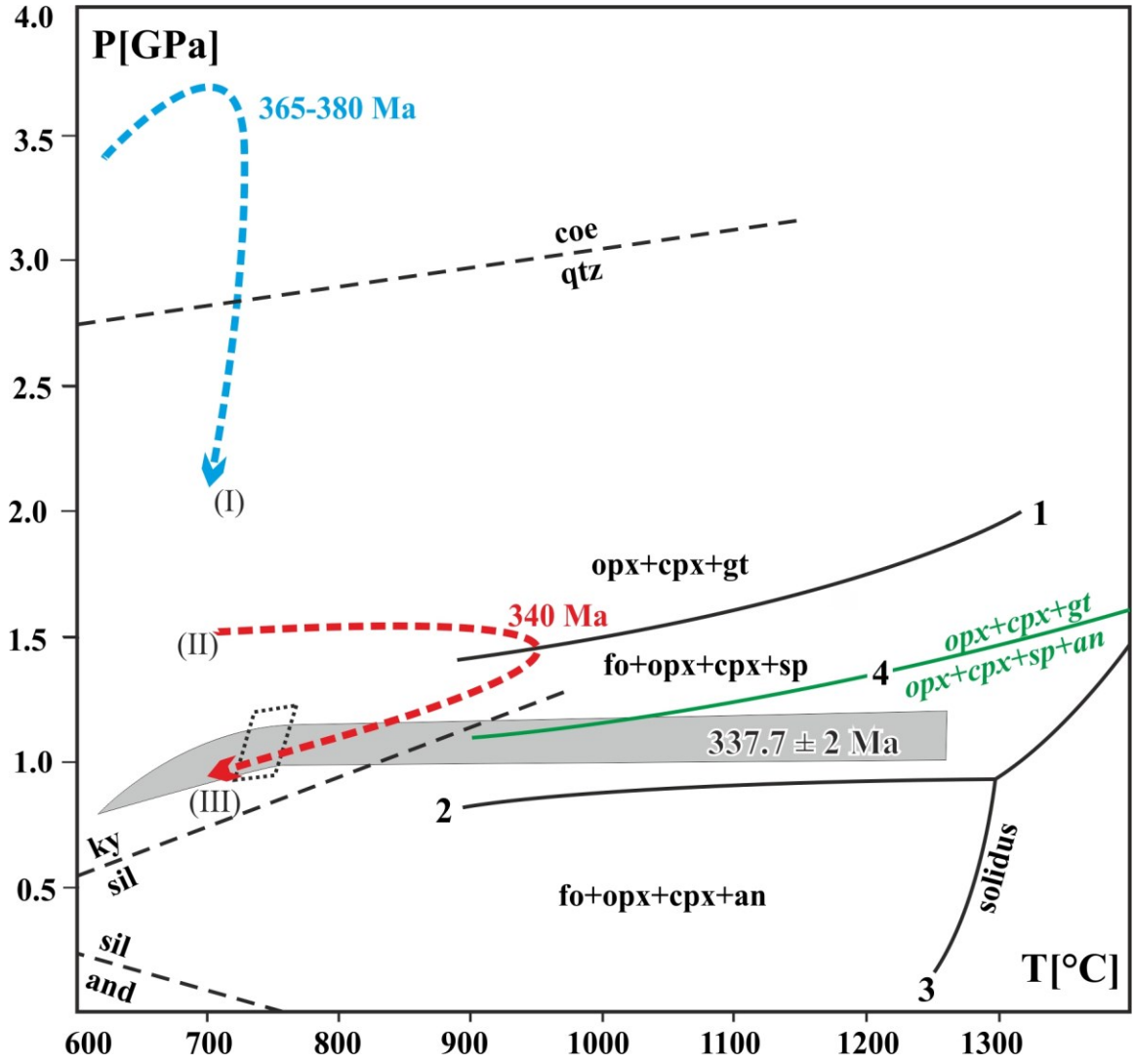

Fig. 11. P–T diagram showing cooling history of spinel-bearing metagabbro and subsequent amphibolite facies metamorphism (III). The univariant (1, 2, 3) and solidus (4) boundaries are from Gasparik (2003). Line (4) delineates the two pyroxene + anorthite + spinel-bearing assemblage from two pyroxene + garnet field. Lines (I) and (II) indicate earlier UHP and subsequent granulite facies metamorphism, respectively in the surrounding granulite (Jedlicka et al., 2015; Perraki and Faryad, 2014).

6.9. Conclusions

To summarize, observations in the mafic–ultramafic body and its relation to the surrounding granulite revealed the following:

1. The mafic–ultramafic rocks of the Ronov body formed by a continuous process of magma emplacement in the middle–lower crustal levels and subsequent deformation and metamorphism in the amphibolite facies conditions.

2. Based on the presence of almost pure anorthite plagioclase in metagabbro, the different varieties of rocks were formed by fractionation of mantle related magma, without contamination of crustal material during magma ascent.

3. Subsolidus and metamorphic reactions occurred by isobaric cooling in the depth of about 25–30 km. Post-consolidation reactions led to formation of garnet and amphibole that occurred by isobaric cooling up to 700–750 °C.

4. Variscan age of magmatic crystallization of the mafic-ultramafic body was coeval with granulite facies metamorphism and supports the interpretation of the asthenospheric magma as heating source of granulite facies metamorphism in the Moldanubian Zone.

5. Based on the calculated P-T conditions and age data of the mafic-ultramafic body and surrounding granulite, they both shared the same exhumation path from their middle–lower crustal position at the end of Variscan orogeny.

6.10. Acknowledgements

This research was supported by the Czech Science Foundation (project 13-06958S). We gratefully acknowledge Arne Willner and an anonymous reviewers for their constructive comments.

PART VII

7.1. Discussion and Conclusions

A wide spectrum of metamorphic rocks from broad area of the Bohemian Massif was investigated in presented chapters above. Starting from crustal lithology rocks represented by felsic a mafic granulites from northern part of Moldanubian Zone (Kutná Hora Complex) and from East Sudetes (Rychleby Mountains), through mafic rocks such as eclogites and metagabbros occurring as numerous bodies and forming a long belt in the Monotonous unit of the Moldanubian Zone and in the Ronov Massif, respectively and finally finishing with the ultramafic mantle rocks – ganet peridotites, pyroxenites and garnetites enclosed in crustal felsic granulites and migmatites in the southern part of the Moldanubian Zone (Nové Dvory, Dunkelsteinerwald). Special attention was focused on garnet composition within these rocks. Variation in mineral chemistry determines zoning, which could be characteristic for different conditions in P-T space. According to that, we were able to trace the possible metamorphic history of the rocks. Inclusions of characteristic minerals within garnet, which are not in equilibrium with other minerals presented in the rock, can provide information about previous metamorphic conditions prior to the high-temperature overprint. In combination with thermodynamic modelling it is possible to trace the pre-exhumation history of strongly re-equilibrated rocks in a Variscan orogeny.

7.1.1. Felsic and mafic granulites and their prograde metamorphic history

Similar to other granulite bodies in the Moldanubian Zone, only cooling and decompression P-T paths from UHP-UHT conditions were proposed for granulite in the Kutná Hora Complex and from the Rychleby Mountains (Bakun-Czubarow, 1992; Budzyń et al., 2015; Kryza et al., 1996; Nahodilová et al., 2014; Pouba et al., 1985; Štípská et al., 2004; Vrána et al., 2005). In addition to mineral inclusions, the prograde metamorphic history in both felsic and mafic varieties of granulite is confirmed by the distribution of major and trace elements in garnet. The classic bell-shaped pattern of major and some trace elements is considered to occur due to strong affinity of these elements into garnet and also as the result of fractionation-depletion mechanism during garnet growth (e.g. Hollister, 1966; Otamendi et al., 2002;

Tracy, 1982; Tracy et al., 1976). The annular peak in garnet from the Kutná Hora granulite is interpreted as the result of two stages of garnet growth that occurred during HP-UHP metamorphism and subsequent granulite facies overprint. The first garnet, formed during the HP-UHP event, was partially consumed during exhumation of the rocks, where Y+HREEs released from the resorbed garnet into the matrix were incorporated back into garnet during the second stage in granulite facies conditions in lower to middle crustal positions. In contrast to garnet from granulite in the Kutná Hora Complex, the annular peaks of Y+HREEs near the rim of garnet crystals were not observed in garnet from Rychleby granulite. The lack of annular peaks suggests its formation by a single HP-UHP event, where almost all garnet was created. If a small amount of garnet was formed during the granulite facies stage, it could continuously overgrow the HP garnet without resorption of the core garnet or enrichment of the system by REEs from an external source by fluid or melt. In comparison with the Rychleby Mountains, the granulite in the Kutná Hora shows higher temperature during granulite facies overprint with formation of leucocratic layers as result of partial melting (Nahodilová et al., 2011) and overgrowth of granulite facies garnet with annular peaks of Y+REEs. Higher temperature and degree of granulite facies overprint was responsible for local garnet resorption-regrowth in the Kutná Hora Complex.

The preservation of prograde zoning in garnet is an important attribute for constraining P-T history and geodynamic reconstruction of the subduction and/or collision zone. From the pseudosection modelling, mainly based on grossular isopleths, we interpret a steep geothermal gradient in a subduction environment from its initial stage at low-pressure, low-temperature conditions (0.6 GPa / 400 °C for Kutná Hora Complex and 0.8-0.9 GPa / 460 °C for Rychleby Mountains) up to UHP conditions (3.2–4.0 GPa / 700 °C for Kutná Hora Complex and 2.4-2.5 GPa / 550 °C for Rychleby Mountains) for these granulites. UHP conditions were confirmed by the finding of micro-diamond and coesite by Perraki and Faryad (2014) and coesite pseudomorphs by Bakun-Czubarow (1992).

There are two alternative scenarios to explain the exhumation of felsic rocks from mantle depths and their subsequent granulite-facies metamorphism. The first is decompression and heating to granulite-facies conditions of 1.5–2.0 GPa

at 800–1000 °C as estimated for the felsic granulite in the Moldanubian Zone and also in East Sudetes (Bakun-Czubarow, 1992; Budzyń et al., 2015; Carswell and O'Brien, 1993; Kotková and Harley, 1999 Kryza et al., 1996; Nahodilová et al., 2014; Pouba et al., 1985; Štípská et al., 2004; Tajčmanová et al., 2006; Vrána, 1992; Vrána et al., 2005). However, an isothermal decompression to the granulite-facies stage would result in total homogenization of the prograde compositional zoning in garnet (Chakraborty and Ganguly, 1992; Carlson, 2006; Vielzeuf et al., 2005), unless the exhumation rate from mantle depths to crustal levels was too fast. The second scenario is an isothermal decompression from UHP conditions at intermediate temperature. After the rocks were exhumed to lower or middle crustal levels, they were subjected to heating at granulite-facies conditions. Such a model for granulite-facies metamorphism in the Moldanubian Zone has been explained by slab breakoff and mantle upwelling as a potential heat source for the granulite-facies metamorphism (Faryad et al., 2015).

7.1.2. UHP metamorphism of eclogites and garnet peridotites

Textural relations and estimated P–T conditions of eclogite bodies within amphibolite facies basement rocks in the Moldanubian Zone enable us to constrain the earlier subduction history of HP–UHPM rocks. The calculated temperature conditions for eclogites in the amphibolite facies Monotonous and Varied units are 600–650 °C. Maximum pressure, calculated based on the pseudosection method and equilibrium reactions among minerals, is 2.3 GPa. When comparing P–T conditions of eclogites in amphibolite facies units from the Moldanubian Zone with those occurring in the Erzgebirge and Sudetes [the Saxothuringian Zone, Massonne and Koppe (2005), Klemd and Bröcker (1999)], both show a P–T gradient of 7–9 °C/km with prograde P–T paths crossing the epidote and lawsonite eclogite facies boundary. These features, as well as preservation of strong compositional zoning of garnet with taramite inclusions, suggest a rapid and/or relatively cool subduction environment.

Metamorphic P–T conditions estimated for garnet peridotites and eclogites from Nové Dvory (Medaris et al., 2005; Nakamura et al., 2004) and from Dunkelsteinerwald (Becker, 1997a, 1997b; Carswell, 1991) indicated that they

passed UHP conditions at temperatures above 1000 or 1100 °C. All these rocks occur within felsic granulites, which together with mafic and ultramafic bodies shared granulite facies metamorphism at about 900–1000 °C (Faryad et al., 2010b; Kotková, 2007; O'Brien and Carswell, 1993; Tajčmanová et al., 2006). Despite such high-temperature metamorphic events, compositional zoning in garnet from eclogites is preserved. This suggests that the UHP and subsequent granulite facies metamorphism were not long enough to entirely homogenize the major element composition in garnet. The increase of Ca and decrease of Mg in the core of garnet grains, both in garnet clinopyroxenite and eclogite, can be interpreted as the result of pressure increase and temperature decrease. This fits with the transformation of spinel to garnet and formation of garnet lamellae both in Al-rich clino- and orthopyroxene. The granulite facies process can be also reproduced from the zoning profile near the rim of garnet grains, where Mg shows increase and Ca decrease. A short-term granulite facies overprint is documented by preservation of prograde zoning garnet in felsic granulite (Faryad et al., 2010b).

7.1.3. Geodynamic implications

Recent studies of felsic granulite in the Gföhl Unit of the Moldanubian Zone (Faryad et al., 2010b; 2015; Jedlicka et al., 2015; Perraki and Faryad, 2014) and from some eclogites in the Monotonous and Variegated units (Faryad and Fišera, 2015; Scott et al., 2013) showed that they both experienced an earlier HP-UHP event and were subsequently overprinted by granulite-amphibolite facies metamorphism in lower and middle crustal positions at 0.7-1.5 GPa. In most cases, the eclogite bodies within granulite were interpreted as result of tectonic imbrication of rocks, which differs in their metamorphic history (Nakamura et al., 2004; Medaris et al., 2006).

The two stage metamorphic history, the first at HP-UHP and the second in MP granulite facies conditions, was established for both granulites in the Moldanubian Zone and in the East Sudetes (part II, III of this thesis). In the Moldanubian Zone, granulite facies metamorphism is assumed to have occurred after exhumation of the HP-UHP rocks by a syn-convergent mechanism into lower-middle crustal

positions (Faryad et al., 2015). The heat source for this short-lived granulite facies metamorphism is explained by slab break-off and mantle upwelling triggering melting and emplacement of magma in a lower stress field beneath the accretionary complex. Extreme heating, produced by mafic-ultramafic intrusions, resulted in granulite facies overprint of the already exhumed HP-UHP bodies and migmatisation of their host lithologies (part VI of the thesis). After this short-lived thermal process, the high-grade rocks were transported to the upper crustal levels due to the subduction of the Rheic oceanic plate (Finger et al., 2007) and subsequent tectonic underplating of the Brunovistulian Block beneath the Moldanubian Zone (Schulmann et al., 2005).

The eclogites and serpentinites are part of the amphibolite facies Monotonous and Varied units. The calculated P–T conditions from eclogite bodies in the Moldanubian Zone indicate low geothermal gradient and suggest their formation by rapid subduction and exhumation process (part V of the thesis). The occurrence of eclogite bodies with serpentinite along ca 250 km zone southeast of the Teplá–Barrandian Block is interpreted as Variscan suture formed by closure of the Moldanubian Ocean (Franke, 2000). The Moldanubian suture is part of the main Variscan suture that can be traced within other allochthonous massifs along the European Variscan Belt from the Bohemian Massif to the Iberian Massif in the southwest (Faryad et al., 2015; Franke, 2000). In the Bohemian Massif, it continues from the Moldanubian Zone to Sudetes in the northwest. The Moldanubian suture might be responsible for formation and exhumation of the UHP granulite bodies in the Moldanubian Zone.

LIST OF REFERENCES

Ackermann, L., Jelínek, E., Medaris, G., Ježek, J., Siebel, W., Strnad, L., 2009. Geochemistry of Fe-rich peridotites and associated pyroxenites from Horní Bory, Bohemian Massif: insights into subduction-related melt–rock reactions. Chemical Geology 259, 152–167.

Ackermann, L., Pašava, J., Erban, V., 2013. Re-Os geochemistry and geochronology of the Ransko gabbro-peridotite massif, Bohemian Massif. Mineralium Deposita 48, 799–804.

Ai, Y., 1994. A revision of the garnet–clinopyroxene Fe^{2+}–Mg exchange geothermometer. Contributions to Mineralogy and Petrology 115, 467–473.

Aleksandrowski, P., Kryza, R., Mazur, S., Żaba, J., 1997. Kinematic data on major Variscan strike-slip faults and shear zones in the Polish Sudetes, northeast Bohemian Massif. Geological Magazine 134, 727–739.

Aleksandrowski, P., Mazur, S., 2002. Collage tectonics in the northeasternmost part of the Variscan Belt: the Sudetes, Bohemian Massif. In: Palaeozoic Amalgamation of Central Europe (Eds. J. A. Winchester, T. C. Pharaoh and J. Verniers). Geological Society, London, Special Publication 201, 237–277.Anders, E., Grevasse, N., 1989. Abundance of the elements: Meteoritic and Solar. Geochimica et Cosmochimica Acta 53, 197-214.

Anczkiewicz, R., Szczepański, J., Mazur, S., Storey, C., Crowley, Q., Villa, I. M., Thirlwall, M. F., Jeffries, T. E., 2007. Lu-Hf geochronology and trace element distribution in garnet: Implications for uplift and exhumation of ultra-high pressure granulites in the Sudetes, SW Poland. Lithos 95, 363–380.

Andersen, T., Austrheim, H., Burke, E.A.J., 1990. Fluid inclusions in granulites and eclogites from the Bergen Arcs, Caledonides of W. Norway. Mineralogical Magazine 54, 145–158.

Anderson, D. E., Buckley, G. R., 1973. Zoning in garnets: Diffusion models. Contributions to Mineralogy and Petrology 40, 87-104.

Ashwal, L.D., 1993. Anorthosites. Minerals and Rocks Series Volume 21. Springer-Verlag Berlin, Heidelberg, New York, London, Paris, Tokyo, Hong Kong.

Babuška, V., Plomerová, J., 2013. Boundaries of mantle–lithosphere domains in the Bohemian Massif as extinct exhumation channels for high-pressure rocks. Gondwana Research 23, 973-987.

Bakun-Czubarow, N., 1992. Quartz pseudomorphs after coesite and quartz exsolutions in eclogitic clinopyroxenes of the Złote Mountains in the Sudetes (SW Poland). Archiwum Mineralogiczne 48, 3–25.

Bakun-Czubarow, N., 1998. Ilmenite-bearing eclogites of the West Sudetes — their geochemistry and mineral chemistry. Archiwum Mineralogiczne 51, 29–110.

Banno, S., Enami, M., Hirajima, T., Ishiwatari, A., Wang, Q.C., 2000. Decompression P–T path of coesite eclogite to granulite from Weihai, eastern China. Lithos 52, 97–108.

Beard, B. L., Medaris, L. G., Johnson, C. M., Brueckner, H. K., Mísař, Z., 1992. Petrogenesis of Variscan high-temperature group-A eclogites from the Moldanubian zone of the Bohemian Massif, Czechoslovakia. Contributions to Mineralogy and Petrology 111, 468-483.

Bebout, G.E., Ryan, J.G., Leeman, W.P., Bebout, A.E., 1999. Fractionation of trace elements by subduction zone metamorphism — effect of convergent margin thermal evolution. Earth and Planetary Science Letters 171, 63–82.

Becker, H., 1997a. Petrological constraints on the cooling history of high-temperature garnet peridotite massifs in lower Austria. Contributions to Mineralogy and Petrology 128, 272–286.

Becker, H., 1997b. Sm–Nd garnet ages and cooling history of high-temperature garnet peridotite massifs and high-pressure granulites from lower Austria. Contributions to Mineralogy and Petrology 127, 224–236.

Benisek, A., Dachs, E., Kroll, H., 2010. A ternary feldspar-mixing model based on calorimetric data: development and application. Contributions to Mineralogy and Petrology 160, 327-337.

Bhattacharya, A., Mohanty, L., Maji, A., Sen, S. K., Raith, M., 1992. Non-ideal mixing in the phlogopite-annite binary: constraints from experimental data on Mg-Fe Partitioning and a reformulation of the biotite-garnet geothermometer. Contributions toMineralogy and Petrology, 111, 87-93.

Blackburn, W. H., Navarro, E., 1977. Garnet zoning and polymetamorphism in the eclogitic rocks of Isla de Margarita, Venezuela. Canadian Mineralogist 15, 257-266.

Brey, G.P., Doroshev, A.M., Girnis, A.V., Turkin, A.I., 1999. Garnet–spinel–olivine–orthopyroxene equilibria in the FeO–MgO–Al2O3–SiO2–Cr2O3 system: I. Composition and molar volumes of minerals. European Journal of Mineralogy 11, 599–617.

Brown, M., Korhonen, F., 2009. In: Gupta, A.K., Dagupta, S. (Eds.), Some remarks on Melting and extreme metamorphism of crustal rocks. Springer-Verlag, Physics and chemistry of the Earth's interior, pp. 67–88.

Bröcker, M., Cosca, M., Klemd, R., 1997. Geochronologie von Eklogiten und assoziierten Nebengesteinen des Orlica–Snieznik Kristallins (Sudeten, Poland): Ergebnisse von U–Pb, Sm–Nd, Rb–Sr und Ar–Ar Untersuchungen. Terra Nostra 97, 29–30.

Bröcker, M., Klemd, R., 1996. Ultrahigh-pressure metamorphism in the Snieznik Mountains (Sudetes, Poland): P–T constraints and geological implications. Journal of Geology 104, 417–433.

Bröcker, M., Klemd, R., Cosca, M., Brock, W., Larionov, A.N., Rodionov, N., 2009. The timing of eclogite facies metamorphism and migmatization in the Orlica–Snieznik complex, Bohemian Massif: constraints from a multimethod geochronological study. Journal of Metamorphic Geology 27, 385–403.

Brueckner, H. K., 1998. Sinking intrusion model for the emplacement of garnet-bearing peridotites into continent collision orogens. Geology 26, 631–634.

Brueckner, H. K., Medaris, L. G., 2000. A general model for the intrusion and evolution of “mantle” garnet peridotites in high pressure and ultrahigh-pressure metamorphic terranes. Journal of Metamorphic Geology 18, 123–133.

Brueckner, H. K., Medaris, L. G., Bakun-Czubarow, N., 1991. Nd–Sm age and isotope patterns from Variscan eclogites of the eastern Bohemian Massif. Neues Jahrbuch für Mineralogie - Abhandlungen 163, 169–196.

Brunet, F., Bonneau, V., Irifune, T., 2006. Complete solid-solution between $Na_3Al_2(PO_4)_3$ and $Mg_3Al_2(SiO_4)_3$ garnets at high pressure. American Mineralogist 91, 211-215.

Budzyń, B., Jastrzębski, M., Kozub-Budzyń, G., Konečný, P., 2015. Monazite Th-U-total Pb geochronology and P-T thermodynamic modelling in a revision of the HP-HT metamorphic record in granulites from Stary Gierałtów (NE Orlica–Śnieźnik Dome, SW Poland). Geological Quarterly 59, 700-717.

Bues, C., Zulauf, G., 2000. Microstructural evolution and geologic significance of garnet pyriclasites in the Hoher-Bogen shear zone (Bohemian Massif, Germany). International Journal of Earth Sciences 88, 803–813.

Bues, C., Dörr, W., Fiala, J., Vejnar, Z., Zulauf, G., 2002. Emplacement depths and radiometric ages of Paleozoic plutons of the Neukirchen-Kdyně massif: differential

uplift and exhumation of Cadomian basement due to Carboniferous orogenic collapse (Bohemian Massif). Tectonophysics 352 (1–2), 225–243.

Cameron, E.P., French, W.J., 1977. Relationship of order of crystallization of basalt melts to their classification and to definition of rocks series. Mineralogical Magazine 41, 239–251.

Carlson, W. D., 1989. The significance of intergranular diffusion to the mechanisms and kinetics of porphyroblast crystallization. Contributions to Mineralogy and Petrology 103, 1-24.

Carlson, W. D., 2006. Rates of Fe, Mg, Mn, and Ca diffusion in garnet. American Mineralogist 91, 1-11.

Carlson, W. D., 2012. Rates and mechanism of Y, REE and Cr diffusion in garnet. American Mineralogist 97, 1598-1618.

Carlson, W. D., Gale, J. D., Wright, K., 2014. Incorporation of Y and REEs in aluminosilicate garnet: Energetics from atomistic simulation. American Mineralogist 99, 1022-1034.

Carlson, R. W., Irving, A.J., 1994. Depletion and enrichment history of subcontinental lithospheric mantle: an Os, Sr, Nd and Pb isotopic study of ultramafic xenoliths from the northwestern Wyoming craton. Earth and Planetary Science Letters 126, 457–472.

Carswell, D. A., 1991. Variscan high P-T metamorphism and uplift history in the Moldanubian Zone of the Bohemian Massif in lower Austria. European Journal of Mineralogy 3, 323-342.

Carswell, D. A., Jamtweit, D., 1990. Variscan Sm–Nd ages for the high-pressure metamorphism in the Moldanubian Zone of the Bohemian Massif, Lower Austria. Neues Jahrbuch für Mineralogie - Abhandlungen 162, 69–78.

Carswell, D. A., O'Brien, P. J., 1993. Thermobarometry and geotectonic significance of high-pressure granulites: examples from the Moldanubian zone of the Bohemian Massif in Lower Austria. Journal of Petrology 34, 427-459.

Culek, A., 1951. Svatokřížský shluk hlubinných basických hornin u Ronova n. D. Rozpravy II. 56. Třídy České Akademie, pp. 1–25.

Cháb, J., Stráník, Z., Eliáš, M., 2007.Geologická mapa České republiky 1:500.000. Česká geologická služba, Praha.

Chakraborty, S., Ganguly, J., 1992. Cation diffusion in aluminosilicate garnets: Experimental determination in spessartine-almandine diffusion couples, evaluation of effective binary diffusion coefficients, and applications. Contributions to Mineralogy and Petrology 111, 74-86.

Chamberlain, C. P., Conrad, M. E., 1993. Oxygen-isotope zoning in garnet: A record of volatile transport. Geochimica et Cosmochimica Acta 57, 2613-2629.

Chemenda, A. I., Mattauer, M., Malavieille, J., Bokun, A. N., 1995. A mechanism for syn-collisional rock exhumation and associated normal faulting - results from physical modeling. Earth and Planetary Science Letters 132, 225-232.

Cheng, H., Nakamura, E., Kobayashi, K., Zhou, Z., 2007. Origin of atoll garnets in eclogites and implications for the redistribution of trace elements during slab exhumation in a continental subduction zone. American Mineralogist 92, 1119-1129.

Chernoff, C. B., Carlson, W. D., 1999. Trace element zoning as a record of chemical disequilibrium during garnet growth. Geology 27, 555-558.

Chopin, C., 2003. Ultrahigh-pressure metamorphism: tracing continental crust into the mantle. Earth and Planetary Science Letters 212, 1–14.

Chopin, F., Schulmann, K., Skrzypek, E., Lehmann, J., Dujardin, J. R., Martelat, J. E., Lexa, O., Corsini, M., Edel, J. B., Štípská, P., Pitra, P., 2012a. Crustal influx, indentation, ductile thinning and gravity redistribution in a continental wedge: building a Moldanubian mantled gneiss dome with underthrust Saxothuringian material (European Variscan Belt). Tectonics, 31, 1–27.

Chopin, F., Schulmann, K., Štípská, P., Martelat, J. E., Pitra, P., Lexa, O., Petri, B., 2012b. Microstructural and metamorphic evolution of a high pressure granitic orthogneiss during continental subduction (Orlica-Snieznik dome, NE Bohemian Massif). Journal of Metamorphic Geology, 30, 347–376.

Coggon, R., Holland, T. J. B., 2002. Mixing properties of phengitic micas and revised garnet-phengite thermobarometers. Journal of Metamorphic Geology 20, 683-696.

Connolly, J. A. D., 2005. Computation of phase-equilibria by linear programming: a tool for geodynamic modelling and its application to subduction zone decarbonation. Earth and Planetary Science Letters 236, 524-541.

Cooke, R.A., 2000. High-pressure/temperature metamorphism in the St. Leonhard Granulite Massif, Austria: evidence from intermediate pyroxene-bearing granulites. International Journal of Earth Sciences 89, 631–651.

Cygan, R. T., Lasaga, A. C., 1982. Crystal-growth and the formation of chemical zoning in garnets. Contributions to Mineralogy and Petrology 79, 187-200.

Dale, J., Holland, T., Powell, R., 2000. Hornblende-garnet-plagioclase thermobarometry: a natural assemblage calibration of the thermodynamics of hornblende. Contributions to Mineralogy and Petrology 140, 353–362.

Dale, J., Powell, R., White, R.W., Elmer, F.L., Holland, T.J.B., 2005. A thermodynamic model for Ca-Na clinoamphiboles in Na_2O-CaO-FeO-MgO-Al_2O_3-SiO_2-H_2O-O for petrological calculations. Journal of Metamorphic Geology 23, 771-791.

Dallmeyer, R. D., Franke, W., Weber, K., 1995. Pre-Permian Geology of Central and Eastern Europe. Springer-Verlag, 1-593.

Dallmeyer, R.D., Urban, M., 1998. Variscan vs. Cadomian tectonothermal activity in northwestern sectors of the Teplá–Barrandian zone, Czech Republic: constraints from 40Ar/39Ar ages. Geologische Rundschau 87, 94–1o6.

Dasgupta, S., Sengupta, P., Guha, D., Fukuoka, M., 1991. A refined garnet-biotite Fe-Mg exchange geothermometer and its application in amphibolites and granulites. Contributions to Mineralogy and Petrology 109, 130-137.

Dawson, J. B., Carswell, D. A., 1990. High-temperature and ultra-high-pressure eclogites. In: Carswell, D. A. (ed.) Eclogite Facies Rocks. Blackie, 314-349.

Demidjuk, Z., Turner, S., Sandiford, M., George, R., Foden, J., Etheridge, M., 2007. U series isotope and geodynamic constraints on mantle melting processes beneath the Newer Volcanic Province in South Australia SEP 30. Earth and Planetary Science Letters 261 (3–4), 517–533.

Dobrzhinetskaya, L.F., 2012. Microdiamonds - frontier of ultrahigh-pressure metamorphism. Gondwana Research 21, 207–223.

Dobrzhinetskaya, L., Faryad, S.W., 2011. Frontiers of ultra-high pressure metamorphism: view from field and laboratory. In: Dobrzhinetskaya, L., Faryad, S.W., Wallis, S., Cuthbert, S. (Eds.), Ultrahigh Pressure Metamorphism: 25 Years after the Discovery of Coesite and Diamond. Elsevier, pp. 1–4o.

Don, J., Dumicz, M., Wojciechowska, I., Żelaźniewicz, A., 1990. Lithology and tectonics of the Orlica-Snieznik Dome, Sudetes – Recent state of knowledge. Neues Jahrbuch für Mineralogie, Abhandlungen 179, 159–188.

Don, J., Skácel, J., Gotowała, R., 2003. The boundary zone of the East and West Sudetes on the 1:50 000 scale geological map of the Velké Vrbno, Staré Město and Śnieźnik Metamorphic Units. Geologia Sudetica 35, 25–59.

Dunham, A. C., Wilkinson, F. C. F., 1985. Sulfide droplets and the Unit 11/12 chromite band, Rhum – a mineralogical study. Geological Magazine 122, 539–548.

Edel, J.B., Schulmann, K., Holub, V.F., 2003. Anticlockwise and clockwise rotations of the Eastern Variscides accommodated by dextral lithospheric wrenching: palaeomagnetic and structural evidence. Journal of the Geological Society of London 160, 209–218.

Erambert, M., Austrheim, H., 1993. The effect of fluid and deformation on zoning and inclusion patterns in poly-metamorphic garnets. Contributions to Mineralogy and Petrology 115, 204-214.

Ernst, W.G., 1988. Tectonic history of subduction zones inferred from retrograde blueschist P–T paths. Geology 16, 1081–1085. Faryad, S.W., 2009. The Kutná Hora Complex (Moldanubian zone, Bohemian Massif): a composite of crustal and mantle rocks subducted to HP/UHP conditions. Lithos 109, 193–208.

Ernst, W.G., Liou, J.G., 2000. Ultrahigh-pressure Metamorphism and Geodynamics in Collision-type Orogenic Belts: International Book Series, vol. 4. Geological Society of America, p. 293.

Faryad, S. W., 2009. The Kutná Hora Complex (Moldanubian zone, Bohemian Massif): A composite of crustal and mantle rocks subducted to HP/UHP conditions. Lithos 109, 193-208.

Faryad, S. W., 2011. Distribution and geological position of high-/ultrahigh-pressure units within the European Variscan Belt: a review, in: Dobrzhinetskaya, L., Faryad, S.W., Wallis, S., Cuthbert, S. (ed.) Ultrahigh Pressure Metamorphism: 25 Years After the Discovery of Coesite and Diamond, Elsevier, 361-397.

Faryad, S. W., 2012. High-pressure polymetamorphic garnet growth in eclogites from the Mariánské Lázně Complex (Bohemian Massif). European Journal of Mineralogy 24, 483–497.

Faryad, S. W., Bernhardt, H.J., 1996. Taramite-bearingmetabasites from Rakovec (Gemeric Unit, The Western Carpathians). Geologica Carpathica 47, 349–357.

Faryad, S. W., Chakraborty, S., 2005. Duration of Eo-Alpine metamorphic event obtained from multicomponent diffusion modelling of garnet: A case study from the Eastern Alps. Contributions to Mineralogy and Petrology 150, 305-318.

Faryad, S. W., Fišera, M., 2015. Olivine-bearing symplectites in fractured garnet from eclogite, Moldanubian Zone (Bohemian Massif) – a short-lived, granulite facies event. Journal of Metamorphic Geology 33(6), 597-612.

Faryad, S. W., Jedlicka, R., Collett, S., 2013a. Eclogite facies rocks of the Monotonous unit, clue to Variscan suture in the Moldanubian Zone (Bohemian Massif). Lithos 179, 353–363.

Faryad, S. W., Jedlicka, R., Ettinger, K., 2013b. Subduction of lithospheric upper mantle recorded by solid phase inclusions and compositional zoning in garnet: example from the Bohemian Massif. Gondwana Research 23 (3), 944–955.

Faryad, S. W., Kachlík, V., 2013. New evidence of blueschist facies rocks and their geotectonic implication for Variscan suture(s) in the Bohemian Massif. Journal of Metamorphic Geology 31, 63-82.

Faryad, S. W., Dolejš, D., Machek, M., 2009. Garnet exsolution in pyroxene from clinopyroxenites in the Moldanubian zone: constraining the early pre-convergence history of ultramafic rocks in the Variscan orogen. Journal of Metamorphic Geology 27, 655-671.

Faryad, S. W., Kachlík, V., Sláma, J., Hoinkes, G., 2015. Implication of corona formation in a metatroctolite to the granulite facies overprint of HP-UHP rocks in the Moldanubian zone (Bohemian Massif). Journal of Metamorphic Geology 33, 295-310.

Faryad, S. W., Kachlík, V., Sláma, J., Jedlicka, R., 2016. Coincidence of gabbro and granulite formation and their implication for Variscan HT metamorphism in the Moldanubian Zone (Bohemian Massif), example from the Kutná Hora Complex. Lithos 264, 56-69.

Faryad, S. W., Klápová, H., Nosál, L., 2010a. Mechanism of formation of atoll garnet during high-pressure metamorphism. Mineralogical Magazine 74, 111-126.

Faryad, S. W., Nahodilová, R., Dolejš, D., 2010b. Incipient eclogite facies metamorphism in the Moldanubian granulites revealed by mineral inclusions in garnet. Lithos 114, 54-69.

Faryad, S. W., Perraki, M., Vrána, S., 2006. P–T evolution and reaction textures in retrogressed eclogites from Světlík, the Moldanubian Zone (Czech Republic). Mineralogy and Petrology 88, 297–319.

Faryad, S.W., Žák, J., 2016. High-pressure granulites of the Podolsko complex, Bohemian Massif: an example of crustal rocks that were subducted to mantle depth

and survived a pervasive mid-crustal high-temperature overprint. Lithos 246-247, 246–260.

Faure, M., Cocherie, A., Gache, J., Esnault, C., Guerrot, C., Rossi, P., Lin, W., Li, Q., 2014. Middle Carboniferous intracontinental subduction in the outer zone of the Variscan Belt (Montagne Noire Axial Zone, French Massif Central); multimethod geochronological approach of polyphase metamorphism. In: Schulmann, K., Martinez Catalán, J.R., Lardeaux, J.M., Janoušek, V., Oggiano, G. (Eds.), The Variscan Orogeny. Geological Society London. Special Publications 405, pp. 289–311.

Ferrando, S., Frezzotti, M.L., Dallai, L., Compagnoni, R., 2005. Multiphase solid inclusions in UHP rocks (Su–Lu, China): remnants of supercritical silicate-rich aqueous fluids released during continental subduction. Chemical Geology 223, 68–81.

Fiala, J., Jelínek, E., 1992. The Borek quarry near Chotěboř. International Workshop, High- Pressure Granulites-Lower Crustal Metamorphism. Excursion Guide. Czech Geological Survey, pp. 42–47.

Finger, F., Steyrer, H.P., 1995. A tectonicmodel for the eastern Variscides: indications from a chemical study of amphibolites in the south-eastern Bohemian Massif. Geologica Carpathica 46, 137–150 (Bratislava).

Finger, F., Gerdes, A., Janoušek, V., René, M., Riegler, G., 2007. Resolving the Variscan evolution of the Moldanubian sector of the Bohemian Massif: the significance of the Bavarian and the Moravo–Moldanubian tectonometamorphic phases. Journal of Geosciences 52, 9-8.

Franke, W., 2000. The mid-European segment of the Variscides: tectonostratigraphic units, terranes, boundaries and plate evolution. In: Franke, W., Haak, V., Oncken, O., Tanner, D. (ed.) Orogenic Processes: Quantification and Modelling in the Variscan Belt.Geological Society of London. Special Publication 179, 35-61.

Franke, W., Żelaźniewicz, A., 2000. The eastern termination of the Variscides: terrane correlation and kinematic evolution. In: Orogenic Processes: Quantification and Modelling in the Variscan Belt (eds Franke, W., Haak, V., Oncken, O. and Tanner, D.). Geological Society, London, Special Publications, 179, 63–85.

Friedl, G., Cooke, R., Finger, F., McNaughton, N., Fletcher, I., 2011. Timing of Variscan HP–HT metamorphism in the Moldanubian Zone of the Bohemian Massif: U–Pb SHRIMP dating on multiply zoned zircons from a granulite from the Dunkelsteiner Wald Massif, Lower Austria. Mineralogy and Petrology 102, 63–75.

Fu, B., Touret, J.L.R., Zheng, Y.F., 2001. Fluid inclusions in coesite-bearing eclogites and jadeite quartzite at Shuanghe, Dabie Shan (China). Journal of Metamorphic Geology 19, 531–547.

Fuchs, G., Matura, A., 1976. Zur Geologie des Kristallin der sudlichen Bohmischen Masse. Jahrbuch der Geologischen Bundesanstalt 119, 1–43.

Ganguly, J., Saxena, S. K., 1984. Mixing properties of alumino-sili-cate garnets: constraints from natural and experimental data, and applications to geothermometry. American Mineralogist 69, 88-97.

Gao, X.Y., Zheng, Y.F., Chen, Y.X., 2011. Dehydration melting of ultrahigh-pressure eclogites in the Dabie orogen: evidence from multiphase solid inclusions in garnet. Journal of Metamorphic Geology 1–20.

Gasparik, T., 2003. Phase diagrams for Geoscientists - An Atlas of the Earth's Interior. Springer-Berlin.

Grocholski, W., 1967. Structure of the Sowie Mts. Geologia Sudetica 3, 181-249.

Grütter, H., Latti, D., Menzies, A., 2006. Cr-saturation arrays in concentrate garnet compositions from kimberlite and their use in mantle barometry. Journal of Petrology 47, 801–820.

Grześkowiak, A., 2003. On the Mineralogy and Origin of the Śnieźnik versus Gieraltów Gneisses, Miedzygórze Unit, OSD, West Sudetes. GeoLines 16, 36–37.

Guy, A., Edel, J.B., Schulmann, K., Tomek, C., Lexa, O., 2011. A geophysical model of the Variscan orogenic root (Bohemian Massif): implications for modern collisional orogens. Lithos 124, 144–157.

Hawthorne, F.C., Oberti, R., Harlow, G.E., Maresch, W.V., Martin, R.F., Schumacher, J.C., Welch, M.D., 2012. Nomenclature of the amphibole supergroup. American Mineralogist 97, 2031–2048.

Henderson, P., 1975. Reaction trends shown by chrome-spinels of Rhum layered intrusion. Geochimica et Cosmochimica Acta 39, 1035–1044.

Hickmott, D. D., Shimizu, N., Spear, F. S., Selverstone, J., 1987. Trace-element zoning in a metamorphic garnet. Geology 15, 573-576.

Hickmott, D. D., Shimizu, N., 1989. Trace element zoning in garnet from Kwoiek area, British Columbia: disequilibrium partitioning during garnet growth? Contributions to Mineralogy and Petrology 104, 619-630.

Hickmott, D. D., Spear, F. S., 1992. Major- and trace-element zoning in garnets from calcareous pelites in the NW Shelburne Falls quadrangle, Massachusetts: garnet growth histories in retrograded rocks. Journal of Petrology 33, 965-1005.

Hilton, D.R., Fischer, T.P., Marty, B., 2002. Noble gases and volatile recycling at subduction zones. In: Porcelli, D., et al. (Ed.), Noble Gases in Geochemistry and Cosmochemistry: Reviews in Mineralogy and Geochemistry, 47, pp. 319–370.

Hirsch, D. M., Prior, D. J., Carlson, W. D., 2003. An overgrown model to explain multiple dispersed high-Mn regions in the cores of garnet porphyroblasts. American Mineralogist 88, 131-141.

Hodges, K. V., Crowley, P. D., 1985. Error estimation in empirical geothermometry and geobarometry for pelitic systems. American Mineralogist 70, 702-709.

Hodges, K. V., Spear F. S., 1982. Geothermometry, geobarometry and the Al2SiO5 triple point at Mt Mooslanke, New Hampshire. American Mineralogist 67, 1118-1134.

Holdaway, M. J., 2000. Application of new experimental and garnet Margules data to the garnet-biotite geothermometer. American Mineralogist 85, 881-892.

Holland, T. J. B., Baker, J., Powell, R., 1998. Mixing properties and activity-composition relationships of chlorites in the system MgO-FeO-Al_2O_3-SiO_2-H_2O. European Journal of Mineralogy 10, 395-406.

Holland, T. J. B., Powell, R., 1996. Thermodynamics of order-disorder in minerals. 2. Symmetric formalism applied to solid solutions. American Mineralogist 81, 1425-37.

Holland, T. J. B., Powell, R., 1998. An internally consistent thermodynamic data set for phases of petrological interest. Journal of Metamorphic Geology 16, 309-343.

Holland, T. J. B., Powell, R., 2001. Calculation of phase relations involving haplogranitic melts using an internally consistent thermodynamic dataset. Journal of Petrology 42, 673-83.

Holland, T. J. B., Powell, R., 2003. Activity-composition relations for phases in petrological calculations: an asymmetric multicomponent formulation. Contributions to Mineralogy and Petrology 145, 492–501.

Hollister, L. S., 1966. Garnet zoning: an interpretation based on the Rayleigh fractionation model. Science 154, 1647-1651.

Holub, F.J., 1997. Ultrapotassic plutonic rocks of the durbachite series in the Bohemian Massif: Petrology, geochemistry and petrogenetic interpretation. Sborník geologických věd, Ložisková geologie - mineralogie. 31, pp. 5–26.

Holub, F.V., Munshi, R.L., 1984. Subsolidus reaction rims between olivine and calcic plagioclase in the Svatý Kříž Massif, eastern Bohemia. Krystalinikum 17, 47–58.

Hoshide, T., Obata, M., 2014. Spinel inclusions in olivine and plagioclase crystals in a layered gabbro: a marker and a tracer for primary phenocrysts in a differentiating magma reservoir. Contributions to Mineralogy and Petrology 168. http://dx.doi.org/10.1007/s00410-014-1049-8.

Jackson, S.E., Pearson, N.J., Griffin, W.L., Belousova, E.A., 2004. The application of laser ablation-inductively coupled plasma-mass spectrometry to in situ U–Pb zircon geochronology. Chemical Geology 211, 47–69.

Jakeš, P., 1997. Melting in high-P region-case of Bohemian granulites. Acta Universitatis Carolinae. Geologica 41, 113-125.

Jamtveit, B., Wogelius, R. A., Fraser, D. G., 1993. Zonation patterns of skarn garnets: Records of hydrothermal system evolution. Geology 21, 113-116.

Janák, M., Cornell, D., Frotzheim, N., de Hoog, C.J., Broska, I., Vrabec, M., Hurai, V., 2009. Eclogite-hosting metapelites fromthe Pohorje Mountains (Eastern Alps): P–T evolution, zircon geochronology and tectonic implications. European Journal of Mineralogy 21, 1191–1212.

Janoušek, V., Finger, F., Roberts, M. P., Frýda, J., Pin, C., Dolejš, D., 2004. Deciphering petrogenesis of deeply buried granites: whole-rock geochemical constraints on the origin of largely undepleted felsic granulites from the Moldanubian Zone of the Bohemian Massif. Transactions of the Royal Society of Edinburgh, Earth Sciences 95, 141-154.

Janoušek, V., Holub, F.V., 2007. The causal link between HP-HT metamorphism and ultrapotassic magmatism in collisional orogens: case study from the Moldanubian Zone of the Bohemian Massif. Proceedings of the Geologists Association 118, 75–86.

Jastrzębski, M., 2009. A Variscan continental collision of the West Sudetes and the Brunovistulian terrane: a contribution from structural and metamorphic record of the Stronie Formation, the Orlica-Śnieżnik Dome, SW Poland. International Journal of Earth Sciences 98, 1901–1923.

Jastrzębski, M., Żelaźniewicz, A., Nowak, I., Murtezi, M., Larionov, A. N., 2010. Protolith age and provenance of metasedimentary rocks in Variscan allochthon units: U-Pb SHRIMP zircon data from the Orlica-Snieznik Dome, West Sudetes. Geological Magazine 147, 416-433.

Jedlicka, R., Faryad, S.W., Hauzenberger, C., 2015. Prograde metamorphic history of UHP granulites from the Moldanubian Zone (Bohemian Massif) revealed by major element and Y + REE zoning in garnets. Journal of Petrology 56, 2069–2088.

Jochum, K. P., Weis, U., Stoll, B., Kuzmin, D., Yang, Q., Raczek, I., Jacob, D. E., Stracke, A., Birbaum, K., Frick, D. A., Günther, D., Enzweiler, J., 2011. Determination of Reference Values for NIST SRM 610–617 Glasses Following ISO Guidelines. Geostandards and Geoanalytical Research 35, 397-429.

Jochum, K. P., Willbold, M., Raczek, I., Stoll, B., Herwig, K., 2005. Chemical characterisation of the USGS reference glasses GSA-1G, GSC-1G, GSD-1G, GSE-1G, BCR-2G, BHVO-2G and BIR-1G using EPMA, ID-TIMS, ID-ICP-MS and LA-ICP-MS. Geostandards and Geoanalytical Research 29(3), 285–302.

Kawakami, T., Hokada, T., 2010. Linking P-T path with development of discontinuous phosphorus zoning in garnet during high-temperature metamorphism - an example from Lützow-Holm Complex, East Antarctica. Journal of Mineralogical and Petrological Sciences 105, 175-186.

Kent, A.J.R., 2008. Melt inclusions in basaltic and related volcanic rocks. Reviews in Mineralogy and Geochemistry 69, 273–331.

Kinzler, R.J., Grove, T.L., 1992. Primary magmas of mid-ocean ridge basalts. 1. Experiments and methods. Journal of Geophysical Research - Solid Earth 97, 6885–6906.

Klápová, H., Konopásek, J., Schulmann, K., 1998. Eclogites from the Czech part of the Erzgebirge: multistage metamorphic and structural evolution. Journal of the Geological Society 155, 567–583.

Klemd, R., Bröcker, M., 1999. Fluid influence on mineral reactions in ultrahigh-pressure granulites: a case study in the Snieznik Mts. (West Sudetes, Poland). Contributions to Mineralogy and Petrology 136, 358–373.

Klemd, R., Bröcker, M., Schramm, J., 1995. Characterization of amphibolite-facies fluids of Variscan eclogites from the Orlica-Śnieżnik Dome (Sudetes, SW Poland). Chemical Geology 119, 101–113.

Klemme, S., O'Neill, H.S.C., 2000. The effect of Cr on the solubility of Al in orthopyroxene: experiments and thermodynamic modelling. Contributions to Mineralogy and Petrology 140, 85–98.

Kobayashi, T., Hirajima, T., Kawakami, T., Svojtka, M., 2011. Metamorphic history of garnet-rich gneiss at Ktiš in the Lhenice shear zone, Moldanubian Zone of the

southern Bohemian Massif, inferred from inclusions and compositional zoning of garnet. Lithos 124, 46–65.

Kohn M. J., Spear, F., 2000. Retrograde net transfer reaction insurance for pressure-temperature estimates. Geology 28, 1127–1130.

Konrad-Schmolke, M., O´Brien, P. J., De Capitani, C., Carswell, D. A., 2008a. Garnet growth at high- and ultra-high pressure conditions and the effect of element fractionation on mineral modes and composition. Lithos 103, 309-332.

Konrad-Schmolke, M., Zack, T., O´Brien, P. J., Jacob, D. E., 2008b. Combined thermodynamic and rare earth element modelling of garnet growth during subduction: Examples from ultrahigh-pressure eclogite of the Western Gneiss Region, Norway. Earth and Planetary Science Letters 272, 488-498.

Konzett, J., Frost, D., 2009. The High P-T Stability of Hydroxyl-apatite in Natural and Simplified MORB – an Experimental Study to 15 GPa with Implications for Transport and Storage of Phosphorus and Halogens in Subduction Zones. Journal of Petrology 50, 2043-2062.

Košler, J., Konopásek, J., Sláma, J., Vrána, S., 2014. U–Pb zircon provenance of Moldanubian metasediments in the Bohemian Massif. Journal of the Geological Society of London 171, 83–95.

Kotková, J., 2007. High-pressure granulites of the Bohemian Massif: recent advances and open questions. Journal of Geosciences 52, 45-71.

Kotková, J., Harley, S. L., 1999. Formation and evolution of high-pressure leucogranulites: experimental constraints and unresolved issues. Physics and Chemistry of the Earth, Part A-Solid Earth 24, 299-304.

Kotková, J., Harley, S. L., 2010. Anatexis during High-pressure Crustal Metamorphism: Evidence from Garnet-Whole-rock REE Relationships and Zircon-Rutile Ti-Zr Thermometry in Leucogranulites from the Bohemian Massif. Journal of Petrology 51, 1967-2001.

Kotková, J., Harley, S. L., Fišera, M., 1997. A vestige of very high-pressure (ca. 28 kbar) metamorphism in the Variscan Bohemian Massif, Czech Republic. European Journal of Mineralogy 9, 1017–1033.

Kotková, J., O'Brien, P., Ziemann, M., 2011. Diamond and coesite discovered in Saxony type granulite: solution to the Variscan garnet peridotite enigma. Geology 39, 667–670.

Kotková, J., Schaltegger, U., Leichmann, J., 2010. Two types of ultrapotassic plutonic rocks in the Bohemian Massif — coeval intrusions at different crustal levels. Lithos 115, 163–176.

Koziol, A. M., 1989. Recalibration of the garnet-plagioclase-Al2SiO5-quartz (GASP) geobarometer and applications for natural parageneses. EOS Transactions, American Geophysical Union 70, 493.

Koziol, A. M., Newton, R. C., 1988. Redetermination of the anorthite breakdown reaction and improvement of the plagioclase-garnet-Al2SiO5-quartz geobarometer. American Mineralogist 73, 216-223.

Kroner, U., Romer, R. L., 2010. The Saxo-Thuringian Zone — tip of the Armorican Spur and part of the Gondwana plate. In: Linnemann, U., Romer, R.L. (Eds.), Pre-Mesozoic Geology of Saxo-Thuringia — From the Cadomian Active Margin to the Variscan Orogen. Schweizerbart, Stuttgart, pp. 371–394.

Kröner, A., Hegner, E., 1998. Geochemistry, single zircon ages and Sm-Nd systematics of granitoid rocks from the Gory Sowie (Owl Mts), Polish west Sudetes: evidence for early Palaeozoic arc-related plutonism. Journal of the Geological Society 155, 711-724.

Kröner, A., Jaeckel, P., Hegner, E., Opletal, M., 2001. Single zircon ages and whole rock Nd isotopic systematics of early Palaeozoic granitoid gneisses from the Czech and Polish Sudetes (Jizerské hory, Krkonoše Mountains and Orlice-Sněžník Complex). International Journal of Earth Sciences 90, 304–324.

Kröner, A., O'Brien, P., Nemchin, A., Pidgeon, R.T., 2000. Zircon ages for high pressure granulites from South Bohemia, Czech Republic, and their connection to carboniferous high temperature processes. Contributions to Mineralogy and Petrology 138, 127–142.

Kröner, A., Willner, A. P., 1998. Time of formation and peak of Variscan HP–HT metamorphism of quartz-feldspar rocks in the central Erzgebirge, Saxony, Germany. Contributions to Mineralogy and Petrology 132, 1–20.

Krs, M., Krsová, M., Pruner, P., 1995. Palaeomagnetism and palaeogeography of Variscan formations of the Bohemian Massif, comparison with other regions in Europe. Studia Geophysica et Geodaetica 39, 309–319.

Kryza, R., 1981. Migmatization in gneisses of northern part of the Sowie Góry. Geologia Sudetica 16, 7-100.

Kryza, R., Mazur, S., Pin, C., 2003. Subduction- and non-subduction-related igneous rocks in the central European variscides: geochemical and Nd isotope evidence from the Klodzko Metamorphic Complex, Polish Sudetes. Geodinamica Acta 16, 39-57.

Kryza, R., Pin, C., 2010. The Central-Sudetic ophiolites (SW Poland): petrogenetic issues, geochronology and palaeotectonic implications. Gondwana Research 17, 292–305.

Kryza, R., Pin, C., Vielzeuf, D., 1996. High-pressure granulites from the Sudetes (south-west Poland): evidence of crustal subduction and collisional thickening in the Variscan Belt. Journal of Metamorphic Geology 14, 531–546.

Kryza, R., Willner, A. P., Massonne, H. J., Muzsynski, A., Schertel, H. P., 2011. Blueschistfacies metamorphism in the Kaczawa Mountains (Sudetes, SW Poland) of the Central-European Variscides: P–T constraints from a jadeite-bearing metatrachyte. Mineralogical Magazine 75, 241–263.

Kusiak, M.A., Dunkley, D.J., Suzuki, K., Kachlík, V., Kedzior, A., Lekki, J., Opluštil, S., 2010. Chemical (non-isotopic) and isotopic dating of Phanerozoic zircon — a case study of durbachite from the Třebíč Pluton, Bohemian Massif. Gondwana Research 17, 153–161.

Lang, H.M., Gilotti, J.A., 2007. Partial melting of metapelites at ultrahigh pressure conditions, Greenland Caledonides. Journal of Metamorphic Geology 25, 129–147.

Lange, U., Bröcker, L., Armstrong, R., Trapp, E., Mezger, K., 2005. Sm–Nd and U–Pb dating of high-pressure granulites from the Złote and Rychleby Mts (Bohemian Massif, Poland and Czech Republic). Journal of Metamorphic Geology 23, 133–145.

Lange, U., Bröcker, M., Trapp, E., 2003. The high - pressure granulites of the Zlote Unit: Sm - Nd and single grain U - Pb zircon ages from the Rychleby Mts. Journal of the Czech Geological Society 48, 1–2.

Lanzirotti, A., 1995. Yttrium zoning in metamorphic garnets. Geochimica Cosmochimica Acta 59, 4105-4110.

Leake, B.E., Woolley, A.R., Birch, W.D., Burke, E.A.J., Ferraris, G., Grice, J.D., Hawthorne, F.C., Kisch, H.J., Krivovichev, V.G., Schumacher, J.C., Stephenson, N.C.N., Whittaker, E.J.W., 2003. Nomenclature of amphiboles: additions and revisions to the International Mineralogical Association's amphibole nomenclature. The Canadian Mineralogist 41, 1355–1370.

Lexa, O., Schulmann, K., Janoušek, V., Štípská, P., Guy, A., Racek, M., 2011. Heat sources and Trigger mechanisms of exhumation of HP granulites in Variscan orogenic root. Journal of Metamorphic Geology 29 (1), 79–102.

Lexa, O., Štípská, P., Schulmann, K., Baratoux, L., Kröner, A., 2005. Contrasting textural record of two distinct metamorphic events of similar P-T conditions and different durations. Journal of Metamorphic Geology 23, 649-666.

Linnemann, U., Romer, R.L., Gerdes, A., Jeffries, T.E., Drost, K., Ulrich, J., 2010. The Cadomian orogeny in the Saxo-Thuringian Zone. In: Linnemann, U., Romer, R.L. (Eds.), Pre-Mesozoic Geology of Saxo-Thuringia — From the Cadomian Active Margin to the Variscan Orogen. Schweizerbart, Stuttgart, pp. 37–58.

Liou, J.G., Ernst, W.G., Zhang, R.Y., Jahn, B.M., 2009. Ultrahigh-pressure minerals and metamorphic terranes - the view from China. Journal of Asian Earth Sciences 35, 199–231.

Liu, J.B., Ye, K., Maruyama, S., Cong, B.L., Fan, H.R., 2001. Mineral inclusions in zircon from gneisses in the ultrahigh pressure zone of the Dabie Mountains, China. Journal of Geology 109, 523–535.

Longhi, J., Vander Auwera, J., Fram, M.S., Duchesne, J.C., 1999. Some phase equilibrium constraints on the origin of Proterozoic (massif) anorthosites and related rocks. Journal of Petrology 40, 339–362.

Ludwig, K.R., 2008. Isoplot 3.70. A geochronological toolkit for Microsoft Excel. Berkeley Geochronology Center Special Publication 4 (77 p). Maaloe, S., 1978. Origin of rhytmic layering. Mineralogical Magazine 42, 337–345.

Machart, J., 1984. Ultramafic rocks in the Bohemian part of Moldanubicum and the Central Bohemian Islet Zone (Bohemian Massif). Krystalinikum 17, 13–32.

Malaspina, N., Hermann, J., Scambelluri, M., Compagnoni, R., 2006. Polyphase inclusions in garnet–orthopyroxenite (Dabie Shan, China) as monitors for metasomatism and fluid related trace element transfer in subduction zone peridotite. Earth and Planetary Science Letters 249, 173–187.

Manning, C.E., 2004. The chemistry of subduction-zone fluids. Earth and Planetary Science Letters 223, 1–16.

Massonne, H.J., Bautsch, H.J., 2004. Ultrahigh and high pressure rocks of Saxony. Field Trip Guide Books. 32nd Int. Geol. Congress, Florence, Italy, vol. 2, p. B21.

Massonne, H.J., Koppe, J., 2005. A low-variance mineral assemblage with talc and phengite in an eclogite from the Saxonian Erzgebirge, central Europe, and its P–T evolution. Journal of Petrology 46, 355–375.

Massonne, H.J., O'Brien, P.J., 2003. The Bohemian Massif and the NW Himalaya. In: Carswel, D.A., Compagnoni, R. (Eds.), Ultrahigh Pressure Metamorphism. EMU Notes in Mineralogy, pp. 145–187.

Matte, P., 1986. Tectonic and plate tectonic model for the Variscan belt of Europe. Tectonophysics 126, 329–374.

Matte, P., 2001. The Variscan collage and orogeny (480–290 Ma) and the tectonic definition of the Armorica microplate: a review. Terra Nova 13, 122–128.

Matte, P., Maluski, H., Rajlich, P., Franke, W., 1990. Terrane boundaries in the Bohemian Massif: results of large-scale Variscan shearing. Tectonophysics 177, 151-170.

Mazur, S., Alexandrowski, 2001. The Tepla(?)/Saxothuringian suture in the Karkonosze– Izera massif, western Sudetes, central European Variscides. International Journal of Earth Sciences 90, 341–360.

Mazur, S., Alexandrowski, P., Kryza, R., Oberc-Dziedzic, T., 2006. The Variscan Orogen in Poland. Geological Quarterly 50, 89–118.

Mazur, S., Aleksandrowski, P., Szczepański, J., 2005. The presumed Teplá-Barrandian/ Moldanubian terrane boundary in the Orlica Mountains (Sudetes, Bohemian Massif): structural and petrological characteristics. Lithos 82, 85–112.

Mazur, S., Szczepański, J., Turniak, K., McNaughton, N.J., 2012. Location of the Rheic suture in the eastern Bohemian Massif: evidence from detrital zircon data. Terra Nova 24, 199-206.

Medaris Jr., L.G., Ackerman, L., Jelínek, E., Michels, Z.D., Erban, V., Kotková, J., 2015. Depletion, cryptic metasomatism, and modal metasomatism (refertilization) of Variscan lithospheric mantle: evidence from major elements, trace elements, and Sr-Nd-Os isotopes in a Saxothuringian garnet peridotite. Lithos 226, 81–97.

Medaris, L. G., Beard, B. L., Jelínek, E., 2006. Mantle-derived, UHP garnet pyroxenite and eclogite in the Moldanubian Gföhl Nappe, Bohemian Massif: a geochemical review, new P-T determinations and tectonic interpretation. International GeologyReview 48, 765–777.

Medaris, L.G., Fournelle, J.H., Ghent, E.D., Jelínek, E., Mísař, Z., 1998. Prograde eclogite in the Gföhl Nappe, Czech Republic: new evidence on Variscan high-pressure metamorphism. Journal of Metamorphic Geology 16, 563–576.

Medaris, L. G., Jelínek, E., Mísař, Z., 1995. Czech eclogites - Terrane settings and implications for variscan tectonic evolution of the Bohemian Massif. European Journal of Mineralogy 7, 7-28.

Medaris, L.G., Wang, H., Jelínek, E., Mihaljevič, M., Jakeš, P., 2005. Characteristics and origins of diverse Variscan peridotites in the Gföhl Nappe, Bohemian Massif, Czech Republic. Lithos 82, 1–23.

Medaris, L.G., Wang, H.F., Mísař, Z., Jelínek, E., 1990. Thermobarometry, diffusion modelling and cooling rates of crustal garnet peridotites: two examples from the Moldanubian zone of the Bohemian Massif. Lithos 25, 189–202.

Mints, M.V., 2015. Granulite-gneiss belt: a special type of tectonic structure, the uniqueness of which is not limited to high-grade metamorphism. Geological Society of America Special Papers 510, 329–332.

Miyashiro, A., 1994. Metamorphic Petrology. UCL press, London. Morse, S.A., 1980. Kiglapait mineralogy. 2. Fe–Ti oxide minerals and the activities of oxygen and silica. Journal of Petrology 21, 685–719.

Moore, S. J., Carlson, W. D., Hesse, M. A., 2013. Origins of yttrium and rare earth element distributions in metamorphic garnet. Journal of Metamorphic Geology 31, 663-689.

Munshi, R.L., 1981. Petrology of gabro amphibolite complex, Ronov-Moravany Area, eastern Bohemia. Acta Universitatis Carolinae, Geologica 1, 19–33.

Naemura, K., Ikuta, D., Kagi, H., Odake, S., Ueda, T., Ohi, S., Kobayashi, T., Svojtka, M., Hirajima, T., 2011. Diamond and other possible ultradeep evidence discovered in the orogenic spinel-garnet peridotite from the Moldanubian Zone of the Bohemian Massif, Czech Republic. In: Dobrzhinetskaya, L., Faryad, S.W., Wallis, S., Cuthbert, S. (Eds.), Ultrahigh Pressure Metamorphism: 25 Years After the Discovery of Coesite and Diamond. Elsevier, pp. 77–111.

Nahodilová, R., Faryad, S. W., Dolejš, D., Tropper, P., Konzett, J., 2011. High-pressure partial melting and melt loss in felsic granulites in the Kutná Hora complex, Bohemian Massif (Czech Republic). Lithos 125, 641-658.

Nahodilová, R., Štípská, P., Powell, R., Košler, J., Racek, M., 2014. High-Ti muscovite as a prograde relict in high pressure granulites with metamorphic Devonian zircon

ages (Běstvina granulite body, Bohemian Massif): Consequence for the relamination model of subducted crust. Gondwana Research 25, 630-648.

Nakamura, D., Svojtka, M., Naemura, K., Hirajima, T., 2004. Very-high-pressure (>4 GPa) eclogites associated with the Moldanubian Zone garnet peridotite (Nové Dvory, Czech Republic). Journal of Metamorphic Geology 22, 593–603.

Nasdala, L., Massonne, H.-J., 2000. Microdiamonds from the Saxonian Erzgebirge, Germany: in situ micro-Raman characterisation. European Journal of Mineralogy 12, 495–498.

Newton, R. C., Charlu, T. V., Kleppa, O. J., 1980. Thermochemistry of the high structural state plagioclases. Geochemica Cosmochemica Acta 44, 933-41.

Nickel, K. G., 1986. Phase equilibria in the system SiO2–MgO–Al2O3–CaO–Cr2O3 (SMACCR) and their bearing on spinel/garnet lherzolite relationships. Neues Jahrbuch für Mineralogie (Abhandlungen) 155, 259–287.

Obata, M., Hirajima, T., Svojtka, M., 2006. Origin of eclogite and garnet pyroxenite from the Moldanubian Zone of the Bohemian Massif, Czech Republic and its implication to other mafic layers embedded in orogenic peridotites. Mineralogy and Petrology 88, 321–340.

O'Brien, P. J., 1997. Garnet zoning and reaction textures in overprinted eclogites, Bohemian Massif, European variscides: a record of their thermal history during exhumation. Lithos 41, 119–133.

O'Brien, P. J., 2008. Challenges in high-pressure granulite metamorphism: reaction textures, compositional zoning, ages and tectonic interpretation with examples from the Bohemian Massif. Journal of Metamorphic Geology 26, 235–251.

O'Brien, P. J., Carswell, D.A., 1993. Tectonometamorphic evolution of the Bohemian Massif: evidence from high pressure metamorphic rocks. Geologische Rundschau 82, 531–555.

O'Brien, P. J., Kröner, A., Jaeckel, P., Hegner, E., Żelaźniewicz, A., Kryza, R., 1997. Petrological and isotopic studies on Palaeozoic high pressure granulites with a medium pressure overprint, Góry Sowie (Owl) Mts., Polish Sudetes. Journal of Petrology 38, 433–456.

O'Brien, P. J., Vrána, S., 1995. Eclogites with a short-lived granulite facies overprint in the Moldanubian Zone, Czech Republic: petrology, geochemistry and diffusion modelling of garnet zoning. Geologische Rundschau 84, 473–488.

O'Driscoll, B., Donaldson, C.H., Daly, J.S., Emeleus, C.H., 2009. The roles of melt infiltration and cumulate assimilation in the formation of anorthosite and a Cr-spinel seamin the Rum Eastern Layered Intrusion, NW Scotland. Lithos 111, 6–20.

Olivier, G. J. H., Corfu, F., Krogh, T. E., 1993. U - Pb ages from SW Poland: evidence for a Caledonian suture zone between Baltica and Gondwana. Journal of the Geological Society London 150, 335–369.

O'Neill, H.S.C., 1981. The transition between spinel lherzolite and garnet lherzolite, and its use as a geobarometer. Contributions to Mineralogy and Petrology 77, 185–194.

Oncken, O., Hindle, D., Kley, J., Elger, K., Victor, P., Schemmann, K., 2007. Deformation of the central Andean upper plate system — facts, fiction, and constraints for plateau models. In: Oncken, O., et al. (Ed.), The Andes — Active Subduction Orogeny. Springer, pp. 3–27.

Osborn, E.F., Tait, D.B., 1952. The system diopside forsterite anorthite. American Journal of Science 250, 413–433.

Otamendi, J. E., de la Rosa, J. D., Patiño Douce, A. E., Castro, A., 2002. Rayleigh fractionation of heavy rare earths and yttrium during metamorphic garnet growth. Geology 30, 159-162.

Parry, M., Štípská, P., Schulmann, K., Hrouda, F., Ježek, J., Kröner, A., 1997. Tonalite sill emplacement at an oblique plate boundary: northeastern margin of the Bohemian Massif. Tectonophysics 280, 61-81.

Paton, C., Woodhead, J.D., Hellstrom, J.C., Hergt, J.M., Greig, A., Maas, R., 2010. Improved laser ablation U–Pb zircon geochronology through robust downhole fractionation correction. Geochemistry, Geophysics, Geosystems 11, Q0AA06. http://dx.doi.org/ 10.1029/2009GC002618.

Perchuk, A. L., Burchard, M., Maresch, W.V., Schertl, H.-P., 2008. Melting of hydrous and carbonate mineral inclusions in garnet host in ultrahigh pressure experiments. Lithos 103, 25–45.

Perchuk, L. L., Lavrent'eva, L. Y., 1983. Experimental investigation of exchange equilibria in the system cordierite–garnet–biotite. In: Saxena, S. K. (ed.) Kinetics and Equilibrium in Mineral Reactions. Advances in Physical Geochemistry 3, 199-239.

Perraki, M., Faryad, S. W., 2014. First finding of microdiamond, coesite and other UHP phases in felsic granulites in the Moldanubian Zone: Implications for deep

subduction and a revised geodynamic model for Variscan Orogeny in the Bohemian Massif. Lithos 202-203, 157-166.

Peřestý, V., Lexa, O., Holder, R., Jeřábek, P., Racek, M., Štípská, P., Schulmann, K., Hacker, B., 2016. Metamorphic inheritance of Rheic passive margin evolution and its early-Variscan overprint in the Tepla-Barrandian Unit, Bohemian Massif. Journal of Metamorphic Geology, DOI: 10.1111/jmg.12234.

Petrus, J.A., Kamber, B.S., 2012. VizualAge: a novel approach to laser ablation ICP-MS U–Pb geochronology data reduction. Geostandards and Geoanalytical Research 36, 247–270.

Philippot, P., 1993. Fluid–melt±rock interaction in mafic eclogites and coesite-bearing metasediments: constraints on volatile recycling during subduction. Chemical Geology 108, 93–112.

Pouba, Z., Fiala, J., Paděra, K., 1987. The granulite body near Běstvina in the Železné Hory Mts. Časopis pro Mineralogy a Geology 32, 73-78.

Pouba, Z., Paděra, K., Fiala, J., 1985. Omphacite granulite from the NE margin area of the Bohemian Massif (Rychleby Mts.). Neues Jahrbuch für Mineralogie, Abhandlungen 151, 29–52.

Powell, R., Holland, T. J. B., 1999. Relating formulations of the thermodynamics of mineral solid solutions: Activity modelling of pyroxenes, amphiboles, and micas. American Mineralogist 84, 1-14.

Powell, R., Holland, T., Worley, B., 1998. Calculating phase diagrams involving solid solutions via non-linear equations, with examples using THERMOCALC. Journal of Metamorphic Geology 16, 577-588.

Presnall, D.C., Dixon, S.A., Dixon, J.R., Odonnell, T.H., Brenner, N.L., Schrock, R.L., Dycus, D.W., 1978. Liquidus phase relations on join diopside-forsterite-anorthite from 1 atm to 20 kbar – their bearing on generation and crystallization of basaltic magma. Contributions to Mineralogy and Petrology 66, 203–220.

Prince, C. I., Košler, J., Vance, D., Günther, D., 2000. Comparison of laser ablation ICP-MS and isotope dilution REE analyses-implications for Sm-Nd garnet geochronology. Chemical Geology 168, 255-274.

Proyer, A., 2003. The preservation of high pressure rocks during exhumation: metagranites and metapelites. Lithos 70, 183-194.

Pyle, J. M., Spear, F. S., 1999. Yttrium zoning in garnet: Coupling of major and accessory phases during metamorphic reactions. Geological Materials Research 1, 1-49.

Ravna, E.J.K., 2000. The garnet–clinopyroxene Fe^{2+}–Mg geothermometer: an updated calibration. Journal of Metamorphic Geology 18, 211–219.

Sadofsky, S. J., Bebout, G. E., 2003. Record of forearc devolatilization in low-T, high-P/T metasedimentary suites: significance for models of convergent margin chemical cycling. Geochemistry, Geophysics, Geosystems 4 (4), 9003, http://dx.doi.org/10.1029/2002GC000412.

Sajeev, K., Windley, B. F., Hegner, E., Komiya, T., 2012. High-temperature, high-pressure granulites (retrograde eclogites) in the central region of the Lewisian, NW Scotland: crustal-scale subduction in the Neoarchean. Gondwana Research, http://dx.doi.org/10.1016/j.gr.2012.05.002.

Schaltegger, U., Schmitt, A.K., Horstwood, M.S.A., 2015. U–Th–Pb zircon geochronology by ID-TIMS, SIMS, and laser ablation ICP-MS: Recipes, interpretations, and opportunities. Chemical Geology 402, 89–110.

Schellart, W.P., Rawlinson, N., 2010. Convergent platemargin dynamics: newperspectives from structural geology, geophysics and geodynamicmodelling. Tectonophysics 483, 4–19.

Schmädicke, E., Okrusch, M., Schmidt, W., 1992. Eclogite-facies rocks in the Saxonian Erzgebirge, Germany: high pressure metamorphism under contrasting P–T conditions. Contributions to Mineralogy and Petrology 110, 226–241.

Schmädicke, E., Gose, J., Will, T.M., 2010. The P-T evolution of ultra high temperature garnet-bearing ultramafic rocks from the Saxonian Granulitgebirge Core Complex, Bohemian Massif. Journal of Metamorphic Geolology 28, 489–508.

Schmidt, M.W., Poli, S., 1998. Experimentally based water budgets for dehydrating slabs and consequences for arc magma generation. Earth and Planetary Science Letters 163, 361–379.

Schovánek, P., 1977. Petrography of selected ultramafic rocks from the Bohemian Massif and chemical composition of their minerals. Unpulished Phd thesis, Faculty of Sciences, Charles University, Prague, p. 256.

Schulmann, K., Gayer, R., 2000. A model for a continental accretionary wedge developed by oblique collision: the NE Bohemian Massif. Journal of the Geological Society 157, 401-416.

Schulmann, K., Konopásek, J., Janoušek, V., Lexa, O., Lardeaux, J. M., Edel, J. B., Štípská, P., Ulrich, S., 2009. An Andean type Palaeozoic convergence in the Bohemian Massif. Comptes Rendus Geosciences 341, 266–286.

Schulmann, K., Kröner, A., Hegner, E., Wendt, I., Konopásek, J., Lexa, O., Štípská, P., 2005. Chronological constraints on the pre-orogenic history, burial and exhumation of deep-seated rocks along the eastern margin of the Variscan Orogen, Bohemian Massif, Czech Republic. American Journal of Science 305, 407-448.

Schulmann, K., Lexa, O., Štípská, P., Racek, M., Tajčmanová, L., Konopásek, J., Edel, J. B., Peschler, A., Lehmann, J., 2008. Vertical extrusion and horizontal channel flow of orogenic lower crust: key exhumation mechanisms in large hot orogens? Journal of Metamorphic Geology 26, 273–297.

Schwandt, C. S., Papike, J. J., Shearer, C. K., 1996. Trace element zoning in pelitic garnet of the Black Hills, South Dakota. American Mineralogist 81, 1195-1207.

Scott, J. M., Konrad-Schmolke, M., O'Brien, P. J., Günter, C., 2013. High-T, low-P formation of rare olivine-bearing symplectites in Variscan eclogite. Journal of Petrology 54, 1375–1398.

Sempere, T., Folguera, A., Gerbault, M., 2008. New insights into Andean evolution: an introduction to contributions from the 6th ISAG symposium (Barcelona, 2005). Tectonophysics 459, 1–13.

Seston, R., Winchester, J.A., Piasecki, M.A.J., Crowley, Q.G., Floyd, P.A., 2000. A structural model for the western-central Sudetes: a deformed stack of Variscan thrust sheets. Journal of the Geological Society of London 157, 1155–1167.

Shimizu, N., 1998. The geochemistry of olivine-hosted melt inclusions in a FAMOUS basalt ALV519-4-1. Physics of the Earth and Planetary Interiors 107, 183–201.

Skora, S., Baumgartner, L. P., Mahlen, N. J., Johnson, C. M., Pilet, S., Hellebrand, E., 2006. Diffusion-limited REE uptake by eclogite garnets and its consequences for Lu-Hf and Sm-Nd geochronology. Contributions to Mineralogy and Petrology 152, 703-720.

Sláma, J., Košler, J., Condon, D.J., Crowley, J.L., Gerdes, A., Hanchar, J.M., Horstwood, M.S.A., Morris, G.A., Nasdala, L., Norberg, N., Schaltegger, U., Schoene, B., Tubrett, M.N., Whitehouse, M.J., 2008. Plešovice zircon — a new natural reference material for U–Pb and Hf isotopic microanalysis. Chemical Geology 249, 1–35.

Slater, L., McKenzie, D., Gronvold, K., Shimizu, N., 2001. Melt generation and movement beneath Theistareykir, NE Iceland. Journal of Petrology 42, 321–354.

Smith, A.D., 2003. Critical evaluation of Re–Os and Pt–Os isotopic evidence on the origin of intraplate volcanism. Journal of Geodynamics 36, 469–484.

Sobolev, A.V., 1996. Melt inclusions as a source of primary petrographic information. Petrology 4, 209–220.

Sobolev, N.V., Chopin, C., 1995. Principal mineralogic indicator of UHP in crustal rocks. In: Coleman, R.G., Wang, X. (Eds.), Ultra-High-Pressure Metamorphism. Cambridge Univ. Press, Cambridge, UK, pp. 96–131.

Spear, F. S., 1988. Thermodynamic projection and extrapolation of high-variance mineral assemblages. Contributions to Mineralogy and Petrology 98, 346-351.

Spear, F. S., Kohn, M. J., 1996. Trace element zoning in garnet as a monitor of crustal melting. Geology 24, 1099-1102.

Steltenpohl, M. G., Cymerman, Z., Krogh, E. J., Kunk, M. J., 1993. Exhumation of eclogitized continental basement during Variscan lithospheric delamination and gravitational collapse, Sudety Mountains, Poland. Geology 21, 1111–1114.

Strnad L., Mihaljevič M., Šebek O., 2005. Laser ablation and solution ICP-MS determination of REE in USGS BIR-1G, BHVO-2G and BCR-2G glass reference materials. Geostandards and Geoanalytical Research 29, 303-314.

Stüwe, K., 1997. Effective bulk composition changes due to cooling: a model predicting complexities in retrograde reaction textures. Contributions to Mineralogy and Petrology 129, 43-52.

Svensen, H., Jamtveit, B., Banks, D.A., Austrheim, H., 2001. Halogen contents of eclogites facies fluid inclusions and minerals: Caledonides, western Norway. Journal of Metamorphic Geology 19, 165–178.

Synek, J., Oliveriová, D., 1993. Terrane character of the northeast margin of the Moldanubian Zone - the Kutná Hora crystalline complex, Bohemian Massif. Geologische Rundschau 82, 566-582.

Szczepański, J., Anczkiewicz, R., Mazur, S., Thirlwall, M., 2004. Constrains on timing of ultra-high pressure metamorphism in the Orlica-Śnieźnik Dome, West Sudetes. Mineralogical Society of Poland, Special Papers 24, 365–368.

Štědrá, V., Nahodilová, R., 2009. High-pressure metabasic rocks from the Kutna Hora Complex: geological position and petrology of exotic lithologies along the segmented Moldanubian margin, Bohemian Massif. Journal of Geosciences 54, 135–157.

Štípská, P., Powell, R., 2005. Constraining the P–T path of a MORB-type eclogite using pseudosections, garnet zoning and garnet-clinopyroxene thermometry: an example from the Bohemian Massif. Journal of Metamorphic Geology 23, 725-743.

Štípská, P., Chopin, F., Skrzypek, E., Schulmann, K., Pitra, P., Lexa, O., Martelat, J. E., Bollinger, C., Žáčková, E., 2012. The juxtaposition of eclogite and mid-crustal rocks in the Orlica–Śnieżnik Dome, Bohemian Massif. Journal of Metamorphic Geology 30, 213-234.

Štípská, P., Schulmann, K., Kröner, A., 2004. Vertical extrusion and middle crustal spreading of omphacite granulite: a model of syn-convergent exhumation (Bohemian Massif, Czech Republic). Journal of Metamorphic Geology 22, 179–198.

Štípská, P., Schulmann, K., Thompson, A. B., Ježek, J., Kröner, A., 2001. Thermo-mechanical role of a Cambro-Ordovician paleorift during the Variscan collision: the NE margin of the Bohemian Massif. Tectonophysics 332, 239-253.

Tagiri, M., Yano, T., Barikov, A., Nakajima, T., Uchiumi, S., 1995. Mineral paragenesis and metamorphic P–T paths of ultrahigh-pressure eclogites from Kyrgyzstan Tien-Shan. The Island Arc 4, 280–292.

Tait, J.A., Bachtadse, V., Soffel, H., 1994. Silurian paleogeography of Armorica: new paleomagnetic data from central Bohemia. Journal of Geophysical Research 99, 2897–2907.

Tajčmanová, L., Konopásek, J., Schulmann, K., 2006. Thermal evolution of the orogenic lower crust during exhumation within a thickened Moldanubian root of the Variscan belt of Central Europe. Journal of Metamorphic Geology 24, 119-134.

Teipel, U., Finger, F., Rohrmüller J., 2012. Remnants of Moldanubian HP-HT granulites in the eastern part of the Bavarian Forest (southwestern Bohemian Massif); evidence from SHRIMP zircon dating and whole rock geochemistry. Zeitschrift der Deutschen Gesellschaft fuer Geowissenschaften 163, 137-152.

Timmermann, H., Štědrá, V., Gerdes, A., Noble, S. R., Parrish, R. R., Dörr, W., 2004. The problem of dating high-pressure metamorphism: a U–Pb isotope and geochemical study on eclogites and related rocks of theMariánské Lázně Complex, Czech Republic. Journal of Petrology 45, 1311–1338.

Tollmann, A., 1995. Das Ausmass des variszischer Deckbaues im Moldanubikum. Krystalinikum 18, 117-132.

Tomkins, H. S., Powell, R., Ellis, D. J., 2007. The pressure dependence of the zirconium-in-rutile thermometer. Journal of Metamorphic Geology 25, 703-713.

Tracy, R. J., 1982. Compositional zoning and inclusions in metamorphic minerals. Reviews in Mineralogy 10, 355-397.

Tracy, R. J., Robinson, P., Thompson, A. B., 1976. Garnet composition and zoning in the determination of temperature and pressure of metamorphism, central Massachusetts. American Mineralogist 61, 762-75.

Turniak, K., Mazur, S., Wysoczański, R., 2000. SHRIMP zircon geochronology and geochemistry of the Orlica-Śnieżnik gneisses (Variscan belt of Central Europe) and their tectonic implications. Geodinamica Acta 13, 293-312.

Udovkiny, N.G., Dudek, A., Lang, M., 1977. Eclogites from the Bohemian Massif and from metamorphic rocks in the Soviet Unions. Correlation of Igneous and Metamorphic Rocks (in Russian). Academia Nauk SSSR, Moscow, pp. 101–117.

van Roermund, H.L.M., 2009. Mantle-wedge garnet peridotites from the northernmost ultra-high pressure domain of the Western Gneiss Region, SW Norway. European Journal of Mineralogy 21, 1085–1096.

Vielzeuf, D., Baronnet, A., Perchuk, A. L., Laporte, D., Baker, M. B., 1997. Calcium diffusivity in alumino-silicate garnets: an experimental and ATEM study. Contributions to Mineralogy and Petrology 154, 153-170.

Vielzeuf, D., Veschambre, M., Brunet, F., 2005. Oxygen isotope heterogeneities and diffusion profile in composite metamorphic-magmatic garnets from the Pyrenees. American Mineralogist 90, 463-472.

Villiger, S., Ulmer, P., Muntener, O., 2007. Equilibrium and fractional crystallization experiments at 0.7 GPa; the effect of pressure on phase relations and liquid compositions of tholeiitic magmas. Journal of Petrology 48, 159–184.

Vrána, S., 1992. The Moldanubian Zone in southern Bohemia: Polyphase evolution of imbricated crustal and upper mantle segments. In: Kukal, Z. (ed). Proceedings of the 1st International Conference on the Bohemian Massif, Prague, September 26-October 3, 1988, 331-335.

Vrána, S., Frýda, J., 2003. Ultrahigh-pressure grossular-rich garnetite from the Moldanubian Zone, Czech Republic. European Journal of Mineralogy 15, 43–54.

Vrána, S., Štědrá, V., Fišera, M., 2005. Petrology and geochemistry of the Běstvina granulite body metamorphosed at eclogite facies conditions, Bohemian Massif. Journal of Czech Geological Society 50, 95-106.

Vrána, S., Štědrá, V., Nahodilová, R., 2009. Geochemistry and petrology of high pressure kyanite–garnet–albite–K-feldspar felsic gneisses and granulites from the Kutná Hora Complex, Bohemian Massif. Journal of Geosciences 54, 159–179.

Wager, L.R., Brown, G.M., 1968. Layered Igneous Rocks. Oliver and Boyd Edinburgh.

Webb, S.A.C., Wood, B.J., 1986. Spinel–pyroxene–garnet relationships and their dependence on Cr/Al ratio. Contributions to Mineralogy and Petrology 92, 471–480.

Wendt, J. I., Kröner, A., Fiala, J., Todt, W., 1994. U–Pb zircon and Sm–Nd dating of Moldanubian HP/HT granulites from South Bohemia, Czech Republic. Journal of the Geological Society of London 151, 83–90.

White, R. W., Powell, R., Phillips, G. N., 2003. A mineral equilibria study of the hydrothermal alteration inmafic greenschist facies rocks at Kalgoorlie, Western Australia. Journal of Metamorphic Geology 21, 455–468.

Whitney D. L., Evans B. W., 2010. Abbreviations for names of rock-forming minerals, American Mineralogist 95, 185-187.

Wiedenbeck, M., Alle, P., Corfu, F., Griffin, W.L., Meier, M., Oberli, F., Von Quadt, A., Roddick, J.C., Speigel, W., 1995. 3 natural zircon standards for U–Th–Pb, Lu–Hf, trace-element and Ree analyses. Geostandards Newsletter 19, 1–23.

Willner, A. P., Krohe, A., Maresch, W. V., 2000. Interrelated P–T-t-d paths in the Variscan Erzgebirge Dome (Saxony, Germany): constraints on the rapid exhumation of high pressure rocks from the root zone of a collisional orogen. International Geology Review 42, 64–85.

Willner, A. P., Sebazungu, E., Gerya, T. V., Maresch, W. V., Krohe, A., 2002. Numerical modelling of PT-paths related to rapid exhumation of high-pressure rocks from the crustal root in the Variscan Erzgebirge Dome (Saxony/Germany). Journal of Geodynamics 33, 281-314.

Yang, P., Pattison, D., 2006. Genesis of monazite and Y zoning in garnet from the Black Hills, South Dakota. Lithos 88, 233-253.

Yang, P., Rivers, T., 2002. The origin of Mn and Y annuli in garnet and the thermal dependence of P in garnet and Y in apatite in calcpelite and pelite. Gagnon terrane, western Labrador. Geological Materials Research 4, 1-35.

Young, E. D., Rumble, D., 1993. The origin of correlated variations in in-situ $^{18}O/^{16}O$ and elemental concentrations in metamorphic garnet from southeastern Vermont, USA. Geochimica et Cosmochimica Acta 57, 2585-2597.

Żelaźniewicz, A., 1990. Deformation and metamorphism in Góry Sowie gneiss complex, Sudetes, SW Poland. Neues Jahrbuch für Geologie und Paläontologie Abhandlungen 179, 129-157.

Żelaźniewicz, A., Nowak, I., Larionov, A., Presnyakov, S., 2006. Syntectonic Lower Ordovician migmatite and posttectonic Upper Viséan syenite in the western limb of the Orlica–Śnieźnik Dome, West Sudetes: U-Pb SHRIMP data from zircons. Geologia Sudetica 38, 63–80.

Zhang, Z.M., Shen, K., Xiao, Y., Hoefs, J., Liou, J.G., Zu, Z., 2006. Mineral and fluid inclusions in zircon of UHP metamorphic rocks from the CCSD-main hole. A record of metamorphic evolution and fluid activity. Lithos 92, 378–398.

Zhang, J., Zheng, Y., Zhao, Z., 2009. Geochemical evidence for interaction between oceanic crust and lithospheric mantle in the origin of Cenozoic continental basalts in east-central China. Lithos 110, 305–326.

Zheng, Y.F., Fu, B., Gong, B., Li, L., 2003. Stable isotope geochemistry of ultrahigh pressure metamorphic rocks from the Dabie–Sulu orogen in China: implications for geodynamics and fluid regime. Earth-Science Reviews 62, 105–161.

Zheng, Y.F., Xia, Q.X., Chen, R.X., Gao, X.Y., 2011. Partial melting, fluid supercriticality and element mobility in ultrahigh-pressure metamorphic rocks during continental collision. Earth-Science Reviews 107, 342–374.

Zulauf, G., 1997. Von der Anchizone bis zur Eklogit fazies: Angekippte Krustenprofile als Folge der cadomischen und variscischen Orogenese im Teplá–Barrandium (Böhmische Masse). Geotektonische Forschungen 89, 1–302.

Žáčková, E., Konopásek, J., Jeřábek, P., Finger, F., Košler, J., 2010. Early Carboniferous blueschist facies metamorphism in metapelites of the West Sudetes (Northern Saxothuringian Domain, Bohemian Massif). Journal of Metamorphic Geology 28, 361–379.

Žák, J., Verner, K., Finger, F., Faryad, S.W., Chlupáčová, M., Veselovský, F., 2011. The generation of voluminous S-type granites in the Moldanubian unit, Bohemian Massif, by rapid isothermal exhumation of the metapelitic middle crust. Lithos 121, 25–40.

Žák, J., Verner, K., Janoušek, V., Holub, F. V., Kachlík, V., Finger, F., Hajná, J., Tomek, F., Vondrovic, L., Trubač, J., 2014. A plate-kinematic model for the assembly of the Bohemian Massif constrained by structural relations around granitoid plutons. In: Schulmann, K., Martínez Catalán, J. R., Lardeaux, J. M., Janoušek, V. and Oggiano, G. (eds) The Variscan Orogeny: Extent, Timescale and the Formation of the European Crust. Geological Society, London, Special Publications 405, 169–196.